



1506
UNIVERSITÀ
DEGLI STUDI
DI URBINO
CARLO BO

Università degli Studi di Urbino Carlo Bo

Department of

Applied and Pure Science

Ph.D. PROGRAMME IN: Research Methods in Science and Technology

CYCLE: XXXVI

**Synthesis and Chemical Optimization of New Melatonergic Ligands,
including Multitarget Compounds**

ACADEMIC DISCIPLINE: Medicinal chemistry - CHIM/08

Coordinator: Prof. Alessandro Bogliolo

Supervisor: Prof. Gilberto Spadoni

Ph.D. student: Fabiola Fanini

ACADEMIC YEAR
2022/2023

Preface

The following thesis is divided in two main part.

The *first part* reports medicinal chemistry investigations performed for melatonergic ligands, aimed at the design, synthesis and chemical optimization of new compounds, including the development of multitarget compounds, definition of structure-activity relationships and investigation of their mechanism of action. In the thesis, in addition to the development of suitable synthetic protocols, multiple aspects of melatonergic ligands activity have been investigated including: a) molecular determinants leading to receptor subtype selectivity or improving MLT fluorescence properties; b) the impact of conformational equilibria on the MLT receptor binding (in particular, the abundance of the bioactive conformation of chiral ligands in the solvent); and optimization of pharmacokinetic properties, while preserving the high binding affinity and MT₂ subtype selectivity. A general introduction about the melatonergic system and an overview of the endocannabinoid system, with a particular focus on melatonin receptors and the most important class of melatonergic ligands and monoacylglycerol lipase inhibitors, is provided in **Chapter 1**, introducing the medicinal chemistry framework in which this work is inserted. Finally, in **Chapter 5**, the potential for drug combination strategies, to widen and further enrich the therapeutic opportunities of melatonin derivatives, was investigated by designing and synthesizing a series of multitarget compounds potentially able to activate melatonin receptors and inhibit the enzyme monoacylglycerol lipase.

The *second part* of the thesis describes the results obtained during my visiting period in the Noël Research Group, at University of Amsterdam. In **Chapter 7**, the development of a new methodology for C-C bond formation, characterized by the use of commercially available starting materials in flow photochemical conditions, remarkably without the presence of a photocatalyst, has been reported.

List of publications and additional information

Peer reviewed articles

1. Ferlenghi F, Mari M, Gobbi G, Elisi GM, Mor M, Rivara S, Vacondio F, Bartolucci S, Bedini A, **Fanini F**, Spadoni G. *N*-(Anilinoethyl)amide Melatonergic Ligands with Improved Water Solubility and Metabolic Stability. *ChemMedChem*. **2021**,16(19), 3071-3082
2. Bartolucci S, Retini M, **Fanini F**, Paderni D, Piersanti G. Synthesis and Fluorescence Properties of 4-Cyano and 4-Formyl Melatonin as Putative Melatonergic Ligands. *ACS Omega*. **2023**, 8(24), 22190-22194
3. **Fanini F**, Luridiana A, Mazzarella D, Alfano AI, Van de Heide P, Rincón JA, García-Losada P, Mateos C, Frederick MO, Nuño M, Noël T. Flow photochemical Giese reaction via silane-mediated activation of alkyl bromides. *Tetrahedron Letters* **2023**, 117, 154380
4. Bedini A, Elisi GM, **Fanini F**, Retini M, Scalvini L, Pasquini S, Contri C, Varani K, Spadoni G, Mor M, Vincenzi F, Rivara S. Binding and unbinding of potent melatonin receptor ligands: mechanistic simulations and experimental evidence. *Journal of Pineal Research*, **2024**, 76(2), e12941

Poster presentation

1. Synthesis, optical resolution, absolute configuration and pharmacological characterization of a potent and selective MT₂ melatonin receptor agonist. **Fanini F**.
ISOS 2023 (Corbella summer school), 18th-22nd June 2023, Gargnano (BS), Italy
2. Design and synthesis of dual melatonin agonists-MGL inhibitors with therapeutic potential to treat neuroinflammation diseases. **Fanini F**.
ESMEC 2023 (European school of medicinal chemistry), 2nd-6th July 2023, Urbino (PU), Italy

Conference/summer school attended

3. *HIMS 1st annual symposium*, 15th June 2022, Amsterdam, the Netherlands
4. *ISPROCHEM 2021 (International school of process chemistry)*, online conference, 10th-12th May 2021
5. *ESMEC 2021 (European school of medicinal chemistry)*, 26th June-1st July 2021, Urbino (PU), Italy

Research period abroad

1. *Noël Research group*, University of Amsterdam (Amsterdam, the Netherlands)
Research activity in the field of photochemistry and flow chemistry
March 2022 to December 2022

Table of Contents

Preface.....	III
List of publications and additional information.....	IV
Peer reviewed articles.....	IV
Poster presentation	IV
Conference/summer school attended	IV
Research period abroad	V

First Part

Chapter 1. General introduction	1
1.1 Melatonin	1
1.1.1 <i>Biosynthesis and physiological role.....</i>	<i>1</i>
1.1.2 <i>Melatonin membrane receptors and their potential therapeutic role.....</i>	<i>3</i>
1.1.3 <i>Design and development of melatonin receptor ligands.....</i>	<i>4</i>
1.1.4 <i>Subtype selective MLT receptor ligands</i>	<i>5</i>
1.2 Endocannabinoid system.....	9
1.2.1 <i>2-Arachidonoylglycerol: biosynthesis, mechanism of action, and degradation.....</i>	<i>10</i>
1.2.2 <i>Irreversible and reversible MAGL inhibitors.....</i>	<i>12</i>
1.3 References	15
Chapter 2. Synthesis and characterization of potent MT₂ selective agonists.....	23
2.1 Introduction	23
2.2 Results and discussion.....	26
2.2.1 <i>Chemistry.....</i>	<i>26</i>
2.2.2 <i>Pharmacological results</i>	<i>29</i>
2.3 Conclusion.....	30
2.4 Experimental section.....	31
2.4.1 <i>Materials.....</i>	<i>31</i>
2.4.2 <i>Experimental procedure.....</i>	<i>31</i>

2.4.3	<i>Comparison of the NMR spectra of compound (2R)-3a, obtained by N-acylation of (±)-1 and compound (2R)-3a obtained by reduction and acylation of (2R)-5a</i>	36
2.4.4	<i>Comparison of NMR spectra of compound (2S)-3b, obtained by N-acylation of (±)-1 and compound (2S)-3b obtained by reduction and acylation of (2S)-5b</i>	36
2.4.5	<i>Chiral HPLC analysis</i>	37
2.5	References	39

Chapter 3. Synthesis of 4-substituted melatonin analogues as putative

fluorescent probes for melatonin receptors 40

3.1	Introduction	40
3.2	Results and discussion.....	43
3.3	Conclusion and outlook.....	46
3.4	Experimental section.....	47
3.4.1	<i>Materials</i>	47
3.4.2	<i>Experimental procedure</i>	47
3.5	References	52

Chapter 4. Novel N-(anilinoethyl)amide melatonergic ligands with improved

water solubility and metabolic stability 54

4.1	Introduction	54
4.2	Results and discussion.....	55
4.2.1	<i>Chemistry</i>	55
4.2.2	<i>SAR discussion and biological evaluation</i>	57
4.2.3	<i>Physicochemical characterization</i>	60
4.2.4	<i>Pharmacokinetic evaluation</i>	62
4.3	Conclusion.....	63
4.4	Experimental section.....	64
4.4.1	<i>Materials</i>	64
4.4.2	<i>Experimental procedures</i>	64
4.4.3	<i>Pharmacokinetics studies</i>	73
4.5	References	76

Chapter 5. Design, synthesis and characterization of new dual-acting compounds: MLT agonists and MAGL inhibitors	78
5.1 Introduction	78
5.2 Results and discussion.....	81
5.2.1 <i>Design and pharmacological evaluations of the new dual-acting compounds</i>	81
5.2.2 <i>Chemistry</i>	88
5.3 Conclusion.....	93
5.4 Experimental section.....	94
5.4.1 <i>Materials</i>	94
5.4.2 <i>General procedures</i>	94
5.4.3 <i>Experimental data</i>	98
5.5 References	131
Chapter 6. Appendix.....	134
6.1 Experimental chemistry methods.....	134
6.2 <i>In vitro</i> pharmacology experiments.....	135
6.3 Molecular modelling	136
6.4 Molecular dynamics (MD) simulations	136
6.5 References	136

Second Part

Chapter 7. Hydrofunctionalization of olefins driven by a photoinduced halogen atom transfer in flow conditions	138
7.1 Introduction	138
7.1.1 <i>Photochemistry</i>	140
7.1.2 <i>Flow chemistry: advantages and application in photochemistry</i>	141
7.1.3 <i>Silyl radicals as halogen abstractors</i>	142
7.2 Results and discussion.....	145
7.3 Conclusion.....	149
7.4 Experimental section.....	150

7.4.1	<i>Materials and methods</i>	150
7.4.2	<i>Reactors</i>	151
7.4.3	<i>Optimization Table</i>	152
7.4.4	<i>Experimental procedures</i>	154
7.4.5	<i>Experimental data</i>	155
7.4.6	<i>Mechanistic studies</i>	165
7.5	References	167

List of abbreviations	170
------------------------------------	------------

First part

Chapter 1. General introduction

Complex multifactorial pathologies, such as metabolic syndrome, psychiatric or degenerative central nervous system disorders, and cancer, are often caused by deregulation of multiple pathways, and cannot be effectively treated with a single-target modulation. An innovative and more effective approach is polypharmacology using multifunctional agents capable of modulating multiple biological targets simultaneously. In this context, both endocannabinoid and melatonergic systems can be a great resource for the design and development of new therapeutic agents, particularly in neurodegenerative diseases. Indeed, they are pleiotropic signaling systems involved in almost all aspects of mammalian physiology and pathology, and have many connections with other neurotransmitter systems.

1.1 Melatonin

1.1.1 Biosynthesis and physiological role

Melatonin (*N*-acetyl-5-methoxytryptamine, MLT) is a neurohormone, mainly secreted by the pineal gland¹, although other organ sources have been suggested². This molecule is produced at night via a 4-step pathway from tryptophan, thanks to an array of enzymes tightly regulated, indirectly, by light. Tryptophan-5-hydroxylase catalyzed hydroxylation at position 5 of the indole ring and subsequent decarboxylation allows the formation of serotonin. Then, serotonin is *N*-acetylated and transformed into melatonin via methylation of the hydroxyphenyl group, by two enzymes, serotonin *N*-acetyl transferase (SNAT) and hydroxyindole *O*-methyltransferase (**Figure 1**).³

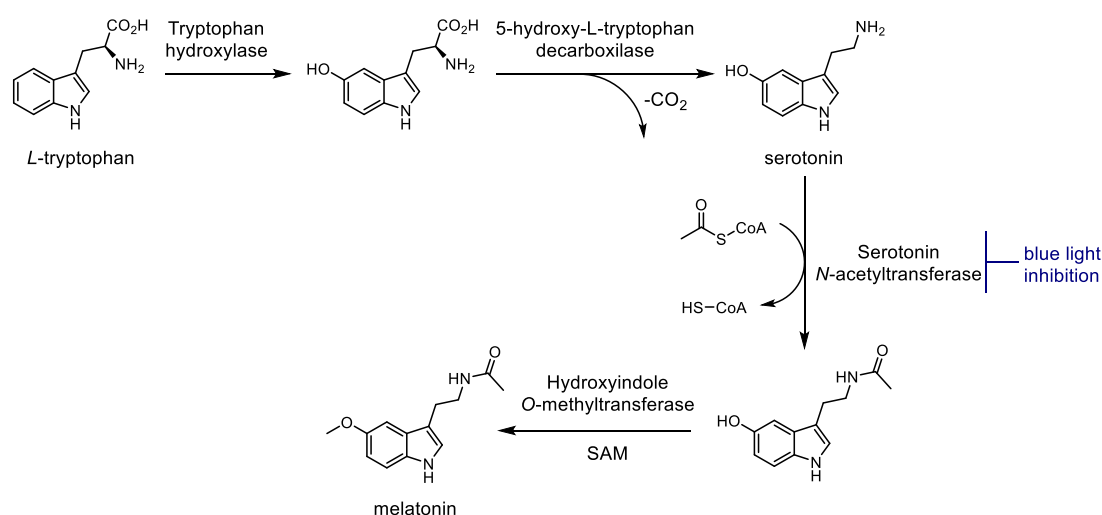


Figure 1 Biosynthesis of melatonin and its inhibition upon blue light exposure. SAM= *S*-adenosyl methionine.

MLT is then released into the systemic circulation following a circadian rhythm, “transferring” the circadian information from the pineal to the general blood circulation, and then to the peripheral

organs. Circulating melatonin is primarily metabolized in the liver through 6-hydroxylation and subsequent sulphate conjugation, leading to increased water solubility.³ Secondly, demethylation of the methoxy group leads to *N*-acetylserotonin (**Figure 2A**). Instead, in the brain MLT is primarily converted to *N*¹-acetyl-*N*²-formyl-5-methoxykynuramine (AFMK) and then to *N*¹-acetyl-5-methoxykynuramine (AMK) (**Figure 2B**).⁴

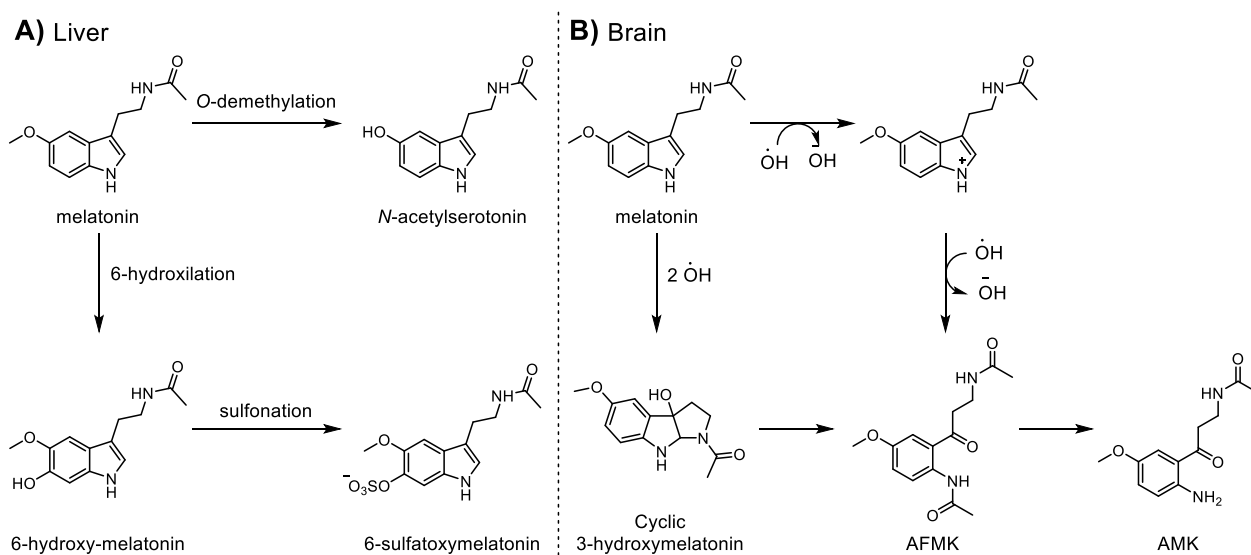


Figure 2 Melatonin metabolic pathways in the liver (**A**) and in the brain (**B**).

Other tissues, such as the retina, produce melatonin in a circadian manner, but in other body regions its production does not depend on the light-dark cycle. Nevertheless, local elevated concentrations of melatonin can be found in some tissues and organs, such as the gut and immune cells.⁵

MLT is generally considered as a natural hormone for inducing sleep and is widely used as a dietary supplement to promote sleep or to alleviate the effects of jet lag.⁶ Although melatonin is one of the most popular sleep-inducing supplement in the United States⁷, it lacks Food and Drug Administration approval due to its rapid efflux and short duration. However, more effective and long-lasting MLT analogs, such as Ramelteon {(*S*)-*N*-[2-(1,6,7,8-tetrahydro-2*H*-indeno-[5,4-*b*]furan-8-yl)ethyl]propionamide}⁸, have been approved for primary chronic insomnia treatment, because of their low side-effect profile as compared to benzodiazepines and other sleeping aids. Other MLT bioisosteres, such as tasimelteon {*N*-[[1*R*,2*R*]-2-(2,3-dihydro-1-benzofuran-4-yl)cyclopropyl]methyl]propenamide}⁹ and agomelatine {*N*-[2-(7-methoxy-1-naphthyl)ethyl]acetamide}¹⁰, are used for non-24-hour sleep-wake disorders in blind individuals and as an atypical anti-depressant for major depressive disorders, respectively. In addition to regulating sleep-wake rhythms, MLT can modulate other physiological processes, including regulation of body temperature, hormone secretion and blood pressure, homeostasis of glucose secretion, pain perception and neuroprotection.

1.1.2 Melatonin membrane receptors and their potential therapeutic role

Even if some non-receptor dependent signaling pathways have been suggested¹¹, MLT exerts most of its physiological and neuroendocrine activities through the activation of two high affinity G-protein-coupled receptors, MT₁ and MT₂, located at the plasma membrane.¹² Melatonin displays picomolar affinity for these receptors, whose activation is mainly coupled to inhibitory G proteins (G_{i/o}) leading to reduction of intracellular cAMP levels. Other signal transduction mechanism have been characterized, comprising G_{q/11} protein, beta-arrestin and protein kinase C.¹³

MT₁ and MT₂ receptors were initially cloned by Reppert's research group¹⁴ together with the Mel1c receptor¹⁵, the expression of which is limited to amphibians, fishes and birds¹⁶. Mel1c, was shown to evolve in mammals into GPR50¹⁷, which lost its capacity to bind to melatonin but gained other roles in the regulation of melatonin receptors¹⁸. Another melatonin-binding site, named MT₃, was described over the years¹⁹ and it turned out to be the enzyme NAD(P)H dehydrogenase quinone 2 (NQO2)²⁰.

In humans MT₁ and MT₂ share 55% and 70% sequence similarity for the overall region and the transmembrane district, respectively. In 2019, the crystal structures of both MT₁ and MT₂, co-crystallized with nonselective agonists, were determined by the X-ray free electron laser method (XFEL), providing valuable information about the agonist binding mode and of the overall binding site composition and extension.^{21,22} Although the reported crystal structures of receptors are in inactive forms (as they were resolved in the presence of several mutated residues), the mutations necessary for crystallization did not modify the overall architecture of the binding site, nor the arrangement and interactions undertaken by the ligands. In fact, a recent cryo-EM structure of the ternary complex of the MT₁ receptor with ramelteon and G_i-protein revealed a very similar three-dimensional structure of the ligand binding site.²³ The resolved structures of MT₁ and MT₂ receptors exhibit high similarity and conservation of ligand-interacting residues, with only one amino acid different between (A104/G117). The MT₂ receptor is characterized by a wider binding site in the region accommodating substituents in position 2 of the indole ring of melatonin.²²

MLT and other nonselective agonists showed similar interactions with receptor residues: the major interactions include aromatic stacking of the heterocyclic core with ECL2 hydrophobic residue F179/192 (in MT₁ and MT₂, respectively), and two hydrogen bonds via their methoxy oxygen (or dihydrofuran oxygen in the case of ramelteon) and amide side chain with Q162/175 and N181/194ECL2, respectively (**Figure 3**).^{21,22}

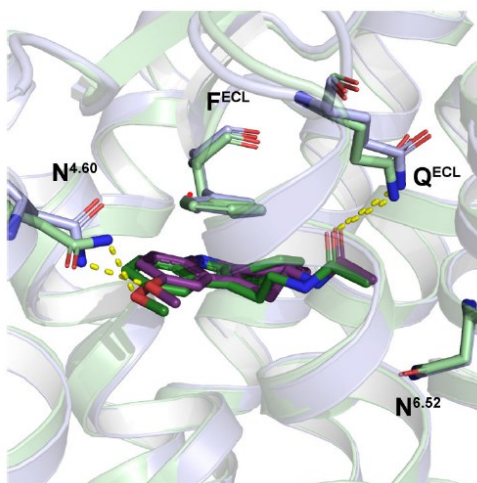


Figure 3 is taken from ref. 22. Comparison of 2-phenyl-melatonin ligand conformations in MT₁ (green) and MT₂ (violet); hydrogen bonds are shown as yellow dashed lines. N=asparagine, F=phenylalanine, Q= glutamine.

A structural peculiarity differentiating melatonin receptors by other Class A GPCRs, is that the orthosteric binding site of both receptors is tightly sealed from solvent by extracellular loop 2 (ECL2), thus strongly hampering ligand recruitment from the solvent. Potential ligand access to the orthosteric binding site is provided by a hydrophobic channel between the TM helices IV and V that opens towards the lipid bilayer.

Over the years, it has become increasingly apparent that targeting MLT receptors is of clinical interest for the treatment of pathologies affecting the CNS (including sleep disorders, depression or neuropathological states in which neuroinflammation plays a central role)²⁴, and other body districts, such as metabolic disorders like diabetes and obesity²⁵, cancer²⁶, or pain²⁷. Even if different aspects of MLT receptors functions and activity require further investigation, such as tissue distribution, biased signaling, and the impact of receptor dimerization/oligomerization on activity, it appears that some activities are sustained by the activation of either one or the other receptor subtype and, in some cases, the two subtypes produce opposite effects.²⁸ For example, MT₁ receptors inhibit neuronal firing of the suprachiasmatic nucleus, which controls pineal melatonin production, and has been linked to neuroprotective activity. The MT₂ subtype has been implicated in the control of non-rapid eye movement (NREM) sleep²⁹ and immune system activation, while MT₁ mediates rapid eye movement (REM) phases of the vigilance state in sleep architecture³⁰.

1.1.3 Design and development of melatonin receptor ligands

Therapeutic potential of targeting MT₁ and MT₂ receptors have prompted many research groups to develop several interesting MLT receptor ligands, including the therapeutic drugs ramelteon, agomelatine and tasimelteon. Some pharmaceutical companies have also developed time-released melatonin tablets, to ameliorate the sleep quality of elderly patients³¹ and autistic children³².

Initial attempts to design new melatonergic ligands were mainly based on ligand-based approaches. Many compounds displaying high binding affinity, but no selectivity toward MT₁ or MT₂ receptors, have been obtained by bioisosteric replacements of the indole with other aromatic systems and/or by structure modifications at specific aromatic ring positions. For example, in the approved melatonergic drugs agomelatine and ramelteon the indole scaffold has been replaced by naphthalene and indane (**Figure 4**), respectively. Higher affinity and agonist potency have been achieved by introducing an iodine, a bromine, an alkyl or an aryl group in a position equivalent to C2 of melatonin.

Other common strategies used to develop high affinity MLT ligands were structural simplification (e.g., phenyl-propyl-amides³³, *N*-anilinoethylamides³⁴, phenoxy-ethylamides³⁵), or introduction of conformational constraints on groups involved in drug-receptor interactions. For example, ramelteon with an ether oxygen incorporated into a dihydrofuran ring shows higher affinity than melatonin (17-fold for MT₁ and 2-fold for MT₂)³⁶. Conformational restriction of the *N*-acylamino side chain, exemplified in the tricyclic ligands **I**³⁷, **II**³⁸, and **III**³⁹, is generally well-tolerated with many analogs reaching binding affinity of the parent hormone (**Figure 4**).

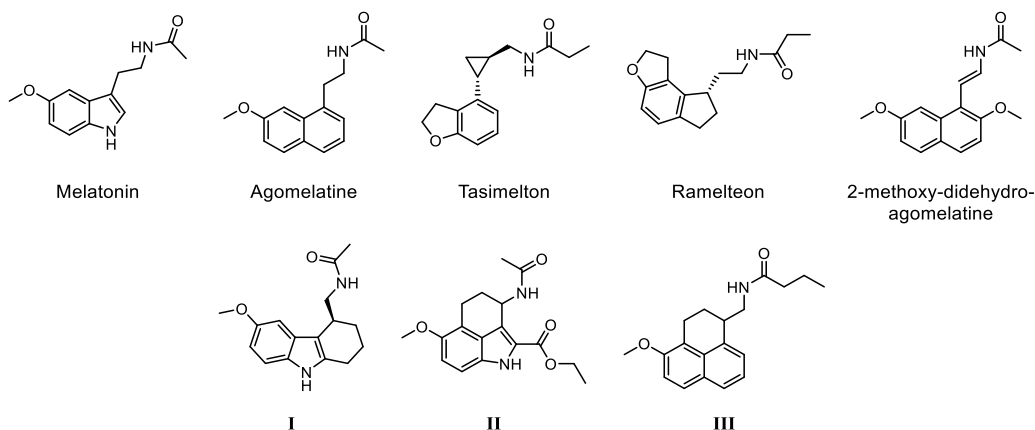


Figure 4 Melatonin and examples of non-selective melatonergic ligands obtained by replacement of melatonin's indole scaffold by other aromatic rings and/or by conformational restriction.

1.1.4 Subtype selective MLT receptor ligands

Although MT₁ and MT₂ receptors may have distinctive *in vivo* functions, none of the most clinically advanced MLT ligands discriminates between the two subtypes. Therefore, in the last few decades, the industrial and academic medicinal chemistry research has been active in the design of subtype-selective ligands as potential candidates for drug development and/or valuable pharmacological tools to investigate the distinct roles, not yet fully elucidated, of MT₁ and MT₂ receptors in several pathophysiological processes.²⁴ Different ligand- and structure based techniques were used to design and develop diverse classes of potential subtype selective ligands, comprising benzofuran (**IVa-c**), tetrahydronaphthalenic derivatives (**Va-b**), tetrahydroisoquinoline (**VIa-b**), 6,7-

dihydro-5H-benzo[*c*]azepino[2,1-*a*]indoles (K185), 2-*N*-acylaminoalkylindoles (such as UCM454), and the two historically reference ligands 4-P-PDOT⁴⁰ and luzindole⁴¹ (**Figure 6**).

Computational strategies, including pharmacophore models integrated with 3D-QSAR analyses, contributed to their development in particular of MT₂-selective ligands. A pharmacophore model for MT₂-selective partial agonists and antagonists was obtained associating the presence of substituents in position 1 or 2 of the indole ring and not coplanar with it, to selectivity toward the MT₂ subtype and reduced intrinsic activity.^{42,43} This model of MT₂-selective antagonism, also statistically supported by 3D-QSAR analysis⁴⁴, was then used to design novel classes of topologically different MT₂-selective receptor antagonists, characterized by a tricyclic dibenzocycloheptene (UCM549, in **Figure 6**)⁴⁵ nucleus which incorporates, in the same structure, both the aromatic core of the MLT nucleus and the out-of-plane substituent (**Figure 5**)

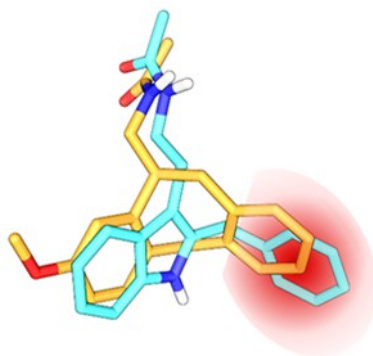


Figure 5 Superimposition of luzindole (cyan carbons) and (*S*)-UCM549 (orange carbons): aromatic substituents occupying the out-of-plane red region induce selectivity for the MT₂ receptor and decrease the intrinsic activity.

Tetracyclic derivative K185, whose 2-phenyl group ring linked to the indole would be placed with an out-of-plane arrangement, behaves as an MT₂ antagonist, in agreement with the rationale leading to the above described dibenzocycloheptene derivatives. Structural simplification of some dibenzo seven-membered tricyclic antagonists, leading to more flexible compounds but retaining the key structural requirements outlined above (i.e., two aromatic rings and an amide side chain in a suitable arrangement), led to the discovery of a series of *N*-(3,3-diphenylpropenyl)alkanamides (e.g. UCM764, **Figure 6**) some of which exhibited MT₂ binding affinity higher than MLT and a remarkable selectivity for the MT₂ receptor.⁶ Substitution of benzhydryl carbon atom of the *N*-(3,3-diphenylpropyl)alkanamido series with a nitrogen one led to a novel class of *N*-(substituted-anilinoalkyl)amido ligands (such as UCM924), whose intrinsic activity and MT₁/MT₂ subtype selectivity can be modulated by the introduction of substituents with different sizes on the aniline nitrogen.³⁴ Indeed, substituents with limited size on the aniline nitrogen (e.g., a methyl group, UCM793) afforded potent MT₁/MT₂ nonselective agonists, while bulkier substituents led to selectivity for the MT₂ receptor and to limited intrinsic activity, moving toward a partial agonism for

the phenyl derivative UCM765 to antagonism in the case of the very MT_2 -selective β -naphthyl derivative UCM800 (**Figure 6**). Subsequently, the *N*-anilinoethylamide scaffold was rigidified to give the novel series of 2-acylaminomethyl-tetrahydroquinolines, including MT_1 / MT_2 non selective ligands and MT_2 selective ligands; interestingly the introduction of a benzyl group on the tetrahydroquinoline nitrogen led to a highly potent MT_2 selective full agonist (UCM1014, **Figure 6**).⁴⁶

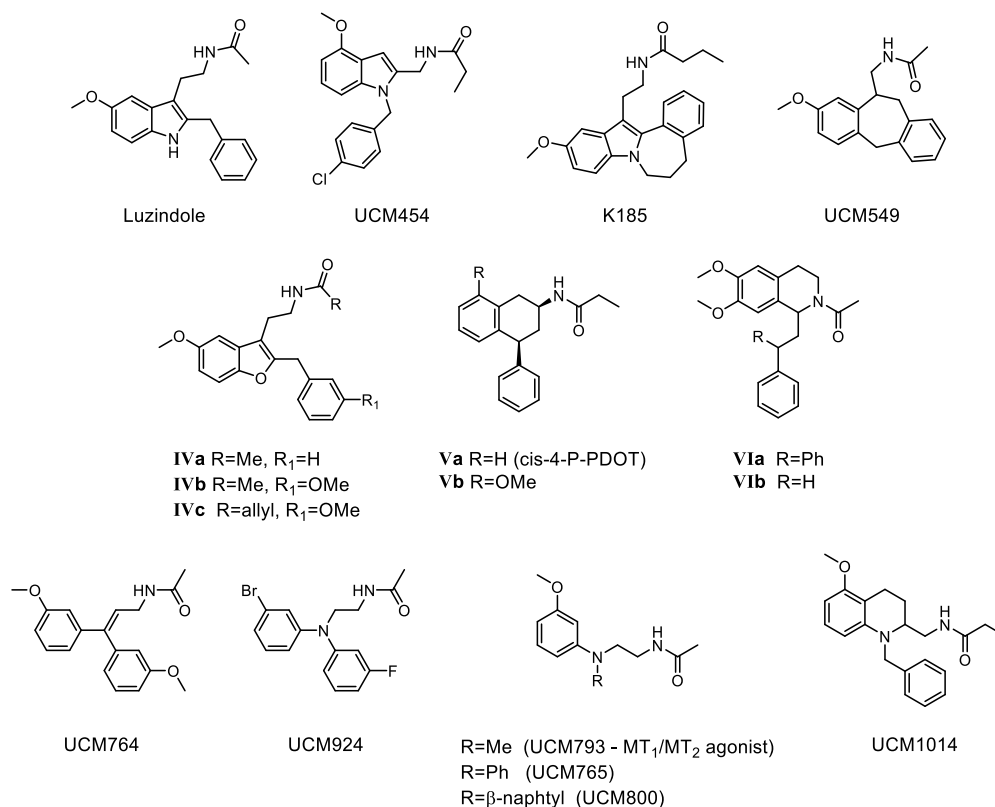


Figure 6 Examples of MT_2 -selective melatonergic ligands.

The search for new MLT ligands has also been expanded to MT_1 -selective derivatives, but the obtained results are far from encouraging, with few compounds currently available, usually displaying limited selectivity for this receptor subtype. The most common structural feature of the MT_1 -preferring ligands is the presence of a longer/bulkier, usually lipophilic, substituent replacing the methoxy group of MLT. The first approach used to develop MT_1 selective ligands was the preparation of symmetric dimers, by coupling two moieties deriving from known ligands (i.e. agomelatine or UCM793) through an appropriate spacer, as exemplified by compounds **VII**⁴⁷ and UCM876⁴⁸ (**Figure 7**). Some other MT_1 -preferring ligands (approximately 20-40 fold selectivity) were obtained by introducing a 4-phenylbutyl group at the C-2 position of the bicyclic scaffold benzoxazole, mimicking the methoxyphenyl fragment of MLT, as exemplified by compound **VIII**⁴⁹ in **Figure 7**. Some other compounds (UCM871, and **IXa-b**) displaying about 10-90 fold preference toward MT_1 receptors, were subsequently obtained by applying the same approaches to other

scaffolds.^{50,51,52} Crystal structures of MT₁ and MT₂ receptors has opened up new opportunities for virtual discovery of new melatonergic chemotypes in clouding subtype selective ligands. A virtual screening, based on docking of a chemical library containing 150 million compounds into the binding sites of MT₁ crystal structure, allowed the discovery of 15 new chemical scaffolds, topologically unrelated to known melatonin receptor ligands with affinities in the micromolar range. Structure-based optimization of some of these compounds led to two interesting MT₁ selective inverse agonists (UCSF7447 and UCSF3384, **Figure 7**), topologically unrelated to previously explored chemotypes.⁵³

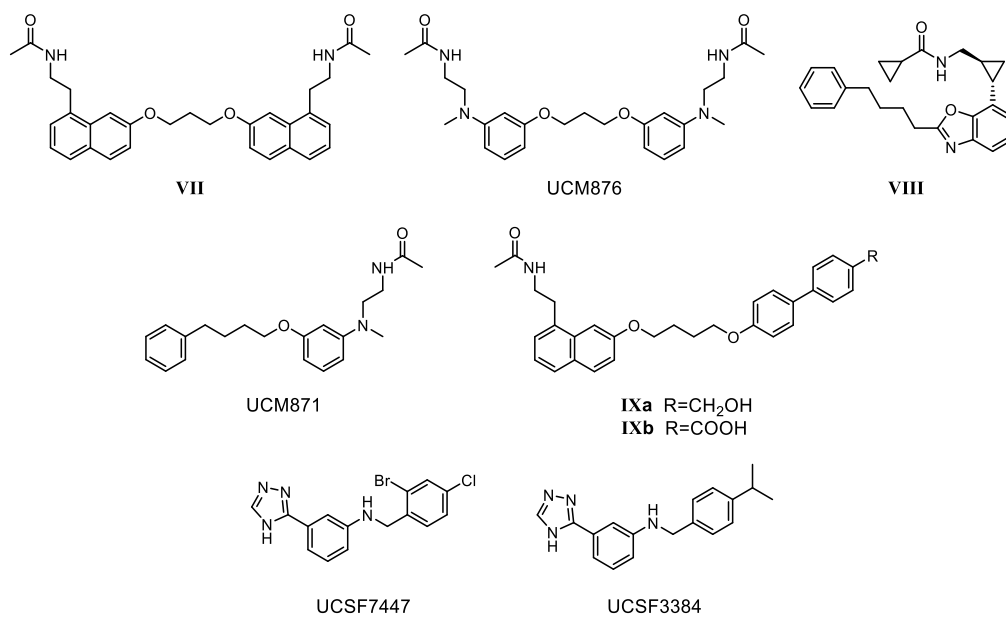


Figure 7 Examples of MT₁-selective melatonergic ligands.

1.2 Endocannabinoid system

The endocannabinoid system (ECS) is a complex neuromodulatory network involved in the regulation of several cognitive and physiological processes.⁵⁴ The endocannabinoid signaling seems to be altered and hypofunctional in many neurological diseases; therefore targeting this system could provide new therapeutic strategies for the treatment of many different (CNS) disorders, particularly in neurodegenerative diseases such as Parkinson's disease, Alzheimer's disease, Huntington's disease, multiple sclerosis, amyotrophic lateral sclerosis, strokes, traumatic brain injury, pain, and epilepsy.⁵⁵

The ECS comprises:

- the G protein-coupled receptors CB₁ and CB₂ which are found throughout the mammalian body, but are particularly abundant in the brain (CB₁) and immune cells (CB₂);
- endogenous lipid-based mediators known as endocannabinoids (ECs);
- the enzymes involved in the biosynthesis and degradation of ECs.⁵⁶

The most important ECs are 2-arachidonoylglycerol (2-AG) and anandamide (AEA), which are synthesized through stimulus-dependent cleavage (“on-demand”) from membrane phospholipids precursors. AEA is synthesized from its arachidonic acid precursors and phosphatidylethanolamine by the sequential actions of two intracellular enzymes: *N*-acyltransferase (NAT) and *N*-acyl phosphatidylethanolamine phospholipase D (NAPE-PLD).⁵⁶ 2-AG is produced through a two-step process in which phospholipase C-beta (PLC-beta) hydrolyzes phosphatidylinositol-4,5-bisphosphate (PIP₂) to generate 1,2-DAG, which is then cleaved by diacylglycerol lipase-alpha (DGL-alpha) to yield 2-AG.⁵⁷ Once they have activated specific receptors, AEA and 2-AG are rapidly inactivated through a two-steps mechanism, involving a selective carrier-based cellular uptake followed by enzymatic hydrolysis. The enzyme fatty acid amide hydrolase (FAAH) is primarily responsible for the degradation of AEA. 2-AG is deactivated in large part by the presynaptic serine hydrolase monoacylglycerol lipase (MAGL) and in minor part by other hydrolases (e.g., serine hydrolase/hydrolase 6 (ABDH-6), serine hydrolase/hydrolase 12 (ABDH-12), and cyclooxygenase (COX-2), which convert 2-AG into arachidonic acid and glycerol.⁵⁸

1.2.1 2-Arachidonoylglycerol: biosynthesis, mechanism of action, and degradation

Many neurological diseases (particularly anxiety and depression)⁵⁹ and neurodegenerative processes are often associated with hypofunctionality of the ECS tone⁶⁰. In these conditions a possible therapeutic strategy could be to inhibit endocannabinoid degradation by synthetic molecules, thus restoring the altered turnover of endocannabinoids and indirectly activating CB receptors only in the tissues where the alteration occurs, avoiding the side effects of direct receptor activation. For these reasons, and considering that the physiological levels of 2-AG are much higher than those of AEA, remarkable efforts have been made both by academia and pharmaceutical companies to develop potent and selective MAGL inhibitors.

In the mammalian brain 2-AG is the most abundant endocannabinoid; it is released upon demand from postsynaptic neurons in response to a wide range of stimuli (including inflammatory conditions, neuronal injury and exposure to oxidative stress)⁶¹ and acts as a retrograde messenger by binding and activating CB₁ receptors expressed on presynaptic neurons, modulating excitatory (e.g., glutamatergic) and inhibitory (e.g., GABAergic) neurotransmission, and other receptors.⁶² In addition, 2-AG is an important intermediate in lipid metabolism, particularly as a source of arachidonic acid for prostaglandin synthesis.⁶³ 2-AG also acts on peripheral CB₁ and CB₂ receptors to mediate, among other effects, immune modulation⁶⁴ and inhibition of cancer cell growth⁶⁵. Enhancements of 2-AG levels in different tissues, that can be achieved through inhibition of MAGL, can mitigate cellular damage caused by widespread stimuli.

MAGL belongs to the α/β serine hydrolase superfamily and shares with the other members of this group a conserved β -sheet core hosting, at the bottom of a long channel delimited by hydrophobic residues (which is thought to accommodate the lipophilic chain of 2-AG), the Ser122–His269–Asp239 catalytic triad.⁶⁶ Close to Ser122, the NH backbone groups of Ala51 and Met123 form the oxyanion hole, which is believed to stabilize the tetrahedral anionic transition state generated during 2-AG hydrolysis. Beyond the oxyanion hole, the binding channel terminates with a cleft, lined by a set of polar residues that include Arg57, His121, and Tyr194 and connected by a narrow opening to the solvent, providing an exit route for the glycerol fraction released after hydrolysis of 2-AG. The structure of MAGL is illustrated in **Figure 8A**.⁶⁶

An interesting structural feature of this enzyme is the presence of a lid domain that surrounds and hides its catalytic task. Within this domain, a region comprising helix α 4 and the loop connecting helices α 4 and α 5 forms a wide flexible hydrophobic U-shaped structure, that serve both as a portal preventing or allowing the substrate access to the catalytic site (**Figure 8B**).⁶⁷

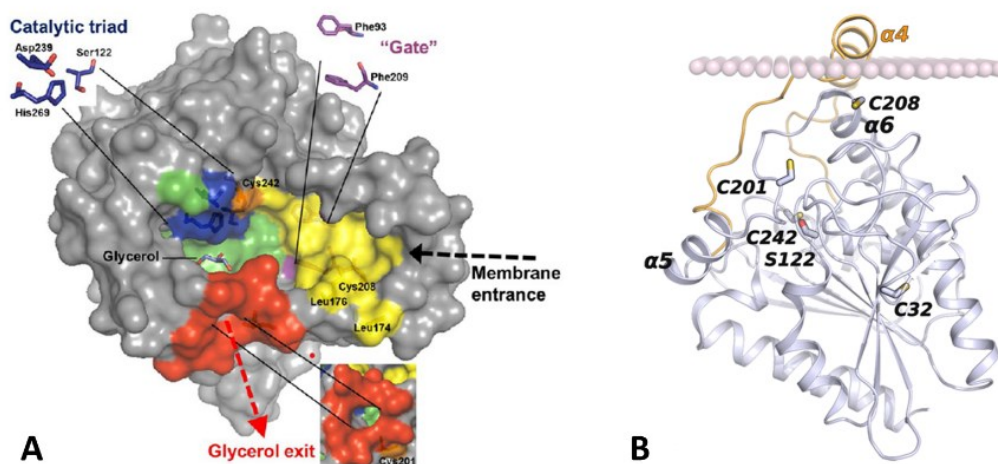
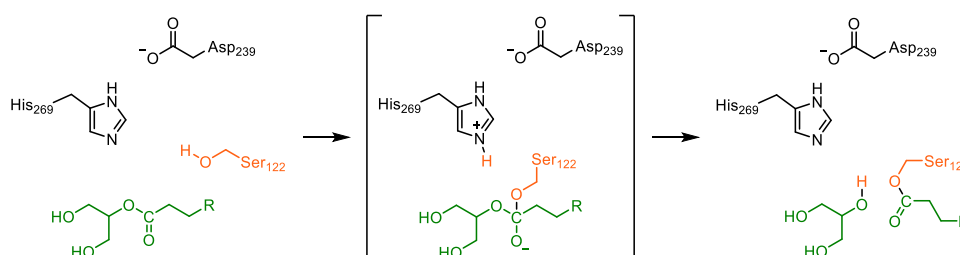


Figure 8 Overview of the structure of MAGL. **A**) The model highlights the membrane entrance and the hydrophobic gate (yellow and pink), the catalytic triad (blue), the polar cleft to be occupied by glycerol (green), and the polar hole for glycerol exit (red). **B**) Crystal structure of human MAGL showing the U-shape conformation of the access tunnel to the catalytic side. Ser122 belongs to the catalytic triad. The three cysteine residues, Cys242 close to the active site, Cys201, and Cys208, are implicated in the allosteric modulation of MAGL.

Another essential feature of MAGL is the presence of three cysteine residues, Cys242, Cys201, and Cys208, that modulate the catalytic activity in important ways. Cys242 is located close to the catalytic Ser122 and is directly involved in catalysis.⁶⁶ On the other hand, Cys201 and Cys208, located far from the active site (on the loop connecting helices $\alpha 5$ and $\alpha 6$, and on the first turn of helix $\alpha 6$, respectively), are responsible for an allosteric modulation of MAGL activity.⁶⁸ An increase of oxidative signals within cells, as in the case of hydrogen peroxide accumulation, enhances 2-AG levels⁶⁹ by inhibiting MAGL through oxidation of the regulatory cysteines Cys201 and Cys208 located on the surface of the enzyme⁷⁰; the resulting spatial modification promotes the closure of the “lid domain”, thus reducing substrate recruitment. These findings can be exploited for the development of allosteric MAGL inhibitors.⁷¹

The catalytic mechanism for MAGL acylation by 2-AG is similar to that shared by other esterases.⁷² This includes a first step in which the nucleophilic serine attacks the carbonyl carbon of 2-AG, generating a tetrahedral intermediate stabilized by oxyanion hole, and a second step in which this intermediate decomposes with the consequent formation of the acylenzyme and elimination of the glycerol (**Scheme 1**).



Scheme 1 Mechanism of MAGL acylation by 2-AG.

1.2.2 Irreversible and reversible MAGL inhibitors

Over the years, the search for potent MAGL inhibitors has led to the identification of different classes of compounds ranging from allosteric cysteine-targeting modulators⁷¹ to orthosteric inhibitors, comprising both covalent agents (i.e., carbamates⁷³ and tertiary ureas⁷⁴) and noncovalent inhibitors⁷⁵, that can be firstly classified as irreversible and or reversible inhibitors according to their mechanism of inhibition; some target the cysteine residues (allosteric inhibition) or the serine (orthosteric inhibition). The first classes of compounds targeting cysteines to be discovered included *N*-substituted maleimides (such as *N*-arachidonoylmaleimide: IC₅₀ = 0.14 μM)⁷⁶ and disulfide derivatives⁷⁷ that covalently and irreversibly block the enzymatic activity through the interaction with Cys242 and Cys208 of human MAGL to form Michael addition or disulfide products (**Figure 9**).

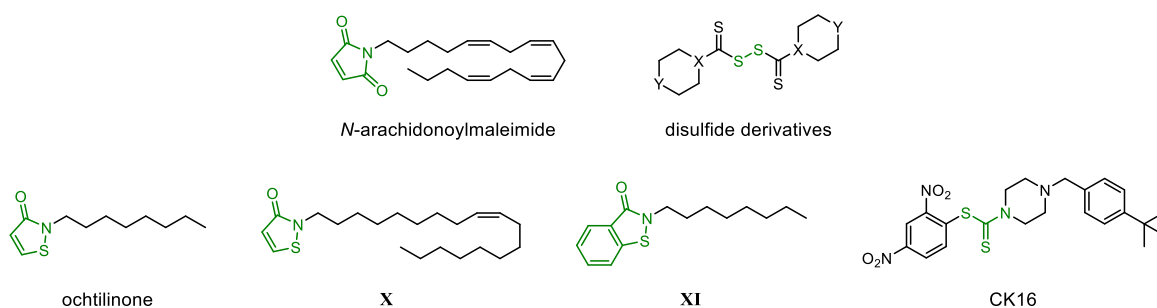


Figure 9 Example of MAGL inhibitors targeting cysteine residues.

Isothiazolinone-based MAGL inhibitors were subsequently identified (octhilinone, IC₅₀ = 88 nM), derivative X (IC₅₀ = 43 nM), and benzisothiazolinone XI (IC₅₀ = 59 nM) displaying activities in the nanomolar range and blocking MAGL activity through a partially reversible mechanism (formation of a disulfide adduct with the enzyme)⁷⁸, together with thioamide-base inhibitors, such as CK37 exhibiting moderate activity, but able to increase dramatically the 2-AG levels *in vivo* (**Figure 9**).

Among the carbamate derivatives, URB602 (**Figure 10**) was the first MAGL inhibitor to be identified in a screening of a library of *O*- and *N*-biphenyl carbamates.⁷⁹ It acts through a partially reversible, noncompetitive mechanism and displays moderate potency (IC₅₀ = 28 μM). However, its utility as pharmacological tool was limited by its tendency to interfere with the activities of a variety of other serine hydrolases.

In an effort to optimize carbamates as selective scaffolds for MAGL inactivation over FAAH, more potent and selective compounds were subsequently discovered (see **Figure 10**), which differ mechanistically from URB602, because they inhibit MAGL activity by forming covalent adducts with the enzyme's catalytic Ser122. For example, Cravatt and co-workers identified the potent and selective inhibitor JZL184 [IC₅₀ (MAGL) = 6 nM vs IC₅₀ (FAAH) = 4 μM], without off-target effects towards cannabinoid receptors and other catalytic serine-containing enzyme.⁸⁰ The

replacement of the *O*-*p*-nitrophenyl leaving group by an *O*-hexafluoroisopropoxy (HIPF) carbamate yielded compound KML29 (IC₅₀ = 5.9 nM in human MAGL) displaying enhanced MAGL activity and selectivity over FAAH and other serine hydrolases.⁸¹ Other described HIPF carbamates include the piperidine SAR127303⁸², identified by Sanofi R&D, the 3-substituted azetidines **XII** and **XIII**⁸³, recently reported by Pfizer, and the 4-benzylpiperazine derivative ABX-1431⁸⁴, developed by Abide Therapeutics. Currently, the covalent, irreversible MAGL inhibitor ABX-1431 is in clinical phase 1b studies for the treatment of post-traumatic stress disorder as well as for other indications, such as neuromyelitis optica and multiple sclerosis.

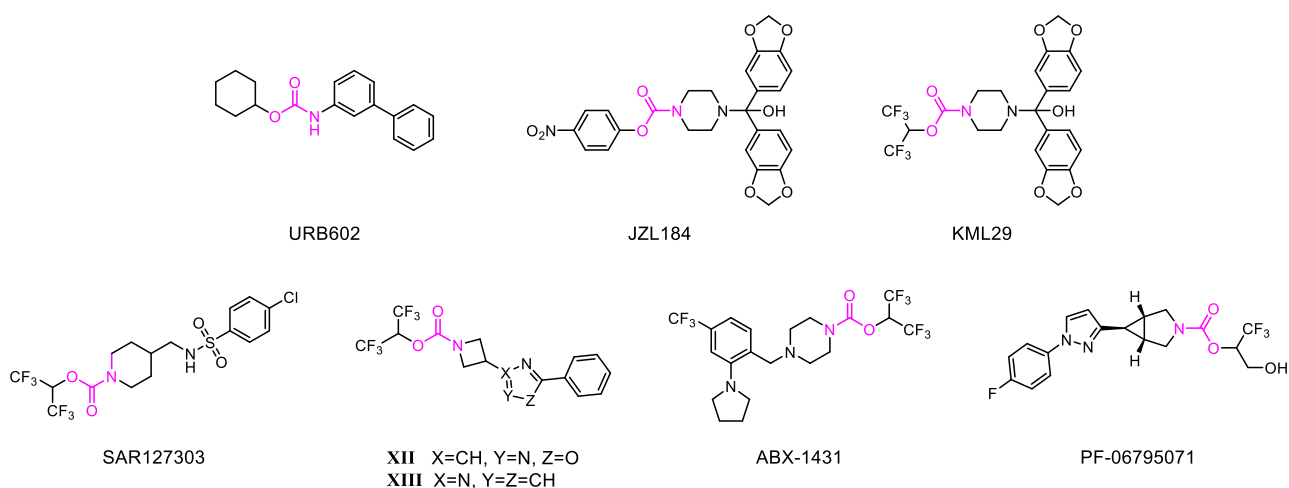


Figure 10 Examples of carbamate-based MAGL inhibitors.

Replacement of the HIPF leaving group by a trifluoromethyl glycol moiety yielded a potent (IC₅₀ = 3 nM), selective, and brain penetrant MAGL inhibitor (PF-06795071) with a suitable PK profile (higher solubility and lower chemical reactivity) to assess its *in vivo* efficacy.⁷³

Another relevant class of covalent MAGL inhibitors is that of azole ureas that owes its inhibitory activity to the presence of a tertiary urea incorporating an azole ring acting as leaving group.⁸⁵ A prototypical example of this class is the piperazine triazole urea SAR629, that reacts with Ser122 forming a stable carbamoylated adduct (**Figure 11**).

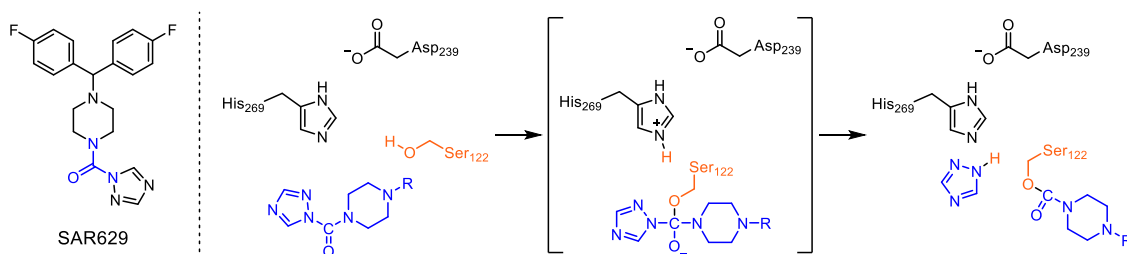


Figure 11 SAR 629 and its catalytic mechanism for MAGL carbamoylation.

Recently, reversible inhibitors (i.e., those compounds that bind temporarily to MAGL, disabling its catalytic activity for a limited period of time) have also been described. Some of the most representative reversible MAGL inhibitors are reported in **Figure 12** and includes the naturally

occurring terpenoids, pristimerin and euphol, and the piperazinyl azetidiny amide ZYH patented by Janssen Pharmaceutica in 2010⁸⁶, the benzo[*d*][1,3]dioxol-5-ylmethyl 6-phenylhexanoate **XIV**⁸⁷, benzoylpiperidine derivatives **XV**⁷⁵, piperazinyl pyrrolidin-2-ones **XVI**⁸⁸, and LEI-515, the most potent reversible and peripherally restricted inhibitor for MAGL up to date (pIC₅₀ = 9.30)⁸⁹.

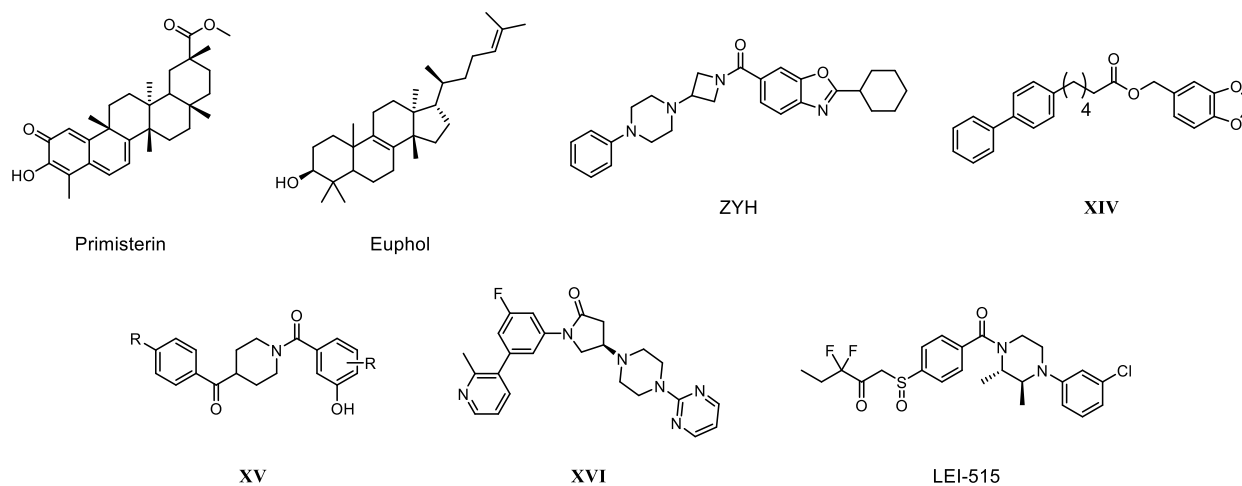


Figure 12 Example of reversible MAGL inhibitors.

1.3 References

- ¹ Boutin JA, Audinot V, Ferry G, Delagrangre P. Molecular tools to study melatonin pathways and actions. *Trends Pharmacol Sci.* **2005**, 26(8), 412-9
- ² Huether G. The contribution of extrapineal sites of melatonin synthesis to circulating melatonin levels in higher vertebrates. *Experientia.* **1993**, 49(8), 665-70
- ³ Klein DC, Weller JL. Indole metabolism in the pineal gland: a circadian rhythm in *N*-acetyltransferase. *Science.* **1970**, 169(3950), 1093-5
- ⁴ Hirata F, Hayaishi O, Tokuyama T, Seno S. *In vitro* and *in vivo* formation of two new metabolites of melatonin. *J Biol Chem.* **1974**, 249(4), 1311-3
- ⁵ Hardeland R, Cardinali DP, Srinivasan V, Spence DW, Brown GM, Pandi-Perumal SR. Melatonin--a pleiotropic, orchestrating regulator molecule. *Prog Neurobiol.* **2011**, 93(3), 350-84
- ⁶ Bedini A, Spadoni G, Gatti G, Lucarini S, Tarzia G, Rivara S, Lorenzi S, Lodola A, Mor M, Lucini V, Pannacci M, Scaglione F. Design and synthesis of *N*-(3,3-diphenylpropenyl)alkanamides as a novel class of high-affinity MT₂-selective melatonin receptor ligands. *J Med Chem.* **2006**, 49(25), 7393-403
- ⁷ Erland LA, Saxena PK. Melatonin Natural Health Products and Supplements: Presence of Serotonin and Significant Variability of Melatonin Content. *J Clin Sleep Med.* **2017**, 13(2), 275-281
- ⁸ Neubauer DN. A review of ramelteon in the treatment of sleep disorders. *Neuropsychiatr Dis Treat.* **2008**, 4(1), 69-79
- ⁹ Traynor K. Tasimelteon approved for circadian disorder in blind adults. *Am J Health Syst Pharm.* **2014**, 71(5), 350
- ¹⁰ de Bodinat C, Guardiola-Lemaitre B, Mocaër E, Renard P, Muñoz C, Millan MJ. Agomelatine, the first melatonergic antidepressant: discovery, characterization and development. *Nat Rev Drug Discov.* **2010**, 9(8), 628-42
- ¹¹ Luo C, Yang Q, Liu Y, Zhou S, Jiang J, Reiter RJ, Bhattacharya P, Cui Y, Yang H, Ma H, Yao J, Lawler SE, Zhang X, Fu J, Rozental R, Aly H, Johnson MD, Chiocca EA, Wang X. The multiple protective roles and molecular mechanisms of melatonin and its precursor N-acetylserotonin in targeting brain injury and liver damage and in maintaining bone health. *Free Radic Biol Med.* **2019**, 130, 215-233
- ¹² Jockers R, Delagrangre P, Dubocovich ML, Markus RP, Renault N, Tosini G, Cecon E, Zlotos DP. Update on melatonin receptors: IUPHAR Review 20. *Br J Pharmacol.* **2016**, 173(18), 2702-25
- ¹³ Cecon E, Boutin JA, Jockers R. Molecular Characterization and Pharmacology of Melatonin Receptors in Animals. *Receptors* **2023**, 2(2), 127–147

-
- ¹⁴ Reppert SM, Weaver DR, Ebisawa T. Cloning and characterization of a mammalian melatonin receptor that mediates reproductive and circadian responses. *Neuron*. **1994**, 13(5), 1177-85; Reppert SM, Godson C, Mahle CD, Weaver DR, Slaugenhaupt SA, Gusella JF. Molecular characterization of a second melatonin receptor expressed in human retina and brain: the Mel1b melatonin receptor. *Proc Natl Acad Sci U S A*. **1995**, 12, 92(19), 8734-8
- ¹⁵ Ebisawa T, Karne S, Lerner MR, Reppert SM. Expression cloning of a high-affinity melatonin receptor from *Xenopus* dermal melanophores. *Proc Natl Acad Sci U S A*. **1994**, 91(13), 6133-7
- ¹⁶ Vanecek J. Cellular mechanisms of melatonin action. *Physiol Rev*. **1998**, 78(3), 687-721
- ¹⁷ Dufourny L, Levasseur A, Migaud M, Callebaut I, Pontarotti P, Malpoux B, Monget P. GPR50 is the mammalian ortholog of Mel1c: evidence of rapid evolution in mammals. *BMC Evol Biol*. **2008**, 8, 105
- ¹⁸ Clement N, Renault N, Guillaume JL, Cecon E, Journé AS, Laurent X, Tadagaki K, Cogé F, Gohier A, Delagrangé P, Chavatte P, Jockers R. Importance of the second extracellular loop for melatonin MT₁ receptor function and absence of melatonin binding in GPR50. *Br J Pharmacol*. **2018**, 175(16), 3281-3297
- ¹⁹ Duncan MJ, Takahashi JS, Dubocovich ML. 2-[¹²⁵I]iodomelatonin binding sites in hamster brain membranes: pharmacological characteristics and regional distribution. *Endocrinology*. **1988**, 122(5), 1825-33
- ²⁰ Nosjean O, Ferro M, Coge F, Beauverger P, Henlin JM, Lefoulon F, Fauchere JL, Delagrangé P, Canet E, Boutin JA. Identification of the melatonin-binding site MT₃ as the quinone reductase 2. *J Biol Chem*. **2000**, 275(40), 31311-7
- ²¹ Stauch B, Johansson LC, McCorvy JD, Patel N, Han GW, Huang XP, Gati C, Batyuk A, Slocum ST, Ishchenko A, Brehm W, White TA, Michaelian N, Madsen C, Zhu L, Grant TD, Grandner JM, Shiriaeva A, Olsen RHJ, Tribo AR, Yous S, Stevens RC, Weierstall U, Katritch V, Roth BL, Liu W, Cherezov V. Structural basis for ligand recognition at the human MT₁ melatonin receptor. *Nature*. **2019**, 569(7755), 284–288
- ²² Johansson LC, Stauch B, McCorvy JD, Han GW, Patel N, Huang XP, Batyuk A, Gati C, Slocum ST, Li C, Grandner JM, Hao S, Olsen RHJ, Tribo AR, Zaare S, Zhu L, Zatspein NA, Weierstall U, Yous S, Stevens RC, Liu W, Roth BL, Katritch V, Cherezov V. XFEL structures of the human MT₂ melatonin receptor reveal basis of subtype selectivity. *Nature*. **2019**, 569(7755), 289–292
- ²³ Okamoto HH, Miyauchi H, Inoue A, Raimondi F, Tsujimoto H, Kusakizako T, Shihoya W, Yamashita K, Suno R, Nomura N, Kobayashi T, Iwata S, Nishizawa T, Nureki O. Cryo-EM structure of the human MT₁-G_i signaling complex. *Nat Struct Mol Biol*. **2021**, 28(8), 694-701
- ²⁴ Zlotos DP, Jockers R, Cecon E, Rivara S, Witt-Enderby PA. MT₁ and MT₂ melatonin receptors: ligands, models, oligomers, and therapeutic potential. *J Med Chem*. **2014**, 57(8), 3161-85
- ²⁵ Karamitri A, Jockers R. Melatonin in type 2 diabetes mellitus and obesity. *Nat Rev Endocrinol*. **2019**, 15(2), 105-125

-
- ²⁶ Liu J, Clough SJ, Hutchinson AJ, Adamah-Biassi EB, Popovska-Gorevski M, Dubocovich ML. MT₁ and MT₂ Melatonin Receptors: A Therapeutic Perspective. *Annu Rev Pharmacol Toxicol.* **2016**, 56, 361-83
- ²⁷ López-Canul M, Comai S, Domínguez-López S, Granados-Soto V, Gobbi G. Antinociceptive properties of selective MT(2) melatonin receptor partial agonists. *Eur J Pharmacol.* **2015**, 764, 424-432
- ²⁸ Dubocovich ML, Markowska M. Functional MT₁ and MT₂ melatonin receptors in mammals. *Endocrine.* **2005**, 27(2), 101-10
- ²⁹ Ochoa-Sanchez R, Comai S, Lacoste B, Bambico FR, Dominguez-Lopez S, Spadoni G, Rivara S, Bedini A, Angeloni D, Fraschini F, Mor M, Tarzia G, Descarries L, Gobbi G. Promotion of non-rapid eye movement sleep and activation of reticular thalamic neurons by a novel MT₂ melatonin receptor ligand. *J Neurosci.* **2011**, 31(50), 18439-52
- ³⁰ Gobbi G, Comai S. Sleep well. Untangling the role of melatonin MT₁ and MT₂ receptors in sleep. *J Pineal Res.* **2019**, 66(3), e12544
- ³¹ Garfinkel D, Laudon M, Nof D, Zisapel N. Improvement of sleep quality in elderly people by controlled-release melatonin. *Lancet.* **1995**, 346(8974), 541-4
- ³² Cortesi F, Giannotti F, Sebastiani T, Panunzi S, Valente D. Controlled-release melatonin, singly and combined with cognitive behavioural therapy, for persistent insomnia in children with autism spectrum disorders: a randomized placebo-controlled trial. *J Sleep Res.* **2012**, 21(6), 700-9
- ³³ Garratt PJ, Travard S, Vonhoff S, Tsotinis A, Sugden D. Mapping the melatonin receptor. 4. Comparison of the binding affinities of a series of substituted phenylalkyl amides. *J Med Chem.* **1996**, 39(9), 1797-805
- ³⁴ Rivara S, Lodola A, Mor M, Bedini A, Spadoni G, Lucini V, Pannacci M, Fraschini F, Scaglione F, Sanchez RO, Gobbi G, Tarzia G. *N*-(substituted-anilinoethyl)amides: design, synthesis, and pharmacological characterization of a new class of melatonin receptor ligands. *J Med Chem.* **2007**, 50(26), 6618-26
- ³⁵ Carocci A, Catalano A, Lovece A, Lentini G, Duranti A, Lucini V, Pannacci M, Scaglione F, Franchini C. Design, synthesis, and pharmacological effects of structurally simple ligands for MT(1) and MT(2) melatonin receptors. *Bioorg Med Chem.* **2010**, 18(17), 6496-511
- ³⁶ Koike T, Takai T, Hoashi Y, Nakayama M, Kosugi Y, Nakashima M, Yoshikubo S, Hirai K, Uchikawa O. Synthesis of a novel series of tricyclic dihydrofuran derivatives: discovery of 8,9-dihydrofuro[3,2-c]pyrazolo[1,5-a]pyridines as melatonin receptor (MT₁/MT₂) ligands. *J Med Chem.* **2011**, 54(12), 4207-4218
- ³⁷ Davies DJ, Garratt PJ, Tocher DA, Vonhoff S, Davies J, Teh MT, Sugden D. Mapping the melatonin receptor. 5. Melatonin agonists and antagonists derived from tetrahydrocyclopent[b]indoles, tetrahydrocarbazoles and hexahydrocyclohept[b]indoles. *J Med Chem.* **1998**, 41(4), 451-67
- ³⁸ Spadoni G, Balsamini C, Diamantini G, Di Giacomo B, Tarzia G, Mor M, Plazzi PV, Rivara S, Lucini V, Nonno R, Pannacci M, Fraschini F, Stankov BM. Conformationally restrained melatonin analogues: synthesis,

binding affinity for the melatonin receptor, evaluation of the biological activity, and molecular modeling study. *J Med Chem.* **1997**, 40(13), 1990-2002

³⁹ Jellimann C, Mathé-Allainmat M, Andrieux J, Kloubert S, Boutin JA, Nicolas JP, Bennejean C, Delagrangé P, Langlois M. Synthesis of phenalene and acenaphthene derivatives as new conformationally restricted ligands for melatonin receptors. *J Med Chem.* **2000**, 43(22), 4051-62

⁴⁰ Dubocovich ML, Masana MI, Jacob S, Sauri DM. Melatonin receptor antagonists that differentiate between the human Mel1a and Mel1b recombinant subtypes are used to assess the pharmacological profile of the rabbit retina ML1 presynaptic heteroreceptor. *Naunyn Schmiedebergs Arch Pharmacol.* **1997**, 355(3), 365-75

⁴¹ Dubocovich ML. Luzindole (N-0774): a novel melatonin receptor antagonist. *J Pharmacol Exp Ther.* **1988**, 246(3), 902-10

⁴² Mor M, Spadoni G, Di Giacomo B, Diamantini G, Bedini A, Tarzia G, Plazzi PV, Rivara S, Nonno R, Lucini V, Pannacci M, Fraschini F, Stankov BM. Synthesis, pharmacological characterization and QSAR studies on 2-substituted indole melatonin receptor ligands. *Bioorg Med Chem.* **2001**, 9(4), 1045-57

⁴³ Spadoni G, Balsamini C, Diamantini G, Tontini A, Tarzia G, Mor M, Rivara S, Plazzi PV, Nonno R, Lucini V, Pannacci M, Fraschini F, Stankov BM. 2-*N*-acylaminoalkylindoles: design and quantitative structure-activity relationship studies leading to MT₂-selective melatonin antagonists. *J Med Chem.* **2001**, 30, 44(18), 2900-12

⁴⁴ Rivara S, Mor M, Silva C, Zuliani V, Vacondio F, Spadoni G, Bedini A, Tarzia G, Lucini V, Pannacci M, Fraschini F, Plazzi PV. Three-dimensional quantitative structure-activity relationship studies on selected MT₁ and MT₂ melatonin receptor ligands: requirements for subtype selectivity and intrinsic activity modulation. *J Med Chem.* **2003**, 46(8), 1429-39

⁴⁵ Lucini V, Pannacci M, Scaglione F, Fraschini F, Rivara S, Mor M, Bordi F, Plazzi PV, Spadoni G, Bedini A, Piersanti G, Diamantini G, Tarzia G. Tricyclic alkylamides as melatonin receptor ligands with antagonist or inverse agonist activity. *J Med Chem.* **2004**, 47(17), 4202-12

⁴⁶ Spadoni G, Bedini A, Lucarini S, Mari M, Caignard DH, Boutin JA, Delagrangé P, Lucini V, Scaglione F, Lodola A, Zanardi F, Pala D, Mor M, Rivara S. Highly Potent and Selective MT₂ Melatonin Receptor Full Agonists from Conformational Analysis of 1-Benzyl-2-acylaminoethyl-tetrahydroquinolines. *J Med Chem.* **2015**, 58(18), 7512-25

⁴⁷ Descamps-François C, Yous S, Chavatte P, Audinot V, Bonnaud A, Boutin JA, Delagrangé P, Bennejean C, Renard P, Lesieur D. Design and synthesis of naphthalenic dimers as selective MT₁ melatonergic ligands. *J Med Chem.* **2003**, 46(7), 1127-9

⁴⁸ Spadoni G, Bedini A, Orlando P, Lucarini S, Tarzia G, Mor M, Rivara S, Lucini V, Pannacci M, Scaglione F. Bivalent ligand approach on *N*-{2-[(3-methoxyphenyl)methylamino]ethyl}acetamide: synthesis, binding

affinity and intrinsic activity for MT(1) and MT(2) melatonin receptors. *Bioorg Med Chem.* **2011**, 19(16), 4910-6

⁴⁹ Sun LQ, Chen J, Takaki K, Johnson G, Iben L, Mahle CD, Ryan E, Xu C. Design and synthesis of benzoxazole derivatives as novel melatonergic ligands. *Bioorg Med Chem Lett.* **2004**, 14(5), 1197-200

⁵⁰ Mésangeau C, Pérès B, Descamps-François C, Chavatte P, Audinot V, Coumaillieu S, Boutin JA, Delagrangue P, Bennejean C, Renard P, Caignard DH, Berthelot P, Yous S. Design, synthesis and pharmacological evaluation of novel naphthalenic derivatives as selective MT₁ melatonergic ligands. *Bioorg Med Chem.* **2010**, 18(10), 3426-3436

⁵¹ Di Giacomo B, Bedini A, Spadoni G, Tarzia G, Fraschini F, Pannacci M, Lucini V. Synthesis and biological activity of new melatonin dimeric derivatives. *Bioorg Med Chem.* **2007**, 15(13), 4643-50

⁵² Rivara S, Pala D, Lodola A, Mor M, Lucini V, Dugnani S, Scaglione F, Bedini A, Lucarini S, Tarzia G, Spadoni G. MT₁-selective melatonin receptor ligands: synthesis, pharmacological evaluation, and molecular dynamics investigation of *N*-{[(3-*O*-substituted)anilino]alkyl}amides. *ChemMedChem.* **2012**, 7(11), 1954-64

⁵³ Stein RM, Kang HJ, McCorvy JD, Glatfelter GC, Jones AJ, Che T, Slocum S, Huang XP, Savych O, Moroz YS, Stauch B, Johansson LC, Cherezov V, Kenakin T, Irwin JJ, Shoichet BK, Roth BL, Dubocovich ML. Virtual discovery of melatonin receptor ligands to modulate circadian rhythms. *Nature.* **2020**, 579(7800), 609-614

⁵⁴ Di Marzo V, Stella N, Zimmer A. Endocannabinoid signalling and the deteriorating brain. *Nat Rev Neurosci.* **2015**, 16(1), 30-42

⁵⁵ Stella N. Cannabinoid and cannabinoid-like receptors in microglia, astrocytes, and astrocytomas. *Glia.* **2010**, 58(9), 1017-30

⁵⁶ Scotter EL, Abood ME, Glass M. The endocannabinoid system as a target for the treatment of neurodegenerative disease. *Br J Pharmacol.* **2010**, 160(3), 480-98

⁵⁷ Murataeva N, Straiker A, Mackie K. Parsing the players: 2-arachidonoylglycerol synthesis and degradation in the CNS. *Br J Pharmacol.* **2014**, 171(6), 1379-91

⁵⁸ Dinh TP, Carpenter D, Leslie FM, Freund TF, Katona I, Sensi SL, Kathuria S, Piomelli D. Brain monoglyceride lipase participating in endocannabinoid inactivation. *Proc Natl Acad Sci U S A.* **2002**, 99(16), 10819-24

⁵⁹ Micale V, Di Marzo V, Sulcova A, Wotjak CT, Drago F. Endocannabinoid system and mood disorders: priming a target for new therapies. *Pharmacol Ther.* **2013**, 138(1), 18-37

⁶⁰ Hillard CJ. Role of cannabinoids and endocannabinoids in cerebral ischemia. *Curr Pharm Des.* **2008**, 14(23), 2347-61

-
- ⁶¹ Matthews AT, Lee JH, Borazjani A, Mangum LC, Hou X, Ross MK. Oxyradical stress increases the biosynthesis of 2-arachidonoylglycerol: involvement of NADPH oxidase. *Am J Physiol Cell Physiol.* **2016**, 311(6), C960-C974
- ⁶² Baggelaar MP, Maccarrone M, van der Stelt M. 2-Arachidonoylglycerol: A signaling lipid with manifold actions in the brain. *Prog Lipid Res.* **2018**, 71, 1-17
- ⁶³ Nomura DK, Morrison BE, Blankman JL, Long JZ, Kinsey SG, Marcondes MC, Ward AM, Hahn YK, Lichtman AH, Conti B, Cravatt BF. Endocannabinoid hydrolysis generates brain prostaglandins that promote neuroinflammation. *Science.* **2011**, 334(6057), 809-13
- ⁶⁴ a) Gokoh M, Kishimoto S, Oka S, Mori M, Waku K, Ishima Y, Sugiura T. 2-arachidonoylglycerol, an endogenous cannabinoid receptor ligand, induces rapid actin polymerization in HL-60 cells differentiated into macrophage-like cells. *Biochem J.* **2005**, 386(Pt 3), 583-9; b) Oka S, Ikeda S, Kishimoto S, Gokoh M, Yanagimoto S, Waku K, Sugiura T. 2-arachidonoylglycerol, an endogenous cannabinoid receptor ligand, induces the migration of EoL-1 human eosinophilic leukemia cells and human peripheral blood eosinophils. *J Leukoc Biol.* **2004**, 76(5), 1002-9
- ⁶⁵ a) Nithipatikom K, Endsley MP, Isbell MA, Wheelock CE, Hammock BD, Campbell WB. A new class of inhibitors of 2-arachidonoylglycerol hydrolysis and invasion of prostate cancer cells. *Biochem Biophys Res Commun.* **2005**, 332(4), 1028-33; b) Bifulco M, Laezza C, Pisanti S, Gazerro P. Cannabinoids and cancer: pros and cons of an antitumour strategy. *Br J Pharmacol.* **2006**, 148(2), 123-35
- ⁶⁶ Scalvini L, Piomelli D, Mor M. Monoglyceride lipase: Structure and inhibitors. *Chem Phys Lipids.* **2016**, 197, 13-24
- ⁶⁷ Tyukhtenko S, Ma X, Rajarshi G, Karageorgos I, Anderson KW, Hudgens JW, Guo JJ, Nasr ML, Zvonok N, Vemuri K, Wagner G, Makriyannis A. Conformational gating, dynamics and allostery in human monoacylglycerol lipase. *Sci Rep.* **2020**, 10(1), 18531
- ⁶⁸ King AR, Dotsey EY, Lodola A, Jung KM, Ghomian A, Qiu Y, Fu J, Mor M, Piomelli D. Discovery of potent and reversible monoacylglycerol lipase inhibitors. *Chem Biol.* **2009**, 16(10), 1045-52
- ⁶⁹ Van der Stelt M, Mazzola C, Esposito G, Matias I, Petrosino S, De Filippis D, Micale V, Steardo L, Drago F, Iuvone T, Di Marzo V. Endocannabinoids and beta-amyloid-induced neurotoxicity *in vivo*: effect of pharmacological elevation of endocannabinoid levels. *Cell Mol Life Sci.* **2006**, 63(12), 1410-24
- ⁷⁰ Scalvini L, Vacondio F, Bassi M, Pala D, Lodola A, Rivara S, Jung KM, Piomelli D, Mor M. Free-energy studies reveal a possible mechanism for oxidation-dependent inhibition of MGL. *Sci Rep.* **2016**, 6, 31046
- ⁷¹ Castelli R, Scalvini L, Vacondio F, Lodola A, Anselmi M, Vezzosi S, Carmi C, Bassi M, Ferlenghi F, Rivara S, Møller IR, Rand KD, Daglian J, Wei D, Dotsey EY, Ahmed F, Jung KM, Stella N, Singh S, Mor M, Piomelli D. Benzisothiazolinone Derivatives as Potent Allosteric Monoacylglycerol Lipase Inhibitors That Functionally Mimic Sulfenylation of Regulatory Cysteines. *Journal of Medicinal Chemistry* **2020**, 63(3), 1261-1280

-
- ⁷² Smith AJ, Müller R, Toscano MD, Kast P, Hellinga HW, Hilvert D, Houk KN. Structural reorganization and preorganization in enzyme active sites: comparisons of experimental and theoretically ideal active site geometries in the multistep serine esterase reaction cycle. *J Am Chem Soc.* **2008**,130(46), 15361-73
- ⁷³ McAllister LA, Butler CR, Mente S, O'Neil SV, Fonseca KR, Piro JR, Cianfrogna JA, Foley TL, Gilbert AM, Harris AR, Helal CJ, Johnson DS, Montgomery JI, Nason DM, Noell S, Pandit J, Rogers BN, Samad TA, Shaffer CL, da Silva RG, Uccello DP, Webb D, Brodney MA. Discovery of Trifluoromethyl Glycol Carbamates as Potent and Selective Covalent Monoacylglycerol Lipase (MAGL) Inhibitors for Treatment of Neuroinflammation. *J Med Chem.* **2018**, 61(7), 3008-3026
- ⁷⁴ Bertrand T, Augé F, Houtmann J, Rak A, Vallée F, Mikol V, Berne PF, Michot N, Cheuret D, Hoornaert C, Mathieu M. Structural basis for human monoglyceride lipase inhibition. *J Mol Biol.* **2010**, 396(3), 663-73
- ⁷⁵ Granchi C, Lapillo M, Glasmacher S, Bononi G, Licari C, Poli G, El Boustani M, Caligiuri I, Rizzolio F, Gertsch J, Macchia M, Minutolo F, Tuccinardi T, Chicca A. Optimization of a Benzoylpiperidine Class Identifies a Highly Potent and Selective Reversible Monoacylglycerol Lipase (MAGL) Inhibitor. *J Med Chem.* **2019**, 62(4), 1932-1958
- ⁷⁶ Zvonok N, Pandarinathan L, Williams J, Johnston M, Karageorgos I, Janero DR, Krishnan SC, Makriyannis A. Covalent inhibitors of human monoacylglycerol lipase: ligand-assisted characterization of the catalytic site by mass spectrometry and mutational analysis. *Chem Biol.* **2008**, 15(8), 854-62
- ⁷⁷ Matuszak N, Muccioli GG, Labar G, Lambert DM. Synthesis and in vitro evaluation of N-substituted maleimide derivatives as selective monoglyceride lipase inhibitors. *J Med Chem.* **2009**, 52(23), 7410-20
- ⁷⁸ King AR, Lodola A, Carmi C, Fu J, Mor M, Piomelli D. A critical cysteine residue in monoacylglycerol lipase is targeted by a new class of isothiazolinone-based enzyme inhibitors. *Br J Pharmacol.* **2009**, 157(6), 974-83
- ⁷⁹ Hohmann AG, Suplita RL, Bolton NM, Neely MH, Fegley D, Mangieri R, Krey JF, Walker JM, Holmes PV, Crystal JD, Duranti A, Tontini A, Mor M, Tarzia G, Piomelli D. An endocannabinoid mechanism for stress-induced analgesia. *Nature.* **2005**, 435(7045), 1108-12
- ⁸⁰ Long JZ, Li W, Booker L, Burston JJ, Kinsey SG, Schlosburg JE, Pavón FJ, Serrano AM, Selley DE, Parsons LH, Lichtman AH, Cravatt BF. Selective blockade of 2-arachidonoylglycerol hydrolysis produces cannabinoid behavioral effects. *Nat Chem Biol.* **2009**, 5(1), 37-44
- ⁸¹ Chang JW, Niphakis MJ, Lum KM, Cognetta AB 3rd, Wang C, Matthews ML, Niessen S, Buczynski MW, Parsons LH, Cravatt BF. Highly selective inhibitors of monoacylglycerol lipase bearing a reactive group that is bioisosteric with endocannabinoid substrates. *Chem Biol.* **2012**, 19(5), 579-88
- ⁸² Griebel G, Pichat P, Beeské S, Leroy T, Redon N, Jacquet A, Françon D, Bert L, Even L, Lopez-Grancha M, Tolstykh T, Sun F, Yu Q, Brittain S, Arlt H, He T, Zhang B, Wiederschain D, Bertrand T, Houtmann J, Rak A, Vallée F, Michot N, Augé F, Menet V, Bergis OE, George P, Avenet P, Mikol V, Didier M, Escoubet J. Selective

blockade of the hydrolysis of the endocannabinoid 2-arachidonoylglycerol impairs learning and memory performance while producing antinociceptive activity in rodents. *Sci Rep.* **2015**, 5, 7642

⁸³ Butler CR, Beck EM, Harris A, Huang Z, McAllister LA, Am Ende CW, Fennell K, Foley TL, Fonseca K, Hawrylik SJ, Johnson DS, Knafels JD, Mente S, Noell GS, Pandit J, Phillips TB, Piro JR, Rogers BN, Samad TA, Wang J, Wan S, Brodney MA. Azetidine and Piperidine Carbamates as Efficient, Covalent Inhibitors of Monoacylglycerol Lipase. *J Med Chem.* **2017**, 60(23), 9860-9873

⁸⁴ Cisar JS, Weber OD, Clapper JR, Blankman JL, Henry CL, Simon GM, Alexander JP, Jones TK, Ezekowitz RAB, O'Neill GP, Grice CA. Identification of ABX-1431, a Selective Inhibitor of Monoacylglycerol Lipase and Clinical Candidate for Treatment of Neurological Disorders. *J Med Chem.* **2018**, 61(20), 9062-9084

⁸⁵ Aaltonen N, Savinainen JR, Ribas CR, Rönkkö J, Kuusisto A, Korhonen J, Navia-Paldanius D, Häyrynen J, Takabe P, Käsnänen H, Pantsar T, Laitinen T, Lehtonen M, Pasonen-Seppänen S, Poso A, Nevalainen T, Laitinen JT. Piperazine and piperidine triazole ureas as ultrapotent and highly selective inhibitors of monoacylglycerol lipase. *Chem Biol.* **2013**, 20(3), 379-90

⁸⁶ Chevalier KM, Dax SL, Flores CM, Liu L, Macielag MJ, McDonnell ME, Nelen MI, Prouty S, Todd M, Zhang S-P, Zhu B, Nulton EL, Clemente J. Preparation of (Hetero)aromatic Piperazinyl Azetidiny Amides as Monoacylglycerol Lipase (MGL) Inhibitors. *WO2010124121*, **2010**

⁸⁷ Hernández-Torres G, Cipriano M, Hedén E, Björklund E, Canales Á, Zian D, Feliú A, Mecha M, Guaza C, Fowler CJ, Ortega-Gutiérrez S, López-Rodríguez ML. A reversible and selective inhibitor of monoacylglycerol lipase ameliorates multiple sclerosis. *Angew Chem Int Ed.* **2014**, 53(50), 13765-70

⁸⁸ Aida J, Fushimi M, Kusumoto T, Sugiyama H, Arimura N, Ikeda S, Sasaki M, Sogabe S, Aoyama K, Koike T. Design, Synthesis, and Evaluation of Piperazinyl Pyrrolidin-2-ones as a Novel Series of Reversible Monoacylglycerol Lipase Inhibitors. *J Med Chem.* **2018**, 61(20), 9205-9217

⁸⁹ Jiang M, Huizenga MCW, Wirt JL, Paloczi J, Amedi A, van den Berg RJBHN, Benz J, Collin L, Deng H, Di X, Driever WF, Florea BI, Grether U, Janssen APA, Hankemeier T, Heitman LH, Lam TW, Mohr F, Pavlovic A, Ruf I, van den Hurk H, Stevens AF, van der Vliet D, van der Wel T, Wittwer MB, van Boeckel CAA, Pacher P, Hohmann AG, van der Stelt M. A monoacylglycerol lipase inhibitor showing therapeutic efficacy in mice without central side effects or dependence. *Nat Commun.* **2023**, 14(1), 8039

Chapter 2. Synthesis and characterization of potent MT₂ selective agonists

This chapter is based on: Bedini A, Elisi GM, **Fanini F**, Retini M, Scalvini L, Pasquini S, Contri C, Varani K, Spadoni G, Mor M, Vincenzi F, Rivara S. Binding and unbinding of potent melatonin receptor ligands: mechanistic simulations and experimental evidence. *Journal of Pineal Research*, **2024**, 76(2), e12941.

2.1 Introduction

Structural modification of features of the melatonin structure (the methoxy group, the alkylamide chain, and the aromatic ring) leads to ligands with different binding affinity, receptor subtype selectivity, and intrinsic activity.¹ Several studies evidenced that the introduction of substituents at the β position of the acylaminoethyl chain could have a positive effect on the binding affinity (**Figure 13**).

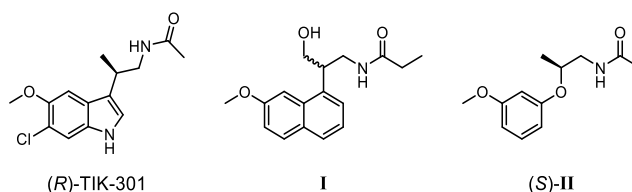


Figure 13 Melatonin analogs with substituents at the β position of the acylaminoethyl chain.

For example, β -methyl-6-chloro-melatonin TIK-301, developed by Eli Lilly, is characterized by a higher binding affinity and metabolic stability than MLT (**Figure 13**).² The introduction of substituents at the β position of the acylaminoethyl chain was also evaluated by Servier industries on agomelatine derivatives. The methyl and the fluoromethyl groups led to an increase in the binding affinity, and introduction of the β -hydroxymethyl substituent gave compound **I**, for which the (*R*)-stereoisomer proved to be the eutomer (**Figure 13**).³ Stereoselective behavior of receptor recognition can also be observed for *N*-[2-(3-methoxyphenoxy)ethyl]acetamide derivatives, with compound (*S*)-**II** to be the eutomer (**Figure 13**).⁴

Docking and molecular dynamic (MD) simulations within the receptor (studying the interplay of the conformational equilibria of the ligand in the solvent and bound to receptor) were used to understand enantioselectivity of β -methyl substituted compounds. The evidence collected suggested that the slight gain of affinity could not be related to a better accommodation within the binding site. On the contrary, the insertion of the β -methyl group could alter the conformational equilibria of the unsubstituted precursor and induce a conformational selection, which could favor the final conformation adopted by the ligands in the binding site.

Previous ligand-based studies as well as the availability of conformationally constrained compounds and stereoselective ligands, provided information regarding the bioactive conformation of MLT. Two pharmacophore models^{5,6} suggested a MLT bioactive conformation in which the ethylamido side chain was not coplanar with the indole ring, and oriented perpendicular to it, with the ethylene C-C bond having an *anti* arrangement. However, the spatial arrangement of MLT side chain could be satisfied by two opposite orientations: above or below the plane defined by the indole ring. The synthesis of the conformationally-constrained stereoselective agonist UCM426, characterized by a tetrahydrobenzo-indole scaffold with the alkylamido chain in axial arrangement confirmed by X-ray diffraction studies, and the high binding affinity displayed by the (*S*)-enantiomer allowed to define the orientation of the MLT ethylamide chain in the bioactive conformation with respect to the indole ring (**Figure 14**).⁷

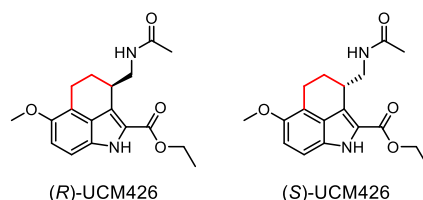


Figure 14 Conformational constrained agonists (*R*)-UCM426 and (*S*)-UCM426.

Indeed, in the bioactive conformation of MLT, the side chain is located below the plane of the indole ring drawing the methoxy group on the left side (**Figure 15**). This arrangement of the pharmacophore elements was also properly reproduced by the *S*-enantiomer (eutomer) of ramelteon.

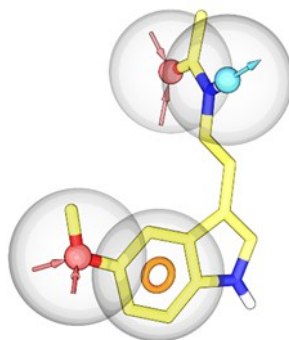


Figure 15 Bioactive conformation of MLT, confirmed by crystal structures of receptor-ligand complexes.

The information has then be used to design and develop the interesting series of 2-acylaminomethyl-tetrahydroquinolines, through the rigidification of the *N*-anilinoethylamide scaffold (inclusion of the carbon atom bound to the aniline nitrogen into a six membered ring). One of the most potent (picomolar affinity) and MT₂-selective compound, **UCM1014**, belongs to this class; it is characterized by the presence of the methoxy group in position 5 (topologically corresponding to 5-position of the MLT indole ring) and of a benzyl substituent on the tetrahydroquinoline nitrogen atom that shifts the axial/equatorial conformational equilibrium of the side chain to the axial arrangement,

fulfilling the requirements of the agonist pharmacophore.⁸ While **UCM1014** was tested as a racemic mixture, both enantiomers (with unassigned absolute configuration) of its de-methoxy analog (*R*)-**III** and (*S*)-**III** were also tested, evidencing a stereoselective behavior. Therefore, high stereoselectivity is also expected for **UCM1014** (*Figure 16*).

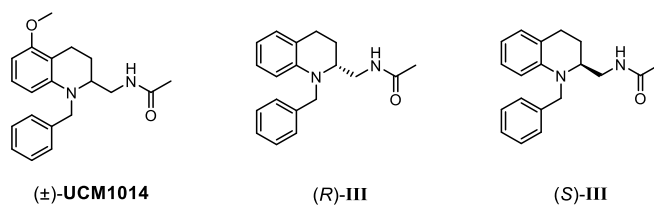


Figure 16 (±)-**UCM1014** and its de-methoxy analogs.

Molecular modelling simulations reproducing binding complexes, in collaboration with the University of Parma, and experimental NMR studies were performed to predict/rationalize the putative enantioselectivity of the two enantiomers. Docking results evaluated with GScore scoring function did not substantially discriminate the two enantiomers ($-10.7 \text{ kcal}\cdot\text{mol}^{-1}$ for (*R*)-**UCM1014** vs $-10.8 \text{ kcal}\cdot\text{mol}^{-1}$ for (*S*)-**UCM1014**). The docked pose of both enantiomers in the MT₂ receptor could establish a hydrogen bond between the alkylamide side chain and Gln194, but assuming different conformations of the tetrahydroquinoline nucleus and of the acylaminoethyl side chain. After energy minimization of the docking complexes, (*R*)-**UCM1014** methylamide chain was placed with an axial arrangement, while (*S*)-**UCM1014** methylamide had an equatorial one. Furthermore, experimentally NMR data of **UCM1014** in solution showed that the conformations with the tetrahydroquinoline ring having axial side chain are strongly favored. Since only the energetically favored axial arrangement of the propionylaminomethyl side chain can be superposed to that of the bioactive conformation of **UCM426** (*Figure 17*), (*R*)-**UCM1014** was predicted as the eutomer.

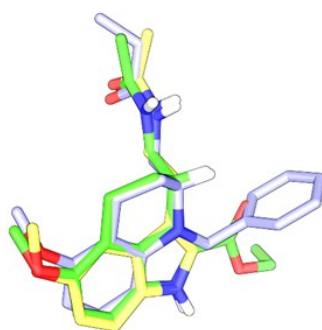


Figure 17 Superimposition of melatonin (yellow carbons) on the stereoselective (*S*)-**UCM426** (green carbons) and (*R*)-**UCM1014** (grey carbons) according to the pharmacophore model devised for agonist compounds.

To confirm the different activity of the two enantiomers, separation of the enantiomers or stereoselective synthesis is needed, as well as the assignment of their absolute configuration. To obtain the two separate **UCM1014** enantiomers we planned different strategies. Unfortunately, attempts of direct enantioselective synthesis, like organocatalytic enantioselective dearomatization of

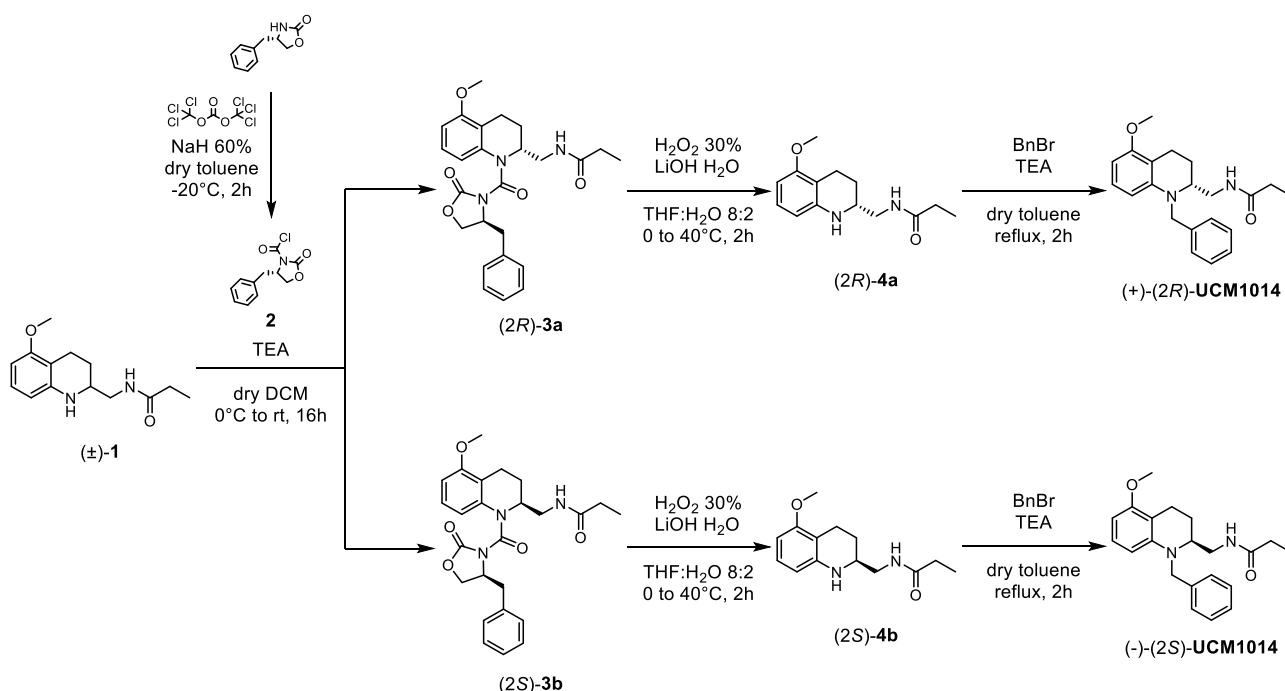
N-acyl-5-methoxyquinolinium salts with nucleophiles or asymmetric hydrogenation of *N*-[(5-methoxyquinolin-2-yl)methyl]propionamide, failed or not gave considerable results. Therefore, we considered optical resolution strategies of the racemate. The absence of an easily derivatizable functional group in the **UCM1014** molecule, prompted us to explore the chiral resolution of a synthetic precursor of (±)-**UCM1014**, such as the 2-propionamidomethyl tetrahydroquinoline (±)-**1** (**Scheme 2**).

After several attempts we were able to resolve the above racemate by using (4*S*)-4-benzyl-2-oxo-oxazolidine-3-carbonyl chloride **2** as resolving reagent, and chromatographic separation of the resulting diastereomers. After removal of the chiral auxiliary, each stereoisomer was converted into the final **UCM1014** enantiomer through synthetic steps that do not involve the stereocenter.

2.2 Results and discussion

2.2.1 Chemistry

The synthetic route adopted for synthesizing the two enantiomers of **UCM1014**, displayed in **Scheme 2**, involves a separation of the two diastereomers **3a** and **3b** by flash chromatography.

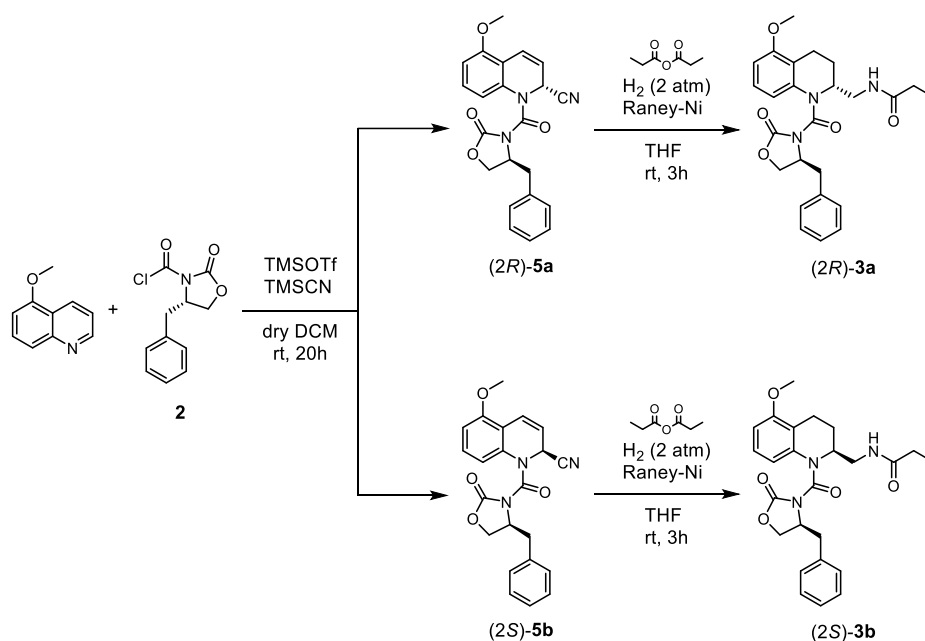


Scheme 2 Synthesis of (+)-(2*R*)-**UCM1014** and (-)-(2*S*)-**UCM1014**.

The two diastereomers were obtained by acylation of the crucial precursor of **UCM1014**, (±)-*N*-[(5-methoxy-1,2,3,4-tetrahydroquinolin-2-yl)methyl]propionamide, (±)-**1** (synthesized following a reported procedure⁸), with the (4*S*)-4-benzyl-2-oxooxazolidine-3-carbonyl chloride **2** as resolving reagent. The latter was previously prepared by reacting the Evans chiral auxiliary [(4*S*)-4-benzyl-2-oxazolidinone] with triphosgene in the presence of NaH. The subsequent chromatography

purification afforded the two diastereomers **3a** and **3b**. Removal of the chiral auxiliary from each single diastereomer by treatment with lithium hydroxide/hydrogen peroxide⁹ and subsequent *N*¹-benzylation provided the enantiopure (+)-UCM1014 (ee \geq 99%) and (-)-UCM1014 (ee \geq 97 %).

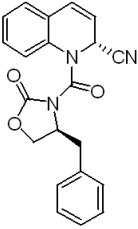
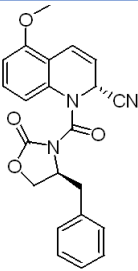
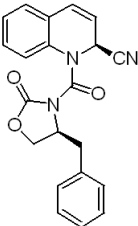
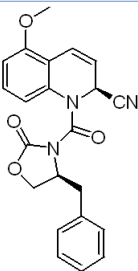
To assign the absolute configuration of the two enantiomers, we first determined the absolute configurations of their precursors **5a** and **5b**. According to the previously reported diastereoselective Reissert reaction onto quinoline¹⁰, 5-methoxyquinoline was treated with the Evans chiral auxiliary **2** in the presence of trifluoromethanesulfonate (TMSOTf) (promoting the crucial exchange of Cl⁻ for TfO⁻, to improve the diastereoselectivity of the reaction); the subsequent addition of trimethylsilyl cyanide (TMSCN) afforded the two diastereomeric Reissert compounds (2*R*)-**5a** and (2*S*)-**5b**, with a diastereomeric ratio 1:2, that were separated by flash chromatography (*Scheme 3*).



Scheme 3 Synthesis of the precursors (2*R*)-**5a** and (2*S*)-**5b**, crucial for assigning the configurations of both UCM1014 enantiomers.

The absolute configuration of the two diastereomers (2*R*)-**5a** and (2*S*)-**5b** can be deduced by the partially observed diastereoselectivity of the Reissert reaction (with the 2*S*-compound more abundant than the 2*R*-compound) and by comparison of their ¹H NMR spectra with those of the corresponding des-methoxy analogs (2*R*)-**6a** and (2*S*)-**6b**, whose absolute configuration was previously unambiguously assigned through X-ray crystallography¹⁰ (*Table 1*). As highlighted in *Table 1*, the diagnostic chemical shifts of (2*R*)-**5a** are in congruence with those of the des-methoxy analog (2*R*)-**6a** as well as the ones of (2*S*)-**5b** are completely in accordance with those of the des-methoxy analog (2*S*)-**6b**.

Table 1 Comparison of ^1H NMR chemical shifts of the previously described des-methoxy compounds (2*R*)-**6a**, (2*S*)-**6b**, with the synthesized 5-methoxy compounds (2*R*)-**5a**, (2*S*)-**5b**. The diagnostic peaks are in bold and blue.

Diastereomers	^1H NMR
des-methoxy analog (2<i>R</i>)-6a	
(<i>R</i>)-1-((<i>S</i>)-4-benzyl-2-oxooxazolidine-3-carbonyl)-1,2-dihydroquinoline-2-carbonitrile	
 <p>(2<i>R</i>)-6a</p>	^1H NMR (200 MHz, CDCl_3) δ 7.40-7.05 (m, 9H, H-Ar), 6.83 (d, $J = 9.2$ Hz, 1H, $\text{CH}=\text{CH}$), 6.09 (dd, $J = 9.2$ Hz, $J = 6.2$ Hz, 1H, $=\text{CH}-\text{CHN}$), 5.74 (d, $J = 6.2$ Hz, 1H, CHN), 4.65-4.50 (m, X part of ABX system, 1H, CHBn), 4.25-4.10 (m, 2H, CH_2O), 3.70 and 2.89 (AB part of ABX system, $J_{AB} = 13.2$ Hz, $J_{AX} = 9.8$ Hz, $J_{BX} = 3.8$ Hz, 2H, CH_2Ph) ¹⁰
5-methoxy analog (2<i>R</i>)-5a	
(<i>R</i>)-1-((<i>S</i>)-4-benzyl-2-oxooxazolidine-3-carbonyl)-5-methoxy-1,2-dihydroquinoline-2-carbonitrile	
 <p>(2<i>R</i>)-5a</p>	^1H NMR (400 MHz, CDCl_3) δ 7.40 – 7.18 (m, 7H), 6.78 (d, 1H, $J = 8.5$ Hz), 6.72 (d, 1H, $J = 8.5$ Hz), 6.04 (dd, 1H, $J = 9.5$ and 6.5 Hz), 5.71 (d, 1H, $J = 6.5$ Hz), 4.57-4.52 (m, 1H), 4.25-4.16 (m, 2H), 3.88 (s, 3H), 3.74 (dd, , 1H, $J = 13.5$ and 3.5 Hz), 2.89 (dd, 1H, $J = 13.5$ and 10.0 Hz)
des-methoxy analog (2<i>S</i>)-6b	
(<i>S</i>)-1-((<i>S</i>)-4-benzyl-2-oxooxazolidine-3-carbonyl)-1,2-dihydroquinoline-2-carbonitrile	
 <p>(2<i>S</i>)-6b</p>	^1H NMR (200 MHz, CDCl_3) δ 7.35-7.15 (m, 8H, H-Ar), 7.05-6.95 (m, 1H, H-Ar), 6.83 (d, $J = 9.2$ Hz, 1H, $\text{CH}=\text{CH}$), 6.04 (dd, $J = 9.2$ Hz, $J = 6.4$ Hz, 1H, $=\text{CH}-\text{CHN}$), 5.76 (dd, $J = 6.4$ Hz, $J = 0.8$ Hz, 1H, CHN), 4.85-4.75 (m, X part of ABX system, 1H, CHBn), 4.35-4.15 (m, 2H, CH_2O), 3.41 and 2.97 (AB part of ABX system, $J_{AB} = 13.2$ Hz, $J_{AX} = 9.4$ Hz, $J_{BX} = 3.4$ Hz, 2H, CH_2Ph) ¹⁰
5-methoxy analog (2<i>S</i>)-5b	
(<i>S</i>)-1-((<i>S</i>)-4-benzyl-2-oxooxazolidine-3-carbonyl)-5-methoxy-1,2-dihydroquinoline-2-carbonitrile	
 <p>(2<i>S</i>)-5b</p>	^1H NMR (400 MHz, CDCl_3) δ 7.40 – 7.29 (m, 3H), 7.25 – 7.20 (m, 3H), 7.18 (dd, 1H, $J_1 = J_2 = 8.5$ Hz), 6.73 (dd, 1H, $J = 8.5$ and 1.0 Hz), 6.68 (d, 1H, $J = 8.0$ Hz), 5.99 (dd, 1H, $J = 9.5$ and 6.5 Hz), 5.73 (dd, 1H, $J = 6.5$ and 1.0 Hz), 4.82-4.74 (m, 1H), 4.28 (dd, 1H, $J_1 = 9.0$ and 8.5 Hz), 4.15 (dd, 1H, $J = 9.5$ and 9.0 Hz), 3.88 (s, 3H), 3.44 (dd, 1H, $J = 13.5$ and 3.5 Hz), 2.96 (dd, 1H, $J = 13.5$ and 9.5 Hz)

Hydrogenation of each diastereomer (2*R*)-**5a** and (2*S*)-**5b** in the presence of propionic anhydride gave the same diastereomers (2*R*)-**3a** and (2*S*)-**3b**, previously prepared by acylation of

(±)-**1** with the Evans chiral auxiliary (*Scheme 2*). As illustrated in *Scheme 2*, removal of the Evans oxazolidinone chiral auxiliary from each single diastereomer (2R)-**3a** and (2S)-**3b** by treatment with lithium hydroxide and hydrogen peroxide⁹, followed by *N*^l-benzylation afforded enantiopure (+)-(2R)-UCM1014, and (-)-(2S)-UCM1014, respectively.

2.2.2 Pharmacological results

Pharmacology experiments were performed at the University of Ferrara. Binding affinity and functional activity assays were performed in CHO cells stably expressing the human MT₁ and MT₂ receptors. *Table 2* shows the experimental binding affinity of melatonin, (±)-UCM1014, and of the two enantiomers, (*R*)-UCM1014 and (*S*)-UCM1014, for human MT₁ and MT₂ receptors expressed in CHO cells.

Table 2 Binding affinity of melatonin and UCM1014, (*R*)-UCM1014 and (*S*)-UCM1014 for MT₁ and MT₂ receptors. ^a

Compound	MT ₁ K _i (nM)	MT ₂ K _i (nM)
Melatonin	0.240 ± 0.016	0.326 ± 0.022
UCM1014	18.3 ± 1.6	0.058 ± 0.004
(<i>R</i>)-UCM1014	7.23 ± 0.61	0.045 ± 0.004
(<i>S</i>)-UCM1014	91 ± 8	2.10 ± 0.17

^aK_i values were calculated from IC₅₀ values. Results are given as mean ± SEM (n=3).

Furthermore, the two enantiomers were evaluated for their intrinsic activity with the cAMP assay (*Table 3*), confirming the agonist behavior exhibited as a racemic mixture.

Table 3 Potency of melatonergic ligands for human MT₁ and MT₂ receptors in cAMP assay. ^a

Compound	MT ₁ IC ₅₀ (nM)	MT ₁ pharmacological behaviour	MT ₂ IC ₅₀ (nM)	MT ₂ pharmacological behaviour
Melatonin	0.277 ± 0.024	full agonist	0.975 ± 0.087	full agonist
UCM1014	31 ± 2	full agonist	0.436 ± 0.035	full agonist
(<i>R</i>)-UCM1014	12.4 ± 1.1	full agonist	0.245 ± 0.019	full agonist
(<i>S</i>)-UCM1014	290 ± 23	full agonist	9.32 ± 0.77	full agonist

^aIC₅₀ is the concentration of compound that reduces by 50% the production of cAMP is induced by 1 μM of forskolin. Results are given as mean ± SEM (n=3).

As depicted in *Table 2*, the (*R*)-UCM1014 resulted in being the eutomer, with about 160-fold selectivity for the MT₂ receptor. Molecular dynamics simulations were applied to evaluate the conformational preferences of the enantiomers in solution. They evidenced that, while the eutomer (*R*)-UCM1014 was able to bind the receptor in a low-energy, highly abundant conformation with

axial amide side chain arrangement, the conformation of the (*S*)-diastomer that can be accommodated in the binding site (with equatorial amide side chain arrangement) was poorly populated in solution. Therefore, the observed stereoselective behavior could be ascribed to a conformational selection operated by the receptor that alters the conformational equilibria by inducing an enrichment of those conformations (with axial amide side chain arrangement) of the enantiomer able to bind the receptor.

2.3 Conclusion

The synthesis of the two enantiomers of (±)-**UCM1014** has been reported, together with the determination of their absolute configuration. Pharmacological assays, performed on cells expressing cloned human MT₁ and MT₂ receptors, revealed the (+)-(2*R*)-enantiomer as the enantiomer, with about 160-fold selectivity for the MT₂ receptor and full agonist behavior. Docking studies into the melatonin receptor crystal structure coupled to evaluation of conformational equilibria in solution by MD and NMR led to the conclusion that the observed high stereoselective binding is related to the axial arrangement of the side chain that can be superposed to that of the bioactive conformation of MLT only for (+)-(2*R*)-enantiomer.

2.4 Experimental section

2.4.1 Materials

(4*S*)-4-Benzyl-2-oxazolidinone and 5-methoxyquinoline were purchased from commercial suppliers and used without further purification.

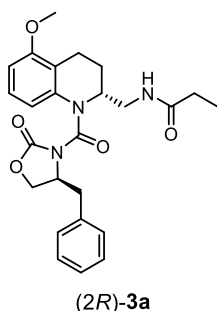
2.4.2 Experimental procedure

***N*-(((*R*)-1-(((*S*)-4-benzyl-2-oxooxazolidine-3-carbonyl)-5-methoxy-1,2,3,4-tetrahydroquinolin-2-yl)methyl)propionamide (*2R*)-3a and *N*-(((*S*)-1-(((*S*)-4-benzyl-2-oxooxazolidine-3-carbonyl)-5-methoxy-1,2,3,4-tetrahydroquinolin-2-yl)methyl)propionamide (*2S*)-3b**

NaH (60% in mineral oil, 3.6 equiv., 122 mg, 3.05 mmol) was added at 0°C to a solution of (4*S*)-4-benzyl-2-oxazolidinone (3.0 equiv., 452 mg, 2.55 mmol) in dry toluene (13.5 mL) under nitrogen atmosphere and the resulting mixture was heated under reflux for 2h. After cooling to room temperature, the suspension was added dropwise to a solution of triphosgene (1.8 equiv., 454 mg, 1.53 mmol) in dry toluene (6 mL) stirred at -20°C. After the addition, the mixture was stirred at -20°C for an additional 2h, and then filtration and distillation of the solvent gave the crude carbonyl chloride **2** as a white solid, which was used without any further purification.

TEA (396 mg, 3.91 mmol) and a solution of the above crude acyl chloride **2** in dry DCM (5 mL) were added to a solution of (±)-**1** (1.0 equiv., 210 mg, 0.85 mmol) in dry DCM (10 mL) cooled at 0°C. Then the reaction mixture was stirred for 16h at room temperature, quenched by the addition of an aqueous saturated solution of NaHCO₃, and extracted with DCM. The combined organic phases were washed with brine, dried over Na₂SO₄, and concentrated under reduced pressure to give a crude residue. The two diastereomers (*2R*)-**3a** and (*2S*)-**3b** were separated by silica gel flash column chromatography (cyclohexane:EtOAc 3:7 as eluent). Overall yield 77%

(*2R*)-**3a**



White solid.

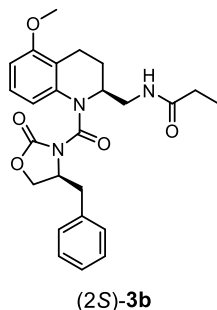
ESI MS (*m/z*) 452 [M+H]⁺

¹H NMR (400 MHz, CDCl₃) δ 7.37–7.22 (m, 5H), 7.05 (dd, 1H, *J*₁ = *J*₂ = 8.0 Hz), 6.71 (bs, 1H), 6.63 (d, 1H, *J* = 8.0 Hz), 6.58 (d, 1H, *J* = 8.0 Hz), 4.59–4.52 (m, 1H), 4.45–4.40 (m, 1H), 4.17–4.09 (m, 2H), 3.81 (s, 3H), 3.73 (dd, 1H, *J* = 13.5 and 3.0 Hz), 3.41–3.36 (m, 1H), 3.26–3.19 (m, 1H), 2.90–2.78 (m, 2H), 2.69

– 2.61 (m, 1H), 2.45–2.37 (m, 1H), 2.23 (q, 2H, *J* = 7.5 Hz), 1.80–1.70 (m, 1H), 1.17 (t, 3H, *J* = 7.5 Hz)

^{13}C NMR (100 MHz, CDCl_3) δ 174.1, 157.0, 154.4, 151.9, 137.5, 135.7, 129.4, 129.0, 127.2, 126.6, 120.4, 113.6, 106.8, 66.6, 58.1, 55.4, 53.9, 42.4, 38.4, 29.7, 26.7, 17.9, 9.9

(2S)-3b



White solid.

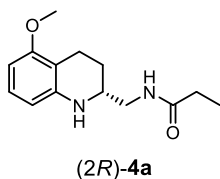
ESI MS (m/z) 452 $[\text{M}+\text{H}]^+$

^1H NMR (400 MHz, CDCl_3) δ 7.37–7.29 (m, 3H), 7.22–7.20 (m, 2H), 7.11 (dd, 1H, $J_1 = J_2 = 8.0$ Hz), 6.84 (bs, 1H), 6.69–6.66 (m, 2H), 4.77–4.65 (m, 1H), 4.62–4.55 (m, 1H), 4.20 (t, 1H, $J = 9.0$ Hz), 4.05 (t, 1H, $J = 9.0$ Hz), 3.83 (s, 3H), 3.46–3.44 (m, 1H), 3.41–3.24 (m, 2H), 2.87 (ddd, 1H, $J_1 = 7.5$; $J_2 = J_3 = 15$ Hz), 2.80–2.74 (m, 1H), 2.63 (ddd, 1H, $J_1 = J_2 = 6.5$ Hz; $J_3 = 15$ Hz), 2.22 (q, 2H, $J =$

7.5 Hz), 2.13 (m, 1H), 1.77 (m, 1H), 1.14 (t, 3H, $J = 7.5$ Hz)

^{13}C NMR (100 MHz, CDCl_3) δ 174.3, 156.9, 154.1, 151.8, 136.8, 134.8, 129.1, 129.0, 127.5, 126.6, 121.0, 115.6, 107.2, 67.7, 56.6, 55.5, 54.0, 42.1, 38.5, 29.6, 27.0, 17.9, 9.8

(R)-N-((5-methoxy-1,2,3,4-tetrahydroquinolin-2-yl)methyl)propionamide (2R-4a)



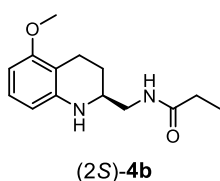
30% H_2O_2 (12 equiv., 0.30 mL, 4.44 mmol) was added dropwise to a stirred solution of propionamide (2R)-3a (1 equiv., 168 mg, 0.37 mmol) in a mixture of THF: H_2O 8:2 (11 mL) cooled at 0°C . After approximately 1 min of stirring, a solution of $\text{LiOH} \cdot \text{H}_2\text{O}$ (4.8 equiv., 75 mg, 1.78 mmol) in H_2O (2.2 mL) was added

dropwise to the reaction mixture, and the stirring continued at 40°C for 4h.⁹ The reaction was quenched by adding an aqueous solution of Na_2SO_3 1.5 M (0.70 mL), concentrated under reduced pressure, and extracted with DCM. The combined organic phases were dried over Na_2SO_4 and concentrated under reduced pressure to give a crude residue, which was purified by silica gel flash column chromatography (DCM:EtOAc 7:3 as eluent) to afford compound (2R)-4a, as a white solid, 58% yield.

$[\alpha]^{15}_{\text{D}} = -51.72$ (c 0.406 in CHCl_3)

Experimental NMR data are in agreement with those previously reported.⁸

(S)-N-((5-methoxy-1,2,3,4-tetrahydroquinolin-2-yl)methyl)propionamide (2S)-4b



Compound (2S)-4b was obtained using the procedure above described starting from (2S)-3b.

Flash chromatography: silica gel, DCM:EtOAc 7:3 as eluent.

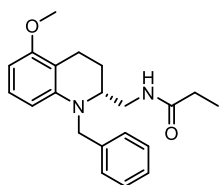
White solid, 57% yield.

$[\alpha]^{15}_{\text{D}} = +45.5$ (c 0.459 in CHCl_3)

Experimental NMR data are in agreement with those previously reported.⁸

(R)-N-((1-benzyl-5-methoxy-1,2,3,4-tetrahydroquinolin-2-yl)methyl)propionamide

[(+)-(2R)-UCM1014]



(+)-(2R)-UCM1014

A solution of (2R)-4a (1 equiv., 45 mg, 0.18 mmol), TEA (2.0 equiv., 0.5 mL, 0.36 mmol) and benzyl bromide (1.6 equiv., 0.40 mL, 0.29 mmol) in dry toluene (3 mL) was refluxed for 2h under nitrogen atmosphere. After cooling to room temperature, the reaction mixture was poured into water and extracted with EtOAc. The combined organic phases were washed with brine and dried over Na₂SO₄. After evaporation of the solvent by distillation under reduced pressure, the residue was purified by silica gel flash column chromatography (cyclohexane:EtOAc 1:1 as eluent) to afford the final compound (+)-(2R)-UCM1014.

Crystallization with diethyl ether:petroleum ether. White solid, 87% yield.

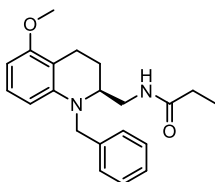
$[\alpha]_{\text{D}}^{18} = +26.3$ (*c* 0.422 in CHCl₃)

Chiral HPLC: 100% ee; *t*_R 20.40 min.

Physicochemical data are in agreement with those previously reported for the racemate.⁸

(S)-N-((1-benzyl-5-methoxy-1,2,3,4-tetrahydroquinolin-2-yl)methyl)propionamide

[(-)-(2S)-UCM1014]



(-)-(2S)-UCM1014

Compound (-)-(2S)-UCM1014 was obtained using the procedure above described starting from (2S)-4b.

Flash chromatography: silica gel cyclohexane:EtOAc 1:1 as eluent.

Crystallization with diethyl ether:petroleum ether. White solid, 81% yield.

$[\alpha]_{\text{D}}^{18} = -28.5$ (*c* 0.417 in CHCl₃)

Chiral HPLC: 97% ee; *t*_R 22.58 min.

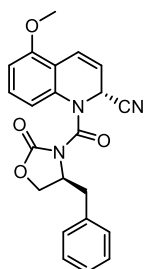
Physicochemical data are in agreement with those previously reported for the racemate.⁸

(R)-1-((S)-4-benzyl-2-oxooxazolidine-3-carbonyl)-5-methoxy-1,2-dihydroquinoline-2-carbonitrile (2R)-5a and (S)-1-((S)-4-benzyl-2-oxooxazolidine-3-carbonyl)-5-methoxy-1,2-dihydroquinoline-2-carbonitrile (2S)-5b

TMSOTf (2 equiv., 0.31 mL, 2.52 mmol) was added to a solution of (4S)-4-benzyl-2-oxooxazolidine-3-carbonyl chloride **2** (2 equiv., 602 mg, 2.52 mmol) and 5-methoxyquinoline (1.5 equiv., 200 mg, 1.25 mmol) in dry DCM (2.5 mL) under nitrogen atmosphere and the resulting mixture was stirred for 3h at room temperature. Then, TMSCN (2 equiv., 0.31 mL, 2.52 mmol) was added to the reaction mixture and the solution was allowed to stir for other 20h.¹⁰ The mixture was diluted with

DCM, washed with a saturated aqueous solution of NaHCO₃ and brine. The organic phase was dried over Na₂SO₄ and concentrated under reduced pressure to give a crude mixture of the two diastereomers which were separated by silica gel flash column chromatography (gradient cyclohexane:EtOAc 8:2 to 7:3 as eluent). Overall yield: 20%

(2R)-5a



Crystallization with diethyl ether/petroleum ether: white solid.

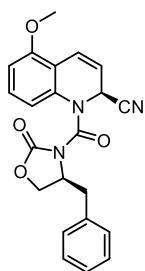
M.p.: 179-180°C

ESI MS (*m/z*): 390 [M+H]⁺

¹H NMR (400 MHz, CDCl₃) δ 7.40 – 7.18 (m, 7H), 6.78 (d, 1H, *J* = 8.5 Hz), 6.72 (d, 1H, *J* = 8.5 Hz), 6.04 (dd, 1H, *J* = 9.5 and 6.5 Hz), 5.71 (d, 1H, *J* = 6.5 Hz), 4.57– 4.52 (m, 1H), 4.25-4.16 (m, 2H), 3.88 (s, 3H), 3.74 (dd, 1H, *J* = 13.5 and 3.5 Hz), 2.89 (dd, 1H,

J = 13.5 and 10.0 Hz)

(2S)-5b



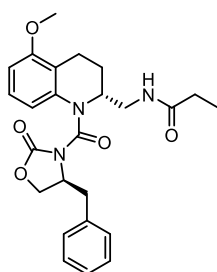
Crystallization with diethyl ether/petroleum ether: white solid.

M.p.: 174-175°C

ESI MS (*m/z*): 390 [M+H]⁺

¹H NMR (400 MHz, CDCl₃) δ 7.40 – 7.29 (m, 3H), 7.25 – 7.20 (m, 3H), 7.18 (dd, 1H, *J*₁ = *J*₂ = 8.5 Hz), 6.73 (dd, 1H, *J* = 8.5 and 1.0 Hz), 6.68 (d, 1H, *J* = 8.0 Hz), 5.99 (dd, 1H, *J* = 9.5 and 6.5 Hz), 5.73 (dd, 1H, *J* = 6.5 and 1.0 Hz), 4.82-4.74 (m, 1H), 4.28 (dd, 1H, *J*₁ = 9.0 and 8.5 Hz), 4.15 (dd, 1H, *J* = 9.5 and 9.0 Hz), 3.88 (s, 3H), 3.44 (dd, 1H, *J* = 13.5 and 3.5 Hz), 2.96 (dd, 1H, *J* = 13.5 and 9.5 Hz)

Synthesis of (2R)-3a by reduction and acylation of (2R)-5a.

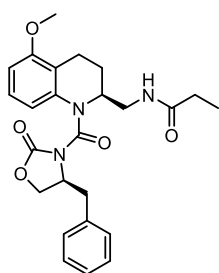


(2R)-3a

A solution of (2R)-5a (1 equiv., 30 mg, 0.08 mmol) and propionic anhydride (16 equiv., 0.16 mL, 1.28 mmol) in THF (0.8 mL) was hydrogenated (2 atm) over Raney-Ni for 3h at room temperature. The catalyst was filtered on Celite and the resulting filtrate was concentrated *in vacuo*. The residue was purified by silica gel flash chromatography (cyclohexane:EtOAc 3:7 as eluent) to afford compound (2R)-3a as a white solid, 75% yield.

¹H NMR data are in agreement with those reported for (2R)-3a, described above.

Synthesis of (2*S*)-3b by reduction and acylation of (2*S*)-5b.



(2*S*)-3b

Compound (2*S*)-3b was obtained using the procedure above described starting from (2*S*)-5b.

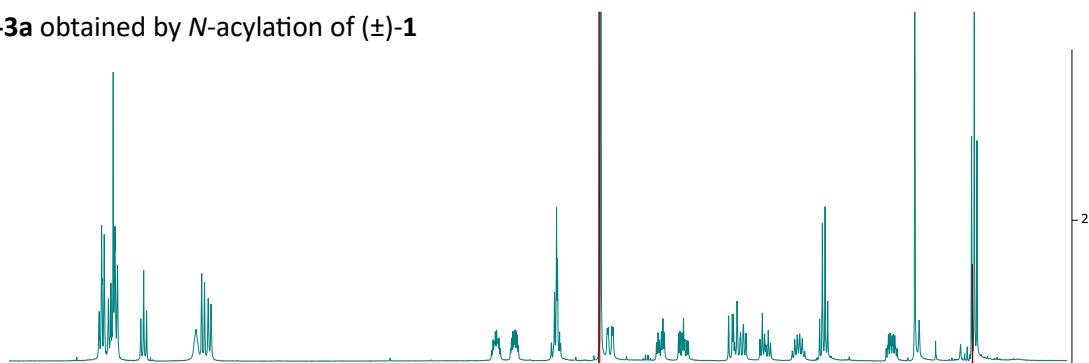
Flash chromatography: silica gel cyclohexane:EtOAc 3:7 as eluent.

White solid, 63% yield.

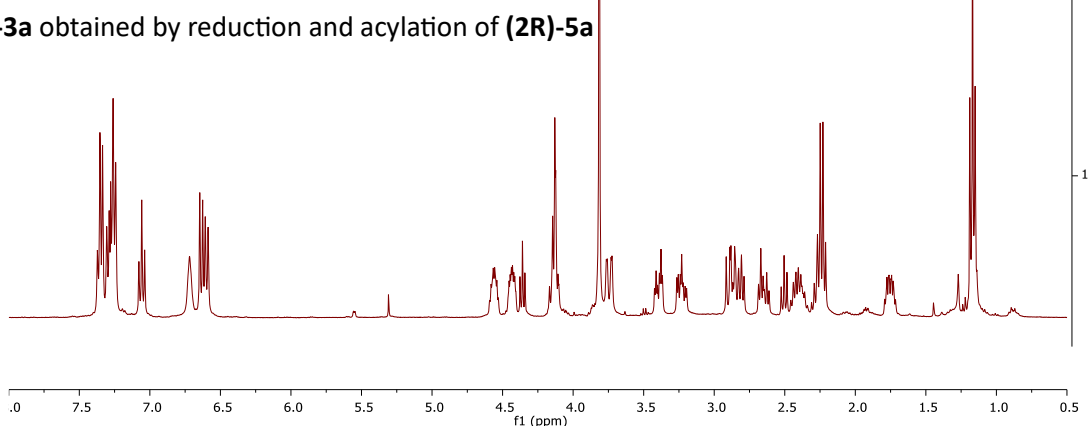
¹H NMR data are in agreement with those reported for (2*S*)-3b, described above.

2.4.3 Comparison of the NMR spectra of compound **(2R)-3a**, obtained by N-acylation of (\pm) -**1** and compound **(2R)-3a** obtained by reduction and acylation of **(2R)-5a**

(2R)-3a obtained by N-acylation of (\pm) -**1**

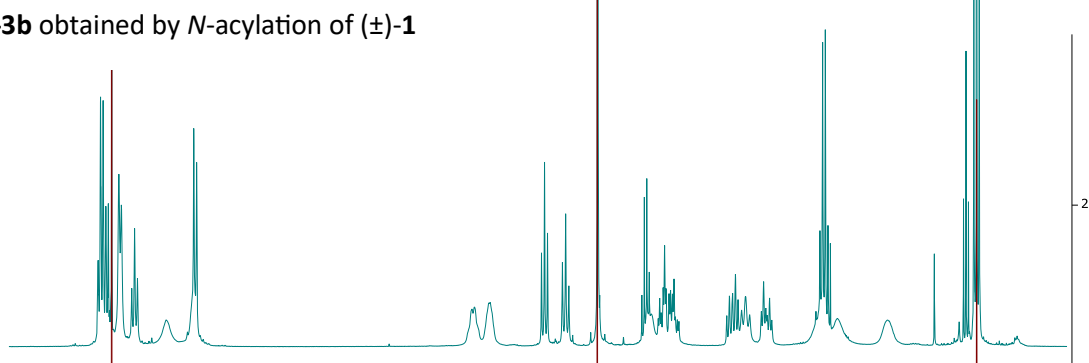


(2R)-3a obtained by reduction and acylation of **(2R)-5a**

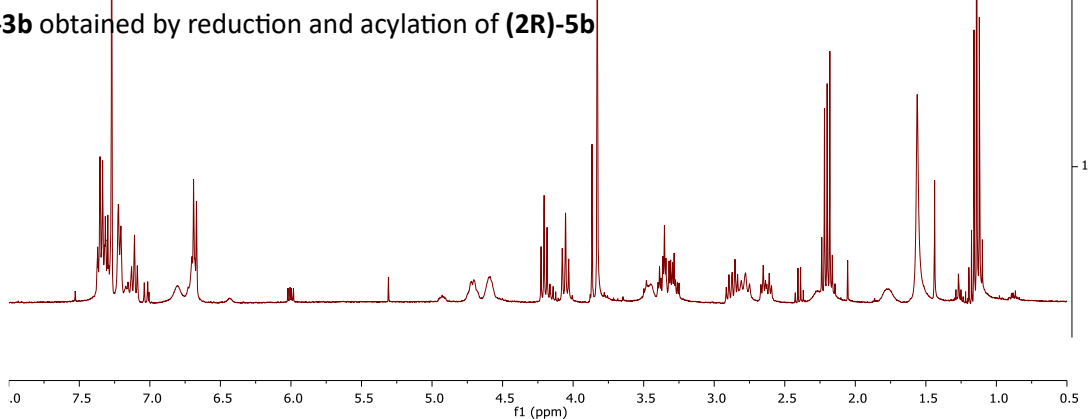


2.4.4 Comparison of NMR spectra of compound **(2S)-3b**, obtained by N-acylation of (\pm) -**1** and compound **(2S)-3b** obtained by reduction and acylation of **(2S)-5b**

(2S)-3b obtained by N-acylation of (\pm) -**1**



(2S)-3b obtained by reduction and acylation of **(2R)-5b**



2.4.5 Chiral HPLC analysis

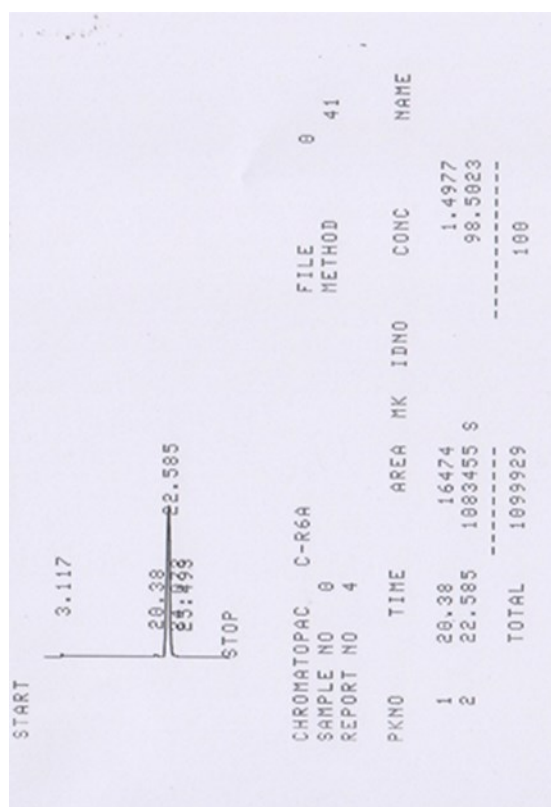
Chromatogram of (±)-UCM1014



Chromatogram of (+)-(2R)-UCM1014



Chromatogram of (-)-(2S)-UCM1014



2.5 References

-
- ¹ Zlotos DP, Jockers R, Cecon E, Rivara S, Witt-Enderby PA. MT₁ and MT₂ melatonin receptors: ligands, models, oligomers, and therapeutic potential. *J Med Chem.* **2014**, 57(8), 3161-85
- ² Mulchahey J, Goldwater D, Zemlan F. A single blind, placebo controlled, across groups dose escalation study of the safety, tolerability, pharmacokinetics and pharmacodynamics of the melatonin analog β -methyl-6-chloromelatonin. *Life Sci.* **2004**, 75(15), 1843–1856
- ³ Ettaoussi M, Sabaouni A, Pérès B, Landagaray E, Nosjean O, Boutin JA, Caignard DH, Delagrangé P, Berthelot P, Yous S. Synthesis and pharmacological evaluation of a series of the agomelatine analogues as melatonin MT₁/MT₂ agonist and 5-HT_{2C} antagonist. *ChemMedChem.* **2013**, 8(11), 1830-45
- ⁴ Carocci A, Catalano A, Lovece A, Lentini G, Duranti A, Lucini V, Pannacci M, Scaglione F, Franchini C. Design, synthesis, and pharmacological effects of structurally simple ligands for MT₁ and MT₂ melatonin receptors. *Bioorg Med Chem.* **2010**, 18(17), 6496-511
- ⁵ Jansen JM, Copping S, Gruppen G, Molinari EJ, Dubocovich ML, Grol CJ. The high affinity melatonin binding site probed with conformationally restricted ligand--I. Pharmacophore and minireceptor models. *Bioorg Med Chem.* **1996**, 4(8), 1321-32
- ⁶ Spadoni G, Balsamini C, Diamantini G, Di Giacomo B, Tarzia G, Mor M, Plazzi PV, Rivara S, Lucini V, Nonno R, Pannacci M, Frascini F, Stankov BM. Conformationally restrained melatonin analogues: synthesis, binding affinity for the melatonin receptor, evaluation of the biological activity, and molecular modeling study. *J Med Chem.* **1997**, 40(13), 1990-2002
- ⁷ Rivara S, Diamantini G, Di Giacomo B, Lamba D, Gatti G, Lucini V, Pannacci M, Mor M, Spadoni G, Tarzia G. Reassessing the melatonin pharmacophore-enantiomeric resolution, pharmacological activity, structure analysis, and molecular modeling of a constrained chiral melatonin analogue. *Bioorg Med Chem.* **2006**, 14(10), 3383-91
- ⁸ Spadoni G, Bedini A, Lucarini S, Mari M, Caignard DH, Boutin JA, Delagrangé P, Lucini V, Scaglione F, Lodola A, Zanardi F, Pala D, Mor M, Rivara S. Highly Potent and Selective MT₂ Melatonin Receptor Full Agonists from Conformational Analysis of 1-Benzyl-2-acylaminomethyl-tetrahydroquinolines. *J Med Chem.* **2015**, 58(18), 7512-25
- ⁹ Evans DA, Britton TC, Ellman JA. Contrasteric carboximide hydrolysis with lithium hydroperoxide. *Tetrahedron Lett.* **1987**, 28(49), 6141-614
- ¹⁰ Pauvert M, Collet SC, Bertrand M-J, Guingant AY, Evain M. Synthesis of chiral *N*-protected 1,2-dihydroquinoline-2-carbonitrile and 1,2-dihydro-isoquinoline-1-carbonitrile via an asymmetric Reissert reaction. *Tetrahedron Lett.* **2005**, 46(17), 2983-2987

Chapter 3. Synthesis of 4-substituted melatonin analogues as putative fluorescent probes for melatonin receptors

This chapter is based on: Bartolucci S, Retini M, **Fanini F**, Paderni D, Piersanti G. Synthesis and Fluorescence Properties of 4-Cyano and 4-Formyl Melatonin as Putative Melatonergic Ligands. *ACS Omega*. **2023**, 8(24), 22190-22194

3.1 Introduction

G-protein coupled receptors (GPCRs) are studied for their importance in intracellular signaling and intercellular communication and their implications in physio-pathological conditions. Crystallography, radiolabeled compounds, mutagenesis, and biophysical methods are the main approaches for studying their activities and ligand binding specificity.¹ Generally, crystallography studies help to elucidate their structure, providing information about the binding sites and the ligand entrance channel.¹ Instead, assays based on radioactive probes (usually tritiated or iodinated ligands) are used to determine receptor-ligand binding characteristics and receptor-receptor interactions.²

The detection and pharmacological characterization of melatonin receptors became possible owing to the development of two specific radioligands, [³H]-melatonin³ ([³H]-MLT) and 2-[¹²⁵I]-iodomelatonin⁴ (2-[¹²⁵I]-MLT) in the 1980s. The vast majority of studies use 2-[¹²⁵I]-MLT as a radioligand due to its higher specific activity. The radiolabeled compound 2-[¹²⁵I]-MLT has also been used for determining the distribution of the two receptors, finding out that they are present both in the CNS and peripheral tissues. Both radioligands are full agonists and are non-specific for either melatonin receptor subtype. Two other iodinated radioligands, [¹²⁵I]DIV880 and [¹²⁵I]S70254, have been recently developed, that are full and partial MT₂-selective agonists, respectively.⁵ However, experiments using radioactive compounds are complex due to the impossibility of avoiding the multistep washing (making it more complicated to run kinetic studies) and the hazardous nature of the radioactive compounds.

Fluorescent ligands represent a valid alternative to radioligands for kinetic, saturation, and competition binding assays. Advantages such as lack of exposure to radioactivity coupled to the reduced costs related to licensing and disposal render them accessible for most laboratories. The design and development of fluorescent probes are challenging because of issues linked to retaining high binding affinity and avoiding non-specific binding. The most common method for obtaining fluorescent probes relies on connecting the pharmacophore with the fluorophore through a linker.⁶ However, it is worth mentioning that isotope tagging has minimal or no effects on the affinity of the probes. On the other hand, fluorophore labeling of parent ligands will inevitably affect binding

affinity and/or efficacy (even reversal of agonist-antagonist activity upon fluorophore conjugation has been reported), considering that often the fluorophore itself is even bigger than the parent ligand.⁷

Some fluorescent melatonin receptor ligands have been reported, some of which retained acceptable binding affinity for these receptors. In 2007, Chou and coworkers described the synthesis of 7-azamelatonin, with dual emission at 330 nm and 550 nm respectively and a pIC₅₀ of 6.9 on MT₁ receptor.⁸ Subsequently, four fluorescent ligands were synthesized via Lewis acid-mediated condensation of 2-formyl melatonin with a series of substituted pyrroles, yielding melatonin-BODIPY fused fluorescent ligands **I-IV** (**Figure 18 A**).⁹

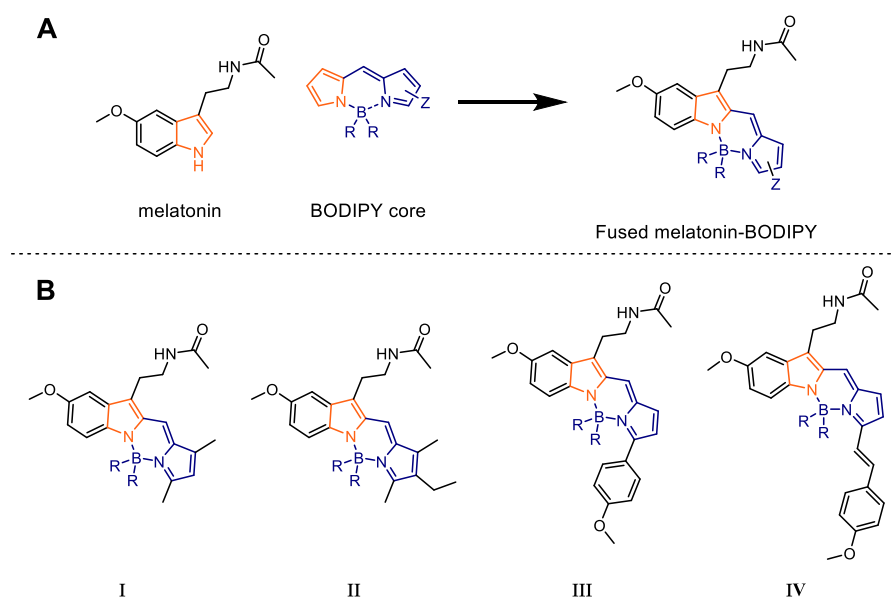


Figure 18 A) General structure of fluorescent ligands obtained by fusing melatonin to BODIPY: the pyrrole core of the BODIPY overlaps with the indole one (in orange) and BODIPY (in blue); **B)** melatonin-BODIPY ligands.

Compound **I** and **IV** showed moderate affinities towards MT₁R and MT₂R ($K_i=32-71$ nM on MT₁R and $K_i=10-26$ nM on MT₂R). The emission spectra of compound **III** and **IV**, characterized by a more extended conjugation than compounds **I** and **II**, were at lower energy than **I** and **II**.⁹

Finally, hydrophilic and lipophilic fluorescent ligands with (sub)- μ M affinities for MLT receptors were synthesized by coupling sulfo-Cy3 cyanin fluorophore and BODIPY FL to the azamelatonin templates (**Figure 19**). Unfortunately, both displayed high nonspecific binding (ICOA-13) and high intracellular uptake (ICOA-9). Notably, functional assays performed using ICOA-9 and ICOA-13 indicated the suitability of the synthesized compounds in determining the contribution of MTRs on the plasma and mitochondrial membrane to melatonin signaling cascades.¹⁰

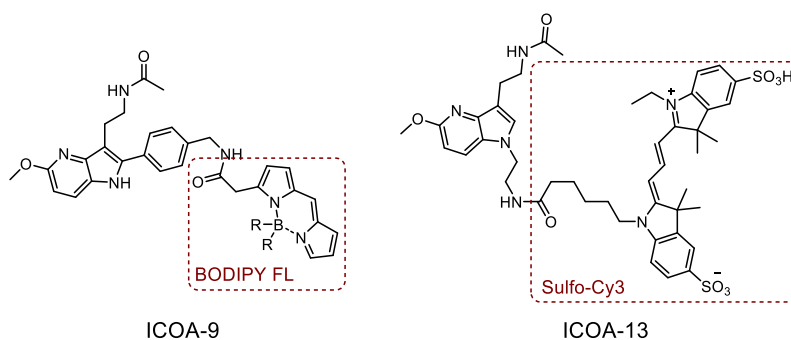


Figure 19 Structure of ICOA-9, fluorescent ligand bearing BODIPY FL tag, and ICOA-13, fluorescent ligand bearing sulfo-Cy3 tag.

Some coumarin-based MLT_R fluorescent ligands were developed by replacing the indole core with a chromen-2-one ring. Unfortunately, the synthesized ligands showed low affinities for MTRs in radioligand binding assays with the only exception of compound **V** ($K_i=13$ nM on MT₁R and $K_i=3.4$ nM on MT₂R) (**Figure 20**).¹¹

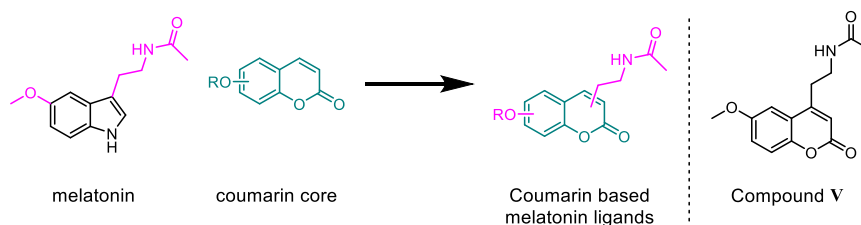


Figure 20 Example of coumarin-based fluorescent melatonin ligands obtained by replacing the indole ring with chromen-2-one ring.

Unfortunately, most of the above reported MLT fluorescent ligands showed high nonspecific binding and intracellular uptake, rendering these tracers not very suitable for fluorescence imaging and fluorescence-based binding studies. Furthermore, the X-ray crystal structure reveal for both receptors narrow ligand entry channels and small orthosteric ligand binding pockets, presenting additional challenges for fluorescent tracer development.

MLT shows fluorescence properties, which, unfortunately, are useless in biological assay due to the overlap of the primary band absorption with one of the *L*-tyrosine and *L*-tryptophan residues present in proteins. However, since the fluorescence of MLT is due mainly to the indole ring, the introduction of substituents, able to extend the ring conjugation, can modify the band absorption/emission wavelength, providing the appropriate fluorescent characteristics. Therefore, a possible approach for the development of new MLT fluorescent probes could be to introduce small modification on the natural ligand scaffold, improving its intrinsic fluorescence and retaining a suitable binding affinity.

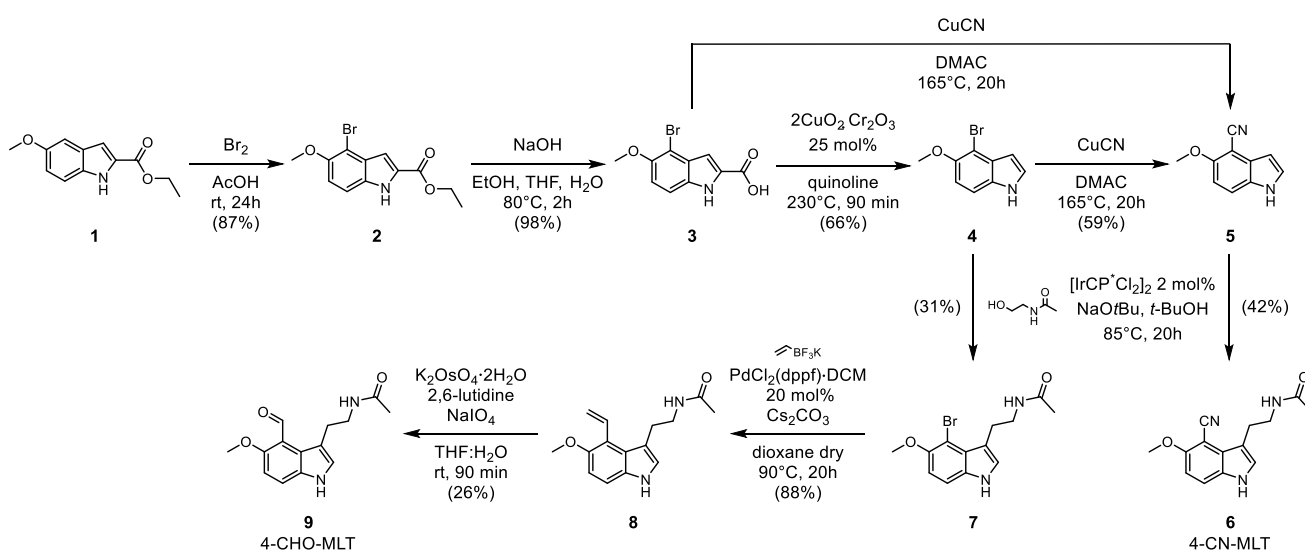
A similar approach has recently been applied to tryptophan, an amino acid structurally related to MLT, having intrinsic fluorescent properties, but its absorption and emission are in the UV wavelength. Indeed, recent photophysical reports have demonstrated that suitable substitutions on the

indole ring of tryptophan derivatives may induce a significant change in fluorescence behavior.¹² The best results for tryptophan derivatives have been obtained by introducing a nitrile or a formyl group on the C^4 indole position. In particular, tryptophan derivatives such as 4CN-Trp*-Gly and *N*-Alpha-Acetyl-4-Cyano-L-Tryptophan Methyl Ester (4CN-Trp) display a long lifetime, good photostability, good absorption (also at 325 nm), and a fluorescence above 415 nm in water, which makes it a blue chromophore.¹² Also C-4-aldehyde-derivatized indoles, including 4-formyl tryptophan derivatives¹³, displayed good fluorescence (with a red-shifted absorption and emission in the green region of the visible spectrum), high quantum yield, and a long lifetime.¹⁴

Considering the above described structure-fluorescence relationships for tryptophan derivatives, we synthesized new C^4 -formyl-MLT and C^4 -CN-MLT putative fluorescent ligands, hoping that these modifications may lead to compounds with a suitable fluorescent profile and retaining good MLT receptors binding affinity. If these structural modifications give interesting results, they could be conveniently extended to selective ligands for each MLT receptor subtype.

3.2 Results and discussion

The synthesis of the 4-cyano-melatonin (4-CN-MLT) and 4-formyl-melatonin (4-CHO-MLT) is shown in **Scheme 4**. The common intermediate, 4-bromo-5-methoxyindole **4**, was obtained starting from the C^4 -selective bromination of the commercially available 5-methoxy-2-carboxyethyl indole **1**, subsequent hydrolysis of the ester, followed by copper-catalyzed decarboxylation. The intermediate **4** can be readily converted into the desired 4-CN-MLT through the insertion of the cyano moiety using CuCN in dimethylacetamide, followed by selective C^3 -indole alkylation with *N*-acetyl ethanolamine. Interestingly, intermediate **3** can directly undergo decarboxylation and cyanation with the only presence of CuCN in dimethylacetamide providing the nitrile compound **5**.



Scheme 4 Synthesis of 4-cyano-melatonin (4-CN-MLT) and 4-formyl-melatonin (4-CHO-MLT).

The critical C^3 -indole alkylation step is performed using a green borrowing hydrogen process, using $[\{Cp^*IrCl_2\}_2]$ as catalyst (2 mol%) and sodium *tert*-butoxide as a base, providing the final product **6** (42% yield) and the intermediate **7** (31% yield), with water as the only byproduct. Suzuki cross-coupling between **7** and potassium vinyl trifluoroborate (vinyl-BF₃K) provided the installation of the vinyl group (88%). Oxidative cleavage of the C=C double bond using the Lemieux–Johnson oxidation in the presence of a catalytic amount of osmium tetroxide, an excess of sodium periodate, and a non-nucleophilic base such as 2,6-lutidine provided selectively the desired 4-CHO-MLT.

With the 4-CN-MLT and 4-CHO-MLT in hand, the optical properties of the synthesized compound were investigated in different solvents and compared with those of MLT (**Figure 21**).

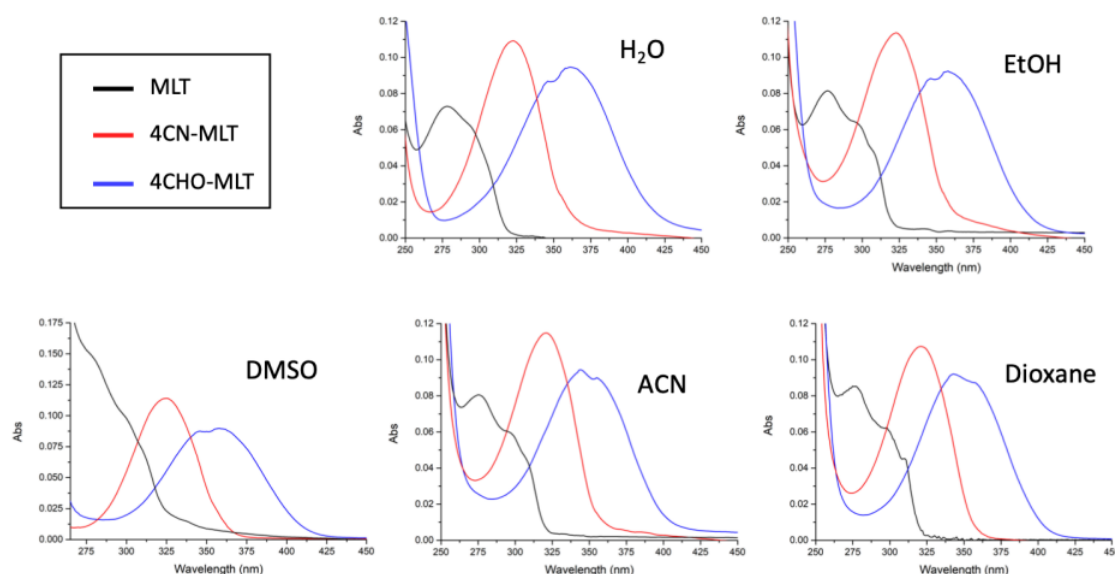


Figure 21 Absorption spectra of MLT (dark grey), 4-CN-MLT (red), and 4-CHO-MLT (blue), recorded at 10 μ M in the indicated solvent.

In an aqueous solution, the UV-Vis spectra show absorption bands at 324 nm for 4-CN-MLT and 362 nm for 4-CHO-MLT. As expected, the absorption wavelengths of **6** and **9** are red shifted compared to those of MLT, confirming that an electron-withdrawing group on an indole ring, especially in the C^4 , provides a red shift of λ_{max} . Solvatochromic studies were performed in different aprotic and protic polar solvents (EtOH, DMSO, ACN, and 1,4-dioxane) because the solvents influences the ground and excited states of molecule dipoles (**Figure 21**). The 4-CHO-MLT has a greater red shift of the λ_{max} in water (362 nm) compared to the other solvents, while there is no significant difference in the absorption band for 4-CN-MLT, which remains constant in the different solvents (between 322 and 325 nm).

After determining the λ_{max} , the fluorescence properties of the two compounds have been registered and compared with the MLT ones (**Figure 22**).

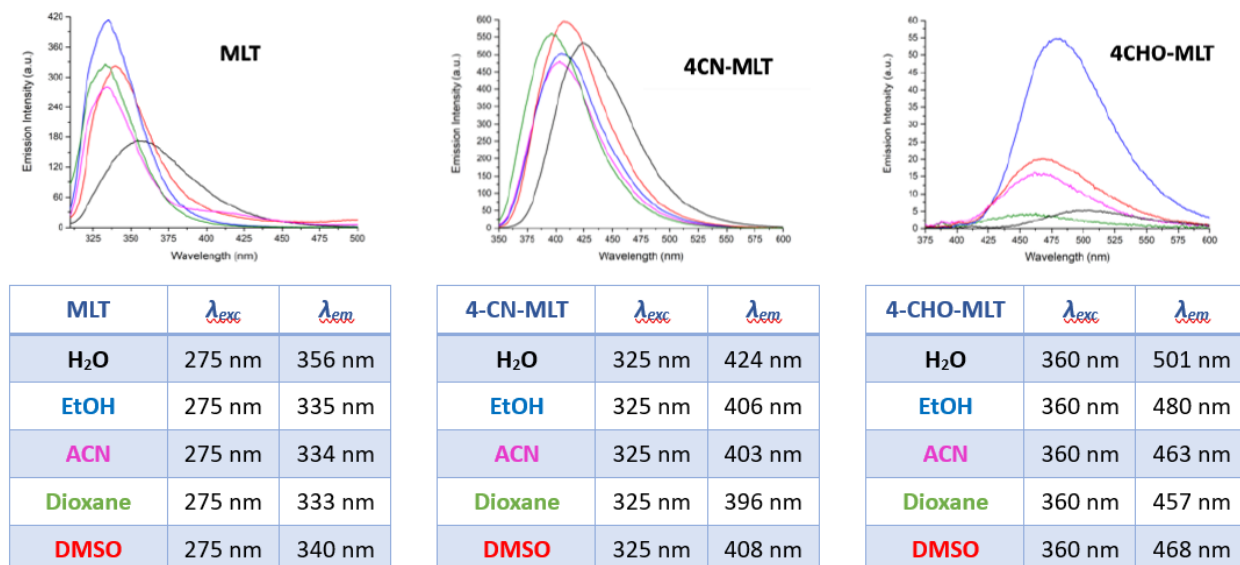


Figure 22 Emission spectra of MLT, 4-CN-MLT, and 4-CHO-MLT, recorded at 10 μ M in all studied solvents.

The emission spectra of both compounds **6** and **9** are in the visible spectral region and show a red shift compared to the one of MLT, as already observed for the absorption spectra. In particular, the 4-CN-MLT has a single emission band at around 410 nm. The fluorescence of 4-CHO-MLT is more intense in EtOH than in the other solvent, where it shows a peak at 480 nm, making it a cyan fluorophore (**Figure 23**). Additionally, other fluorescent properties of the 4-CHO-MLT have been evaluated. The quantum yield was decent (value of 0.049), the brightness was appropriate ($B = 1120 \text{ mM}^{-1}\text{cm}^{-1}$), and the photostability was excellent.

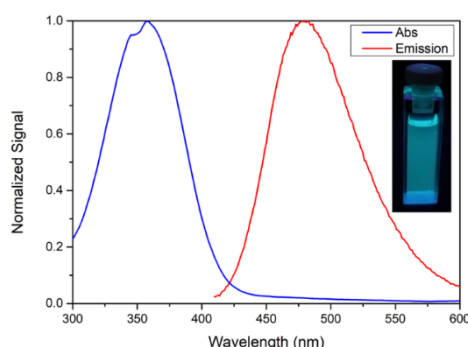


Figure 23 Normalized absorption (blue) and fluorescence (red) spectra of 4-CHO-MLT in EtOH. The excitation wavelength for the fluorescence measurement was 360 nm. As shown in the inset, 4-CHO-MLT, is a cyan product.

The new synthesized 4-substituted MLT derivatives were evaluated for their binding affinity at human MT₁ and MT₂ receptors stably transfected in rat fibroblast NIH3T3 cells using 2-[¹²⁵I]iodomelatonin as radioligand, and the results are reported in **Table 4**, together with those of the reference compound melatonin. Unfortunately, the introduction of electron-withdrawing groups in

the C^4 -indole MLT position resulted to be detrimental for binding to MLT receptors; both compounds show only modest affinities for MT₁ and MT₂ receptors.

Table 4 Binding affinity [K_i (nM)] values of MLT, 4-CN-MLT, and 4-CHO-MLT for the human MLT receptors MT₁ and MT₂.

Compound	MT ₁ K_i (nM)	MT ₂ K_i (nM)
MLT	5.5 ± 0.4	6.3 ± 0.5
4-CN-MLT	2591 ± 168	398 ± 26
4-CHO-MLT	1084 ± 79	424 ± 29

3.3 Conclusion and outlook

A novel and preliminary approach for developing new biologically useful fluorescent probes for melatonin receptors has been reported. The design, synthesis, and fluorescent and pharmacological characterization of two 4-substituted MLT compounds, namely 4-CN-MLT and 4-CHO-MLT, have been described. The extension of the conjugation of MLT by introducing the electron-withdrawing group (formyl and cyano group) provides the desired red shift in the absorption spectra and the emission in the visible region (blue region). Although these novel compounds displayed only modest binding affinities to the MT₁ and MT₂, a new and reliable synthetic procedure for preparing novel C^4 -substituted MLT compounds has been reported.

Recently, the dicyanovinyl group has been installed in the C^4 of tryptophan, finding an excellent fluorescence with a significant Stokes shift in polar solvent (around 139 and 145 nm in DMSO and water, respectively), with an emission band in the visible light in the green and yellow region, and reasonable quantum yield depending on the solvent tested.¹⁵ This modification as well as those achievable by derivatizing the formyl moiety of 4-CHO-MLT (such as oxime, hydrazone, and nitron formation) can be explored to verify the possibility to obtain novel and unusual high affinity MLT fluorescent receptor ligands.

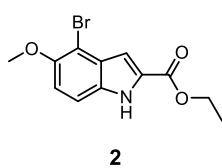
3.4 Experimental section

3.4.1 Materials

All reagents were purchased from best-known commercial suppliers and used without further purification, unless otherwise stated. All reactions were performed under ambient condition, unless otherwise specified.

3.4.2 Experimental procedure

Ethyl 4-bromo-5-methoxy-1*H*-indole-2-carboxylate (**2**)



5-methoxy-1*H*-indole-2-carboxylate **1** (1.0 equiv., 1 g, 4.57 mmol) was stirred in glacial acetic acid (22.9 mL) at 40 °C until only a small amount of indole remained undissolved. Then, bromine (1 equiv., 234 μ L, 4.57 mmol) was added dropwise in open air, maintaining 40°C and a vigorous stirring (800-1000 rpm), and then allowed to stand (200 rpm) at room temperature for 24 h. The resulting dark brown mixture was filtered. The crystalline product was washed sequentially with acetic acid (2 x 4 mL) and cyclohexane (2 x 4 mL) and then dried at 45 °C in vacuo to give **2** as a white solid (1.19 g, 3.98 mmol, 87%).

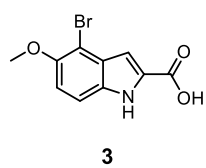
M.p.: 176 °C

MS (ESI): 298, 300 [M+H]⁺

¹H-NMR (CDCl₃, 400 MHz): δ 1.44 (t, J = 7.1 Hz, 3H), 3.95 (s, 3H), 4.44 (q, J = 7.1 Hz, 2H) 7.08 (d, J = 8.9 Hz, 1H), 7.24 (dd, J = 2.2 and 0.8 Hz, 1H), 7.34 (dd, J = 8.9 and 0.8 Hz, 1H), 9.10 (br s, 1H)

Physicochemical data are in agreement with those reported in the literature.¹⁶

4-bromo-5-methoxy-1*H*-indole-2-carboxylic acid (**3**)



Ethyl 4-bromo-5-methoxy-1*H*-indole-2-carboxylate **2** (1.0 equiv., 1.19 g, 3.98 mmol) was suspended in a mixture of THF (1.62 mL) and EtOH (6.5 mL). A aqueous solution of NaOH 3M (3.24 mL) was added and the reaction was stirred for 2h at 80°C. The solution was cooled to 0°C and stirred vigorously for 1h. After, the mixture was acidified (pH 2) using a aqueous solution of HCl 2N. The resulting thick yellow paste was filtered, and the crystalline product was washed with water (3 x 4 mL), and dried at 45 °C in vacuo to give the carboxylic acid **3** (1.05 g, 3.90 mmol, 98%).

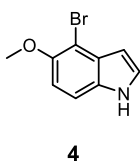
M.p.: 261°C dec

MS (ESI): 268, 270 [M-H]⁻

¹H-NMR (CD₃OD, 400 MHz): δ 3.89 (s, 3H), 7.06 (d, J = 0.8 Hz, 1H), 7.13 (d, J = 8.9 Hz, 1H), 7.40 (dd, J = 8.9 and 0.8 Hz, 1H)

Physicochemical data are in agreement with those reported in the literature.¹⁶

4-bromo-5-methoxy-1*H*-indole (4)



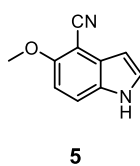
4-Bromo-5-methoxy-1*H*-indole-2-carboxylic acid **3** (1 equiv., 1.05 g, 3.90 mmol) and copper chromite (barium-promoted) (0.25 equiv., 303 mg, 0.975 mmol) were mixed together in freshly distilled quinoline (14 mL). Nitrogen was gently bubbled through the mixture for 5 minutes, then the mixture heated quickly to 220-230°C under nitrogen atmosphere. After 90 minutes the mixture was cooled to room temperature diluted with ethyl acetate (120 ml) and aqueous solution of HCl 2N (75 mL) and stirred for 10 minutes. The mixture was filtered through a pad of Celite, the filtrate dried with Na₂SO₄ and the solvent evaporated. The residue was purified by flash column chromatography on silica gel (ciclohexane:EtOAc 8:2 as eluent) to give 4-bromo-5-methoxy-1*H*-indole **4** (583 mg, 2.58 mmol, 66%).

MS (ESI): 226, 228 [M+H]⁺

¹H-NMR (CDCl₃, 400 MHz): δ 3.94 (s, 3H), 6.57-6.59 (m, 1H), 6.94 (d, *J* = 8.7 Hz, 1H), 7.26-7.28 (m, 1H), 7.31 (dd, *J* = 8.7 and 0.9 Hz, 1H), 8.18 (br s, 1H)

Physicochemical data are in agreement with those reported in the literature.¹⁷

5-methoxy-1*H*-indole-4-carbonitrile (5)



A 10-mL flask was charged with freshly distilled *N,N*-dimethylacetamide (4.3 mL), and the solvent was degassed (15 min) with a vigorous stream of nitrogen. 4-bromo-5-methoxy-1*H*-indole **4** (1.0 equiv., 583 mg, 2.58 mmol) and copper cyanide (0.33 equiv., 690 mg, 7.75 mmol) were added, and the solution was stirred at reflux (165°C) for 20h.

The reaction mixture was cooled to room temperature, poured into a mixture of water (5 mL) and ethyl acetate (5 mL) and filtered through a pad of Celite. The precipitate was washed with EtOAc (3 x 3 mL), and the combined organic phases were separated from the aqueous layer, washed with water (3 x 4 mL) and brine. The solution was dried and concentrated, and the yellow residue was recrystallized (EtOAc:hexane) to give **5** as light yellow solid (rods) (262 mg, 1.52 mmol, 59%).

M.p.: 139-142°C

MS (ESI): 173 [M+H]⁺

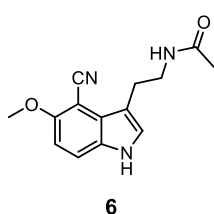
¹H-NMR (CDCl₃, 400 MHz): δ 3.97 (s, 3H), 6.66-6.67 (m, 1H), 6.89 (d, *J* = 8.9 Hz, 1H), 7.36-7.37 (m, 1H), 7.55 (dd, *J* = 8.9 and 0.8 Hz, 1H), 8.39 (br s, 1H)

Physicochemical data are in agreement with those reported in the literature.¹⁶

General procedure for borrowing hydrogen reaction:¹⁸

Under an air atmosphere, a 5 mL vial equipped with a stir bar, was sequentially charged with the appropriate indole **4** or **5** (1.5 equiv.), *N*-(2-hydroxyethyl)acetamide (1 equiv.), [IrCp*Cl₂]₂ (2 mol%), NaOtBu (0.5 equiv.) and *tert*-butanol (2.5 M). The reaction vessel was sealed and the vial was heated to 85°C in a preheated oil bath for 24 h. The mixture was cooled to room temperature and filtered through a SiO₂ plug (EtOAc as eluent). The solvent was evaporated and the residue was purified by flash column chromatography on silica gel.

N-(2-(4-cyano-5-methoxy-1*H*-indol-3-yl)ethyl)acetamide, 4-CN-MLT (**6**)



Compound **6** was obtained following general procedure for borrowing hydrogen reaction (0.7 mmol scale reaction), using 5-methoxy-1*H*-indole-4-carbonitrile **5** (1.5 equiv., 180 mg, 1.05 mmol), *N*-(2-hydroxyethyl)acetamide (1.0 equiv., 72 mg, 0.7 mmol), [IrCp*Cl₂]₂ (0.02 equiv., 11 mg, 0.014 mmol), NaOtBu (0.5 equiv., 34 mg, 0.35 mmol) and *tert*-butanol (1.75 mL).

Flash chromatography: silica gel DCM:acetone 8:2 as eluent.

White solid, 75 mg, 0.29 mmol, 42% yield.

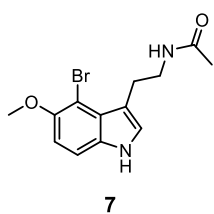
MS (ESI): 258 [M+H]⁺

¹H-NMR (CD₃OD, 400 MHz): δ 1.92 (s, 3H), 3.11 (t, *J* = 7.2 Hz, 2H), 3.49 (t, *J* = 7.2 Hz, 2H), 3.95 (s, 3H), 6.97 (d, *J* = 9.0 Hz, 1H), 7.27 (s, 1H), 7.59 (d, *J* = 9.0 Hz, 1H)

¹³C-NMR (CD₃OD, 400 MHz): δ 22.5, 25.7, 41.8, 57.4, 89.6, 107.3, 112.6, 118.4, 118.6, 128.3, 128.8, 133.5, 159.4, 173.3

HRMS (ESI-TOF) *m/z* calcd. for C₁₄H₁₅N₃NaO₂ [M+Na]⁺: 280.1056; found 280.1067

N-(2-(4-bromo-5-methoxy-1*H*-indol-3-yl)ethyl)acetamide (**7**)



Compound **6** was obtained following general procedure for borrowing hydrogen reaction (1.3 mmol scale reaction), using 4-bromo-5-methoxy-1*H*-indole **4** (1.5 equiv., 440 mg, 1.95 mmol), *N*-(2-hydroxyethyl)acetamide (1 equiv., 134 mg, 1.3 mmol), [IrCp*Cl₂]₂ (0.02 equiv., 21 mg, 0.026 mmol), NaOtBu (0.5 equiv., 62 mg, 0.65 mmol) and *tert*-butanol (3.25 mL).

Flash chromatography: silica gel DCM:MeOH 97:3 as eluent.

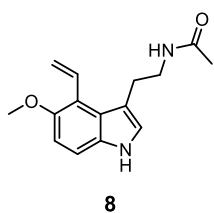
Beige foam, 125 mg, 0.4 mmol, 31%.

MS (ESI): 311, 313 [M+H]⁺

¹H-NMR (CDCl₃, 400 MHz): δ 1.96 (s, 3H), 3.25 (t, *J* = 6.9 Hz, 2H), 3.63 (dd, *J* = 12.9 and 6.9 Hz, 2H), 3.93 (s, 3H), 5.76 (br s, 1H), 6.93 (d, *J* = 8.8 Hz, 1H), 7.07 (d, *J* = 1.8 Hz, 1H), 7.27 (d, *J* = 8.8 Hz, 1H), 8.24 (br s, 1H)

Physicochemical data are in agreement with those reported in the literature.¹⁹

***N*-(2-(5-methoxy-4-vinyl-1*H*-indol-3-yl)ethyl)acetamide (8)¹²**



A 10 mL vial equipped with a stir bar was charged with *N*-(2-(4-bromo-5-methoxy-1*H*-indol-3-yl)ethyl)acetamide **7** (1 equiv., 97 mg, 0.31 mmol), potassium vinyl trifluoroborate (2 equiv., 83 mg, 0.62 mmol), Cs₂CO₃ (3.2 equiv., 323 mg, 0.99 mmol), PdCl₂(dppf)·CH₂Cl₂ complex (0.2 equiv., 51 mg, 0.062 mmol) and subsequently 1,4-dioxane dry (6.2 mL). The mixture was degassed (20 min) with

a vigorous stream of Argon. The vial was transferred to an oil bath pre-heated to 90 °C and the reaction refluxed under Argon for 20 h. The solution was cooled to room temperature and diluted with EtOAc and water. The organic phase was separated and the aqueous phase was extracted with EtOAc (3 x 50 mL). The combined organic phases were dried over Na₂SO₄, concentrated and the residue was purified by flash chromatography (DCM:MeOH 97:3 as eluent) to give the title compound **8** (70 mg, 0.27 mmol, 88%), which can be directly use in the next reaction without purification.

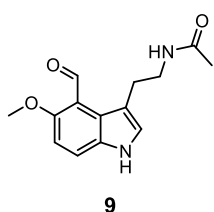
MS (ESI): 259 [M+H]⁺

¹H-NMR ((CD₃)₂CO, 400 MHz): δ 1.85 (s, 3H), 3.0 (t, *J* = 7.4 Hz, 2H), 3.42, (dt, *J* = 7.4 and 5.9 Hz, 2H), 3.80 (s, 3H), 5.48 (dd, *J* = 11.7 and 2.8 Hz, 1H), 5.77 (dd, *J* = 17.7 and 2.8 Hz, 1H), 6.91 (d, *J* = 8.8 Hz, 1H), 7.07 (br s, 1H), 7.15 (d, *J* = 2.4 Hz, 1H), 7.21-7.28 (m, 2H), 9.94 (br s, 1H)

¹³C-NMR ((CD₃)₂CO, 400 MHz): δ 23.0, 28.9, 41.1, 57.6, 110.2, 111.7, 113.8, 119.0, 119.9, 125.9, 126.6, 132.6, 134.3, 152.7, 169.7

HRMS (ESI-TOF) *m/z* calcd. for C₁₅H₁₈N₂NaO₂ [M+Na]⁺: 281.1260; found 281.1269

***N*-(2-(4-formyl-5-methoxy-1*H*-indol-3-yl)ethyl)acetamide, 4-CHO-MLT (9)¹²**



A vial equipped with a stir bar was charged with *N*-(2-(5-methoxy-4-vinyl-1*H*-indol-3-yl)ethyl)acetamide **8** (1 equiv., 70 mg, 0.27 mmol), subsequently dissolved in a mixture of THF (3.8 mL) and H₂O (0.97 mL). Then, K₂OsO₄·2H₂O (0.15 equiv., 14 mg, 0.038 mmol), 2,6-lutidine (4 equiv., 126 μL, 1.08 mmol) and NaIO₄ (3.1 equiv., 179 mg, 0.84 mmol) were added to the stirring biphasic solution. The

reaction was stirred at room temperature for 90 minutes before quenching with a saturated aqueous solution of NaHCO₃ (15 mL) and then extracted with EtOAc (3 x 30 mL). The combined organic phases were dried over Na₂SO₄ and concentrated under reduced pressure. Purification by silica gel chromatography (DCM:MeOH 97:3 as eluent) gave the title compound **9** as an amorphous light brown solid (18 mg, 0.07 mmol, 26%).

MS (ESI): 261 [M+H]⁺

$^1\text{H-NMR}$ ($(\text{CD}_3)_2\text{CO}$, 400 MHz): δ 1.83 (s, 3H), 3.13 (t, $J = 7.1$ Hz, 2H), 3.30-3.35 (m, 2H), 3.96 (s, 3H), 6.96 (br s, 1H), 7.01 (d, $J = 8.9$ Hz, 1H), 7.33 (d, $J = 2.6$ Hz, 1H), 7.68 (d, $J = 8.9$ Hz, 2H), 10.36 (br s, 1H), 10.69 (s, 1H)

$^{13}\text{C-NMR}$ ($(\text{CD}_3)_2\text{CO}$, 400 MHz): δ 22.1, 28.2, 40.9, 56.8, 107.2, 114.5, 117.9, 119.0, 124.1, 128.5, 133.6, 159.5, 168.7, 190.6

HRMS (ESI-TOF) m/z calcd. for $\text{C}_{14}\text{H}_{16}\text{N}_2\text{NaO}_3$ $[\text{M}+\text{Na}]^+$: 283.1053; found 283.1055

3.5 References

- ¹ Granier S, Kobilka B. A new era of GPCR structural and chemical biology. *Nat Chem Biol.* **2012**, 8(8), 670-673
- ² Cottet M, Faklaris O, Zwier JM, Trinquet E, Pin J-P, Durroux T. Original Fluorescent Ligand-Based Assays Open New Perspectives in G-Protein Coupled Receptor Drug Screening. *Pharmaceuticals.* **2011**, 4(1), 202-214
- ³ Niles LP. [³H] melatonin binding in membrane and cytosol fractions from rat and calf brain. *J Pineal Res.* **1987**, 4(1), 89-98
- ⁴ Vakkuri O, Lämsä E, Rahkamaa E, Ruotsalainen H, Leppäluoto J. Iodinated melatonin: preparation and characterization of the molecular structure by mass and 1H NMR spectroscopy. *Anal Biochem.* **1984**, 142(2), 284-9
- ⁵ Schwartz C, Bartell P, Cassone V, Smotherman M. Distribution of 2-[I]iodomelatonin binding in the brain of Mexican free-tailed bats (*Tadarida brasiliensis*). *Brain Behav Evol.* **2009**, 73(1), 16-25
- ⁶ Ma Z, Du L, Li M. Toward fluorescent probes for G-protein-coupled receptors (GPCRs). *J Med Chem.* **2014**, 57(20), 8187-203
- ⁷ Fang Y. Ligand-receptor interaction platforms and their applications for drug discovery. *Expert Opin Drug Discov.* **2012**, 7(10), 969-88
- ⁸ Wu PW, Cheng YM, Hsieh WT, Wang YH, Wei CY, Chou PT. 7-Azamelatonin: efficient synthetic routes, excited-state double proton transfer properties and biomedical implications. *ChemMedChem.* **2007**, 2(7), 1071-1075
- ⁹ Thireau J, Marteaux J, Delagrangé P, Lefoulon F, Dufourny L, Guillaumet G, Suzenet F. Original Design of Fluorescent Ligands by Fusing BODIPY and Melatonin Neurohormone. *ACS Med Chem Lett.* **2013**, 5(2), 158-61
- ¹⁰ Gbahou F, Cecon E, Viault G, Gerbier R, Jean-Alphonse F, Karamitri A, Guillaumet G, Delagrangé P, Friedlander RM, Vilardaga JP, Suzenet F, Jockers R. Design and validation of the first cell-impermeant melatonin receptor agonist. *Br J Pharmacol.* **2017**, 174(14), 2409-2421
- ¹¹ De la Fuente Revenga M, Herrera-Arozamena C, Fernández-Sáez N, Barco G, García-Orue I, Sugden D, Rivara S, Rodríguez-Franco MI. New coumarin-based fluorescent melatonin ligands. Design, synthesis and pharmacological characterization. *Eur J Med Chem.* **2015**, 103, 370-3
- ¹² Micikas RJ, Ahmed IA, Acharyya A, Smith AB, Gai F. Tuning the electronic transition energy of indole via substitution: application to identify tryptophan-based chromophores that absorb and emit visible light. *Phys Chem Chem Phys.* **2021**, 23(11), 6433-6437

-
- ¹³ Hilaire MR, Ahmed IA, Lin CW, Jo H, DeGrado WF, Gai F. Blue fluorescent amino acid for biological spectroscopy and microscopy. *Proc Natl Acad Sci U S A*. **2017**, 114(23), 6005-6009
- ¹⁴ You M, Fan H, Wang Y, Zhang W. Aldehyde-derivatized indoles as fluorescent probes for hydration environments. *Chemical Physics* **2019**, 526, 110438
- ¹⁵ Micikas RJ, Acharyya A, Smith AB, Gai F. Synthesis and characterization of the fluorescence utility of two Visible-Light-Absorbing tryptophan derivatives. *Chemical Physics Letters* **2022**, 795, 139553
- ¹⁶ Kruse L. I.; Meyer M. D. Ergoline synthons. 2. Synthesis of 1,5-dihydrobenz[cd]indol-4(3H)-ones and 1,3,4,5-tetrahydrobenz[cd]indol-4-amines. *J. Org. Chem.* **1984**, 49, 4761–4768
- ¹⁷ Johansson G.; Angbrant J.; Ringom R.; Hammer K.; Ringberg E.; Lindqvist B.; Brandt P.; Beierlein K.; Nilsson B. M. Indoles as 5-HT₆ modulators. *Patent WO2008003703*, **2010**
- ¹⁸ Hall C.J.J.; Goundry W. R. F.; Donohoe T. J. Hydrogen-Borrowing Alkylation of 1,2-Amino Alcohols in the Synthesis of Enantioenriched γ -Aminobutyric Acids. *Angew. Chem. Int. Ed.* **2021**, 60, 6981-6985
- ¹⁹ Somei M.; Fukui Y.; Hasegawa M.; Oshikiri N.; Hayashi T. Syntheses of Melatonin and Its Derivatives. *Heterocycles*, **2000**, 53, 1725-1736

Chapter 4. Novel *N*-(anilinoethyl)amide melatonergic ligands with improved water solubility and metabolic stability

This chapter is based on: Ferlenghi F, Mari M, Gobbi G, Elisi GM, Mor M, Rivara S, Vacondio F, Bartolucci S, Bedini A, **Fanini F**, Spadoni G. *N*-(Anilinoethyl)amide Melatonergic Ligands with Improved Water Solubility and Metabolic Stability. *ChemMedChem.* **2021**, 16(19), 3071-3082

4.1 Introduction

As outlined in the general introduction, different series of melatonergic ligands have been developed over the years. Among these, the class of *N*-anilinoethylamides has proved to be one of the most interesting and versatile. These compounds showed a generally good affinity for MLT receptors and can be easily chemically modified giving predictable modulations of selectivity and intrinsic activity. In particular, the increase of size of the substituent on the aniline nitrogen progressively shifted the selectivity toward the MT₂ receptor and decreased intrinsic activity.

The *N*-methyl derivative UCM793 was a nanomolar nonselective MT₁/MT₂ agonist, the *N*-phenyl derivative UCM765 showed 46-times selectivity for the MT₂ receptor and a partial agonist behavior, and UCM800, carrying a bulky β-naphthyl substituent, resulted a potent MT₂-selective antagonist (**Figure 24**).¹

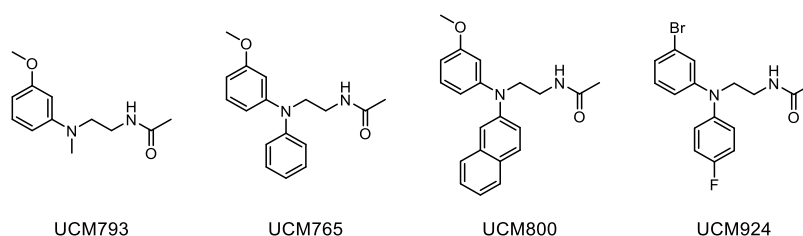


Figure 24 Representative MLT ligands belonging to the *N*-anilinoethylamides class.

Appropriate preclinical studies in rats and mice with UCM765 and its metabolically more stable analogue UCM924 have been conducted to investigate their hypnotic², antinociceptive³ or anxiolytic⁴ properties and to evaluate the involvement of each receptor subtype. When subcutaneously administered to rats (40 mg·kg⁻¹), UCM765 was able to reduce latency and to increase the duration of non-rapid eye movement (NREM) sleep, without affecting REM sleep duration.² This activity was related to the activation of MT₂ receptors, since its hypnotic effect was prevented by the administration of the MT₂-selective antagonist 4-P-PDOT or genetic deletion of the MT₂ receptor.

Despite a sub-nanomolar affinity for MT₂ receptors, UCM765 exhibits hypnotic effects in rats only when administered at high doses and shows a very short half-life in the presence of rat oxidative

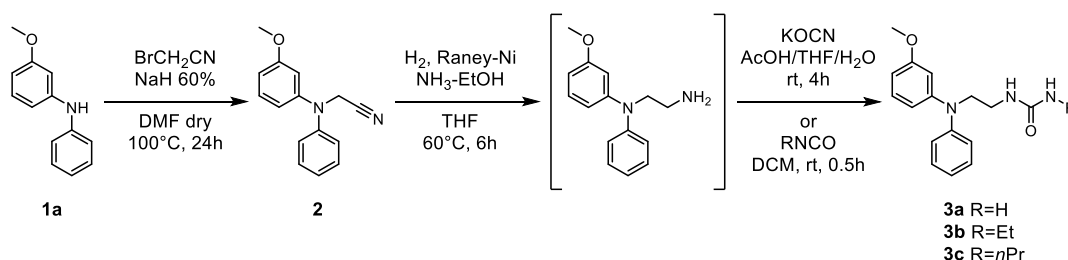
enzymes. The oral bioavailability of UCM765 in rats was less than 2% when administered as a 40% aqueous solution of DMSO.⁵

Therefore, modest metabolic stability associated with poor aqueous solubility greatly limited the use of these compounds in research and functional applications. Thus, to overcome these limitations, we prepared novel *N*-anilinoethylamide derivatives, designed taking advantage of knowledge acquired from previous studies.⁶ Different strategies were pursued in order to enhance the water solubility with respect to the parent compounds UCM765 and UCM924 such as insertion of hydrophilic groups on the phenyl substituent, substituting the amido moiety in the side chain with an urea group, replacement of the UCM765 phenyl ring with a 4-pyridyl substituent and/or increasing the basic nature of the resulting compounds.

4.2 Results and discussion

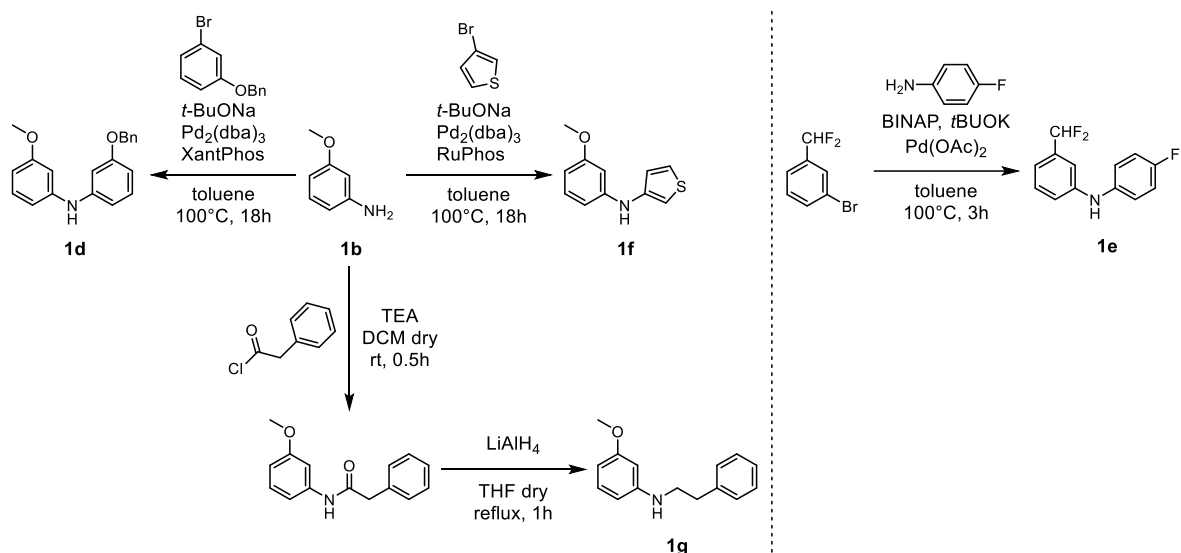
4.2.1 Chemistry

The three melatonin urea-based ligands were synthesized, as shown in **Scheme 5**. The crude *N*¹-3-(methoxyphenyl)-*N*¹-phenylethane-1,2-diamine was obtained by the *N*-cyanoalkylation of 3-methoxy-*N*-phenylaniline **1a** with bromoacetonitrile in the presence of sodium hydride, and subsequent hydrogenation of the intermediate nitrile **2** with Raney Nickel, in the presence of 1M solution of ammonia in EtOH.¹ The reaction of the crude diamine with potassium cyanate in aqueous acidic medium afforded the monosubstituted urea **3a**, while using ethyl- or *n*-propyl isocyanate the disubstituted urea **3b** and **3c** were obtained.



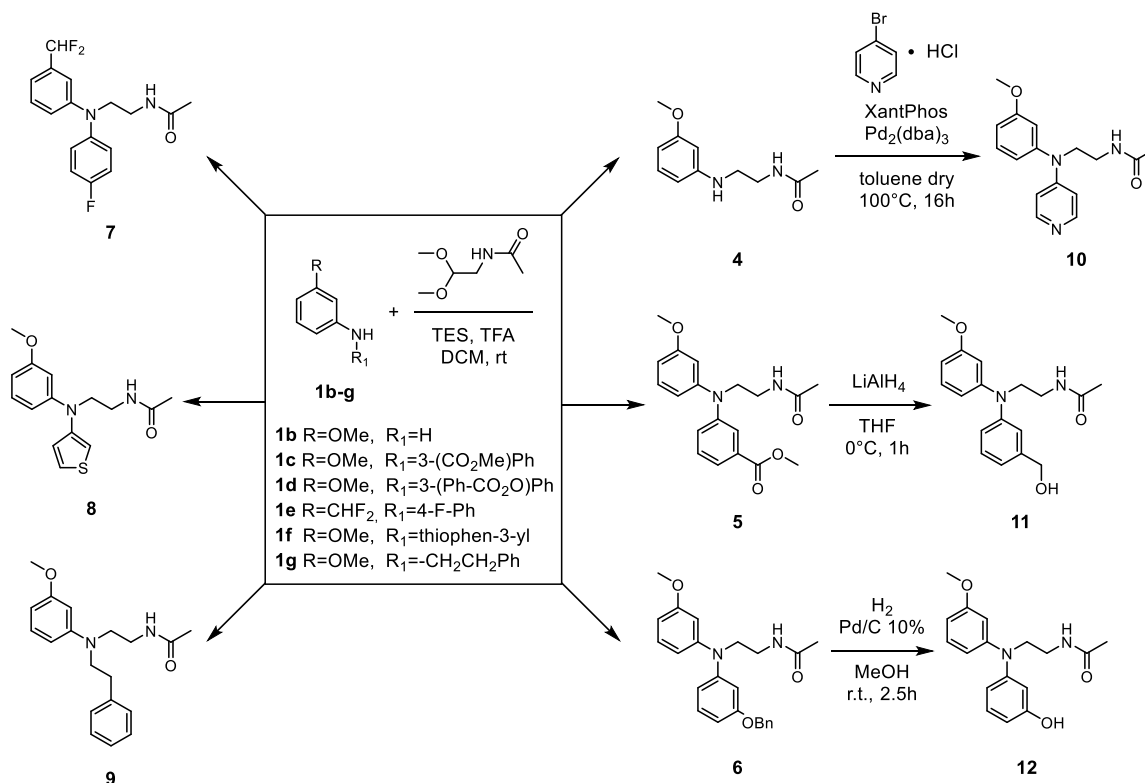
Scheme 5 Synthesis of *N*-[2-(diphenylamino)ethyl]ureas **3a-c**.

The *N*-(anilinoethyl)acetamido derivatives **4-9** were prepared starting from the crucial intermediates **1b-c**, which are commercially available, and **1d-g**, obtained following known procedures for similar compounds (**Scheme 6**). Buchwald–Hartwig amination afforded the desired aniline **1d-f**, using the suitable catalyst depending on the substrate and the appropriate aniline and Br-aryl starting reagents, while **1g** was obtained by *N*-acylation of **1b** with phenylacetyl chloride followed by amide reduction.



Scheme 6 Synthesis of *N,N*-diarylamines **1d-f** and *N*-phenethyl-3-methoxyaniline **1g**.

With the crucial intermediates in our hand, we proceeded to synthesize compounds **4-12** (**Scheme 7**). The reductive *N*-alkylation of the suitable aniline **1b-g** with *N*-(2,2-dimethoxyethyl)acetamide in the presence of triethylsilane and trifluoroacetic acid afforded the final compounds **7, 8, and 9** and the intermediates **4, 5** and **6**.

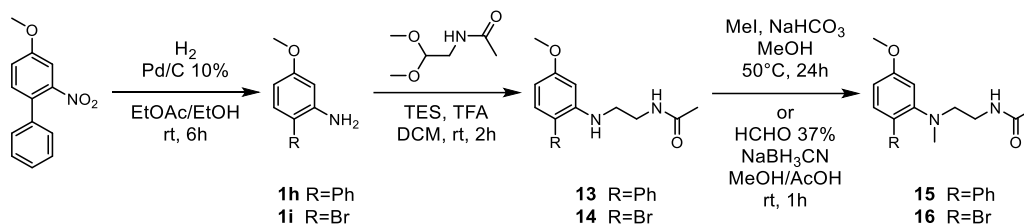


Scheme 7 Synthesis of *N*-[2-(diarylamino)ethyl]amides **7, 8, 10, 11, and 12**, and *N*-[2-(*N*-phenethylanilino)ethyl]acetamide **9**.

The 4-pyridyl aniline derivative **10** was synthesized by palladium-catalysed amination [Pd₂(dba)₃/XantPhos/*t*-BuONa] of **4** with 4-bromopyridine hydrochloride. To prepare the 3-

(hydroxymethyl)phenyl derivative **11**, the corresponding methyl ester **5** was reduced with lithium aluminum hydride, while the 3-hydroxyphenyl analog **12** was obtained by *O*-debenzylation of compound **6**, using H₂/Pd–C.

As illustrated in **Scheme 8**, the *N*-methyl-2-substituted-aniline derivatives **15** and **16** were synthesized by reductive *N*-alkylation of the corresponding 2-substituted anilines **1h** and **1i** with *N*-(2,2-dimethoxyethyl)acetamide (same procedure used for compounds **4-9**) and subsequent *N*-methylation with MeI or reductive amination with HCHO/NaBH₃CN (**15** and **16**, respectively).



Scheme 8 Synthesis of *N*-[2-(2-substituted-5-methoxyanilino)ethyl]acetamides **15** and **16**.

4.2.2 SAR discussion and biological evaluation

In vitro pharmacological studies on the new synthesized compounds was conducted at Cerep (Celle-Lévescault, France), including binding affinity and efficacy assays. Binding affinities were determined displacing 2-[¹²⁵I]-iodomelatonin in competition experiments on human MT₁ and MT₂ receptors expressed in CHO cells and are reported in **Table 5**, together with data for reference compounds UCM765 and UCM924 tested in the same experimental conditions.^{7,8} Regarding the efficacy assays, agonist activity at MT₁ receptors was evaluated using a cell impedance assay exploiting cellular dielectric spectroscopy⁷ and at MT₂ receptors using a cAMP assay via a fluorometric method⁸.

Starting from the lead compound UCM765 several new compounds were developed. Compounds **3a-c**, deriving from bioisosteric modification of the amide in the side chain with an urea group, showed a reduced binding affinity, especially at the MT₁ receptor. The most potent urea was compound **3b** achieving a binding affinity at the MT₂ receptor similar to that of UCM765. The lower affinity of urea analogues compared to amide derivatives has also been observed for other melatonergic ligands, such as agomelatine and its structural analogs⁹ or tetrahydroquinolines¹⁰, but this modification could have improved their water solubility.

Replacement of the metabolically labile methoxy substituent with a difluoromethyl group (**7**) was detrimental for the interaction with the receptors, leading to reduced binding affinities. On the contrary, the 3-thienyl group in compound **8** provided a good alternative to *N*-phenyl substituent of UCM765, resulting in the most potent compound of the series.

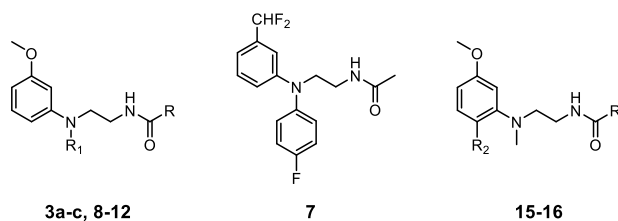


Table 5 Binding affinity of melatonergic ligands at human MT_1 and MT_2 receptors.

Compound	R	R ₁	R ₂	MT ₁ K_i [nM] ^a	MT ₂ K_i [nM] ^a
UCM765				1.6 ± 0.14	0.29 ± 0.10
UCM924				>100	1.4 ± 0.08
3a	NH ₂	Phenyl		>100	10 ± 0.13
3b	NHEt	Phenyl		20 ± 0.45	0.65 ± 0.03
3c	NH <i>n</i> Pr	Phenyl		57 ± 0.10	1.7 ± 0.08
7				>100	35 ± 0.35
8	CH ₃			0.7 ± 0.10	0.07 ± 0.02
9	CH ₃			>100	2.1 ± 0.15
10	CH ₃			>100	>100
11	CH ₃			>100	3.5 ± 0.05
12	CH ₃			53 ± 1.6	1.4 ± 0.15
15			Phenyl	32 ± 0.80	1.7 ± 0.13
16			Br	18 ± 0.70	2.4 ± 0.10

K_i values are calculated from IC_{50} values obtained from competition curves by the method of Cheng and Prusoff¹¹ and are the mean ± standard deviation of three determinations.

The more hydrophilic compounds **10**, **11**, and **12**, obtained by replacement of UCM765 phenyl ring with a 4-pyridyl substituent or by introduction of a *meta*-hydroxymethyl- or a *meta*-hydroxy-substituent on the UCM765 phenyl ring, respectively, showed no appreciable affinity for MT_1 receptor. On the other hand, the hydroxy-substituted compounds **11** and **12** displayed only a limited reduction of binding affinity at the MT_2 receptor. Compounds **11** and **12** should accommodate hydroxyl groups in the aromatic subpocket, which tolerance could be more pronounced at the MT_2 receptor. Moreover, simulations identified Tyr94^{2,58} at the MT_2 receptor as a polar residue able to interact with hydrophilic substituents (**Figure 25A**).

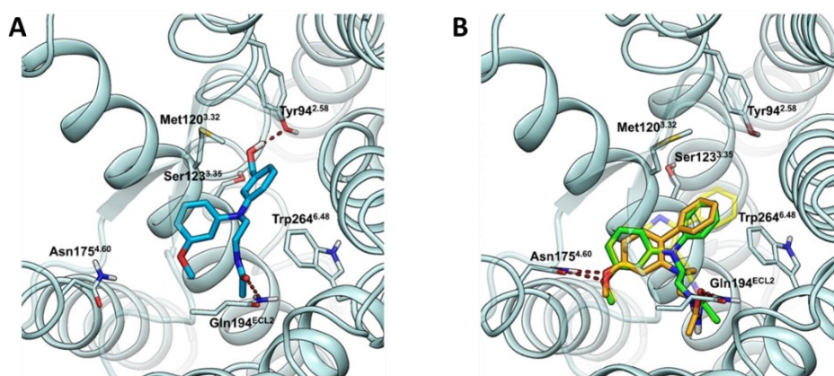


Figure 25 *A)* Representative snapshot of a molecular dynamics simulation of compound **11** in complex with the MT₂ receptor. The ligand forms hydrogen bonds with Gln194 in ECL2 and Tyr94, while the interaction between the methoxy group and Asn175, proposed by docking studies, is lost; *B)* Proposed binding mode for UCM765 (green carbons) and compound **15** (orange carbons) into the MT₂ crystal structure (PDB:6ME6), observed from the extracellular side of the receptor. Hydrogen bonds are shown as red dashed lines. Co-crystallized 2-phenylmelatonin is shown with shaded yellow carbons.

To improve the water solubility of the ligands, while preserving their high binding affinity and selectivity toward the MT₂ receptor, we also designed more basic UCM765 derivatives. In particular, replacement of the diphenylamino scaffold of UCM765 with an *N*-phenyl-*N*-methyl one, and shift of the lipophilic *N*-phenyl substituent on the anisole ring (in the para position with respect to the methoxy group) led to compound **15** characterized by improved water solubility and maintenance of a limited selectivity for the MT₂ receptor. On the other hand, insertion of a bromine atom on the ortho position of the phenyl-methylamino scaffold led to a more soluble derivative (compound **16**) endowed with higher microsomal stability.

Aiming at the same goal, introduction of an ethane spacer, linking the nitrogen of the aniline to the phenyl substituent, gave the more basic derivative **9**. Considering these more basic *N*-alkylanilino-ethylamido derivatives (**9**, **15** and **16**), the phenethyl substituted derivative **9** was tolerated only at the MT₂ receptor, while the *N*-phenyl-*N*-methyl-ethylamides **15** and **16** displayed good binding affinity at both receptors.

The potency and MT₂-selectivity observed for the latter derivatives can be explained by their structural similarity with the lead UCM765. Superposition of docking solutions obtained for UCM765 and compound **15** in the MT₂ receptor crystal structure highlights the same binding site occupation and interactions. Compounds **15** (**Figure 25B**) and **16** have the phenyl and bromine substituents superimposed to the phenyl ring of co-crystallized 2-PhMLT and docked UCM765 in docking calculations, highlighting their complementarity with the binding pocket.

4.2.3 Physicochemical characterization

Experimental lipophilicity and solubility measurements as well as metabolic stability assays in rat and human liver microsomes of the new *N*-anilinoethylamides were performed at the University of Parma, and the results are reported in **Table 6**.

Table 6 Solubility, rat and human microsomal stability, and lipophilicity of melatonergic ligands.

Comp.	Solubility pH 1.0 [$\mu\text{g/ml}$]	Solubility pH 7.4 [$\mu\text{g/ml}$]	$t_{1/2}$ Rat LM ^a	Cl ⁱ ^b Rat LM ^a	$t_{1/2}$ Human LM ^a	Cl ⁱ ^b Human LM ^a	Log $D_{\text{Oct},7.4}$
UCM765	125 \pm 5	104 \pm 5	1.7 \pm 0.4	408 \pm 85	40.8 \pm 1.1	17 \pm 1	2.93 \pm 0.01
UCM924	6.9 \pm 0.1	5.1 \pm 0.2	18.2 \pm 2.8	38.1 \pm 6.0	71.2 \pm 3.4	9.7 \pm 0.5	3.84 \pm 0.05
3a	363.9 \pm 3.7	311.4 \pm 2.6	15.7 \pm 0.4	44.2 \pm 1.0	77.5 \pm 13.4	9.1 \pm 1.5	2.65 \pm 0.02
3b	14.9 \pm 0.6	10.2 \pm 1.7	7.1 \pm 0.5	98.1 \pm 6.8	15.4 \pm 1.0	45.1 \pm 3.0	3.30 \pm 0.02
3c	17.7 \pm 0.9	14.3 \pm 0.1	3.2 \pm 0.3	218.4 \pm 21.2	7.4 \pm 1.2	95.7 \pm 14.7	3.91 \pm 0.02
7	54.9 \pm 1.1	40.6 \pm 0.1	12.2 \pm 1.5	58.0 \pm 8.2	55.4 \pm 6.8	12.8 \pm 1.3	3.45 \pm 0.02
8	161.5 \pm 4.4	92.5 \pm 3.5	4.0 \pm 0.5	175.4 \pm 22.3	40.1 \pm 5.3	17.5 \pm 2.4	2.74 \pm 0.01
9	>1000 ^d	109.6 \pm 6.9	2.9 \pm 0.5	247.3 \pm 34.2	7.2 \pm 0.5	96.7 \pm 6.3	3.44 \pm 0.02
10	>1000 ^d	1019.6 \pm 93.7	100.9% \pm 3.5 ^c	N.D.	101.5% \pm 2.7 ^c	N.D.	0.41 \pm 0.01
11	>1000 ^d	>1000 ^d	2.9 \pm 0.3	241.4 \pm 28.5	64.9 \pm 6.9	10.8 \pm 1.2	2.04 \pm 0.01
12	95.9 \pm 4.2	118.7 \pm 2.8	3.3 \pm 0.6	217.3 \pm 44.6	66.2 \pm 2.8	10.5 \pm 0.4	2.42 \pm 0.02
15	>1000 ^d	339.5 \pm 9.7	1.5 \pm 0.1	468.9 \pm 12.9	11.2 \pm 0.7	61.9 \pm 3.8	3.11 \pm 0.02
16	>1000 ^d	822.9 \pm 34.7	17.6 \pm 1.5	39.6 \pm 3.1	78.5 \pm 12.2	8.9 \pm 1.4	1.85 \pm 0.01

^a LM: Liver Microsomes. ^b Clⁱ: Intrinsic Clearance ($\mu\text{Lmin}^{-1} \text{1mg prot}^{-1}$). ^c Percentage of compound left after 60 min, 37°C. ^d Weighted compound completely dissolved in the chosen buffer at 1000 $\mu\text{g/mL}$. N.D.: not determined. Experiments were performed in triplicate, and values are reported as the mean \pm standard deviation.

Thermodynamic solubility was measured at physiological and acidic pH (pH=1.0). Diarylamine derivatives generally had similar solubility at the two pH values, usually slightly higher at pH=1.0. The most soluble compounds are the primary urea **3a**, the hydrophilic and basic 4-pyridyl derivative **10**, and the *m*-hydroxymethyl-substituted compound **11**. The solubility of the latter compound is greater than 1 mg/mL at both pH values. A higher solubility at acidic than neutral pH

was observed for phenylalkylamides **9**, **15**, and **16**, with a solubility greater than 1 mg/mL at pH=1.0. Compared to UCM765, compound **16** was also significantly more soluble at pH=7.4.

Metabolic stability was evaluated in the presence of rat and human liver microsomes and expressed as pseudo half-life and as intrinsic clearance in **Table 6**. All the compounds were susceptible to oxidative metabolism at different degrees, except for the 4-pyridyl derivative **10**, which remained unaltered after 60 min of incubation with microsomes of both species. The primary urea **3a** was significantly more stable than UCM765. It displayed half-lives close to those of the metabolically protected UCM924.⁵ Alkyl substitutions of the urea group (**3b** and **3c**) reduce the metabolic stability in microsomes of both species. At the same time, it increases the compound lipophilicity ($\text{Log}D_{\text{Oct},7.4}$). The hydroxy-substituted derivatives **11** and **12** slightly increased rat and human microsomal stability by approximately 1.5 fold compared to the unsubstituted precursor UCM765. Besides urea derivative **3a**, the other most stable compounds are **7** and **16**. Compound **7** has a similar half-life to UCM924, while compound **16** shows improved microsomal stability, probably due to the lack of metabolically labile phenyl ring and to lower lipophilicity compared to UCM765.

Taking together all the results of binding affinity, solubility, and metabolic stability, compounds **11** and **16** were selected for further characterization. The *m*-hydroxymethyl derivative **11** retained an MT₂-selective profile with high receptor binding affinity, and a good solubility in both acidic and neutral pH. Its limited metabolic stability might be improved by preparing suitable prodrugs, temporarily masking the hydroxyl group, which is most likely responsible for the short half-life. The *o*-bromo-anilinoethylamido derivative **16** is a potent MLT receptor agonist endowed with better microsomal stability and water solubility.

Then, the two novel melatonin receptor ligands **11** and **16** have been studied in terms of functionality (**Table 7**).

Table 7 Intrinsic activity of select *N*-(anilinoethyl)amides **11** and **16**.

Compound	MT ₁ EC ₅₀ [nM] ^a	E _{max} [%] ^b	MT ₂ EC ₅₀ [nM] ^c	E _{max} [%] ^b
11	53 ± 0.5	32 ± 0.3	6.8 ± 0.3	71 ± 2
16	4.4 ± 0.2	94 ± 4	0.83 ± 0.05	93 ± 2

^a EC₅₀ values obtained from a cell impedance assay. ^b The E_{max} values are referred to as the % of melatonin response. ^c EC₅₀ values obtained from a cAMP assay. Experiments were performed in triplicate, and values are reported as the mean ± standard deviation.

In the cAMP functional assay, compound **11** behaved as an MT₂-selective partial agonist, as UCM765¹. On the other hand, compound **16** displayed a full agonist profile with potency at the MT₂ receptor similar to that of melatonin.

4.2.4 Pharmacokinetic evaluation

To evaluate the *in vivo* behavior of the two melatonergic ligands **11** and **16**, a preliminary pharmacokinetic (PK) study was carried out in male Sprague-Dawley rats and the experiments were conducted at NiKem Research (Baranzate – Milan – Italy). The compounds were administered as intravenous bolus (IV) or oral gavage (PO) at doses of 5 or 40 mg kg⁻¹, respectively. Quantitative analysis was carried out by UPLC/MS/MS, and the plasma concentration profiles are shown in **Figure 26**.

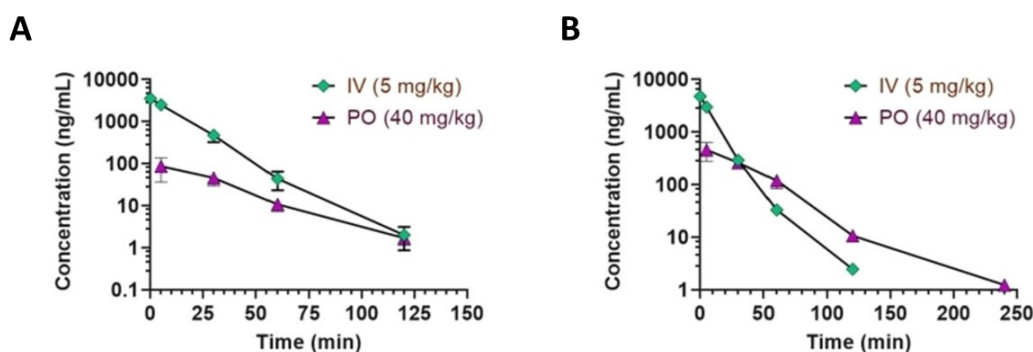


Figure 26 Plasma concentration (semilogarithmic scale) profiles of compounds **11** (A) and **16** (B) in Sprague-Dawley rats after single intravenous (5 mg kg⁻¹) or oral (40 mg kg⁻¹) administration.

The main pharmacokinetic parameters are reported in **Table 8**.

Table 8 Main pharmacokinetic parameters in rat plasma obtained for compounds **11** and **16**.

Parameter ^a	IV bolus (5 mg kg ⁻¹)		PO gavage (40 mg kg ⁻¹)	
	11	16	11	16
AUC _{IV 0-∞} [ng min mL ⁻¹]	66508.2 ± 9656.1	66017.0 ± 7842.4	2626.5 ± 1037.9	19129.8 ± 4802.3
C _{max} [ng mL ⁻¹]	2757.5 ± 478.6	2973.0 ± 383.9	75.6 ± 39.7	455.7 ± 178.5
t _{1/2} [min]	11.5 ± 1.0	13.5 ± 0.3	19.8 ± 1.9	26.2 ± 0.9
CL [mL min ⁻¹ kg ⁻¹]	76.2 ± 10.3	76.4 ± 8.8	-	-
V _{ss} [L kg ⁻¹]	0.9 ± 0.2	0.7 ± 0.1	-	-
F [%]	-	-	0.5	3.6

^a AUC: area under the plasma concentration-time curve of the drug; t_{1/2}: half-life; CL: volume of plasma cleared of the drug per unit time; V_{ss}: volume of distribution at the steady state defined by the amount of drug in the body over the concentration of the drug in the plasma at the steady state; F: percentage of the dose reaching blood circulation after oral administration.

Upon single IV administration, they displayed limited plasma half-life (compound **11**, 11.5 min; compound **16**, 13.5 min) and moderately-high plasma clearance (**11**, 76.2 mL min⁻¹kg⁻¹; **16**, 76.4

mL min⁻¹kg⁻¹). For **11**, the C_{max} was 2757.5 ng mL⁻¹, while for **16**, it was 2973.0 ng mL⁻¹. The steady-state volume of distribution (V_{ss}) was moderate (**11**, 0.9 L kg⁻¹; **16**, 0.7 L kg⁻¹), indicating a moderate propensity to distribute out from the plasma compartment. After PO administration, their plasma half-life was longer (**11**, 19.8 min; **16**, 26.2 min) with a corresponding C_{max} of 75.6 mg mL⁻¹ for **11** and 455.7 ng mL⁻¹ for **16**. The oral bioavailability was very low for **11** and moderate for **16**. Even though far from optimal, the PK profile of compound **16** was more favorable than those of compound **11**, with greater oral absorption and more prolonged plasma exposure, most likely related to its higher *in vitro* liver microsomal stability.

4.3 Conclusion

Novel *N*-(anilinoethyl)amide melatonergic ligands have been designed to improve the physicochemical properties and metabolic stability of the MT₂-selective partial agonist UCM765. Different strategies were applied, including the replacement of metabolically liable substituents, introduction of hydrophilic groups, and structural modifications. *In vitro* studies showed compounds with good receptor binding affinities, such as the thienyl derivative **8**, the *meta*-hydroxymethyl analog **11**, or the *p*-Br-phenylalkylamide derivative **16**, some of which with high water solubility and improved microsomal stability. Compounds **11** and **16** were selected for a preliminary PK study and the (2-Br-5-methoxyanilino)ethylamide derivative **16** provided the most favorable PK profile, showing greater plasma exposure but with a short half-life. Compound **16** can undergoes to further chemical optimization and pharmacological investigation.

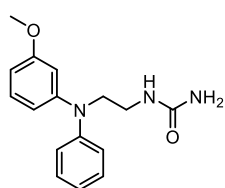
4.4 Experimental section

4.4.1 Materials

3-Methoxy-*N*-phenylaniline (**1a**), 3-methoxyaniline (**1b**), 1-(benzyloxy)-3-bromobenzene, 3-(difluoromethyl)bromobenzene, 3-bromothiophene, 2-bromo-5-methoxyaniline (**1i**) and 4-bromopyridine·HCl were purchased from commercial suppliers and used without further purification.

4.4.2 Experimental procedures

1-(2-((3-methoxyphenyl)(phenyl)amino)ethyl)urea (**3a**)



3a

A solution of the nitrile **2**¹ (1 equiv., 262 mg, 1.1 mmol) in THF (7 mL) and 1M NH₃ in EtOH (1.5 mL) was hydrogenated over Raney nickel (4 atm of H₂) for 6h at 60°C. The catalyst was filtered on a celite pad and the filtrate was concentrated *in vacuo*, to give a crude oily amine which was used in the next step without any further purification. A solution of KOCN (1.7 equiv., 150 mg, 1.85 mmol) in H₂O (0.85 mL) was added dropwise to a solution of the above crude amine in THF/H₂O/acetone (1:1:0.5 mL) and the resulting mixture was stirred at room temperature for 4 h. The reaction mixture was neutralized with a saturated aqueous solution of NaHCO₃, and then extracted with EtOAc. The combined organic phases were washed with brine, dried (Na₂SO₄) and concentrated under reduced pressure. The resulting crude residue was purified by flash chromatography (silica gel; EtOAc as eluent) to give **3a** as a white solid (45% yield). Crystallization: diethyl ether:petroleum ether
M.p.: 78–79 °C

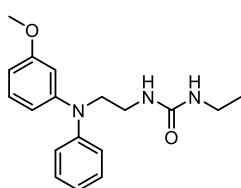
ESI MS (m/z): 286 [M+H]⁺

¹H NMR (400 MHz, CDCl₃) δ: 3.34 (bt, 2H, *J*=6.5 Hz), 3.73 (s, 3H), 3.80 (t, 2H, *J*=6.5 Hz), 4.57 (brs, 2H), 5.39 (brs, 1H), 6.47 (dd, 1H, *J*=2.5 and 8.0 Hz), 6.54–6.57 (m, 2H), 6.96–7.00 (m, 1H), 7.03–7.06 (m, 2H), 7.13 (dd, 1H, *J*₁=*J*₂=8.0 Hz), 7.24–7.28 (m, 2H)

¹³C NMR (100 MHz, CDCl₃) δ: 38.2, 51.8, 55.2, 106.1, 106.3, 112.7, 122.2, 122.4, 129.5, 130.0, 147.6, 149.3, 159.2, 160.6.

HRMS (ESI): *m/z* calculated for C₁₆H₂₀N₃O₂, [M+H]⁺ 286.1556. Found: 286.1555

1-ethyl-3-(2-((3-methoxyphenyl)(phenyl)amino)ethyl)urea (**3b**)



3b

A solution of the nitrile **2**¹ (1.0 equiv., 262 mg, 1.1 mmol) in THF (7 mL) and 1M NH₃ in EtOH (1.5 mL) was hydrogenated over Raney Nickel (4 atm of H₂) for 6h at 60°C. The catalyst was filtered on a celite pad, the filtrate was concentrated *in vacuo*, to give the crude oily *N*^l-3-(methoxyphenyl)-*N*^l-phenylethane-1,2-diamine which was used in the next step without any further

purification. Ethyl isocyanate (1.1 equiv., 1.2 mmol, 0.095 mL) was added to a solution of the above crude amine in DCM (4 mL) and the resulting mixture was stirred at room temperature for 30 min. The solvent was removed by distillation under reduced pressure to give a crude residue that was purified by flash chromatography (silica gel, EtOAc:cyclohexane 1:1 as eluent) to give **3b** as a white solid (87% yield). Crystallization: diethyl ether.

M.p.: 96–97 °C

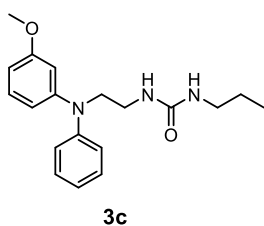
ESI MS (*m/z*): 314 [M+H]⁺

¹H NMR (400 MHz, CDCl₃) δ: 1.06 (t, 3H, *J*=7.0 Hz), 3.11 (q, 2H, *J*=7.0 Hz), 3.38 (t, 2H, *J*=6.5 Hz), 3.73 (s, 3H), 3.82 (t, 2H, *J*=6.5 Hz), 4.69 (brs, 1H), 4.90 (brs, 1H), 6.48 (dd, 1H, *J*=2.5 and 8.0 Hz), 6.53–6.55 (m, 1H), 6.59 (dd, 1H, *J*=2.5 and 8.0 Hz), 6.96–7.00 (m, 1H), 7.05–7.07 (m, 2H), 7.15 (dd, 1H, *J*₁=*J*₂=8.0 Hz), 7.24–7.28 (m, 2H)

¹³C NMR (100 MHz, CDCl₃) δ: 15.4, 35.3, 38.3, 52.0, 55.2, 106.1, 106.2, 112.7, 122.0, 122.2, 129.5, 130.0, 147.6, 149.3, 158.4, 160.6

HRMS (ESI): *m/z* calculated for C₁₈H₂₄N₃O₂, [M+H]⁺ 314.1869. Found: 314.1853

1-(2-((3-methoxyphenyl)(phenyl)amino)ethyl)-3-propylurea (**3c**)



Compound **3c** was prepared following the above described procedure for the synthesis of **3b**, using *n*-propyl isocyanate instead of ethyl isocyanate. White solid (91% yield). Crystallization: diethyl ether:petroleum ether

M.p.: 63–65 °C

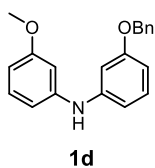
ESI MS (*m/z*): 328 [M+H]⁺

¹H NMR (400 MHz, CDCl₃) δ: 0.79 (t, 3H, *J*=7.5 Hz), 1.32–1.41 (m, 2H), 2.95 (t, 2H, *J*=7.0 Hz), 3.31 (t, 2H, *J*=6.5 Hz), 3.65 (s, 3H), 3.75 (t, 2H, *J*=6.5 Hz), 4.60 (brs, 1H), 4.71 (brs, 1H), 6.40 (dd, 1H, *J*=2.5 and 8.0 Hz), 6.45–6.46 (m, 1H), 6.51 (dd, 1H, *J*=2.5 and 8.0 Hz), 6.88–6.90 (m, 1H), 6.92–6.99 (m, 2H), 7.06 (dd, 1H, *J*₁=*J*₂=8.0 Hz), 7.16–7.20 (m, 2H)

¹³C NMR (100 MHz, CDCl₃) δ: 11.3, 23.3, 38.4, 42.3, 52.1, 55.2, 106.2, 106.3, 112.7, 122.0, 122.2, 129.4, 130.0, 147.6, 149.3, 158.5, 160.6

HRMS (ESI): *m/z* calculated for C₁₉H₂₆N₃O₂, [M+H]⁺ 328.2025. Found: 328.2013

3-(benzyloxy)-*N*-(3-methoxyphenyl)aniline (**1d**)



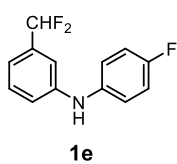
A Schlenk flask was charged with 3-methoxyaniline **1b** (1 equiv., 123 mg, 1 mmol) and 1-(benzyloxy)-3-bromobenzene (1.0 equiv., 264 mg, 1 mmol). Dry toluene (10 mL) was added, followed by *t*-BuONa (1.5 equiv., 144 mg, 1.5 mmol), Pd₂(dba)₃ (0.02 equiv., 18 mg, 0.02 mmol) and XantPhos (0.06 equiv., 34 mg, 0.06 mmol). The mixture was evacuated and purged with argon (3 cycles), then heated to 100 °C under argon for 18 h. The

mixture was cooled to room temperature, quenched by addition of water and then extracted with EtOAc. The organic phase was dried over Na₂SO₄, and concentrated under reduced pressure. The resulting crude product was purified by flash chromatography (silica gel, cyclohexane:EtOAc 8:2 as eluent) to give **1d** as an amorphous solid (88% yield).

ESI MS (*m/z*): 306 [M+H]⁺

¹H NMR (200 MHz, CDCl₃) δ: 3.78 (s, 3H), 5.05 (s, 2H), 5.73 (brs, 1H), 6.49–6.74 (m, 5H), 7.13–7.43 (m, 8H)

3-(difluoromethyl)-*N*-(4-fluorophenyl)aniline (**1e**)

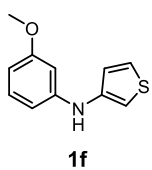


A Schlenk flask was charged with Pd(OAc)₂ (0.05 equiv., 14 mg, 0.06 mmol), (±)-BINAP (0.05 equiv., 41 mg, 0.06 mmol), *t*-BuOK (1.4 equiv., 190 mg, 1.7 mmol), 3-(difluoromethyl)bromobenzene (1.0 equiv., 250 mg, 1.2 mmol) and 4-fluoroaniline (1.0 equiv., 133 mg, 1.2 mmol) under nitrogen atmosphere, followed by the addition of dry toluene (2 mL). The mixture was stirred at 100 °C for 3 h. Then, the reaction mixture was cooled at room temperature and quenched with water and then extracted with DCM. The combined organic phases were dried over Na₂SO₄ and evaporated under reduced pressure. The crude was purified by flash chromatography (silica gel, cyclohexane:EtOAc 9:1 as eluent) to give **1e** as an oil (44% yield).

ESI MS (*m/z*): 238 [M+H]⁺

¹H NMR (200 MHz, CDCl₃) δ: 5.70 (brs, 1H), 6.58 (t, 1H, *J*=56.5 Hz), 7.03–7.14 (m, 7H), 7.28–7.36 (m, 1H)

N-(3-methoxyphenyl)thiophen-3-amine (**1f**)

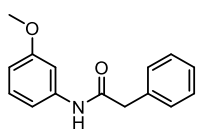


An oven dried Schlenk tube containing a magnetic stirrer bar was evacuated and backfilled with argon. Then, the tube was charged with Pd₂(dba)₃ (0.02 equiv., 11 mg, 0.012 mmol), 2-dicyclohexylphosphino-2',6'-diisopropoxybiphenyl (0.8 equiv., RuPhos, 23 mg, 0.05 mmol), and *t*-BuONa (1.4 equiv., 82 mg, 0.85 mmol). The tube was evacuated and purged with argon (x1) and closed with a septa. 3-Bromothiophene (1.0 equiv., 99 mg, 58 μL, 0.61 mmol) and 3-methoxyaniline **1b** (1.2 equiv., 91 mg, 83 μL, 0.74 mmol) were added via syringe followed by toluene (1.25 mL). The tube was sealed under argon atmosphere with a Teflon screw cap and placed into a pre-heated oil bath (100°C) for 18 h. The reaction mixture was cooled to room temperature, filtered through a celite pad and washed with EtOAc. The solvent was evaporated under reduced pressure and the residue was purified by flash chromatography (silica gel, cyclohexane:EtOAc 9:1 as eluent) to give **1f** as an oil (92% yield).

ESI MS (*m/z*): 206 [M+H]⁺

^1H NMR (200 MHz, CDCl_3) δ : 3.79 (s, 3H), 5.71 (brs, 1H), 6.44 (dd, 1H, $J=2.0$ and 8.5 Hz), 6.55–6.58 (m, 2H), 6.77–6.79 (m 1H), 6.94 (dd, 1H, $J=1.5$ and 5.0 Hz), 7.16 (dd, 1H, $J_1=J_2=8.5$ Hz), 7.25–7.29 (m, 1H)

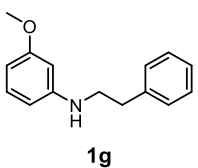
N-(3-methoxyphenyl)-2-phenylacetamide



A solution of 2-phenylacetyl chloride (1.01 equiv., 0.4 mL, 2.47 mmol) in DCM (3.5 mL) was added dropwise to an ice-cooled solution of 3-methoxyaniline **1b** (1.0 equiv., 300 mg, 2.44 mmol) and TEA (1.5 equiv., 0.51 mL, 3.66 mmol) in DCM (3.5 mL), and the resulting reaction mixture was stirred at room temperature for 30 min. After dilution with DCM, the mixture was washed with a saturated aqueous solution of NaHCO_3 followed by brine. The organic phase was dried over Na_2SO_4 , and concentrated to give a crude residue that was purified by flash chromatography (silica gel; cyclohexane:EtOAc 8:2 as eluent) to give the final compound as a white solid (84% yield).

Physicochemical data are in agreement with those previously reported.¹²

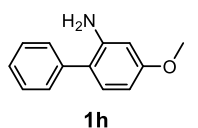
3-methoxy-*N*-phenethylaniline (**1g**)



Solid LiAlH_4 (3.0 equiv., 154 mg, 3.95 mmol) was added portion wise to a stirred ice-cooled solution of *N*-(3-methoxyphenyl)-2-phenylacetamide (1.0 equiv., 320 mg, 1.33 mmol) in dry THF (15 mL) under nitrogen atmosphere. After the addition, the mixture was refluxed for 1 h. The unreacted LiAlH_4 was destroyed by careful addition of water at 0°C , and the resulting mixture was filtered through a celite pad. The filtrate was concentrated *in vacuo*, and the residue was partitioned between EtOAc and water. The combined organic phases were washed with brine, dried over Na_2SO_4 , and concentrated. The crude residue was purified by flash chromatography (silica gel, cyclohexane:EtOAc 8:2 as eluent) to give **1g** as an oil (70% yield).

Physicochemical data are in agreement with those previously reported.¹³

4-methoxy-[1,1'-biphenyl]-2-amine (**1h**)



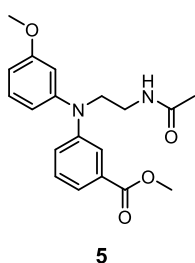
A solution of 4-methoxy-2-nitro-1,1'-biphenyl¹⁴ (1.0 equiv., 530 mg, 2.31 mmol) in a 1:1 mixture of EtOAc:EtOH (46 mL) was hydrogenated (4 atm H_2) over 10% Pd/C (43 mg) for 6 h at room temperature. The catalyst was filtered on a celite pad and the filtrate was concentrated *in vacuo*, to give the oily amine **1h**, which was used without any further purification (99% yield).

Physicochemical data are in agreement with those previously reported.¹⁵

General procedure for reductive *N*-alkylation of anilines.¹⁶

Under nitrogen atmosphere, TFA (1 mL) and TES (2.5 equiv., 0.4 mL, 2.5 mmol) were added to a solution of the opportune aniline (1.0 equiv., 1.0 mmol) and *N*-(2,2-dimethoxyethyl)acetamide (1.4 equiv., 206 mg, 1.4 mmol) in dry DCM (2 mL), and the resulting mixture was stirred for 2 h at room temperature. The reaction mixture was cooled at 0°C and carefully neutralized with an aqueous saturated solution of NaHCO₃. The mixture was diluted with DCM and the aqueous phase was extracted with DCM. The combined organic phases were washed with brine, and dried over Na₂SO₄. The solvent was removed by distillation, and the crude residue was purified by column chromatography to afford the desired compound.

Methyl 3-((2-acetamidoethyl)(3-methoxyphenyl)amino)benzoate (5)



Compound **5** was synthesized according to the above described general procedure using **1c**.¹⁷ Flash chromatography: silica gel, EtOAc as eluent.

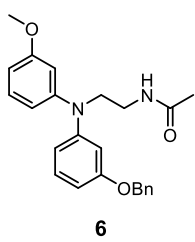
Oil, 81% yield.

ESI MS (*m/z*): 258 [M+H]⁺

¹H NMR (200 MHz, CDCl₃) δ: 3.80 (s, 3H), 3.91 (s, 3H), 5.83 (brs, 1H), 6.54 (dd, 1H, *J*=2.0 and 8.0 Hz), 6.65–6.71 (m, 2H), 7.21 (dd, 1H, *J*₁=*J*₂=8.0 Hz), 7.26–7.38

(m, 2H), 7.58–7.61 (m, 1H), 7.74–7.75 (m, 1H)

N-(2-((3-(benzyloxy)phenyl)(3-methoxyphenyl)amino)ethyl)acetamide (6)



Compound **6** was synthesized according to the above-described general procedure starting from **1d**. Flash chromatography: silica gel, EtOAc as eluent.

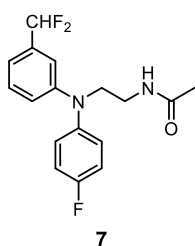
Oil, 80% yield.

ESI MS (*m/z*): 391 [M+H]⁺

¹H NMR (400 MHz, CDCl₃) δ: 1.92 (s, 3H), 3.49 (m, 2H), 3.77 (s, 3H), 3.86 (t, 2H, *J*=6.5 Hz), 5.02 (s, 2H), 5.62 (brs, 1H), 6.60 (dd, 1H, *J*=2.5 and 8.0 Hz), 6.60–6.63 (m, 2H),

6.65–6.66 (m, 2H), 7.17–7.21 (m, 2H), 7.32–7.41 (m, 6H)

N-(2-((3-(difluoromethyl)phenyl)(4-fluorophenyl)amino)ethyl)acetamide (7)



Compound **7** was synthesized according to the above-described general procedure starting from **1e**. Flash chromatography: silica gel, EtOAc:cyclohexane 7:3 as eluent.

White solid, 77% yield. Crystallization: diethyl ether-petroleum ether

M.p.: 76–77 °C

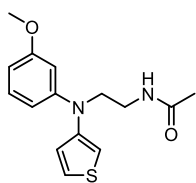
ESI MS (m/z): 323 $[M+H]^+$

^1H NMR (400 MHz, CDCl_3) δ : 1.95 (s, 3H), 3.48 (m, 2H), 3.85 (t, 2H, $J=6.5$ Hz), 5.80 (brs, 1H), 6.54 (t, 1H, $J=56.5$ Hz), 6.93–6.97 (m, 3H), 7.04–7.14 (m, 4H), 7.25–7.60 (m, 1H)

^{13}C NMR (100 MHz, CDCl_3) δ : 23.1, 37.6, 51.3, 113.4 (t, $J=6.2$ Hz), 114.8 (t, $J=237.2$ Hz), 116.4 (t, $J=6.2$ Hz), 116.7 (d, $J=22.3$ Hz), 118.8 (t, $J=1.8$ Hz), 126.7 (d, $J=8.2$ Hz), 129.7, 135.5 (t, $J=21.8$ Hz), 142.8 (d, $J=3.0$ Hz), 148.7, 159.7 (d, $J=43.0$ Hz), 170.6

HRMS (ESI): m/z calculated for $\text{C}_{17}\text{H}_{18}\text{F}_3\text{N}_2\text{O}$, $[M+H]^+$ 323.1371. Found: 323.1359

***N*-2-((3-methoxyphenyl)(thiophen-3-yl)amino)ethyl)acetamide (8)**



8

Compound **8** was synthesized according to the above-described general procedure starting from **1f**. Flash chromatography: silica gel, EtOAc as eluent.

Yellowish solid, 66% yield. Crystallization: diethyl ether:petroleum ether

M.p.: 76–77 °C

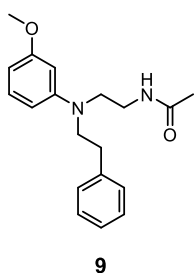
ESI MS (m/z): 291 $[M+H]^+$

^1H NMR (400 MHz, CDCl_3) δ : 1.93 (s, 3H), 3.50 (m, 2H), 3.77 (s, 3H), 3.83 (t, 2H, $J=6.5$ Hz), 5.71 (brs, 1H), 6.47 (dd, 1H, $J=2.5$ and 8.0 Hz), 6.54–6.56 (m, 1H), 6.59 (dd, 1H, $J=2.5$ and 8.0 Hz), 6.70–6.78 (m, 1H), 6.88 (d, 1H, $J=5.0$ Hz), 7.15 (t, 1H, $J_1=J_2=8.0$ Hz), 7.25 (d, 1H, $J=5.0$ Hz)

^{13}C NMR (100 MHz, CDCl_3) δ : 23.2, 37.8, 52.0, 55.2, 104.7, 105.8, 110.4, 111.0, 124.1, 125.4, 129.9, 146.4, 149.5, 160.6, 170.4

HRMS (ESI): m/z calculated for $\text{C}_{15}\text{H}_{19}\text{N}_2\text{O}_2\text{S}$, $[M+H]^+$ 291.1167. Found: 291.1167

***N*-2-((3-methoxyphenyl)(phenethyl)amino)ethyl)acetamide (9)**



9

Compound **9** was synthesized according to the above-described general procedure starting from **1g**. Flash chromatography: silica gel, EtOAc as eluent.

Oil, 36% yield.

ESI MS (m/z): 313 $[M+H]^+$

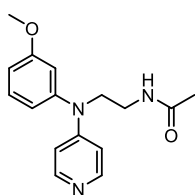
^1H NMR (400 MHz, CDCl_3) δ : 1.83 (s, 3H), 2.79 (t, 3H, $J=7.5$ Hz), 3.23–3.27 (m, 4H), 3.45 (t, 2H, $J=7.5$ Hz), 3.74 (s, 3H), 5.40 (brs, 1H), 6.21–6.38 (m, 3H), 7.06–

7.25 (m, 6H).

^{13}C NMR (100 MHz, CDCl_3) δ : 23.2, 33.3, 37.5, 50.8, 53.1, 55.2, 99.5, 101.8, 105.9, 126.4, 128.6, 128.9, 130.2, 139.5, 149.2, 161.0, 170.3

HRMS (ESI): m/z calculated for $\text{C}_{19}\text{H}_{24}\text{N}_2\text{O}_2\text{Na}$, $[M+H]^+$ 335.1735. Found: 335.1747

N-2-((3-methoxyphenyl)(pyridin-4-yl)amino)ethylacetamide (**10**)



10

A Schlenk flask was charged with 4-bromopyridine·HCl (1.3 equiv., 100 mg, 0.48 mmol) and *N*-{2-[(3-methoxyphenyl)amino]ethyl}acetamide **4** (1.0 equiv., 121 mg, 0.62 mmol).¹ Dry toluene (5 mL) was added, followed by *t*-BuONa (1.9 equiv., 115 mg, 1.2 mmol), Pd₂(dba)₃ (0.015 equiv., 9 mg, 0.01 mmol) and XantPhos (0.05 equiv., 17 mg, 0.03 mmol). The mixture was evacuated and purged with argon (3 cycles), then heated to 100°C for 16 h under argon. After cooling to room temperature, the mixture was quenched by addition of water and then extracted with EtOAc. The combined organic phases were dried over Na₂SO₄ and concentrated by distillation under reduced pressure. The crude residue was purified by filtration on a pad of silica gel (DCM:MeOH 9:1 as eluent) to give **10** as an oil (95% yield).

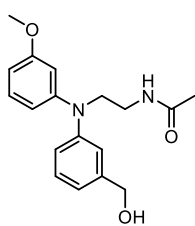
ESI MS (*m/z*): 286 [M+H]⁺

¹H NMR (400 MHz, CDCl₃) δ: 1.90 (s, 3H), 3.45 (m, 2H), 3.78 (s, 3H), 3.84 (t, 2H, *J*=6.5 Hz), 6.61 (dd, 2H, *J*=1.5 and 5.0 Hz), 6.71 (brt, 1H), 6.73–6.75 (m, 1H), 6.78 (ddd, 1H, *J*=1.0, 2.5 and 8.0 Hz), 6.84 (ddd, 1H, *J*=1.0, 2.5 and 8.0 Hz), 7.33 (t, 1H, *J*₁=*J*₂=8.0 Hz), 8.08 (dd, 2H, *J*=1.5 and 5.0 Hz)

¹³C NMR (100 MHz, CDCl₃) δ: 23.0, 37.3, 50.4, 55.4, 108.6, 112.5, 113.3, 119.5, 131.0, 145.4, 148.9, 153.9, 161.2, 171.0

HRMS (ESI): *m/z* calculated for C₁₆H₂₀N₃O₂, [M+H]⁺ 286.1556. Found: 286.1549

N-2-((3-(hydroxymethyl)phenyl)(3-methoxyphenyl)amino)ethylacetamide (**11**)



11

A solution of **5** (1.0 equiv., 150 mg, 0.44 mmol) in dry THF (3 mL) was added dropwise to a stirred ice-cooled suspension of LiAlH₄ (2.0 equiv., 34 mg, 0.88 mmol) in dry THF (3 mL) under a nitrogen atmosphere, and the resulting mixture was stirred at 0°C for 1 h. The unreacted LiAlH₄ was destroyed by careful addition of water at 0°C. The resulting mixture was filtered through a celite pad, and the filtrate was concentrated *in vacuo*, and partitioned between EtOAc and water. The organic phase was washed with brine, dried over Na₂SO₄, and concentrated by distillation under reduced pressure. The crude residue was purified by flash chromatography (silica gel, EtOAc as eluent) to give **11** as an oil (84% yield).

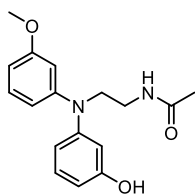
ESI MS (*m/z*): 315 [M+H]⁺

¹H NMR (400 MHz, CDCl₃) δ: 1.84 (s, 3H), 3.36 (brs, 1H), 3.40 (m, 2H), 3.72 (s, 3H), 3.80 (t, 1H, *J*=6.5 Hz), 4.57 (s, 2H), 6.35 (brt, 1H), 6.46 (ddd, 1H, *J*=1.0, 2.5 and 8.0 Hz), 6.52–6.54 (m, 1H), 6.56 (ddd, 1H, *J*=1.0, 2.5 and 8.0 Hz), 6.90–6.93 (m, 2H), 7.08–7.09 (m, 1H), 7.12 (t, 1H, *J*₁=*J*₂=8.0 Hz), 7.20 (t, 1H, *J*₁=*J*₂=8.0 Hz)

^{13}C NMR (100 MHz, CDCl_3) δ : 22.9, 37.7, 50.9, 55.2, 64.8, 106.3, 106.4, 112.8, 120.0, 120.7, 120.9, 129.4, 130.0, 142.7, 147.6, 149.1, 106.6, 171.1

HRMS (ESI): m/z calculated for $\text{C}_{18}\text{H}_{22}\text{N}_2\text{O}_3\text{Na}$, $[\text{M}+\text{H}]^+$ 337.1528. Found: 337.1541

N-(2-((3-hydroxyphenyl)(3-methoxyphenyl)amino)ethyl)acetamide (**12**)



12

A solution of **6** (1.0 equiv., 120 mg, 0.4 mmol), in MeOH (10 mL) was hydrogenated (1 atm H_2) over 10 % Pd/C (0.05 equiv., 20 mg, 0.02 mmol) for 2.5 h at room temperature. The catalyst was filtered on a celite pad and the filtrate was concentrated *in vacuo*. The crude residue was purified by flash chromatography (silica gel, EtOAc as eluent) to give **12** as a white solid (80% yield). Crystallization:

diethyl ether.

M.p.: 110 °C

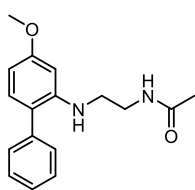
ESI MS (m/z): 301 $[\text{M}+\text{H}]^+$

^1H NMR (400 MHz, CDCl_3) δ : 1.93 (s, 3H), 3.47 (m, 2H), 3.76 (s, 3H), 3.83 (t, 2H, $J=6.5$ Hz), 5.76 (brs, 1H), 6.47 (ddd, 1H, $J=1.0, 2.5$ and 8.0 Hz), 6.52 (ddd, 1H, $J=1.0, 2.5$ and 8.0 Hz), 6.55 (ddd, 1H, $J=1.0, 2.5$ and 8.0 Hz), 6.59 (dd, 1H, $J_1=J_2=2.5$ Hz), 6.61 (dd, 1H, $J_1=J_2=2.5$ Hz), 6.65 (ddd, 1H, $J=1.0, 2.5$ and 8.0 Hz), 7.09 (dd, 1H, $J_1=J_2=8.0$ Hz), 7.18 (dd, 1H, $J_1=J_2=8.0$ Hz)

^{13}C NMR (100 MHz, CDCl_3) δ : 23.1, 38.0, 51.0, 55.3, 107.3, 107.5, 107.8, 108.7, 112.5, 114.3, 130.1, 130.2, 148.8, 149.0, 157.3, 160.7, 171.0

HRMS (ESI): m/z calculated for $\text{C}_{17}\text{H}_{21}\text{N}_2\text{O}_3$, $[\text{M}+\text{H}]^+$ 301.1552. Found: 301.1563

N-(2-((4-methoxy-[1,1'-biphenyl]-2-yl)amino)ethyl)acetamide (**13**)



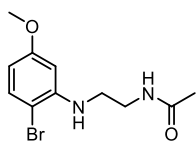
13

Compound **13** was synthesized according to the reductive *N*-alkylation general procedure starting from **1h**. Flash chromatography: silica gel, EtOAc as eluent. Amorphous solid, 65 % yield.

ESI MS (m/z): 285 $[\text{M}+\text{H}]^+$

^1H NMR (200 MHz, CDCl_3) δ : 1.93 (s, 3H), 3.23–3.29 (m, 2H), 3.37–3.46 (m, 2H), 3.84 (s, 3H), 4.20 (brs, 1H), 5.65 (brs, 1H), 6.34–6.36 (m, 1H), 6.36 (dd, 1H, $J=2.5$ and 8.0 Hz), 7.03 (d, 1H, $J=8.0$ Hz), 7.31–7.49 (m, 5H)

N-(2-((2-bromo-5-methoxyphenyl)amino)ethyl)acetamide (**14**)



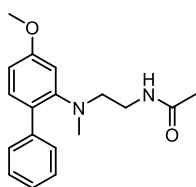
14

Compound **14** was synthesized according to reductive *N*-alkylation general procedure starting from **1i**. Flash chromatography: silica gel, EtOAc as eluent. Amorphous solid, 70% yield.

ESI MS (*m/z*): 287 [M+H]⁺

¹H NMR (200 MHz, CDCl₃) δ: 2.02 (s, 3H), 3.29–3.35 (m, 2H), 3.48–3.57 (m, 2H), 3.78 (s, 3H), 4.58 (brs, 1H), 5.84 (brs, 1H), 6.18 (dd, 1H, *J*=3.0 and 9.0 Hz), 6.26 (d, 1H, *J*=3.0 Hz), 7.30 (d, 1H, *J*=9.0 Hz)

N-(2-((4-methoxy-[1,1'-biphenyl]-2-yl)(methyl)amino)ethyl)acetamide (**15**)



15

A suspension of **13** (1.0 equiv., 284 mg, 1 mmol), NaHCO₃ (1.0 equiv., 84 mg, 1 mmol) and methyl iodide (6.5 equiv., 0.4 mL, 6.5 mmol) in dry MeOH (11 mL) was stirred at 50 °C for 24 h. Then, the mixture was concentrated and poured into water, extracted with EtOAc, and the combined organic phases were washed with brine, dried over Na₂SO₄ and concentrated under reduced pressure. The residue was purified by flash chromatography (silica gel, DCM:EtOAc 8:2 as eluent) to give **15** as an oil (74 % yield)

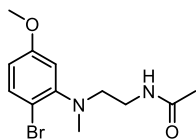
ESI MS (*m/z*): 299 [M+H]⁺

¹H NMR (400 MHz, CDCl₃) δ: 1.65 (s, 3H), 2.54 (s, 3H), 2.71 (t, 2H, *J*=6.5 Hz), 3.04 (m, 2H), 3.75 (s, 3H), 5.16 (brs, 1H), 6.61 (dd, 1H, *J*=2.5 and 8.5 Hz), 6.70 (d, 1H, *J*=2.5 Hz), 7.09 (d, 1H, *J*=8.5 Hz), 7.20–7.25 (m, 1H), 7.30–7.36 (m, 4H)

¹³C NMR (100 MHz, CDCl₃) δ: 23.1, 36.9, 40.8, 55.3, 55.5, 107.6, 108.5, 126.6, 128.3, 129.5, 130.1, 132.0, 141.1, 151.9, 159.9, 170.1

HRMS (ESI): *m/z* calculated for C₁₈H₂₃N₂O₂, [M+H]⁺ 299.1760. Found: 299.1751

N-(2-((2-bromo-5-methoxyphenyl)(methyl)amino)ethyl)acetamide (**16**)



16

Sodium cyanoborohydride (2.4 equiv., 100 mg, 1.20 mmol) and a 37 % HCHO aqueous solution (0.5 mL) were added to a solution of **14** (1.0 equiv., 143 mg, 0.5 mmol), in MeOH (5 mL) and AcOH (to pH=5), and the resulting mixture was stirred at room temperature for 1 h. After distillation of the solvent, the residue was partitioned in water and EtOAc. The combined organic phase was dried over Na₂SO₄ and concentrated by distillation under reduced pressure to afford a crude residue which was purified by flash chromatography (silica gel, cyclohexane:EtOAc 6:4 as eluent) to give **16** as white solid (78% yield). Crystallization: diethyl ether-petroleum ether.

M.p.: 94–96 °C

ESI MS (*m/z*): 301 [M+H]⁺

¹H NMR (400 MHz, CDCl₃) δ: 1.97 (s, 3H), 2.70 (s, 3H), 3.09 (t, 2H, *J*=6.0 Hz), 3.39 (m, 2H), 3.78 (s, 3H), 6.30 (brs. 1H), 6.56 (dd, 1H, *J*=3.0 and 9.0 Hz), 6.72 (d, 1H, *J*=3.0 Hz), 7.45 (d, 1H, *J*=9.0 Hz)

¹³C NMR (100 MHz, CDCl₃) δ: 23.3, 36.8, 41.7, 54.2, 55.5, 109.8, 110.6, 111.7, 133.8, 151.3, 160.0, 170.2

HRMS (ESI): *m/z* calculated for C₁₂H₁₈BrN₂O₂, [M+H]⁺ 301.0552. Found: 301.0552

4.4.3 Pharmacokinetics studies

Metabolic stability assays in rat and human liver microsomes

Stock solutions of melatonin receptor ligands were prepared in DMSO immediately before use; cosolvent concentration in final samples was kept constant at 1 % v/v. Each compound (final concentration: 5 μM) was incubated in the presence of rat or human liver microsomes (final concentration: 1 mg protein/mL) and of a NADPH-regenerating system (final concentrations: 2 mM NADP⁺, 10 mM glucose-6-phosphate, 0.4 U mL⁻¹ glucose-6-phosphate dehydrogenase, 5 mM MgCl₂) in a 10 mM Phosphate Buffered Saline (PBS) solution, pH 7.4, at 37 °C. Compound was added after a 10 min pre-incubation at 37 °C and, at stated time points, depending on compound kinetics, sample aliquots were withdrawn, metabolic reaction was quenched by acetonitrile addition (1 : 2), and after a centrifugation step (9000 g, 10 min, 4 °C) the supernatant was analyzed by HPLC-UV-VIS.

Apparent half-lives (*t*_{1/2} in min) for the metabolic clearance of compounds were calculated from the pseudo first-order rate constants (*k*) obtained by linear regression of the log chromatographic peak area versus time plots and are reported as means of three experiments ± standard deviation. Intrinsic clearance (CL_i) values of the compounds were calculated using the following equation: CL_i (μL×min⁻¹×mg protein⁻¹)=*k*×V where V (μL×mg protein⁻¹)=incubation volume/mg protein added.

Pooled rat and human liver microsomes (20 mg/mL) were supplied by BD Biosciences (BD Biosciences, Woburn, MA, USA). Acetonitrile and methanol were HPLC grade and were supplied by Sigma-Aldrich (Sigma-Aldrich srl, Milan, Italy). Water was freshly bidistilled before use. All other reagents were purchased in the highest purity available.

Experimental lipophilicity

Distribution coefficients (log *D*_{oct, 7.4}) were determined employing the reference shake-flask method¹⁸ in the biphasic *n*-octanol/water partition system, at room temperature (25±1 °C) and at

physiological pH 7.4. Chosen buffer was 50 mM zwitterionic MOPS (3-morpholinopropanesulfonic acid), pH 7.4 to avoid ionic couple partitioning, with ionic strength adjusted to 0.15 M by KCl addition. Compounds, after partitioning overnight, and dilution of both phases with methanol, were dosed in the HPLC-UV system, as detailed below. Reported $\log D_{\text{Oct},7.4}$ values are the mean of three measurements \pm standard deviation.

Solubility measurements

Thermodynamic solubility values were measured in two different buffers (pH 1.0; pH 7.4) by the shake flask method.¹⁹ 1 mg of each compound was placed in 1 mL of appropriate buffer and shaken at room temperature overnight. The resulting suspension was centrifuged (10 min, 10000 g, 20 °C) and the supernatant analyzed by HPLC-UV. Solubility values were interpolated from calibration curves prepared from concentrated DMSO stock solutions of each compound. Reported solubility values are the mean of three measurements \pm standard deviation.

Sample analysis by HPLC-UV

A Shimadzu High Performance Liquid Chromatography (HPLC) system coupled to UV-VIS detection (Shimadzu Corp., Kyoto, Japan) was employed to analyze melatonin receptor ligands in metabolic stability and physicochemical characterization assays. It consisted of a LC-10ADvp solvent delivery module, a 20 μ L Rheodyne sample injector (Rheodyne LLC, Rohnert Park, CA, USA) and a SPD-10Avp UV-VIS detector. PeakSimple 2.83 software was employed for data acquisition and HPLC peak integration. HPLC columns were a RP-C18 Supelco Discovery (Supelco, Bellefonte, PA, USA), 5 μ m, 150 \times 4.6 mm i.d. for all compounds except **10**, and a Phenomenex Gemini, 5 μ m, 150 \times 4.6 mm i.d. for compound **10** (Phenomenex). Elution conditions were optimized for each compound at a flow rate of 1 mL min⁻¹ employing mobile phases consisting of water and acetonitrile at different percentages, while UV detection was set at $\lambda = 254$ nm. For compound **10**, the mobile phase consisted of a 10 mM ammonium acetate buffer pH 7.0 and methanol and the UV detection was set at $\lambda = 281$ nm.

***In vivo* pharmacokinetic studies**

The *in vivo* pharmacokinetic experiments were conducted at NiKem Research (Baranzate – Milan – Italy). PK studies were performed using Sprague-Dawley CD (albino) male rats (7–9 weeks-old, weight 160–200 grams, Charles River Lab. Italia, Calco). Animals were housed under standard conditions and had free access to water and standard laboratory rodent diet. Care and husbandry of animals were in conformity with the institutional guidelines, in compliance with national and international laws and policies (EEC Council Directive 86/609, OJL 358 m, 1, Dec. 122, 1987; NIH

Guide for the care and Use of Laboratory Animals, NIH Publication No. 86–23, 1985). The compounds were dissolved in water containing 3 % DMSO and 20 % Encapsin (and a stoichiometric amount of HCl for **11**) at a concentration of 2.5 mg mL⁻¹ for the IV (bolus) dose, or in water containing 5 % DMSO and 10 % encapsin (and a stoichiometric amount of HCl for **11**) at a concentration of 4 mg mL⁻¹ for PO (gavage) dose. Rats were randomly assigned to four treatment groups ($n=3$) and received a single IV bolus dose (5 mg kg⁻¹) or a single oral administration (40 mg kg⁻¹) through oral gavage of compound **11** or **16**. Serial blood samples (200 mL) were collected from caudal vein at 5, 30, 60, 120, 480 and 1440 min after IV injection, or at 15, 30, 60, 120, 480 and 1440 min after PO administration. Blood samples were collected in heparinized eppendorfs (Heparin Vister 5000 U.I./mL_Marvecs Pharma), gently mixed and placed on ice; then blood was centrifuged (3500×g, at 4 °C for 15 min), the plasma was collected and immediately frozen at -80 °C until submission to UPLC/MS/MS analysis. For the sample preparation, 100 µL of plasma spiked with 5 µL of internal standard (I.S.; **16** for compound **11** and **11** for compound **16**; 2.5 µg mL⁻¹;) were added to a SW96 deep well plate (Waters) containing 300 µL of acetonitrile. The plate was shaken for 10 min and then centrifuged at 3000 rpm for 15 min. UPLC/MS/MS analyses were performed on an Acquity UPLC, coupled with a sample organizer and interfaced with a triple quadrupole Premiere XE (Waters, Milford, USA). LC runs (inj. vol. 5 µL) were carried out at 50 °C on Acquity BEH C₁₈ columns (1.7 µm, 2.1×50 mm) at a flow rate of 0.45 mL min⁻¹. Mobile phases consisted of a phase A (water) and a phase B (0.1 % formic acid in acetonitrile). The column was conditioned with 2 % phase B for 0.2 min, then brought to 100 % phase B within 0.6 min and maintained at these conditions for 1.1 min. Analyses were carried out using a positive electrospray ionization [ESI(+)] interface in multiple reaction monitoring (MRM) mode. Capillary 3.5 Kv; extractor 3 V; source T 140 °C, desolvation T 450 °C. Transitions: for compound **11** Q1/Q3 315.2/86, CV 14, CE16+315.2/238 CV 14, CE19; for I.S. (compound **16**): 301.1/86 CV 14 CE16; LLOQ: 1 ng mL⁻¹. Transitions: for compound **16** Q1/Q3: 301.1/86CV 14 CE16; for I.S. (compound **11**) 315.2/238CV 14, CE19; LLOQ: 1 ng mL⁻¹. Pharmacokinetic analysis was performed by non-compartmental analysis (NCA) using the WinNonlin 5.1 software (Pharsight, Mountain View, CA, USA. Absolute oral bioavailability (F) was calculated by linear trapezoidal rule using the relationship: $F = [\text{dose}_{\text{IV}} \times \text{AUC}_{\text{oral } 0-\infty} / \text{dose}_{\text{oral}} \times \text{AUC}_{\text{IV } 0-\infty}] \times 100$.

4.5 References

- ¹ Rivara S, Lodola A, Mor M, Bedini A, Spadoni G, Lucini V, Pannacci M, Fraschini F, Scaglione F, Sanchez RO, Gobbi G, Tarzia G. *N*-(substituted-anilinoethyl)amides: design, synthesis, and pharmacological characterization of a new class of melatonin receptor ligands. *J Med Chem.* **2007**, 50(26), 6618-26
- ² Ochoa-Sanchez R, Comai S, Lacoste B, Bambico FR, Dominguez-Lopez S, Spadoni G, Rivara S, Bedini A, Angeloni D, Fraschini F, Mor M, Tarzia G, Descarries L, Gobbi G. Promotion of non-rapid eye movement sleep and activation of reticular thalamic neurons by a novel MT₂ melatonin receptor ligand. *J Neurosci.* **2011**, 31(50), 18439-52
- ³ Lopez-Canul M, Palazzo E, Dominguez-Lopez S, Luongo L, Lacoste B, Comai S, Angeloni D, Fraschini F, Boccella S, Spadoni G, Bedini A, Tarzia G, Maione S, Granados-Soto V, Gobbi G. Selective melatonin MT₂ receptor ligands relieve neuropathic pain through modulation of brainstem descending antinociceptive pathways. *Pain.* **2015**, 156(2), 305-317
- ⁴ Ochoa-Sanchez R, Rainer Q, Comai S, Spadoni G, Bedini A, Rivara S, Fraschini F, Mor M, Tarzia G, Gobbi G. Anxiolytic effects of the melatonin MT(2) receptor partial agonist UCM765: comparison with melatonin and diazepam. *Prog Neuropsychopharmacol Biol Psychiatry.* **2012**, 39(2), 318-25
- ⁵ Rivara S, Vacondio F, Fioni A, Silva C, Carmi C, Mor M, Lucini V, Pannacci M, Caronno A, Scaglione F, Gobbi G, Spadoni G, Bedini A, Orlando P, Lucarini S, Tarzia G. *N*-(Anilinoethyl)amides: design and synthesis of metabolically stable, selective melatonin receptor ligands. *ChemMedChem.* **2009**, 4(10), 1746-55
- ⁶ Ferlenghi F, Mari M, Gobbi G, Elisi GM, Mor M, Rivara S, Vacondio F, Bartolucci S, Bedini A, Fanini F, Spadoni G. *N*-(Anilinoethyl)amide Melatonergic Ligands with Improved Water Solubility and Metabolic Stability. *ChemMedChem.* **2021**, 16(19), 3071-3082
- ⁷ Dupré C, Bruno O, Bonnaud A, Giganti A, Nosjean O, Legros C, Boutin JA. Assessments of cellular melatonin receptor signaling pathways: β -arrestin recruitment, receptor internalization, and impedance variations. *Eur J Pharmacol.* **2018**, 818, 534-544
- ⁸ Beresford IJ, Browning C, Starkey SJ, Brown J, Foord SM, Coughlan J, North PC, Dubocovich ML, Hagan RM. GR196429: a nonindolic agonist at high-affinity melatonin receptors. *J Pharmacol Exp Ther.* **1998**, 285(3), 1239-45
- ⁹ a) Duroux R, Rami M, Landagaray E, Ettaoussi M, Caignard DH, Delagrangé P, Melnyk P, Yous S. Synthesis and biological evaluation of new naphtho- and quinolinocyclopentane derivatives as potent melatonergic (MT₁/MT₂) and serotonergic (5-HT_{2C}) dual ligands. *Eur J Med Chem.* **2017**, 141, 552-566; b) Landagaray E, Ettaoussi M, Rami M, Boutin JA, Caignard DH, Delagrangé P, Melnyk P, Berthelot P, Yous S. New quinolinic derivatives as melatonergic ligands: Synthesis and pharmacological evaluation. *Eur J Med Chem.* **2017**, 127, 621-631

-
- ¹⁰ Spadoni G, Bedini A, Lucarini S, Mari M, Caignard DH, Boutin JA, Delagrange P, Lucini V, Scaglione F, Lodola A, Zanardi F, Pala D, Mor M, Rivara S. Highly Potent and Selective MT₂ Melatonin Receptor Full Agonists from Conformational Analysis of 1-Benzyl-2-acylaminomethyl-tetrahydroquinolines. *J Med Chem.* **2015**, 58(18), 7512-25
- ¹¹ Cheng Y, Prusoff WH. Relationship between the inhibition constant (K_i) and the concentration of inhibitor which causes 50 per cent inhibition (I_{50}) of an enzymatic reaction *Biochem. Pharmacol.* **1973**, 22, 3099–3108
- ¹² Mamillapalli, NC, Sekar, G. Chemoselective Reductive Deoxygenation and Reduction of α -Keto Amides by using a Palladium. *Catalyst. Adv. Synth. Catal.* **2015**, 357, 3273-3283
- ¹³ Larrosa M, Guerrero C, Rodriguez R, Cruces J. Selective Copper-Promoted Cross-Coupling of Aromatic Amines with Alkyl Boronic Acids. *Synlett* **2010**, 14, 2101-2105
- ¹⁴ Kamino BA, Mills B, Reali C, Gretton MJ, Brook MA, Bender TP. Liquid Triarylamine: The Scope and Limitations of Piers–Rubinsztajn Conditions for Obtaining Triarylamine–Siloxane Hybrid Materials. *J. Org. Chem.* **2012**, 77(4), 1663–1674
- ¹⁵ Elumalai V, Bjørsvik HR. Indium powder as the reducing agent in the synthesis of 2-amino-1,1'-biphenyls. *Tetrahedron Letters*, **2016**, 57(11), 1224-1226
- ¹⁶ Righi M, Bedini A, Piersanti G, Romagnoli F, Spadoni G. Direct, One-Pot Reductive Alkylation of Anilines with Functionalized Acetals Mediated by Triethylsilane and TFA. Straightforward Route for Unsymmetrically Substituted Ethylenediamine. *The Journal of Organic Chemistry* **2011**, 76(2), 704-707
- ¹⁷ Adeniji AO, Twenter BM, Byrns MC, Jin Y, Chen M, Winkler JD, Penning TM. Development of potent and selective inhibitors of aldo-keto reductase 1C3 (type 5 17 β -hydroxysteroid dehydrogenase) based on *N*-phenylaminobenzoates and their structure-activity relationships. *J Med Chem.* **2012**, 55(5), 2311-23
- ¹⁸ a) Benigni R. The first US National Toxicology Program exercise on the prediction of rodent carcinogenicity: definitive results. *Mutat Res.* **1997**, 387(1), 35-45; b) Mor M, Silva C, Vacondio F, Plazzi PV, Bertoni S, Spadoni G, Diamantini G, Bedini A, Tarzia G, Zusso M, Franceschini D, Giusti P. Indole-based analogs of melatonin: in vitro antioxidant and cytoprotective activities. *J Pineal Res.* **2004**, 36(2), 95-102
- ¹⁹ Lipinski CA, Lombardo F, Dominy BW, Feeney PJ. Experimental and computational approaches to estimate solubility and permeability in drug discovery and development settings. *Adv Drug Deliv Rev.* **2001**, 46(1-3), 3-26

Chapter 5. Design, synthesis and characterization of new dual-acting compounds: MLT agonists and MAGL inhibitors

5.1 Introduction

The pharmacological treatment of complex diseases, such as metabolic syndrome, psychiatric or degenerative CNS disorders, and cancer requires the modulation of the different biological targets implicated in the pathology, in order to generate sufficient therapeutic efficacy. Therefore, these diseases could be treated more successfully with multiple target drugs. Well-designed and optimally balanced multitarget drugs, in addition to potentially increase therapeutic efficacy through synergies, offer a variety of advantages. In particular, multiple ligands may replace a series of drugs in combination therapy, with a subsequent decrease in treatment complexity, drug side effects, pharmacokinetic complexity, drug–drug interactions, and patients' adherence. Furthermore, the clinical development of a single multitarget drug is in general more economic, requiring fewer clinical trials than combination of multiple specific drugs. Two interesting and appealing systems to take into consideration for the design of multitarget compounds are the endocannabinoid and melatonergic systems since several studies highlight that their modulation can be helpful in the treatment of multifactorial diseases, particularly those in which neuroinflammation plays a central role.¹ In the mammalian brain 2-AG is the most abundant endocannabinoid and MAGL, catalyzing the transformation of 2-AG to arachidonic acid, has a central role in controlling levels of both 2-AG and the proinflammatory eicosanoid precursor arachidonic acid¹, which can be further converted to proinflammatory eicosanoids. Therefore, this dual role in controlling neuroinflammation through central 2-AG and arachidonic acid regulation supports wide ranging therapeutic potential for MAGL inhibitors. Indeed, hypofunctionality or deregulation of the endocannabinoid system (with changes in endocannabinoid AEA and 2-AG levels and CB receptors) are some common features in neurodegenerative diseases.²

In line with this consideration, the inhibition of FAAH and MAGL, the two major endocannabinoid hydrolyzing enzymes, has demonstrated to be an effective strategy in different preclinical models of these diseases, due to their anti-inflammatory, antioxidant, and neuroprotective effects, with lesser potential to cause side effects than the use of exogenous cannabinoid agonists.

¹ In contrast to the periphery, where arachidonic acid is primarily derived from phospholipids via cytosolic phospholipase A2, in the brain MAGL serves as the primary regulator of arachidonic acid, controlling >85% of 2-AG metabolism. (Blankman JL, Simon GM, Cravatt BF. A comprehensive profile of brain enzymes that hydrolyze the endocannabinoid 2-arachidonoylglycerol. *Chem Biol.* **2007**, 14(12), 1347-56)

Indications emerging from recent literature suggest that also the activation of MT₁ and MT₂ melatonin receptors by MLT and synthetic analogues exerts protection from oxidative stress, pointing to the melatonergic system as a key player in the context of redox homeostasis and neuroprotection.^{3,4}

Over the years, academic and industrial efforts have been strongly focused on the development of selective MAGL inhibitors or MLT receptor agonists, with potential therapeutic application in several CNS diseases. However, the inhibition of the endocannabinoid hydrolyzing enzymes and simultaneous activation of MLT receptors also appears as a promising therapeutic strategy. Despite the above considerations and the potential benefits, the polypharmacological approach concerning the development of dual-targeting agents, combining MAGL inhibition with the activation of MLT receptors remains not explored.

However, a relevant example of dual-agent URB1341 (**Figure 27**), targeting simultaneously MLT receptors and the endocannabinoid hydrolyzing enzyme FAAH, was recently reported. This multitarget compound was obtained by combining pharmacophoric elements of both the FAAH inhibitor URB597 and 2-Br-MLT through an appropriate alkyl chain.

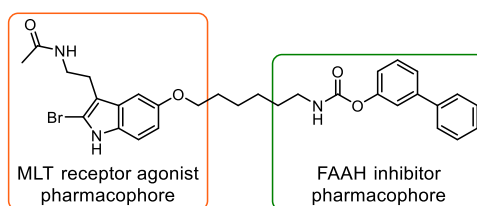


Figure 27 Dual-acting compound UCM1341: MLT agonist and FAAH inhibitor.

UCM1341, having potent (nanomolar) and balanced FAAH inhibitory action and agonistic activity on MT₁/MT₂ melatonin receptors, was able to reduce intraocular pressure in a rabbit model, leading to benefits in the glaucoma treatment.⁵ Interestingly, the same bivalent ligand UCM1341 showed protective effect against inflammation-induced neurodegeneration in *ex vivo* cultures of rat hippocampal explants.⁶ These studies provided evidence that the melatonergic and endocannabinoid systems cooperate to promote neuroprotection against the neuroinflammatory damage, and stimulated further investigations. Looking for novel options to provide neuroprotection, we investigated the possibility to develop dual-targeting agents, combining MAGL inhibition with the activation of MLT receptors. Combination of the two mechanisms is expected to provide a better control of the imbalance in pro-oxidant vs. antioxidant homeostasis and improve recovery from oxidative-stress related cellular damage.

The most advanced classes of covalent MAGL inhibitors are tertiary ureas and carbamates. The common structural features to achieve both high potency towards MAGL and selectivity over other possible off-target serine hydrolases are a reactive warhead able to carbamoylate the nucleophile residue (Ser122), linked to a Y-shaped lipophilic recognition portion, needed to properly fit the

hydrophobic lid domain of MAGL (normally accommodating the long aliphatic chain of the natural substrate 2-AG) (**Figure 28**).

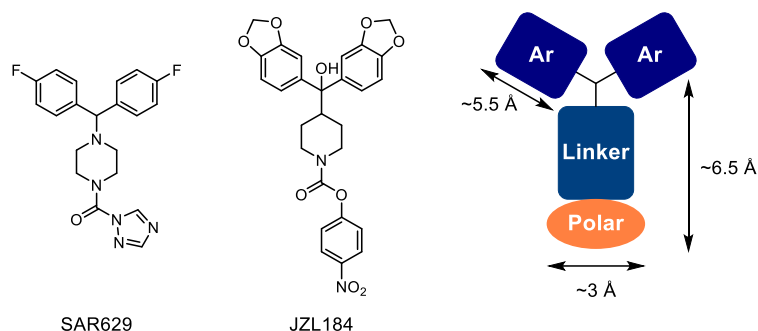


Figure 28 Examples of MAGL inhibitors and typical pharmacophoric points.

In order to facilitate inhibitory acyl transfer with Ser122, carbamates generally contain an alcoholic subunit with a relatively low pK_a , such as 4-nitrophenol and hexafluoroisopropyl alcohol (HFIP), to serve as a suitable leaving group, while urea derivatives have generally an *N*-heterocycle (triazole, tetrazole) as leaving group.

Current knowledge about SARs and the X-ray structures of MGL with Ser122 carbamoylated by inhibitors with different scaffolds⁷ and of MT₁ and MT₂ melatonin receptors in complex with agonist compounds⁸ has been applied to design new dual MLT agonists-MGL inhibitors. The Y-shaped structure of the recognition portion offers the possibility to include the pharmacophoric elements (namely an alkoxy group and an amide side chain attached to an aromatic ring) required for interaction with melatonin receptors in one branch.

Therefore, we designed different series of putative dual-acting compounds, with suitable physicochemical properties, by merging in the same structure the pharmacophore elements required to activate MLT receptors and to carbamoylate the active Ser122 of MAGL (**Figure 29**).

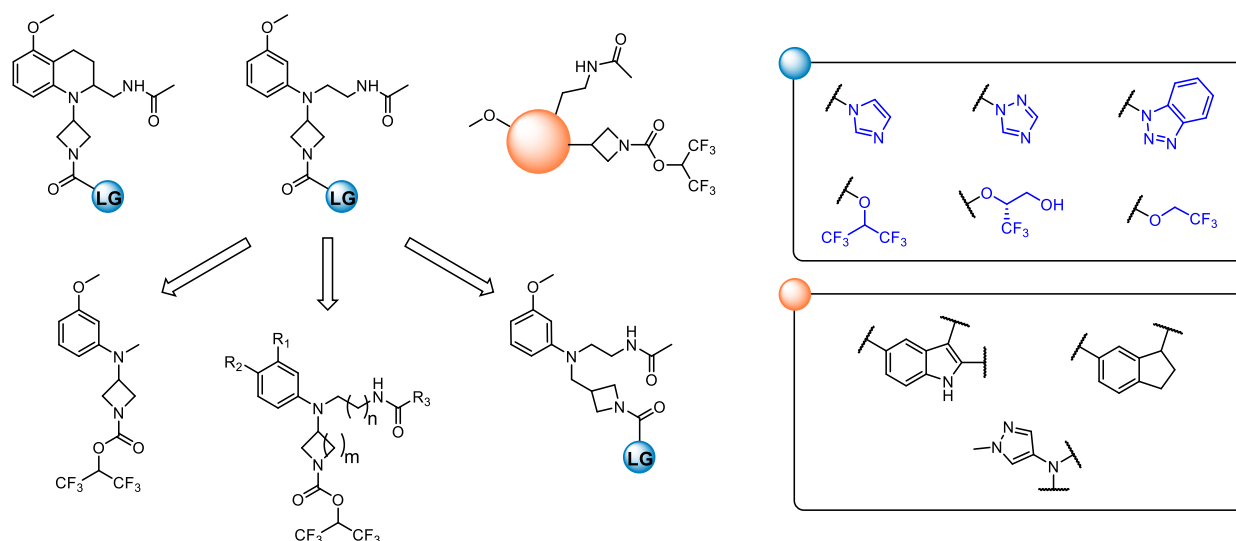


Figure 29 Design of dual-acting compounds by combining relevant structural features of melatonergic ligands and MAGL inhibitors.

5.2 Results and discussion

5.2.1 Design and pharmacological evaluations of the new dual-acting compounds

The first synthesized series of potential dual-acting agents includes compounds obtained by combining, through an azetidine ring, the *N*-anilinoethylamido characteristic moiety of potent MLT ligands with a reactive urea or carbamate warhead having different leaving groups (**Figure 30**).

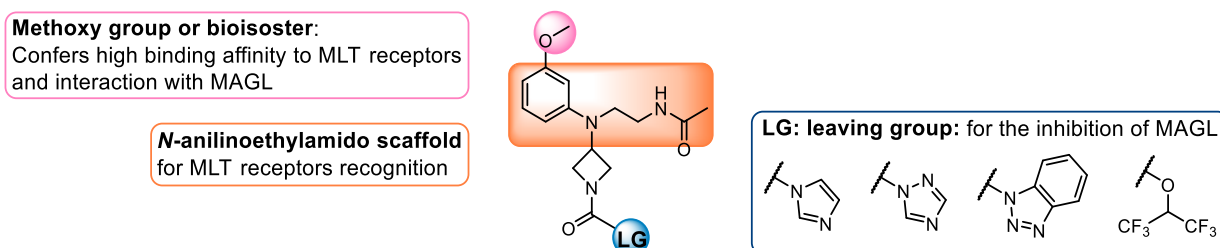
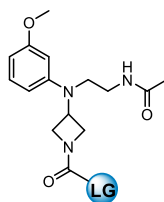


Figure 30 General structure of dual-acting MLT receptors agonists and MAGL inhibitors combining the pharmacophore elements of the two targets.

The new hybrid compounds (**UCM1484-1487**) were evaluated for their binding affinity and intrinsic activity at human MT₁ and MT₂ receptors (stably transfected in Chinese hamster ovary cells using 2-[¹²⁵I]iodomelatonin as radioligand) and for their inhibitory potency toward MAGL *in vitro* (**Table 9**). Pharmacological results indicated the carbamate compound (**UCM1485**) as more promising than urea derivatives (**UCM1484**, **UCM1486** and **UCM1487**).



UCM1484-1487

Table 9 Inhibitory activity on human MAGL and affinity at human MT₁ and MT₂ melatonin receptors of *N*-anilinoethylamido derivatives.

compounds	Leaving Group (LG)	<i>h</i> MAGL IC ₅₀ (nM)	MT ₁ K _i (nM)	MT ₂ K _i (nM)
JJKK-048		0.15±0.01		
UCM1484 7a		2480±168	7647±465	1435±122
UCM1485 9a		275±17	18.2±1.3	26.4±2.1
UCM1486 8a		>10000	1641±135	1753±148
UCM1487 10		93142± 8143	1836± 158	3510± 287

Although all the new compound displayed sub-optimal dual-acting activity, **UCM1485**, structurally characterized by the presence of the *N*-anilinoethylamide scaffold combined with an hexafluoroisopropanol-carbamate, demonstrated that it is possible to fuse the structural elements required for MAGL inhibition and for MLT receptor binding and activation in the same molecule. However, activity of **UCM1485** at the two targets (*hMT*₁ *K*_i = 18.2 nM, *hMT*₂ *K*_i = 26.4 nM, *hMAGL* IC₅₀ = 275 nM), appeared rather unbalanced as MAGL inhibitory potency is about 15 times lower than binding affinity at MLT receptors.

UCM1485 docked into MAGL substrate binding site provided two possible accommodation, where the ethylamido side chain and the methoxy group can exchange their positions, highlighting different solutions for its putative optimization (**Figure 31**).

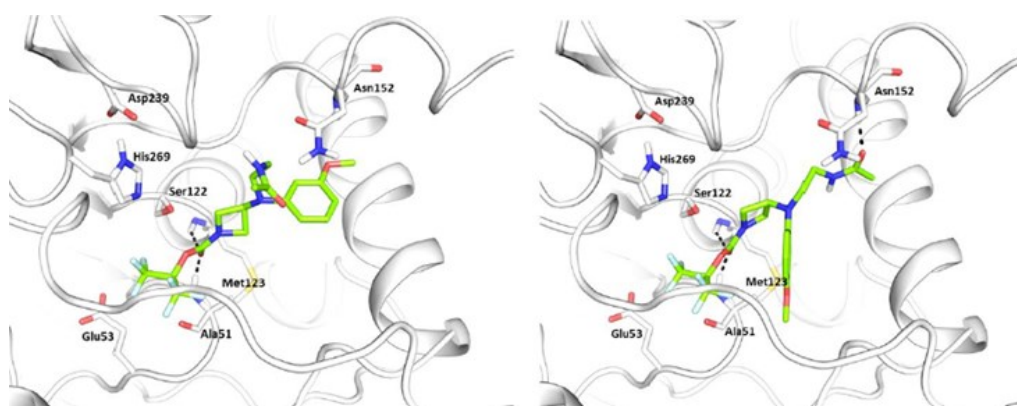


Figure 31 Two possible docking poses for **UCM1485** into MAGL substrate binding site.

With the aim of especially improving MAGL inhibition potency, structural variants were introduced, while conserving the hexafluoroisopropyl carbamate moiety.

Conformational restriction of the flexible alkylamide chain of the *N*-anilinoethylamide ligands gave the corresponding tetrahydroquinoline derivatives **UCM1488-UCM1490** that showed improved potency on MAGL (i.e. **UCM1488** vs **UCM1485**), but at the same time an unexpected significant reduction in binding affinity at *MT*₁ and *MT*₂ receptors was observed (**Table 10**). Also in this series the most potent compound was the one having the hexafluoroisopropanol-carbamate warhead. The observed lower affinity for MLT receptors could depend on the reduced flexibility of the tetrahydroquinoline scaffold and/or greater difficulty in accessing to the binding site.

In an attempt to favor interactions at the MLT receptors, we replaced the *N*-anilinoethylamide scaffold with the *N*-indolyethylamide one of MLT, and contemporary the azetidine-linked-carbamate warhead was introduced at the C-2 indole position, (**UCM1503**, **Table 10**), consistent with SAR for MLT indole derivatives; unfortunately, also this bioisosteric replacement did not allowed to increase MLT receptor binding affinity (*hMT*₁ *K*_i = 718 nM, *hMT*₂ *K*_i = 305 nM, *hMAGL* IC₅₀ = 354 nM).

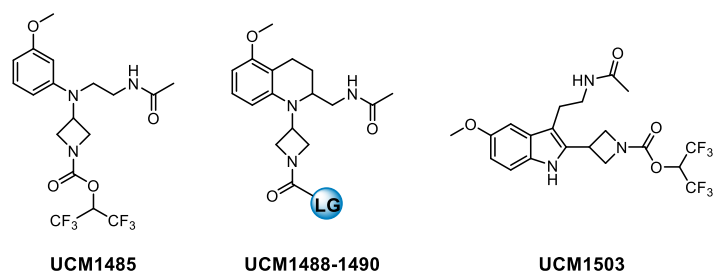


Table 10 Inhibitory activity on human MAGL and affinity at human MT₁ and MT₂ melatonin receptors of the tetrahydroquinoline and N-indolyethylamide derivatives.

compounds	Leaving group (LG)	hMAGL IC ₅₀ (nM)	MT ₁ K _i (nM)	MT ₂ K _i (nM)
JJKK-048		0.15±0.01		
UCM1485 9a		275±17	18.2±1.3	26.4±2.1
UCM1488 9i		169± 11	3187±249	2956±233
UCM1489 8i		>10000	>10000	4697± 392
UCM1490 7i		705±52	>10000	726±59
UCM1503 51		354±24	718±392	305±25

Unfortunately, all the above-mentioned attempts at bioisosteric replacement of the *N*-anilinoethylamide scaffold did not give the desired results, with compound **UCM1485** remaining the most promising structure for lead optimization. The structural modifications introduced in subsequent series were aimed at improve the accommodation of the new compounds on both targets, and their design has been assisted by molecular modelling simulations.

More lipophilic compounds were obtained through replacement of the acetylamino group of **UCM1485** with a propionylamino one (**UCM1493**), addition of a chlorine atom into the anisole moiety (**UCM1499**), or bioisosteric replacement of the methoxy group with a more lipophilic bromine atom (**UCM1497**). The dioxolane derivatives **UCM1498**⁹, deriving from the cyclization of the methoxy group of **UCM1485** on the aniline para position, mimics structural elements already reported both in potent melatonergic ligands and MAGL inhibitors. Alkylamido sidechain lengthening from two to three methylenes (**UCM1494**) is another modification already used on the anilinoethylamides series while retaining a good MLT receptor affinity.

Other structural modifications were made in the linker, used to merge the anilinoethylamido scaffold and the carbamate portion, including the introduction of a methylene spacer (**UCM1501**), or the replacement of the heterocyclic azetidine with a pyrrolidine (**UCM1495**), or a piperidine (**UCM1496**).

A representation of the docking solutions obtained for compound **UCM1501** with both targets is provided in the MT₂ binding site, the ethylamine chain can interact with Gln194 and Asn175, while the *O*-hexafluoroisopropyl carbamate moiety occupies the region corresponding to the C₂ position of melatonin (**Figure 32A**). On the other hand, the carbamate portion occupies the MAGL catalytic site, and its carbonyl group is hydrogen-bonded to the NH of Met123 and Ala51 in the oxyanion hole, close to the catalytic serine Ser122, while the anilinoethylamide portion occupies the region opening to the membrane (**Figure 32B**).

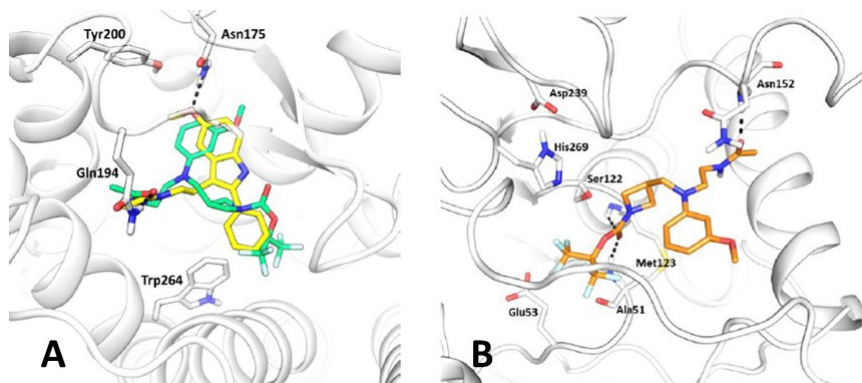


Figure 32 A) docking of compound **UCM1501** (in green) and the 2-Ph-melatonin (in yellow) with the MT₂ receptor. B): docking of compound **UCM1501** in the binding site of MAGL.

In the bioisostere indane derivative **UCM1500** a piperazinyl linker were introduced to reproduce the previously reported scaffold used for piperazinyl-urea melatonergic agonists¹⁰, and its docking pose in the MAGL binding pocket revealed several key interactions (**Figure 33**).

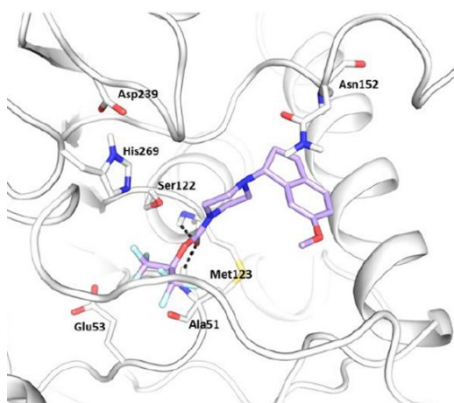


Figure 33 Docking pose of compound **UCM1500**.

Pharmacological results of the new synthesized putative dual-acting compounds **UCM1493-UCM1502** for both considered target are reported **Table 11**.

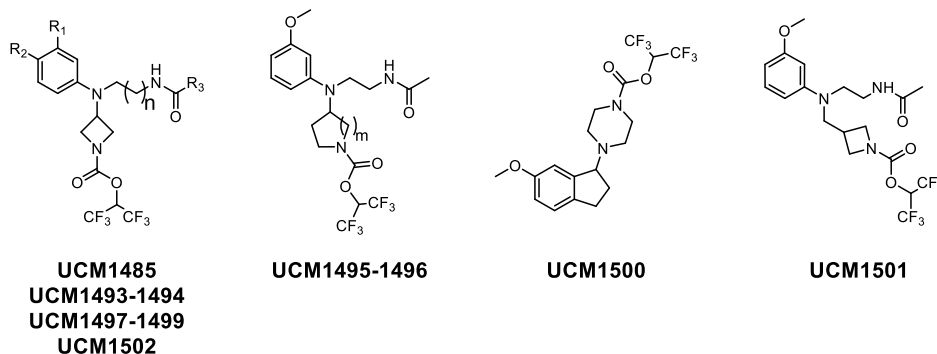


Table 11 Inhibitory activity on human MAGL and affinity at human MT_1 and MT_2 melatonin receptors of the second series.

compounds		Substitutions				<i>h</i> MAGL IC ₅₀ (nM)	MT ₁ K _i (nM)	MT ₂ K _i (nM)
UCM1485	9a	n=1	R ₁ =OMe	R ₂ =H	R ₃ =Me	275±17	18.2±1.3	26.4±2.1
UCM1493	9b	n=1	R ₁ =OMe	R ₂ =H	R ₃ =Pr	220±17	5639± 388	1339± 104
UCM1494	9d	n=2	R ₁ =OMe	R ₂ =H	R ₃ =Me	446±33	>10000	9144± 756
UCM1497	9e	n=1	R ₁ =Br	R ₂ =H	R ₃ =Me	1261±82	>10000	4398± 316
UCM1498	9c	n=1	R ₁ =R ₂ = -OCH ₂ O-		R ₃ =Me	377±25	>10000	>10000
UCM1499	9f	n=1	R ₁ =OMe	R ₂ =Cl	R ₃ =Me	1311±93	>10000	4018± 286
UCM1502	9h	n=1	R ₁ =O(CH ₂) ₄ Ph	R ₂ =H	R ₃ =Me	1294±86	3961± 392	6850± 469
UCM1495	37a	m=1				321±22	>10000	>10000
UCM1496	37b	m=2				7.93± 0.54	>10000	>10000
UCM1500	40					89±6	>10000	6206± 473
UCM1501	17					44±3	7740± 392	5582± 408

Introduction of a methylene unit between the aniline nitrogen and the azetidine (**UCM1501**) or replacement of the azetidine heterocycle with a piperidine (**UCM1496**) or a piperazine (**UCM1500**) moiety led to compounds with remarkable MAGL inhibitory potency. Structural variants on the ethylamido side chain (**UCM1493-UCM1494**), as well as the replacement of the azetidine with a pyrrolidine heterocycle (**UCM1495**) had minimal effect on the ability to inhibit the enzyme. On the contrary, substitution of the methoxy group with a bromine atom (**UCM1497**) or with a longer phenoxyalkyl chain (**UCM1502**), as well as insertion of a chlorine in the *ortho*-position of anisole (**UCM1499**) significantly impacted on the ability to inhibit enzyme activity.

Unfortunately, all the above illustrated structural modification played a strong detrimental role for MLT agonist activity, highlighting a lower steric tolerance of the MLT binding site (or of the lateral entry channel) compared to that of the enzyme.

One of the few compounds retaining a residual receptor binding affinity (micromolar range) was **UCM1501**, which was subsequently structurally modified in order to reduce its steric demand and possibly to favor additional interactions with the MLT receptor binding pocket. For example the high lipophilic hexafluoroisopropyl alcoholic subunit of the carbamate portion has been replaced by 2,2,2-trifluoroethyl alcohol (**UCM1530**) or (*R*)-3,3,3-trifluoropropane-1,2-diol (**UCM1529**). Docking simulation of this latter compounds in the MT₂ receptor binding site revealed additional key interactions between the terminal hydroxymethane group and the Tyr⁹⁴ in the binding pocket (**Figure 34**). A narrow sized compound was obtained by replacement of the anisole moiety of **UCM1501** with the smaller pyrazole ring (**UCM1531**), whose nitrogen atom, similarly to what occurs with the methoxy of MLT, can undertake a hydrogen bond with the Asn175^{4,60} of the MT₂ binding site.

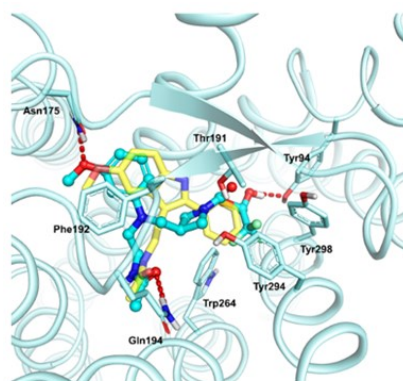


Figure 34 Docking pose of 1,1,1-trifluoromethyl-3-hydroxypropan carbamate derivative **UCM1529** (light blue) and the 2-Ph-MLT (yellow) with the MT₂ receptor. The possible hydrogen bond between the CH₂OH and the Tyr⁹⁴ is highlighted in red.

It has been recently reported the discovery of an interesting peripherally restricted reversible MAGL inhibitor¹¹, structurally characterized by the presence of an α -CF₂-ketone that may function as a warhead. This result stimulated us to take into consideration functional groups different from those normally present in MAGL inhibitors and melatonergic agonists. In this scenario, we synthesized the trifluoro-ketone derivative **UCM1491** and the small-size compound (**UCM1533**) in which the carbamic portion could mimic the typical side chain amido moiety of MLT. In **Figure 35** is illustrated a docking pose of **UCM1533** in the MT₂ receptor, in which are highlighted key interactions of the carbamate moiety or the amido side chain of 2-PhMLT.

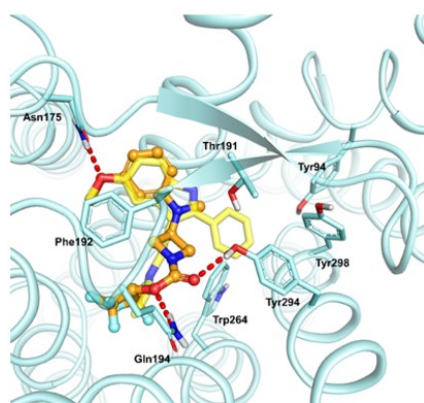


Figure 35 Docking pose of compound **UCM1533** (orange) and 2-Ph-MLT (yellow) in the MT_2 receptor.

As shown in **Table 12**, compound **UCM1533** showed interesting MAGL inhibitory potency, but was unable to activate MLT receptors, as well as all the other putative dual agents tested.

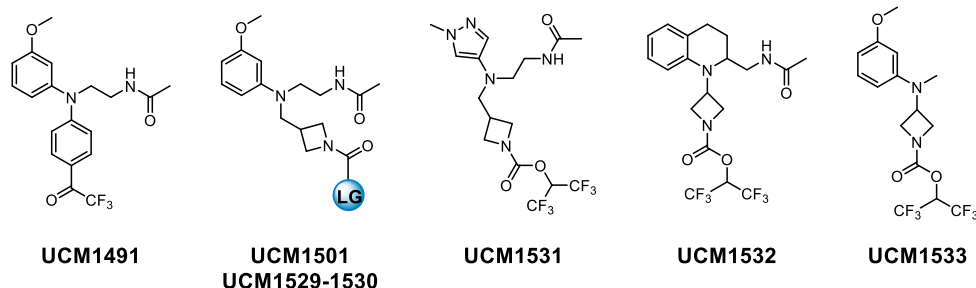


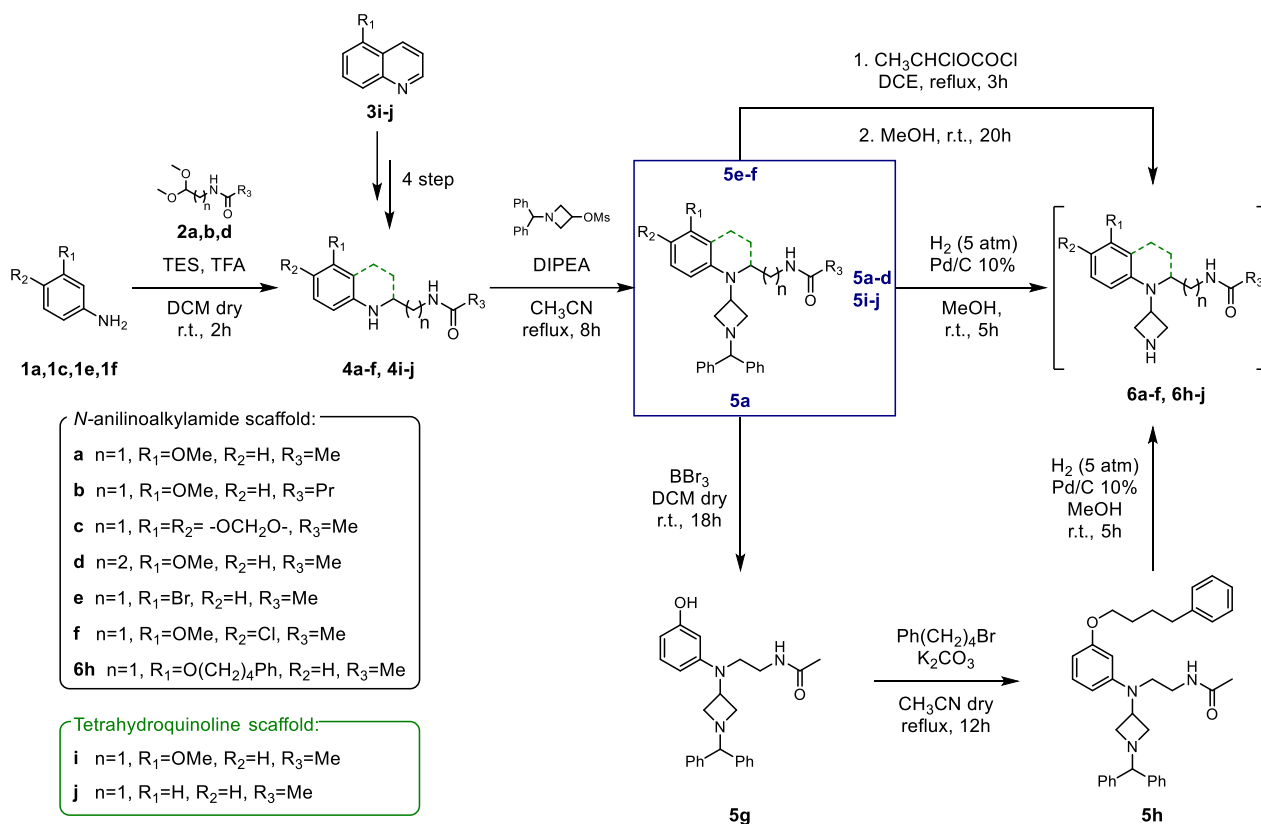
Table 12 Inhibitory activity on human MAGL and affinity at human MT_1 and MT_2 melatonin receptors of the third series.

compounds		Leaving Group (LG)	<i>h</i> MAGL IC ₅₀ (nM)	MT_1 K _i (nM)	MT_2 K _i (nM)
UCM1501	17		44±3	7740± 392	5582± 408
UCM1491	54		43432± 3287	>10000	>10000
UCM1529	19		168±9	>10000	3948± 218
UCM1530	15		7435± 521	1438±91	307±18
UCM1531	28		140±8	>10000	>10000
UCM1532	9j		4392± 287	735±54	356±21
UCM1533	32		9.79±0.68	>10000	>10000

Finally, the potency of **UCM1485**, which showed a balance activity between the two targets, has been evaluated in a cAMP assay for MT_1 and MT_2 receptors. The compound exhibited full agonist behavior for both receptors, with a IC₅₀ (nM) value of 39 ± 5 for MT_1 and 67 ± 5 for MT_2 .

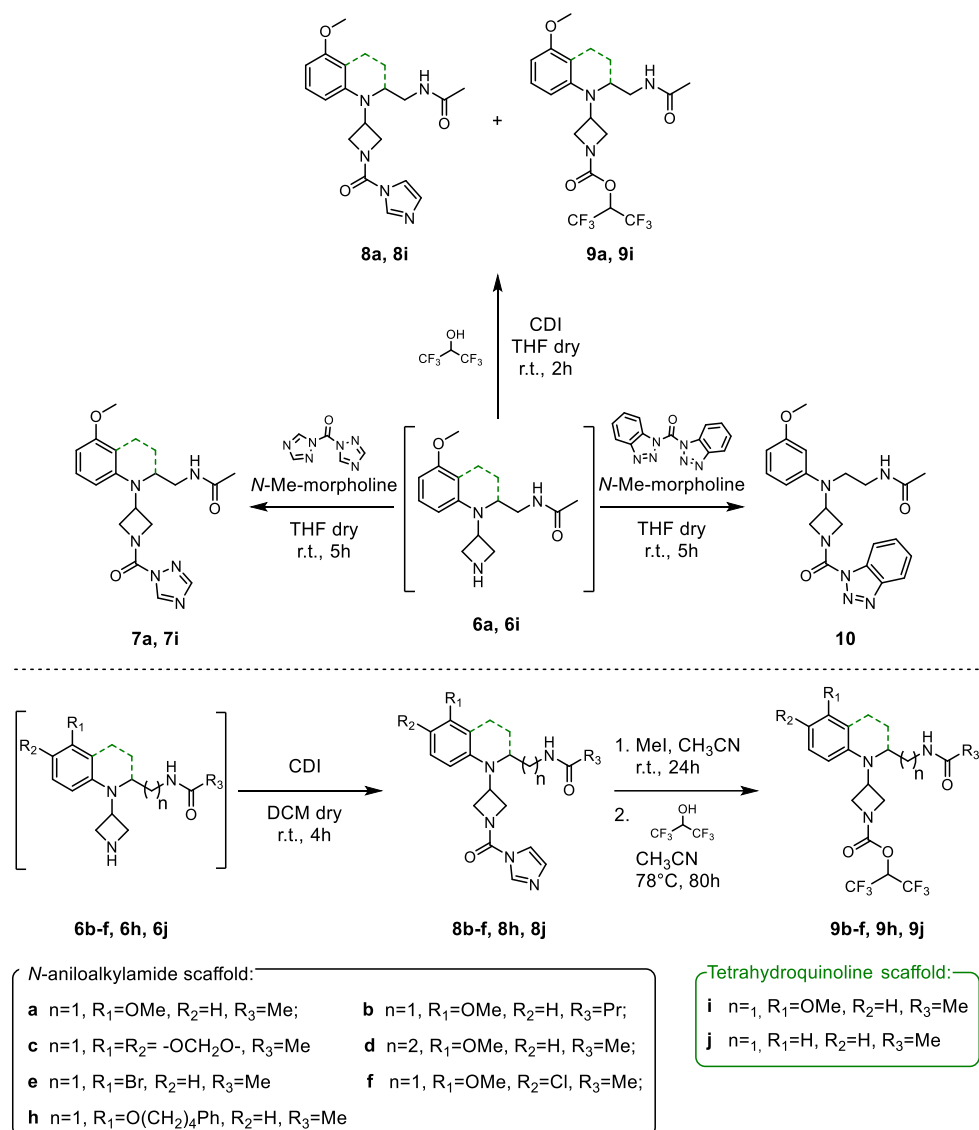
5.2.2 Chemistry

The synthesis of the key intermediates for the preparation of the *N*-anilinoethylamide and the tetrahydroquinolin-2-methanamido derivatives is reported in **Scheme 9**.



Scheme 9 General procedure for preparing the crucial intermediates for synthesizing *N*-anilinoethylamide and the tetrahydroquinolin-2-methanamido derivatives.

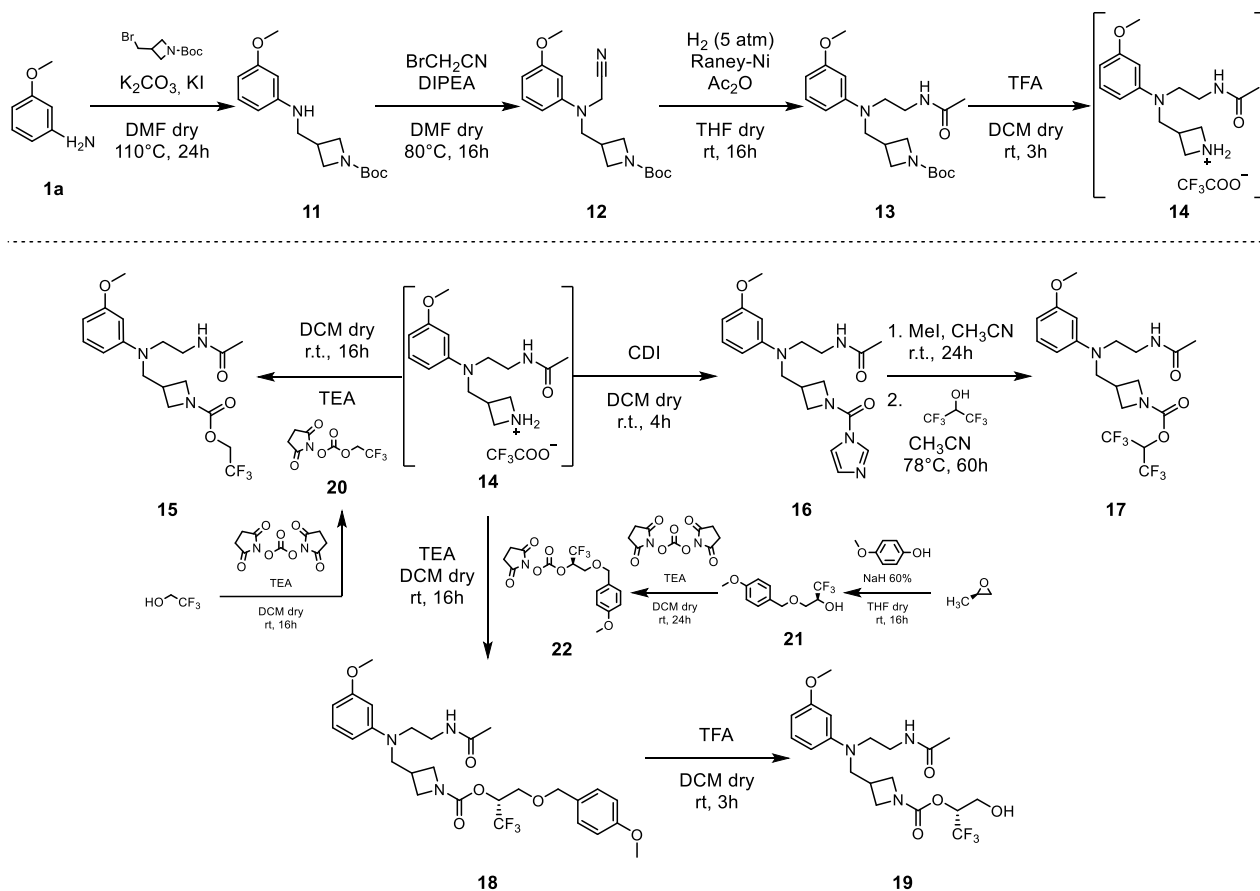
Briefly, the (anilinoalkyl)amido intermediates **4a-f** were prepared by reductive *N*-alkylation of the suitable commercially available anilines **1a**, **1c**, **1e**, and **1f**, with the opportune *N*-(2,2-dimethoxyalkyl)amide in the presence of triethylsilane and trifluoroacetic acid.¹² On the contrary, the tetrahydroquinoline intermediates **4i** and **4j** were prepared from the appropriate quinoline **3i** and **3j**, following a reported procedures¹³. The subsequent treatment of **4a-f** and **4i-j** with *N*-benzhydrylazetididin-3-yl methanesulfonate¹⁴, followed by removal of the *N*-benzhydryl protecting group (H₂ 5 atm over Pd/C for **5a-d** and **5i-j**, or 1-chloroethyl chloroformate for **5e-f**) gave the crucial corresponding azetidines derivatives **6a-f** and **6i-j**. The derivative **6h** can be easily obtained by ether cleavage of the methoxy derivatives **5a** using boron tribromide, followed by *O*-alkylation of the intermediate phenol **5g** with 1-bromo-4-phenylbutane in the presence of K₂CO₃, and final removal of the *N*-benzhydryl group by catalytic hydrogenation. The functionalization of the azetidines derivatives **6a-f** and **6h-j** is illustrated in **Scheme 10**.



Scheme 10 Synthesis of the final *N*-anilinoethylamide derivatives **7a**, **8a**, **9a-f**, **9h** and **10**. Synthesis of the final tetrahydroquinolin-2-methanamido derivatives **7i**, **8i**, **9i**, **9h** and **9j**. *The addition of TEA is required for the preparation of **8e** and **8f**.

The triazole- and benzotriazole-carboxamido derivatives **7a** and **10** were synthesized in good yields by the coupling reaction of the azetidine **6a** with 1,1'-carbonyl-di(1,2,4-triazole) or bis(1*H*-benzo[*d*][1,2,3]triazol-1-yl)methanone, respectively, in the presence of *N*-methylmorpholine.¹⁵ The coupling between tetrahydroquinoline derivative **6i** with 1,1'-carbonyl-di(1,2,4-triazole) afforded the desired compound **7i**. The treatment of the azetidine **6a** with a combination of hexafluoro-2-propanol (HFIP) and CDI in THF afforded the imidazole derivative **8a** and *O*-hexafluoroisopropyl carbamate **9a**. The same reaction with **6i** gave similarly the imidazole derivative **8i** and *O*-hexafluoroisopropyl carbamate **9i**.¹⁶ In order to obtain selectively and in higher yields the desired *O*-hexafluoroisopropyl carbamates, first the azetidine derivatives **6b-f**, **6h**, and **6j** were converted by treatment with CDI into the corresponding imidazole carboxamido derivatives **8b-f**, **8h**, and **8j**, which after methylation to

carbamoylimidazolium salts and treatment with HFIP provided the desired *O*-hexafluoroisopropyl carbamates **9b-f**, **9h** and **9j**.

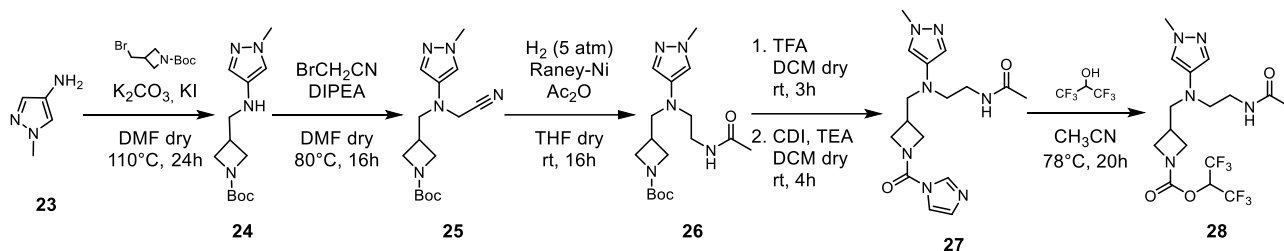


Scheme 11 Synthesis of the *N*-methylazetidines **15**, **17**, and **19**

As illustrated in **Scheme 11**, the synthesis of the *N*-methylazetidines **15**, **17**, and **19** starts with the *N*-alkylation of the *m*-anisidine **1a** with commercially available *N*-Boc-(bromomethyl)azetidine and subsequent *N*-alkylation with bromoacetonitrile (**12**). Reduction and acetylation of the nitrile **12** and final Boc-deprotection with TFA afforded the crucial azetidinium salt **14**, which can undergo the following steps without any further purification. The carbamate moieties were introduced on **14**, in the presence of TEA, by the reaction with compounds 2,5-dioxopyrrolidin-1-yl (2,2,2-trifluoroethyl) carbonate **20** and *(R)*-2,5-dioxopyrrolidin-1-yl (1,1,1-trifluoro-3-((4-methoxybenzyl)oxy)propan-2-yl) carbonate **22**¹⁷ (both bearing *N*-hydroxysuccinimide moiety as leaving group), affording the final compound **15** and compound **18**, respectively. The treatment of **18** with TFA allowed the deprotection of the hydroxy group, providing the final compound **19**. The *O*-hexafluoroisopropyl carbamate derivative **17** was obtained following the same procedure used for the other derivatives (formation of the corresponding imidazole carboxamido derivative **16**, methylation and treatment with HFIP).

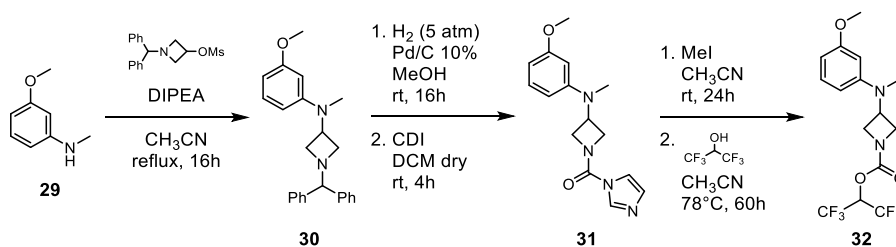
The pyrazole derivative **28** was obtained following a strategy similar to that adopted for *N*-methylazetidines **15**, **17**, and **19**. The key intermediate **26** was prepared by alkylation steps

of the pyrazole **23**, with *N*-Boc-(bromomethyl)azetidine, subsequent treatment of **24** with bromoacetonitrile, followed by reduction and simultaneous acetylation of derivative **25** (*Scheme 12*).



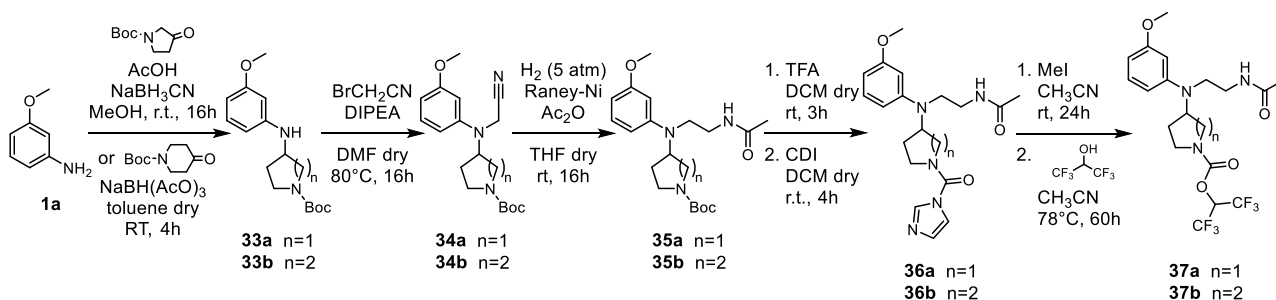
Scheme 12 Synthesis of the pyrazole derivative **28**.

Deprotection of **26** with TFA followed by the reaction of the azetidino intermediate with CDI in the presence of TEA provided the imidazole carboxamido derivative **27**, which was converted into the carbamate **28** by treatment with an excess of HFIP (*Scheme 12*).



Scheme 13 Synthesis of compound **32**.

The dual-acting compound **32** was prepared as depicted in *Scheme 13*. The *N*-alkylation of commercially available anisidine **29** with *N*-benzhydrylazetididin-3-yl methanesulfonate provided the intermediate **30**, which was converted into derivative **31** by *N*-benzhydryl deprotection (H_2 5 atm over Pd/C) followed by reaction with CDI. The general procedure used for the preparation of *O*-hexafluoroisopropyl carbamates afforded the desired compound **32** from **31** (methylation and treatment with HFIP).

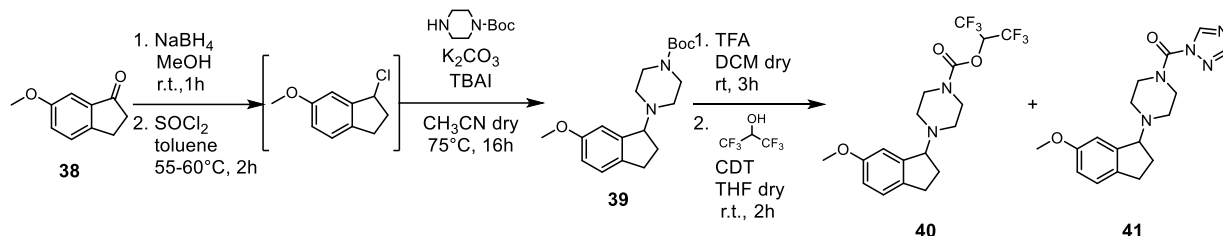


Scheme 14 Synthesis of pyrrolidine and piperidine derivatives **37a** and **37b**.

The pyrrolidine and piperidine derivatives **37a** and **37b** were synthesized, starting with a reductive amination of *m*-anisidine **1a** with *N*-Boc-3-pyrrolidinone or *N*-Boc-4-piperidinone in the presence of sodium cyanoborohydride (for **33a**) or sodium triacetoxyborohydride (for **33b**) (*Scheme 14*). Then, the intermediates **33a-b** were converted into the imidazole carboxamido derivatives **36a-b** using the same procedure described above for compound **27** (alkylation with bromoacetonitrile

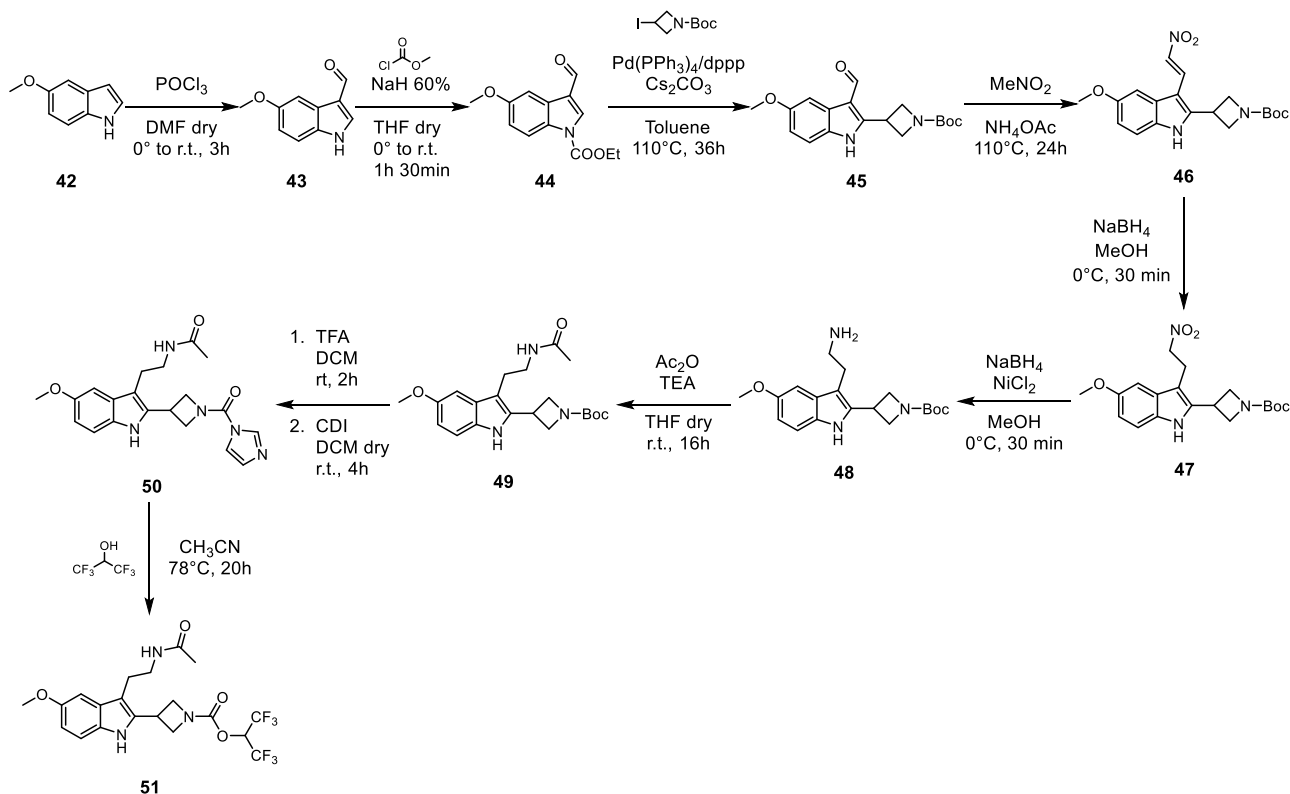
followed by reduction and simultaneously acetylation of the nitrile group). Methylation of compounds **36a-b** afforded the corresponding carbamoylimidazolium salt, which, after treatment with HFIP, provided the final carbamate derivatives **37a-b** (*Scheme 14*).

The synthetic route used for indanylpiperazine derivative **40** is illustrated in *Scheme 15*.



Scheme 15 Synthesis of indanylpiperazine derivative **40**.

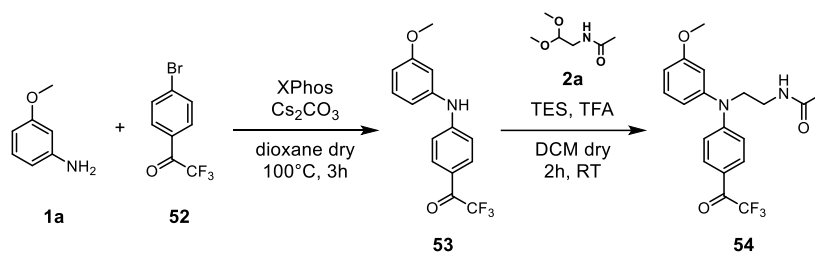
Reduction of the commercially available indanone **38** with sodium borohydride and subsequent chlorination with thionyl chloride afforded a crude, which gave the *N*-protected indanylpiperazine derivative **39** by nucleophilic substitution with *N*-Boc piperazine in the presence of K_2CO_3 and tetra-*N*-butylammonium iodide (TBAI).¹⁸ After *N*-Boc-deprotection with TFA, the resulting piperazine was treated with a combination of HFIP and di(1*H*-1,2,4-triazol-1-yl) (CDT) in THF afforded the *O*-hexafluoroisopropyl carbamate **40** and the triazole carboxamido derivative **41**.



Scheme 16 Synthesis of the 2-azetidinindole derivative **51**.

In *Scheme 16* the synthetic route used to prepare the 2-azetidinindole derivative **51** is outlined. The 3-formyl-indole derivative **44** was obtained by a Vilsmeier reaction and subsequent acylation with ethyl chloroformate. Then, C^2 Pd-catalyzed alkylation of the indole derivative **44** with *N*-Boc-

3-iodoazetidine¹⁹ gave the 2-azetidin-3-formylindole derivative **45**, which was treated with nitromethane to yield the 3-(2-nitrovinyl)-indole derivative **46**. The synthetic sequence continued with two reduction steps of the nitrovinyl group (first with NaBH₄, second NaBH₄ in the presence of NiCl₂) and subsequent *N*-acetylation of the 2-azetidin-tryptamine derivative **48** with acetic anhydride. After *N*-Boc deprotection and reaction with CDI, the *N*-acetyl-2-azetidin-tryptamine derivative **50** was finally converted to the target compound **51** by treatment with an excess of HFIP.



Scheme 17 Synthesis of the trifluoroacetophenone derivative **54**.

The trifluoroacetophenone derivative **54** was prepared by Pd-catalyzed *N*-arylation of 3-methoxyaniline **1a** with 1-(4-bromophenyl)-2,2,2-trifluoroethan-1-one **52** (using Xphos as precatalyst, Cs₂CO₃ as base, and dioxane as solvent), followed by reductive *N*-alkylation of the intermediate *N,N*-diphenylamine **53** with *N*-(2,2-dimethoxyethyl)acetamide **2a** in the presence of triethylsilane and trifluoroacetic acid¹² (*Scheme 17*).

5.3 Conclusion

Different series of putative dual-acting compounds with suitable physicochemical properties were designed by merging in the same structure the pharmacophore elements required to activate melatonin receptors and to carbamoylate the active Ser122 of MGL. The design of the new synthesized compounds has been assisted by molecular modelling simulations to evaluate their complementarity with the two targets. The new compounds were evaluated for their binding affinity and intrinsic activity at human MT₁ and MT₂ receptors and for their inhibitory potency toward MGL *in vitro*. Some of the new synthesized compounds displayed good MGL inhibitory activity and moderate affinity for MLT receptors. The dual-acting compound with the most balanced activity at both targets, is structurally characterized by the presence of the *N*-anilinoethylamido scaffold and the *O*-hexafluoroisopropyl carbamate as leaving group (**UCM1485**). Preliminary pharmacological studies in rat hippocampal explant cultures, showed that this compound exerts neuroprotection against inflammation-induced neurodegeneration in *ex vivo* cultures of rat hippocampal explants, encouraging new and extensive studies with these compounds.

5.4 Experimental section

5.4.1 Materials

Unless otherwise stated, all reagents and solvents were purchased from best-known commercial suppliers and used without further purification.

5.4.2 General procedures

A) General procedure for reductive *N*-alkylation of primary anilines (synthesis of 4a-f and 54).¹²

TFA (1 mL) and TES (2.5 equiv., 2.5 mmol) were added to a solution of the opportune aniline **1a**, **1c**, **1e**, **1f** (1 equiv., 1 mmol) and the suitable acetal **2a**, **2b**, **2d** (1.4 equiv., 1.4 mmol, unless differently specified) in dry DCM (2 mL), and the resulting mixture was stirred at room temperature for 2 h under nitrogen atmosphere. After cooling to 0 °C, the reaction mixture was carefully neutralized with NaHCO₃ aqueous saturated solution and diluted with DCM. The aqueous phase was extracted with DCM and the combined organic phases were washed with brine and dried over Na₂SO₄. The solvent was removed by distillation, and the crude residue was purified by column chromatography to afford the desired compounds **4a-f** and **54**.

B) General procedure for *N*-alkylation of secondary anilines with 1-benzhydrylazetid-3-yl methanesulfonate (synthesis of 5a-f, 13a-b, and 40).¹⁴

A solution of the appropriate arylamine **4a-f**, **4i-j**¹², and **30** (1 equiv., 1 mmol) in dry CH₃CN (4.25 mL) was treated with 1-benzhydrylazetid-3-yl methanesulfonate (1.3 equiv., 1.3 mmol) and DIPEA (2 equiv., 2.00 mmol). The reaction mixture was stirred at reflux (80 °C) overnight. After cooling to room temperature, the mixture was concentrated and purified by silica gel column chromatography to give the desired compounds **5a-f**, **13a-b**, and **40**.

C) General procedure for the *N*-alkylation of secondary anilines with *tert*-butyl 3-(bromomethyl)azetidine-1-carboxylate (synthesis of 11 and 24)

Under nitrogen atmosphere, KI (0.2 equiv., 0.52 mmol) and K₂CO₃ (1.2 equiv., 3.12 mmol) were added to a solution of the anisidine **1a** or pyrazole **23** (1.5 equiv., 3.9 mmol) and *tert*-butyl 3-(bromomethyl)azetidine-1-carboxylate (1 equiv., 2.6 mmol) in dry DMF (7.15 mL). Then, the reaction mixture was heated for 24h at 115 °C. After cooling to room temperature, the suspension was diluted with EtOAc, washed with H₂O, and the aqueous phase was extracted with EtOAc. The combined organic phases were washed with brine (x4), dried over Na₂SO₄, and evaporated under

reduced pressure to yield a crude product, which was purified by flash chromatography to afford the desired compounds **11** and **24**.

D) General procedure for the synthesis of *N*-(cyanomethyl) aniline derivatives (synthesis of **12, **25**, **34a**, and **34b**)**

Under nitrogen atmosphere, the appropriate intermediate **11**, **24**, **33a**, and **33b** (1 equiv., 1.06 mmol) and DIPEA (2 equiv., 2.12 mmol) was dissolved in dry DMF (2.12 mL). Then, the bromoacetonitrile (2 equiv., 2.12 mmol) was added to the solution dropwise at room temperature. After completing the addition, the reaction was stirred at 80°C for 16h. The reaction was quenched, pouring it in a becker with ice-cooled H₂O and then extracted with EtOAc (5 x 10 ml). The combined organic phases were dried over Na₂SO₄ and evaporated under reduced pressure to yield a crude product which was purified by flash chromatography to afford the desired compounds **12**, **25**, **34a**, and **34b**.

E) General procedure for the hydrogenation of the nitrile group and concomitant acylation of the intermediate methanamide (synthesis of **13, **26**, **35a**, and **35b**)**

A solution of *N*-acetonitrile derivatives **12**, **25**, **34a**, and **34b** (1 equiv., 0.79 mmol) and acetic anhydride (5 equiv., 3.95 mmol) in anhydrous THF (7.9 mL) was hydrogenated (5 atm) under stirring for 16h in the presence of Raney Nickel. The mixture was filtered over celite, washing with MeOH. After concentrating the filtrate, the crude was dissolved in EtOAc and washed with an aqueous solution of NaOH 2N, then with brine. The organic phase was dried over Na₂SO₄ and evaporated under reduced pressure to yield a crude product which was purified by flash chromatography to afford the desired compounds **13**, **26**, **35a**, and **35b**.

F1) General procedure for *N*-benzhydryl deprotection of **5a-d, and **5h-j****

A solution of the suitable *N*-benzhydryl azetidine derivatives (1 equiv., 1 mmol) in MeOH (13.8 mL) was hydrogenated over Pd/C 10% (92.3 mg) at 5 atm for 12h at room temperature. The catalyst was filtered on Celite and the filtrate was concentrated in vacuo to give the corresponding crude oily azetidines **6a-d**, and **6h-i** in quantitative yield which were used without any further purification.

F2) General procedure for *N*-benzhydryl deprotection of **5e-f**

1-Chloroethyl chloroformate (1.1 equiv., 1.1 mmol) was added to a solution of the suitable halogenated *N*-benzhydrylazetidines derivative **5e-f** (1 equiv., 1 mmol) in DCE (1.80 mL). The reaction

was stirred at reflux until all the starting material was consumed (around 3h). After cooling to room temperature, the mixture was concentrated and dissolved in methanol (1.80 mL). The mixture was allowed to stir at room temperature for 20h. The reaction was concentrated in vacuo to give the corresponding crude oily azetidines **6e** and **6f** which were used without any further purification.

G) General procedure for the preparation of triazole-carboxamido derivatives (synthesis of 7a and 7i)¹⁵

The opportune *N*-anilino or tetrahydroquinoline ethylamide derivative **6a** or **6i** (1 equiv., 0.54 mmol) in dry THF (4 mL) was added dropwise over 5 minutes to a solution of 1,1'-carbonylditriazole (1.2 equiv., 0.65 mmol) and 4-methylmorpholine (0.01 equiv., 0.05 mmol) in dry THF (4 mL). The reaction mixture was stirred overnight for 5h after which the solvent was evaporated. The residue was taken into EtOAc, washed with water (x2), dried over Na₂SO₄, and concentrated in vacuo. The crude products were purified by silica gel column chromatography to give the desired compounds **7a** and **7i**.

H) General procedure for the preparation of imidazole-carboxamido and hexafluoroisopropanol carbamoyl derivatives (synthesis of 8a, 8i, 9a, and 9i)

To a solution of 1,1'-carbonyldiimidazole (2.5 equiv., 0.56 mmol) in THF (4 mL) was added 1,1,1,3,3,3-hexafluoro-2-propanol (20 equiv., 4.5 mmol). The reaction mixture was stirred at room temperature for 15 min, and then *N*-anilino or tetrahydroquinoline azetidine **6a** or **6i** (1 equiv., 0.22 mmol) was added in one portion. The reaction mixture was stirred for an additional 2 h at room temperature and then concentrated under reduced pressure. The crude was purified by silica gel flash chromatography to give the desired compounds **8a**, **8i**, **9a** and **9i**.

I) General procedure for the preparation of imidazole-carboxamido derivatives 8b-f, 8h, 8j, and 16

1,1'-Carbonyldiimidazole (1.2 equiv., 0.70 mmol) was added to a solution of a generic *N*-heterocycle or azetidine derivatives from deprotection reactions (*Scheme 10* and *Scheme 11*) (1 equiv., 0.58 mmol) in dry DCM (1.15 mL). If specified, TEA (2.5 equiv., 1.74 mmol) was added to the solution. The reaction was stirred at room temperature for 4h. After completion, the solution was diluted with DCM and washed with H₂O (x3). The organic phase was dried over Na₂SO₄ and evaporated under reduced pressure to yield a crude product which was purified by flash chromatography to afford the desired compounds **8b-f**, **8h**, **8j**, and **16**.

J) General procedure for the preparation of imidazole-carboxamido derivatives 27, 36a-b, and 50

TFA (0.38 mL) was added to a solution of the suitable *N*-Boc azetidine (or different heterocycle) derivatives **26**, **34a-b**, and **49** (1 equiv., 0.71 mmol) in DCM (1.05 mL) at room temperature. The reaction was stirred at room temperature until the starting material is completely disappeared (about 2h). Then, the reaction was diluted with DCM and washed with an aqueous saturated solution of NaHCO₃. The aqueous phase was extracted with DCM (x3). The combined organic phases were concentrated in vacuo to give the corresponding crude oily azetidine in quantitative yield which was used without any further purification in the next step. For pyrazoline derivative **26**, the extraction step was avoided due to its propensity to remain solubilized in water; then the reaction mixture was concentrated under reduced-pressure to yield a crude product which was used directly in the next step. Then the obtained crude was dissolved in dry DCM (1.15 mL) and CDI (1.2 equiv., 0.70 mmol) was added to the solution. If specified, TEA (2.5 equiv., 1.74 mmol) was added to the solution. The reaction was stirred at room temperature for 4h. After completion, the solution was diluted with DCM and washed with H₂O (x3). The organic phase was dried over Na₂SO₄ and evaporated under reduced pressure to yield a crude product which was purified by flash chromatography to afford the desired compounds **27**, **36a-b**, and **50**.

K) General procedure for the preparation of hexafluoroisopropanol-carbamate derivatives 9b-f, 9h, 9j, 17, 32, and 37a-b

Methyl iodide (3.5 equiv., 1.1 mmol) is added to a solution of the imidazole-carboxamido derivatives **8b-f**, **16**, **31**, and **36a-b** (1 equiv., 0.31 mmol) in dry CH₃CN (0.62 mL). The reaction was stirred for 24h at room temperature and then concentrated to yield a crude, that is used without any further purification (quantitative yield). 1,1,1,3,3,3-hexafluoropropan-2-ol (1.2 equiv., 0.372 mmol or 2.5 equiv., 0.775 mmol depending on the substrate) is added to a solution of the crude in dry CH₃CN (0.94 mL). The reaction was stirred at 78°C for 60h, and after cooling to room temperature, concentrated under reduced pressure. The crude was purified by silica gel flash chromatography to give the desired final compounds **9b-f**, **9h**, **9j**, **17**, **32**, and **37a-b**.

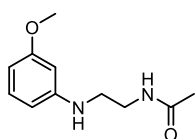
L) General procedure for the preparation of hexafluoroisopropanol-carbamate derivatives 28 and 51

The *N*-carboxamide imidazole derivative (1 equiv., 0.21 mmol) is dissolved in dry ACN (0.57 mL). Then, HFIP (15 equiv., 3.15 mmol) is added to the solution. The reaction was stirred at 78°C for 20h and after cooling to room temperature, concentrated under reduced pressure. The crude is

dissolved in EtOAc, washed with an aqueous solution of NaOH 2N (x2) and then brine. The organic phase was dried over Na₂SO₄ and evaporated under reduced pressure to yield a crude product, which was purified by flash chromatography to afford the desired compounds **28** and **51**.

5.4.3 Experimental data

***N*-(2-((3-methoxyphenyl)amino)ethyl)acetamide (4a)**



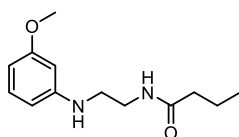
4a

Compound **4a** was prepared following the described general procedure **A** starting from **1a** and *N*-(2,2-dimethoxyethyl)acetamide **2a**.

Flash chromatography: silica gel, EtOAc as eluent. Dark oil, 90% yield.

Physicochemical data are in agreement with those previously reported.¹³

***N*-(2-((3-methoxyphenyl)amino)ethyl)butyramide (4b)**



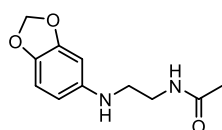
4b

Compound **4b** was prepared following the described general procedure **A** starting from **1a** and *N*-(2,2-dimethoxyethyl)butyramide **2b**¹² (1.00 mmol instead of 1.4 mmol). Flash chromatography: silica gel, cyclohexane:EtOAc 2:8 as eluent. Brown oil, 73% yield.

ESI MS (*m/z*): 237 [M+H]⁺

¹H NMR (400 MHz, Chloroform-*d*) δ 7.08 (t, *J* = 8.0 Hz, 1H), 6.28 (dd, *J* = 8.0, 2.0 Hz, 1H), 6.23 (dd, *J* = 8.0, 2.0 Hz, 1H), 6.17 (t, *J* = 2.0 Hz, 1H), 5.75 (br s, 1H), 4.05 (br s, 1H), 3.77 (s, 3H), 3.51 (q, *J* = 6.0 Hz, 2H), 3.30 – 3.23 (m, 2H), 2.21 – 2.12 (m, 2H), 1.66 (h, *J* = 7.5 Hz, 2H), 0.94 (t, *J* = 7.5 Hz, 3H)

***N*-(2-(benzo[*d*][1,3]dioxol-5-ylamino)ethyl)acetamide (4c)**



4c

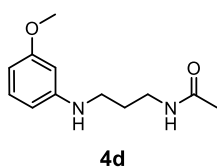
Compound **4c** was prepared following the described general procedure **A** starting from **1c** and *N*-(2,2-dimethoxyethyl)acetamide **2a**.

Flash chromatography: silica gel, EtOAc:MeOH 94:6 as eluent. Brown oil, 96% yield.

ESI MS (*m/z*): 223 [M+H]⁺

¹H NMR (400 MHz, Chloroform-*d*) δ 6.65 (d, *J* = 8.5 Hz, 1H), 6.25 (d, *J* = 2.5 Hz, 1H), 6.05 (dd, *J* = 8.5, 2.5 Hz, 1H), 5.85 (s, 2H), 5.80 (s, 1H), 3.48 (q, *J* = 6.0 Hz, 2H), 3.23 – 3.18 (m, 2H), 1.99 (s, 3H)

N-(3-((3-methoxyphenyl)amino)propyl)acetamide (**4d**)



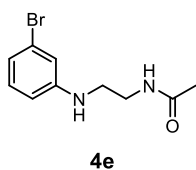
Compound **4d** was prepared following the described general procedure starting **A** from **1a** and *N*-(3,3-dimethoxypropyl)acetamide **2d**¹².

Flash chromatography: silica gel, EtOAc as eluent. Brown oil, 86% yield.

ESI MS (*m/z*): 223 [M+H]⁺

¹H NMR (400 MHz, Chloroform-*d*) δ 7.08 (t, *J* = 8.0 Hz, 1H), 6.33 – 6.22 (m, 2H), 6.21 – 6.15 (m, 1H), 5.64 (br s, 1H), 4.00 (br s, 1H), 3.77 (s, 3H), 3.37 (q, *J* = 6.5 Hz, 2H), 3.17 (t, *J* = 6.5 Hz, 2H), 1.98 (s, 3H), 1.79 (p, *J* = 6.5 Hz, 2H)

N-(2-((3-bromophenyl)amino)ethyl)acetamide (**4e**)



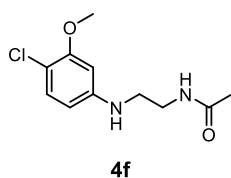
Compound **4e** was prepared following the described general procedure **A** starting from **1e** and *N*-(2,2-dimethoxyethyl)acetamide **2a**.

Flash chromatography: silica gel, EtOAc as eluent. Oil, 90% yield.

ESI MS (*m/z*): 258 [M+H]⁺

¹H NMR (400 MHz, Chloroform-*d*) δ 7.01 (t, *J* = 8.0 Hz, 1H), 6.81 (d, *J* = 8.0 Hz, 1H), 6.73 (s, 1H), 6.52 (dd, *J* = 8.0, 2.0 Hz, 1H), 5.77 (s, 1H), 4.21 (s, 1H), 3.50 (q, *J* = 6.0 Hz, 2H), 3.28 – 3.21 (m, 2H), 2.00 (s, 3H).

N-(2-((4-chloro-3-methoxyphenyl)amino)ethyl)acetamide (**4f**)



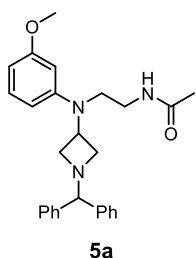
Compound **4f** was prepared following the described general procedure **A** starting from **1f** and *N*-(2,2-dimethoxyethyl)acetamide **2a**.

Flash chromatography: silica gel, EtOAc as eluent. White solid, 88% yield.

ESI MS (*m/z*): 243 [M+H]⁺

¹H NMR (400 MHz, Chloroform-*d*) δ 7.09 (d, *J* = 8.5 Hz, 1H), 6.22 (d, *J* = 2.5 Hz, 1H), 6.13 (dd, *J* = 8.5, 2.5 Hz, 1H), 6.05 (br s, 1H), 4.19 (br s, 1H), 3.83 (s, 3H), 3.48 (q, *J* = 6.0 Hz, 2H), 3.27 – 3.19 (m, 2H), 1.98 (s, 3H)

N-(2-((1-benzhydrylazetid-3-yl)(3-methoxyphenyl)amino)ethyl)acetamide (**5a**)



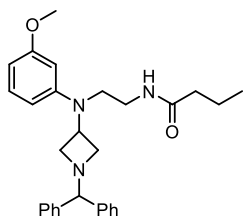
Compound **5a** was prepared following the described general procedure **B** starting from **3a**.

Flash chromatography: silica gel, cyclohexane:EtOAc 1:9 as eluent.

White solid, 70% yield (conversion of **3a**, 73%).

^1H NMR (400 MHz, Chloroform-*d*) δ 7.42 – 7.37 (m, 4H), 7.30 – 7.23 (m, 4H), 7.20 – 7.15 (m, 2H), 7.09 (t, J = 8.0 Hz, 1H), 6.35 (dd, J = 2.5, 1.5 Hz, 1H), 6.33 (dd, J = 2.5, 1.5 Hz, 1H), 6.26 (t, J = 2.5 Hz, 1H), 5.54 (t, J = 6.0 Hz, 1H), 4.33 (br s, 1H), 4.16 (p, J = 6.5 Hz, 1H), 3.74 (s, 3H), 3.62 (td, J = 6.5, 2.0 Hz, 2H), 3.41 – 3.35 (m, 2H), 3.34 – 3.27 (m, 2H), 2.91 (td, J = 7.0, 1.8 Hz, 2H), 1.82 (s, 3H)

***N*-(2-((1-benzhydrylazetid-3-yl)(3-methoxyphenyl)amino)ethyl)butyramide (5b)**



5b

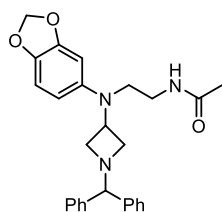
Compound **5b** was prepared following the described general procedure **B** starting from **3b**.

Flash chromatography: silica gel, cyclohexane:EtOAc 1:1 as eluent.

White solid, 67% yield (conversion of **3b**, 80%).

^1H NMR (400 MHz, Chloroform-*d*) δ 7.40 (d, J = 6.9 Hz, 4H), 7.31 – 7.24 (m, 4H), 7.22 – 7.16 (m, 2H), 7.10 (t, J = 8.1 Hz, 1H), 6.38 – 6.32 (m, 2H), 6.26 (t, J = 2.2 Hz, 1H), 5.44 (s, 1H), 4.34 (s, 1H), 4.17 (p, J = 6.7 Hz, 1H), 3.75 (s, 3H), 3.64 (td, J = 6.4, 1.6 Hz, 2H), 3.43 – 3.37 (m, 2H), 3.36 – 3.29 (m, 2H), 2.95 – 2.86 (m, 2H), 2.02 (q, J = 7.5 Hz, 2H), 1.54 (dt, J = 14.8, 7.5 Hz, 2H), 0.89 (t, J = 7.4 Hz, 3H)

***N*-(2-((1-benzhydrylazetid-3-yl)(benzo[*d*][1,3]dioxol-5-yl)amino)ethyl)acetamide (5c)**



5c

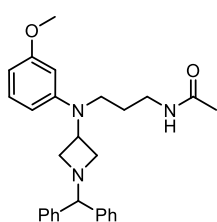
Compound **5c** was prepared following the described general procedure **B** starting from **3c**.

Flash chromatography: silica gel, cyclohexane:EtOAc 2:8 as eluent.

White solid, 77% yield.

^1H NMR (400 MHz, Chloroform-*d*) δ 7.41 – 7.36 (m, 4H), 7.29 – 7.23 (m, 4H), 7.21 – 7.15 (m, 2H), 6.65 (d, J = 8.5 Hz, 1H), 6.44 (d, J = 2.5 Hz, 1H), 6.26 (dd, J = 8.5, 2.5 Hz, 1H), 5.87 (s, 2H), 5.56 (br s, 1H), 4.33 (s, 1H), 3.98 (p, J = 6.5 Hz, 1H), 3.51 (td, J = 6.5, 1.5 Hz, 2H), 3.24 (q, J = 6.0 Hz, 2H), 3.14 (t, J = 6.0 Hz, 2H), 2.85 – 2.79 (m, 2H), 1.89 (s, 3H)

***N*-(3-((1-benzhydrylazetid-3-yl)(3-methoxyphenyl)amino)propyl)acetamide (5d)**



5d

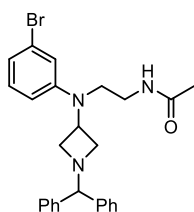
Compound **5d** was prepared following the described general procedure **B** starting from **3d**.

Flash chromatography: silica gel, EtOAc as eluent.

Oil, 62% yield (conversion of **3d**, 75%).

^1H NMR (400 MHz, Chloroform-*d*) δ 7.45 – 7.39 (m, 4H), 7.31 – 7.24 (m, 4H), 7.22 – 7.16 (m, 2H), 7.10 (t, $J = 8.0$ Hz, 1H), 6.37 – 6.29 (m, 2H), 6.23 – 6.20 (m, 1H), 5.75 (br s, 1H), 4.34 (s, 1H), 4.09 (p, $J = 6.5, 5.5$ Hz, 1H), 3.73 (s, 3H), 3.64 (t, $J = 6.5$ Hz, 2H), 3.25 (t, $J = 7.5$ Hz, 2H), 3.13 (q, $J = 6.5$ Hz, 2H), 2.90 (t, $J = 7.2$ Hz, 2H), 1.87 (s, 3H), 1.62 (p, $J = 7.0$ Hz, 2H)

***N*-(2-((1-benzhydrylazetid-3-yl)(3-bromophenyl)amino)ethyl)acetamide (5e)**



5e

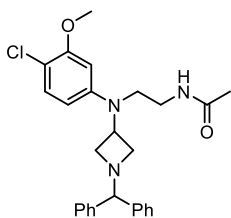
Compound **5e** was prepared following the described general procedure **B** starting from **3e**.

Flash chromatography: silica gel, cyclohexane:EtOAc 2:8 as eluent.

White solid, 67% yield.

^1H NMR (400 MHz, Chloroform-*d*) δ 7.43 – 7.39 (m, 4H), 7.31 – 7.25 (m, 4H), 7.22 – 7.17 (m, 2H), 7.03 (t, $J = 8.0$ Hz, 1H), 6.87 (dd, $J = 7.5, 1.5$ Hz, 1H), 6.83 (t, $J = 2.0$ Hz, 1H), 6.64 (dd, $J = 8.0, 2.0$ Hz, 1H), 5.53 (br s, 1H), 4.34 (s, 1H), 4.16 (p, $J = 6.5$ Hz, 1H), 3.63 (td, $J = 6.5, 1.5$ Hz, 2H), 3.41 (t, $J = 6.5$ Hz, 2H), 3.31 (q, $J = 6.5$ Hz, 2H), 2.92 (td, $J = 7.0, 1.5$ Hz, 2H), 1.86 (s, 3H)

***N*-(2-((1-benzhydrylazetid-3-yl)(4-chloro-3-methoxyphenyl)amino)ethyl)acetamide (5f)**



5f

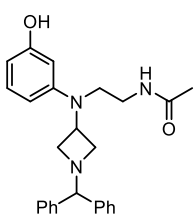
Compound **5f** was prepared following the described general procedure **B** starting from **3f**.

Flash chromatography: silica gel, cyclohexane:EtOAc 2:8 as eluent.

White solid, 67% yield.

^1H NMR (400 MHz, Chloroform-*d*) δ 7.44 – 7.39 (m, 4H), 7.31 – 7.26 (m, 4H), 7.23 – 7.16 (m, 2H), 7.11 (d, $J = 8.5$ Hz, 1H), 6.42 (d, $J = 2.5$ Hz, 1H), 6.21 (dd, $J = 8.5, 2.5$ Hz, 1H), 5.56 (br s, 1H), 4.37 (s, 1H), 4.19 (p, $J = 6.5$ Hz, 1H), 3.86 (s, 3H), 3.64 (t, $J = 7.0$ Hz, 2H), 3.39 (t, $J = 7.0$ Hz, 2H), 3.30 (q, $J = 6.0$ Hz, 2H), 3.01 – 2.90 (m, 2H), 1.87 (s, 3H)

***N*-(2-((1-benzhydrylazetid-3-yl)(3-hydroxyphenyl)amino)ethyl)acetamide (5g)**



5g

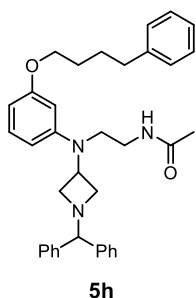
A solution of BBr_3 1M in DCM (5 equiv., 5 mL, 5 mmol) diluted with dry DCM (10 mL) was added dropwise to a solution of the methoxy derivative **5a** (1 equiv., 429 mg, 1.00 mmol) in dry DCM (2 mL) at 0°C , and the resulting mixture was stirred at room temperature for 18h.²⁰ The reaction mixture was neutralized with a 2N aqueous solution of Na_2CO_3 and extracted with EtOAc (x2). The organic phases were combined, dried over Na_2SO_4 , and concentrated under reduced pressure to give the crude which was

purified by flash chromatography (silica gel, DCM:MeOH 98:2 as eluent) to give **5g** as an oil (35% yield, 64% conversion).

¹H NMR (400 MHz, Chloroform-*d*) δ 7.39 (d, *J* = 7.5 Hz, 4H), 7.26 (t, *J* = 7.5 Hz, 4H), 7.21 – 7.15 (m, 2H), 7.00 (t, *J* = 8.0 Hz, 1H), 6.32 – 6.26 (m, 2H), 6.21 (dd, *J* = 8.0, 2.0 Hz, 1H), 5.78 (br s, 1H), 4.34 (s, 1H), 4.13 (p, *J* = 6.5 Hz, 1H), 3.61 (t, *J* = 6.5 Hz, 2H), 3.35 – 3.30 (m, 2H), 3.26 (q, *J* = 7.0, 6.0 Hz, 2H), 2.92 (t, *J* = 7.0 Hz, 2H), 1.80 (s, 3H)

N-(2-((1-benzhydrylazetid-3-yl)(3-(4-phenylbutoxy)phenyl)amino)ethyl)acetamide

(**5h**)

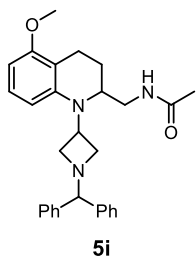


(4-Bromobutyl)benzene (2 equiv., 0.14 mL, 0.82 mmol) was added to a mixture of 3-hydroxy-*N*-(anilinoethyl)amide derivative **5g** (1 equiv., 169 mg, 0.41 mmol) and K₂CO₃ (2.5 equiv., 141 mg, 1.025 mmol) in dry CH₃CN (1.55 mL). The reaction was refluxed for 12h. After cooling to room temperature, the mixture was concentrated. The crude was dissolved in DCM and washed with H₂O and brine.

The organic phase was dried over Na₂SO₄ and concentrated under reduced pressure to give the crude, which was purified by flash chromatography (silica gel, cyclohexane:EtOAc 2:8 as eluent) to give **5h** as a white solid (78% yield).

¹H NMR (400 MHz, Chloroform-*d*) δ 7.41 (d, *J* = 7.0 Hz, 4H), 7.31 – 7.24 (m, 6H), 7.22 – 7.16 (m, 5H), 7.08 (t, *J* = 8.0 Hz, 1H), 6.34 (t, *J* = 2.5 Hz, 1H), 6.32 (t, *J* = 2.5 Hz, 1H), 6.25 (t, *J* = 2.5 Hz, 1H), 5.46 (br s, 1H), 4.34 (s, 1H), 4.17 (p, *J* = 7.0 Hz, 1H), 3.94 – 3.88 (m, 2H), 3.63 (t, *J* = 7.0 Hz, 2H), 3.39 (t, *J* = 6.0 Hz, 2H), 3.32 (q, *J* = 6.0 Hz, 2H), 2.92 (t, *J* = 7.0 Hz, 2H), 2.66 (d, *J* = 7.0 Hz, 2H), 1.84 (s, 3H), 1.79 (t, *J* = 3.5 Hz, 4H)

N-((1-(1-benzhydrylazetid-3-yl)-5-methoxy-1,2,3,4-tetrahydroquinolin-2-yl)methyl)acetamide (**5i**)



Compound **5i** was prepared following the described general procedure **B** starting from **4i**¹³.

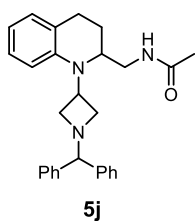
Flash chromatography: silica gel, cyclohexane:EtOAc 3:7 as eluent.

White solid, 69% yield.

¹H NMR (400 MHz, Chloroform-*d*) δ 7.45 – 7.37 (m, 4H), 7.32 – 7.23 (m, 4H), 7.22 – 7.15 (m, 2H), 6.97 (t, *J* = 8.0 Hz, 1H), 6.29 (d, *J* = 8.0 Hz, 1H), 6.09 (d, *J* = 8.0 Hz, 1H), 5.52 (br s, 1H), 4.32 (s, 1H), 4.23 (s, 1H), 3.78 (s, 3H), 3.72 – 3.57 (m, 3H), 3.26 (dt, *J* = 13.0, 6.5 Hz, 1H), 3.13 (dt, *J* = 13.0, 6.5 Hz, 1H), 3.04 – 2.94 (m, 1H), 2.90 – 2.81 (m, 1H), 2.75 (dd, *J* = 17.5, 7.0 Hz, 1H), 2.49 (ddd, *J* = 18.0, 12.5, 7.5 Hz, 1H), 1.98 – 1.88 (m, 4H), 1.84 (ddd, *J* = 13.5, 6.5, 2.0 Hz, 1H).

***N*-((1-(1-benzhydrylazetid-3-yl)-1,2,3,4-tetrahydroquinolin-2-yl)methyl)acetamide**

(5j)



Compound **5j** was prepared following the described general procedure **B** starting from **4j**.¹³

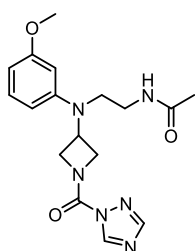
Flash chromatography: silica gel, cyclohexane:EtOAc 3:7 as eluent.

Amorphous solid, 74% yield.

¹H NMR (400 MHz, Chloroform-*d*) δ 7.46 – 7.38 (m, 4H), 7.33 – 7.23 (m, 4H), 7.19

(dtt, *J* = 8.5, 6.5, 1.4 Hz, 2H), 7.02 – 6.96 (m, 2H), 6.67 (td, *J* = 7.5, 1.0 Hz, 1H), 6.38 (dd, *J* = 8.5, 1.0 Hz, 1H), 5.48 (t, *J* = 5.0 Hz, 1H), 4.33 (s, 1H), 4.22 (p, *J* = 7.0 Hz, 1H), 3.71 (td, *J* = 6.5, 2.0 Hz, 1H), 3.66 (td, *J* = 7.0, 3.0 Hz, 1H), 3.64 – 3.58 (m, 1H), 3.29 (dt, *J* = 13.5, 6.5 Hz, 1H), 3.17 (dt, *J* = 13.5, 6.0 Hz, 1H), 3.02 (t, *J* = 7.5 Hz, 1H), 2.87 – 2.82 (m, 1H), 2.80 – 2.66 (m, 2H), 2.02 – 1.91 (m, 1H), 1.90 (s, 3H), 1.89 – 1.82 (m, 1H)

***N*-2-((1-(1H-1,2,4-triazole-1-carbonyl)azetid-3-yl)(3-methoxyphenyl)amino)ethyl acetamide (7a, UCM1484)**



Compound **7a** was prepared following the described general procedure **G** starting from **6a**.

Flash chromatography: silica gel, EtOAc:MeOH 95:5 as eluent.

White solid, 72% yield.

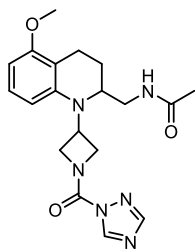
ESI MS (*m/z*): 359 [M+H]⁺

7a, UCM1484

¹H NMR (400 MHz, Chloroform-*d*) δ 8.82 (s, 1H), 7.92 (s, 1H), 7.13 (t, *J* = 8.0 Hz, 1H), 6.43 (dd, *J* = 8.0, 2.5 Hz, 1H), 6.35 (dd, *J* = 8.0, 2.5 Hz, 1H), 6.31 (t, *J* = 2.5 Hz, 1H), 6.18 (br s, 1H), 4.84 (dd, *J* = 10.5, 6.6 Hz, 1H), 4.53 – 4.45 (m, 1H), 4.45 – 4.33 (m, 2H), 4.13 – 4.05 (m, 1H), 3.74 (s, 3H), 3.37 (t, *J* = 7.0 Hz, 2H), 3.30 (q, *J* = 6.0 Hz, 2H), 1.83 (s, 3H)

¹³C NMR (101 MHz, Chloroform-*d*) δ 170.6, 160.7, 152.7, 148.9, 147.3, 144.7, 130.2, 110.0, 105.5, 104.1, 59.7, 55.2, 54.1, 49.4, 48.3, 37.7, 23.0

***N*-((1-(1-(1*H*-1,2,4-triazole-1-carbonyl)azetidin-3-yl)-5-methoxy-1,2,3,4-tetrahydroquinolin-2-yl)methyl)acetamide (**7i**, UCM1490)**



7i, UCM1490

Compound **7i** was prepared following the described general procedure **G** starting from **6i**.

Flash chromatography: silica gel, EtOAc:MeOH 97:3 as eluent.

White solid, 73% yield.

ESI MS (*m/z*): 384 [M+H]⁺

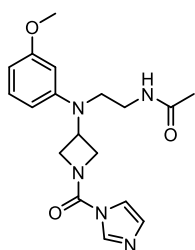
¹H NMR (400 MHz, DMSO-*d*₆) δ 9.07 (s, 1H), 8.20 (s, 1H), 7.80 (t, *J* = 5.0 Hz, 1H), 7.00 (t, *J* = 8.0 Hz, 1H), 6.38 (d, *J* = 8.0 Hz, 1H), 6.12 (d, *J* = 8.0 Hz, 1H), 4.86-4.37 (br s, 2H), 4.62 (dt, *J* = 13.5, 6.5 Hz, 3H), 3.75 (s, 3H), 3.74 – 3.68 (m, 2H), 2.99 (t, *J* = 6.5 Hz, 2H), 2.69 – 2.61 (m, 1H), 2.54 (dd, *J* = 12.5, 6.5 Hz, 2H), 1.95 (ddt, *J* = 9.0, 5.0, 2.0 Hz, 1H), 1.81 (s, 3H), 1.78 – 1.66 (m, 1H)

¹³C NMR (101 MHz, Chloroform-*d*) δ 170.5, 157.7, 152.9, 147.4, 144.8, 143.5, 127.2, 112.2, 106.9, 101.1, 60.7, 59.2, 55.4, 53.7, 50.4, 50.2, 40.2, 23.2, 17.0

***N*-((2-((1-(1*H*-imidazole-1-carbonyl)azetidin-3-yl)(3-methoxyphenyl)amino)ethyl)acetamide (**8a**, UCM1486) and 1,1,1,3,3,3-hexafluoropropan-2-yl 3-((2-acetamidoethyl)(3-methoxyphenyl)amino) azetidino-1-carboxylate and (**9a**, UCM1485)**

Compound **8a** and **9a** were prepared following the described general procedure **H** starting from **6a**. Flash chromatography: silica gel, EtOAc:MeOH 95:5 as eluent to obtain **9a** and EtOAc:MeOH 9:1 as eluent to obtain **8a**.

8a, UCM1486



8a, UCM1486

Oil, 39% yield

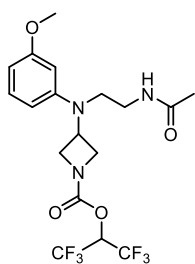
ESI MS (*m/z*): 358 [M+H]⁺

¹H NMR (400 MHz, Chloroform-*d*) δ 7.98 (s, 1H), 7.28 (t, *J* = 1.0 Hz, 1H), 7.16 (t, *J* = 8.0 Hz, 1H), 7.05 – 7.02 (m, 1H), 6.46 (dd, *J* = 8.0, 2.0 Hz, 1H), 6.35 (dd, *J* = 8.0, 2.0 Hz, 1H), 6.30 (t, *J* = 2.0 Hz, 1H), 6.06 (br s, 1H), 4.53 – 4.44 (m, 3H), 4.28 – 4.18 (m, 2H), 3.76 (s, 3H), 3.40 (t, *J* = 6.0 Hz, 2H), 3.32 (q, *J* = 6.0 Hz, 2H), 1.86

(s, 3H)

¹³C NMR (101 MHz, Chloroform-*d*) δ 170.7, 160.8, 150.3, 148.8, 136.4, 130.3, 130.0, 116.8, 109.7, 105.4, 103.9, 55.3, 49.1, 48.2, 37.9, 26.9, 23.0

9a, UCM 1485



Oil, 44% yield

ESI MS (m/z): 458 [M+H]⁺

¹H NMR (400 MHz, Chloroform-*d*) δ 7.17 (t, $J = 8.0$ Hz, 1H), 6.47 (dd, $J = 8.0$, 2.5 Hz, 1H), 6.37 (dd, $J = 8.0$, 2.5 Hz, 1H), 6.32 (t, $J = 2.5$ Hz, 1H), 5.76 (br s, 1H), 5.64 (hept, $J = 6.0$ Hz, 1H), 4.42 (tt, $J = 7.0$, 5.5 Hz, 1H), 4.37 – 4.23 (m, 2H), 4.00 (dd, $J = 9.5$, 5.5 Hz, 2H), 3.78 (s, 3H), 3.39 – 3.35 (m, 2H), 3.35 – 3.26

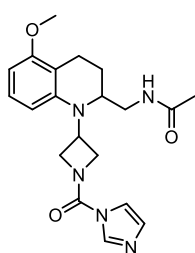
(m, 2H), 1.86 (s, 3H)

¹³C NMR (101 MHz, Chloroform-*d*) δ 170.7, 160.9, 151.8, 148.9, 130.4, 125.66 – 115.91 (m), 110.3, 105.9, 104.5, 67.8 (hept, $J = 34.3$ Hz), 55.3, 54.4, 49.3, 48.5, 37.8, 23.1

***N*-((1-(1-(1*H*-imidazole-1-carbonyl)azetid-3-yl)-5-methoxy-1,2,3,4-tetrahydroquinolin-2-yl)methyl)acetamide (8i, UCM1489) and 1,1,1,3,3,3-hexafluoropropan-2-yl 3-(2-(acetamidomethyl)-5-methoxy-3,4-dihydroquinolin-1(2*H*)-yl)azetidine-1-carboxylate (9i, 1488)**

Compound **8i** and **9i** were prepared following the described general procedure **H** starting from **6i**. Flash chromatography: silica gel, EtOAc as eluent to obtain **9i** and EtOAc:MeOH 9:1 as eluent to obtain **8i**.

8i, UCM1489



Oil, 30% yield

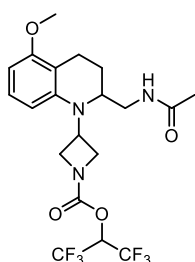
ESI MS (m/z): 384 [M+H]⁺

¹H NMR (400 MHz, Chloroform-*d*) δ 8.15 (s, 1H), 7.37 (s, 1H), 7.10 (s, 1H), 7.06 (t, $J = 8.0$ Hz, 1H), 6.38 (d, $J = 8.0$ Hz, 1H), 6.08 (d, $J = 8.0$ Hz, 1H), 5.90 (br s, 1H), 4.69 (p, $J = 6.5$ Hz, 1H), 4.63 – 4.48 (m, 2H), 4.33 (br s, 1H), 3.86 – 3.81 (m, 1H), 3.80 (s, 3H), 3.23 (dt, $J = 14.0$, 6.0 Hz, 1H), 3.15 (dt, $J = 14.0$, 6.0 Hz, 1H),

2.81 (ddd, $J = 18.0$, 7.0, 2.0 Hz, 1H), 2.52 (ddd, $J = 18.0$, 12.5, 7.0 Hz, 1H), 2.40 (s, 1H), 2.07 – 1.99 (m, 1H), 1.97 (s, 3H), 1.95 – 1.77 (m, 1H)

¹³C NMR (101 MHz, Chloroform-*d*) δ 170.8, 157.9, 150.5, 143.4, 136.6, 130.1, 127.4, 116.9, 112.04, 106.5, 101.1, 55.5, 50.4, 49.9, 40.6, 23.4, 23.2, 17.0

9i, UCM1488



9i, UCM1488

White solid, 29% yield

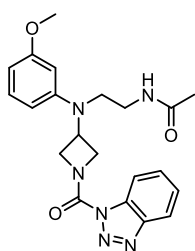
ESI MS (m/z): 484 [M+H]⁺

¹H NMR (400 MHz, Chloroform-*d*) δ 7.05 (d, J = 16.5 Hz, 1H), 6.38 (d, J = 8.0 Hz, 1H), 6.06 (d, J = 8.0 Hz, 1H), 5.73 (br s, 1H), 5.65 (hept, J = 6.0 Hz, 1H), 4.57 (p, J = 6.5 Hz, 1H), 4.44 – 4.24 (m, 3H), 4.06 (dd, J = 9.0, 6.0 Hz, 1H), 3.80 (s, 3H), 3.76 – 3.69 (m, 1H), 3.28 – 3.06 (m, 2H), 2.78 (ddd, J = 18.0, 7.0, 2.0 Hz, 1H), 2.53 (ddd,

J = 18.0, 12.0, 7.0 Hz, 1H), 1.95 (s, 3H), 2.05 – 1.80 (m, 2H)

¹³C NMR (101 MHz, Chloroform-*d*) δ 170.58, 157.86, 151.82, 143.57, 127.27, 125.58 – 116.12 (m), 112.39, 106.93, 101.25, 67.83 (p, J = 34.6 Hz), 56.52, 55.74, 55.47, 54.81, 53.91, 50.81, 40.22, 23.26, 17.16

N-(2-((1-(1H-benzo[*d*][1,2,3]triazole-1-carbonyl)azetidin-3-yl)(3-methoxyphenyl)amino)ethyl)acetamide (10, UCM1487)



10, UCM1487

The *N*-(2-(azetidin-3-yl(3-methoxyphenyl)amino)ethyl)acetamide **6a** (1 equiv., 97 mg, 0.37 mmol) in dry THF (4 ml) was added dropwise over 5 minutes to a solution of bis(1*H*-benzo[*d*][1,2,3]triazol-1-yl)methanone²¹ (1.2 equiv., 116 mg, 0.44 mmol) and 4-methylmorpholine (0.1 equiv., 0.004 ml, 0.037 mmol) in dry THF (40 ml).

The reaction mixture was stirred for 5h after which the solvent was evaporated. The residue was taken into EtOAc and washed with water (x2), dried over Na₂SO₄, and

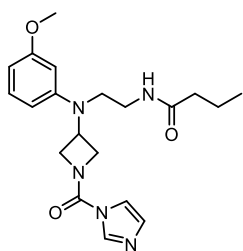
concentrated in vacuo.¹⁵ The crude product was purified by silica gel column chromatography (EtOAc:MeOH 96:4) to give the desired compounds **10** as a white solid, 94% yield.

ESI MS (m/z): 409 [M+H]⁺

¹H NMR (400 MHz, Chloroform-*d*) δ 8.26 (dt, J = 8.5, 1.0 Hz, 1H), 8.09 (dt, J = 8.5, 1.0 Hz, 1H), 7.61 (ddd, J = 8.5, 7.0, 1.0 Hz, 1H), 7.47 (ddd, J = 8.0, 7.0, 1.0 Hz, 1H), 7.23 (t, J = 8.0 Hz, 1H), 6.58 – 6.45 (m, 3H), 5.68 (br s, 1H), 5.08 – 4.99 (m, 1H), 4.76 – 4.68 (m, 1H), 4.59 – 4.49 (m, 2H), 4.37 – 4.26 (m, 1H), 3.82 (s, 3H), 3.50 – 3.44 (m, 2H), 3.43 – 3.36 (m, 2H), 1.89 (s, 3H).

¹³C NMR (101 MHz, Chloroform-*d*) δ 170.1, 160.7, 149.1, 148.7, 144.9, 132.1, 130.1, 129.5, 125.3, 119.6, 114.1, 110.4, 106.0, 104.5, 55.1, 54.0, 49.8, 48.6, 37.6, 26.7, 22.9

***N*-2-((1-(1*H*-imidazole-1-carbonyl)azetid-3-yl)(3-methoxyphenyl)amino)ethyl butyramide (**8b**)**



8b

Compound **8b** was prepared following the described general procedure **I** starting from **6b**.

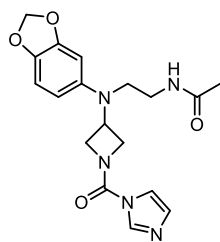
Flash chromatography: silica gel, EtOAc:MeOH 97:3 as eluent.

Oil, 61% yield.

ESI MS (*m/z*): 386 [M+H]⁺

¹H NMR (400 MHz, Chloroform-*d*) δ 7.99 (s, 1H), 7.29 (s, 1H), 7.16 (t, *J* = 8.0 Hz, 1H), 7.05 (s, 1H), 6.46 (dd, *J* = 8.0, 2.0 Hz, 1H), 6.39 – 6.34 (m, 1H), 6.29 (t, *J* = 2.0 Hz, 1H), 5.95 (br s, 1H), 4.50 (s, 3H), 4.24 (s, 2H), 3.76 (s, 3H), 3.40 (t, *J* = 6.0 Hz, 2H), 3.33 (q, *J* = 6.0 Hz, 2H), 2.04 (t, *J* = 7.5 Hz, 2H), 1.56 (h, *J* = 7.5 Hz, 2H), 0.88 (t, *J* = 7.5 Hz, 3H)

***N*-2-((1-(1*H*-imidazole-1-carbonyl)azetid-3-yl)(benzo[*d*][1,3]dioxol-5-yl)amino)ethyl acetamide (**8c**)**



8c

Compound **8c** was prepared following the described general procedure **I** starting from **6c**.

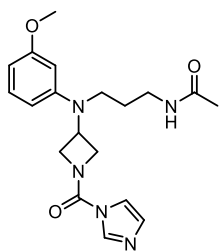
Flash chromatography: silica gel, EtOAc:MeOH 9:1 as eluent.

White solid, 63% yield.

ESI MS (*m/z*): 372 [M+H]⁺

¹H NMR (400 MHz, Chloroform-*d*) δ 7.97 (s, 1H), 7.25 (s, 1H), 7.06 (s, 1H), 6.73 (d, *J* = 8.0 Hz, 1H), 6.52 (d, *J* = 2.0 Hz, 1H), 6.36 (dd, *J* = 8.0, 2.0 Hz, 1H), 5.94 (s, 2H), 5.60 (br s, 1H), 4.36 (t, *J* = 8.0 Hz, 2H), 4.23 (dt, *J* = 12.0, 6.0 Hz, 1H), 4.10 (dt, *J* = 10.5, 5.5 Hz, 2H), 3.25 (q, *J* = 6.0 Hz, 2H), 3.11 (t, *J* = 6.0 Hz, 2H), 1.93 (s, 3H)

***N*-3-((1-(1*H*-imidazole-1-carbonyl)azetid-3-yl)(3-methoxyphenyl)amino)propyl acetamide (**8d**)**



8d

Compound **8d** was prepared following the described general procedure **I** starting from **6d**.

Flash chromatography: silica gel, EtOAc:MeOH 9:1 as eluent.

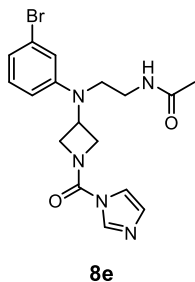
Oil, 69% yield.

ESI MS (*m/z*): 372 [M+H]⁺

¹H NMR (400 MHz, Chloroform-*d*) δ 8.09 (s, 1H), 7.29 (s, 1H), 7.18 (t, *J* = 8.0 Hz, 1H), 7.08 (s, 1H), 6.49 (ddd, *J* = 8.0, 2.5, 1.0 Hz, 1H), 6.37 (ddd, *J* = 8.0, 2.5, 1.0 Hz, 1H), 6.28 (t, *J* = 2.5 Hz, 1H), 5.76 (br s, 1H), 4.48 (t, *J* = 8.0 Hz, 2H), 4.43 – 4.35 (m, 1H), 4.20 (dd, *J* = 9.0, 5.0 Hz, 2H), 3.77 (s, 3H), 3.26 (t, *J* = 7.5 Hz, 2H), 3.20 (q, *J* = 7.0 Hz, 2H), 1.94 (s, 3H), 1.66 (p, *J* = 7.0 Hz, 2H)

***N*-(2-((1-(1*H*-imidazole-1-carbonyl)azetid-3-yl)(3-bromophenyl)amino)ethyl)**

acetamide (8e)



Compound **8e** was prepared following the described general procedure **I** starting from **6e** with the addition of TEA.

Flash chromatography: silica gel, DCM:MeOH 95:5 as eluent.

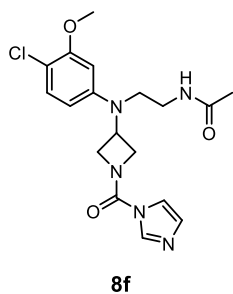
Oil, 25% yield (in three step, including the two step for the *N*-benzhydryl deprotection)

ESI MS (*m/z*): 407 [M+H]⁺

¹H NMR (400 MHz, Chloroform-*d*) δ 8.06 (s, 1H), 7.33 (s, 1H), 7.13 (t, *J* = 8.0 Hz, 1H), 7.09 (s, 1H), 7.02 (ddd, *J* = 8.0, 2.0, 1.0 Hz, 1H), 6.88 (t, *J* = 2.0 Hz, 1H), 6.69 (ddd, *J* = 8.0, 2.5, 1.0 Hz, 1H), 5.80 (t, *J* = 6.0 Hz, 1H), 4.60 – 4.51 (m, 3H), 4.33 – 4.24 (m, 2H), 3.47 (t, *J* = 6.5 Hz, 2H), 3.36 (q, *J* = 6.5 Hz, 2H), 1.90 (s, 3H)

***N*-(2-((1-(1*H*-imidazole-1-carbonyl)azetid-3-yl)(4-chloro-3-methoxyphenyl)amino)**

ethyl)acetamide (8f)



Compound **8f** was prepared following the described general procedure **I** starting from **6f** with the addition of TEA.

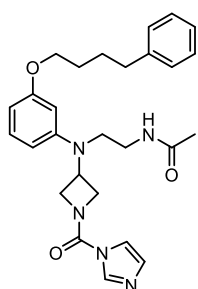
Flash chromatography: silica gel, DCM:MeOH 95:5 as eluent.

White solid, 20% yield (in three step, including the two step for the *N*-benzhydryl deprotection)

ESI MS (*m/z*): 392 [M+H]⁺

¹H NMR (400 MHz, Chloroform-*d*) δ 8.02 (s, 1H), 7.31 – 7.27 (m, 1H), 7.18 (d, *J* = 8.5 Hz, 1H), 7.05 (s, 1H), 6.47 (d, *J* = 2.5 Hz, 1H), 6.27 – 6.18 (m, 1H), 6.04 (br s, 1H), 4.56 – 4.46 (m, 3H), 4.30 – 4.18 (m, 2H), 3.88 (s, 3H), 3.44 – 3.37 (m, 2H), 3.32 (q, *J* = 6.0 Hz, 2H), 1.88 (s, 3H)

***N*-(2-((1-(1*H*-imidazole-1-carbonyl)azetid-3-yl)(3-(4-phenylbutoxy)phenyl)amino)ethyl)acetamide (**8h**)**



8h

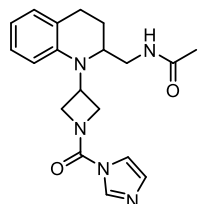
Compound **8h** was prepared following the described general procedure **I** starting from **6h**.

Flash chromatography: silica gel, EtOAc as eluent.

White solid, 48% yield.

¹H NMR (400 MHz, Chloroform-*d*) δ 8.01 (s, 1H), 7.32 – 7.27 (m, 3H), 7.22 – 7.14 (m, 4H), 7.07 (s, 1H), 6.47 (dd, *J* = 8.0, 2.0 Hz, 1H), 6.37 (dd, *J* = 8.0, 2.0 Hz, 1H), 6.34 – 6.27 (m, 1H), 5.60 (br s, 1H), 4.53 – 4.47 (m, 3H), 4.29 – 4.18 (m, 2H), 3.98 – 3.91 (m, 2H), 3.40 (t, *J* = 6.0 Hz, 2H), 3.35 (q, *J* = 6.0 Hz, 2H), 2.69 (t, *J* = 6.5 Hz, 2H), 1.88 (s, 3H), 1.84 – 1.78 (m, 4H)

***N*-(1-(1-(1*H*-imidazole-1-carbonyl)azetid-3-yl)-1,2,3,4-tetrahydroquinolin-2-yl)methyl)acetamide (**8j**)**



8j

Compound **8j** was prepared following the described general procedure **I** starting from **6j**.

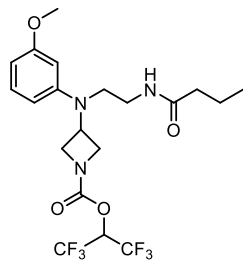
Flash chromatography: silica gel, EtOAc:MeOH 9:1 as eluent.

Amorphous solid, 74% yield

ESI MS (*m/z*): 354 [M+H]⁺

¹H NMR (400 MHz, Chloroform-*d*) δ 8.06 (s, 1H), 7.35 (t, *J* = 1.5 Hz, 1H), 7.17 – 7.03 (m, 2H), 7.08 (s, 1H), 6.77 (t, *J* = 7.5 Hz, 1H), 6.38 (d, *J* = 8.0 Hz, 1H), 5.71 (t, *J* = 5.0 Hz, 1H), 4.67 (p, *J* = 6.5 Hz, 1H), 4.63 – 4.53 (m, 3H), 4.31 (brs, 1H), 3.87 – 3.79 (m, 1H), 3.27 (dt, *J* = 14.0, 5.5 Hz, 1H), 3.17 (dt, *J* = 14.0, 7.0 Hz, 1H), 2.86 – 2.70 (m, 2H), 2.11 – 1.87 (m, 2H), 1.95 (s, 3H)

1,1,1,3,3,3-hexafluoropropan-2-yl 3-((2-butylamidoethyl)(3-methoxyphenyl)amino)azetidine-1-carboxylate (9b**, UCM1493)**



9b, UCM1493

Compound **9b** was prepared following the described general procedure **K** starting from **8b** using 1.2 equivalent of HFIP.

Flash chromatography: silica gel, cyclohexane:EtOAc 1:1 as eluent.

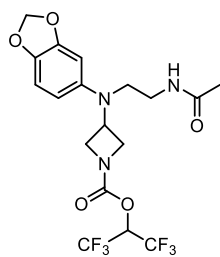
Oil, 64% yield

ESI MS (*m/z*): 486 [M+H]⁺

¹H NMR (400 MHz, Chloroform-*d*) δ 7.19 (t, *J* = 8.0 Hz, 1H), 6.49 (dd, *J* = 8.0, 2.0 Hz, 1H), 6.40 (dd, *J* = 8.0, 2.0 Hz, 1H), 6.33 (t, *J* = 2.0 Hz, 1H), 5.64 (hept, *J* = 6.0 Hz, 1H), 5.47 (br s, 1H), 4.48 – 4.39 (m, 1H), 4.39 – 4.25 (m, 2H), 4.07 – 3.98 (m, 2H), 3.79 (s, 3H), 3.42 – 3.31 (m, 4H), 2.05 (t, *J* = 7.5 Hz, 2H), 1.65 – 1.53 (m, 2H), 0.91 (t, *J* = 7.5 Hz, 3H)

¹³C NMR (101 MHz, Chloroform-*d*) δ 173.4, 160.9, 151.8, 148.9, 130.5, 120.6 (q, *J* = 288.7 Hz), 110.55, 106.06, 104.65, 67.82 (dt, *J* = 69.1, 34.6 Hz), 55.40, 55.31, 54.42, 49.47, 48.83, 38.61, 37.64, 19.03, 13.86

1,1,1,3,3,3-hexafluoropropan-2-yl 3-((2-acetamidoethyl)(benzo[d][1,3]dioxol-5-yl)amino)azetidine-1-carboxylate (9c, UCM1498)



9c, UCM1498

Compound **9c** was prepared following the described general procedure **K** starting from **8c** using 2.5 equivalent of HFIP.

Flash chromatography: silica gel, cyclohexane:EtOAc 1:9 as eluent.

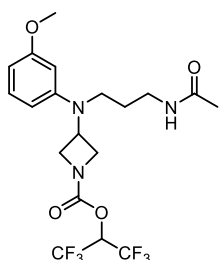
White amorphous solid, 90% yield

ESI MS (*m/z*): 472 [M+H]⁺

¹H NMR (400 MHz, Chloroform-*d*) δ 6.74 (d, *J* = 8.5 Hz, 1H), 6.54 (d, *J* = 2.0 Hz, 1H), 6.38 (dd, *J* = 8.5, 2.0 Hz, 1H), 5.95 (s, 2H), 5.70 (br s, 1H), 5.63 (hept, *J* = 6.0 Hz, 1H), 4.40 (br s, 1H), 4.25 – 4.13 (m, 2H), 3.94 – 3.83 (m, 2H), 3.24 (q, *J* = 6.0 Hz, 2H), 3.06 (t, *J* = 6.0 Hz, 2H), 1.95 (s, 3H)

¹³C NMR (101 MHz, Chloroform-*d*) δ 170.3, 151.9, 148.8, 144.6, 119.3 (dd, *J* = 285.1, 281.6 Hz), 115.3, 108.3, 103.9, 101.5, 67.8 (p, *J* = 34.4 Hz), 55.0, 54.3, 51.6, 51.3, 37.2, 23.7

1,1,1,3,3,3-hexafluoropropan-2-yl 3-((3-acetamidopropyl)(3-methoxyphenyl)amino)azetidine-1-carboxylate (9d, UCM1494)



9d, UCM1494

Compound **9d** was prepared following the described general procedure **K** starting from **8d** using 1.2 equivalent of HFIP.

Flash chromatography: silica gel, EtOAc as eluent.

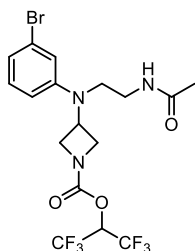
Yellow oil, 51% yield

ESI MS (*m/z*): 472 [M+H]⁺

¹H NMR (400 MHz, Chloroform-*d*) δ 7.18 (t, *J* = 8.0 Hz, 1H), 6.49 (dd, *J* = 8.0, 2.0 Hz, 1H), 6.37 (dd, *J* = 8.0, 2.0 Hz, 1H), 6.28 (t, *J* = 2.0 Hz, 1H), 5.64 (hept, *J* = 6.0 Hz, 1H), 5.42 (br s, 1H), 4.40 – 4.30 (m, 2H), 4.26 (dd, *J* = 15.0, 6.0 Hz, 1H), 4.00 (dd, *J* = 8.5, 4.5 Hz, 2H), 3.79 (s, 3H), 3.26 (dt, *J* = 8.0, 3.5 Hz, 2H), 3.21 (q, *J* = 7.0 Hz, 2H), 1.94 (s, 3H), 1.66 (p, *J* = 7.0 Hz, 2H)

^{13}C NMR (101 MHz, Chloroform-*d*) δ 170.3, 160.8, 151.8, 148.9, 130.3, 120.7 (q, $J = 282.7$ Hz), 111.2, 106.0, 105.2, 67.8 (p, $J = 34.6$ Hz), 55.3, 55.2, 54.3, 49.4, 47.5, 37.6, 27.4, 23.3

1,1,1,3,3,3-hexafluoropropan-2-yl 3-((2-acetamidoethyl)(3-bromophenyl)amino)azetidine-1-carboxylate (9e, UCM1497)



9e, UCM1497

Compound **9e** was prepared following the described general procedure **K** starting from **8e** using 1.2 equivalent of HFIP.

Flash chromatography: silica gel, EtOAc as eluent.

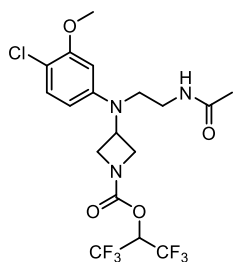
Oil, 58% yield

ESI MS (m/z): 507 $[\text{M}+\text{H}]^+$

^1H NMR (400 MHz, Chloroform-*d*) δ 7.13 (t, $J = 8.0$ Hz, 1H), 7.03 (d, $J = 8.0$ Hz, 1H), 6.90 (br s, 1H), 6.70 (dd, $J = 8.0, 2.0$ Hz, 1H), 5.65 (hept, $J = 6.0$ Hz, 1H), 5.48 (br s, 1H), 4.48 (p, $J = 6.0, 5.5$ Hz, 1H), 4.35 (dt, $J = 17.0, 8.5$ Hz, 2H), 4.03 (dd, $J = 9.0, 5.5$ Hz, 2H), 3.43 (t, $J = 6.0$ Hz, 2H), 3.34 (dt, $J = 11.5, 6.0$ Hz, 2H), 1.89 (s, 3H)

^{13}C NMR (101 MHz, Chloroform-*d*) δ 170.6, 151.8, 148.9, 130.9, 123.8, 123.7, 125.48 – 116.22 (m), 120.0, 115.7, 67.8 (p, $J = 34.7$ Hz), 55.2, 54.3, 49.1, 48.2, 37.7, 23.2

1,1,1,3,3,3-hexafluoropropan-2-yl 3-((2-acetamidoethyl)(4-chloro-3-methoxyphenyl)amino)azetidine-1-carboxylate (9f, UCM1499)



9f, UCM1499

Compound **9f** was prepared following the described general procedure **K** starting from **8f** using 2.5 equivalent of HFIP.

Flash chromatography: silica gel, EtOAc as eluent.

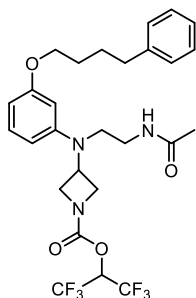
Yellow amorphous solid, 90% yield

ESI MS (m/z): 486 $[\text{M}+\text{H}]^+$

^1H NMR (400 MHz, Chloroform-*d*) δ 7.21 (d, $J = 8.5$ Hz, 1H), 6.51 (d, $J = 2.5$ Hz, 1H), 6.26 (dd, $J = 8.5, 2.5$ Hz, 1H), 5.64 (hept, $J = 6.0$ Hz, 1H), 5.55 (br s, 1H), 4.45 (tt, $J = 7.0, 5.5$ Hz, 1H), 4.32 (dt, $J = 17.5, 8.5$ Hz, 2H), 4.06 – 3.97 (m, 2H), 3.91 (s, 3H), 3.42 – 3.36 (m, 2H), 3.36 – 3.30 (m, 2H), 1.90 (s, 3H)

^{13}C NMR (101 MHz, Chloroform-*d*) δ 170.6, 155.9, 151.8, 147.6, 130.6, 125.17 – 116.29 (m), 114.9, 109.9, 102.7, 67.9 (hept, $J = 34.6$ Hz), 56.4, 55.2, 54.4, 49.4, 48.7, 37.8, 23.2

1,1,1,3,3,3-hexafluoropropan-2-yl 3-((2-acetamidoethyl)(3-(4-phenylbutoxy)phenyl)amino)azetidine-1-carboxylate (9h, UCM1502)



9h, UCM1502

Compound **9h** was prepared following the described general procedure **K** starting from **8h** using 2.5 equivalent of HFIP.

Flash chromatography: silica gel, cyclohexane:EtOAc 3:7 as eluent.

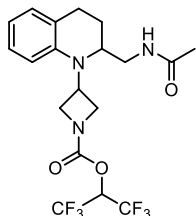
Oil, 90% yield

ESI MS (*m/z*): 576 [M+H]⁺

¹H NMR (400 MHz, DMSO-*d*₆) δ 7.89 (t, *J* = 5.0 Hz, 2H), 7.31 – 7.25 (m, 2H), 7.21 (d, *J* = 6.5 Hz, 2H), 7.17 (tt, *J* = 6.5, 1.5 Hz, 1H), 7.08 (t, *J* = 8.0 Hz, 1H), 6.47 (hept, *J* = 7.0 Hz, 1H), 6.37 – 6.29 (m, 2H), 4.64 – 4.53 (m, 1H), 4.34 (dt, *J* = 21.0, 8.0 Hz, 2H), 3.96 (s, 4H), 3.37 – 3.29 (m, 2H), 3.13 (s, 2H), 2.64 (s, 2H), 1.77 (s, 3H), 1.71 (d, *J* = 3.5 Hz, 4H)

¹³C NMR (101 MHz, DMSO-*d*₆) δ 169.4, 159.8, 151.0, 148.9, 142.0, 129.8, 128.3, 128.2, 125.7, 125.28 – 114.94 (m), 107.2, 104.5, 101.3, 67.0, 66.9 (p, *J* = 33.3 Hz), 55.1, 54.3, 47.9, 46.5, 37.2, 34.8, 28.3, 27.4, 22.5

1,1,1,3,3,3-hexafluoropropan-2-yl 3-(2-(acetamidomethyl)-3,4-dihydroquinolin-1(2H)-yl)azetidine-1-carboxylate (9j, UCM1532)



9j, UCM1532

Compound **9j** was prepared following the described general procedure **K** starting from **8j** using 1.2 equivalent of HFIP.

Flash chromatography: silica gel, cyclohexane:EtOAc 3:7 as eluent.

White solid, 54% yield. Crystallization: diethyl ether:petroleum ether

M.p.: 112-115 °C

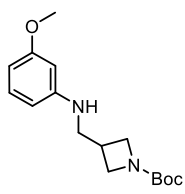
ESI MS (*m/z*): 454 [M+H]⁺

Rotamers are observed when NMR analysis are performed at 25°C. Therefore, NMR analysis have been carried out at 40°C.

¹H NMR (400 MHz, DMSO-*d*₆, 313K) δ 7.93 (t, *J* = 6.0 Hz, 1H), 7.03 – 6.95 (m, 2H), 6.63 (t, *J* = 7.5 Hz, 1H), 6.45 (hept, *J* = 6.5 Hz, 1H), 6.41 (d, *J* = 8.0 Hz, 1H), 4.62 (p, *J* = 7.0 Hz, 1H), 4.46 – 4.35 (m, 1H), 4.35 – 4.27 (m, 2H), 3.95 (dd, *J* = 9.0, 6.0 Hz, 1H), 3.73 – 3.67 (m, 1H), 3.05 – 2.90 (m, 2H), 2.80 (ddd, *J* = 18.0, 12.0, 6.5 Hz, 1H), 2.61 (ddd, *J* = 17.0, 6.0, 3.0 Hz, 1H), 1.90 (ddt, *J* = 12.5, 6.0, 3.0 Hz, 1H), 1.82 (s, 3H), 1.79 – 1.70 (m, 1H)

¹³C NMR (101 MHz, DMSO-*d*₆, 313K) δ 169.3, 150.9, 142.7, 128.9, 126.7, 123.0, 120.1 (q, *J* = 287.7 Hz), 112.2, 66.9 (hept, *J* = 33.5 Hz), 55.7, 54.9, 54.3, 53.4, 50.5, 48.2, 22.8, 22.5, 22.4

***Tert*-butyl 3-(((3-methoxyphenyl)amino)methyl)azetidine-1-carboxylate (11)**



11

Compound **11** was prepared following the described general procedure **C** starting from **1a**.

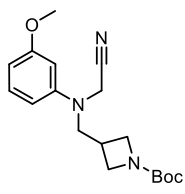
Flash chromatography: silica gel, DCM:EtOAc 9:1 as eluent.

Oil, 50% yield

ESI MS (m/z): 293 [M+H]⁺

¹H NMR (400 MHz, Chloroform-*d*) δ 7.09 (t, J = 8.0 Hz, 1H), 6.32 (dd, J = 8.0, 2.0 Hz, 1H), 6.26 (dd, J = 8.0, 2.0 Hz, 1H), 6.19 (t, J = 2.0 Hz, 1H), 4.03 (t, J = 8.5 Hz, 2H), 3.77 (s, 3H), 3.65 (dd, J = 8.5, 5.0 Hz, 2H), 3.33 (d, J = 7.5 Hz, 2H), 2.80 (ttt, J = 10.5, 7.5, 4.0 Hz, 1H), 1.44 (s, 9H)

***Tert*-butyl 3-(((cyanomethyl)(3-methoxyphenyl)amino)methyl)azetidine-1-carboxylate (12)**



12

Compound **12** was prepared following the described general procedure **D** starting from **11**.

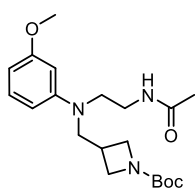
Flash chromatography: silica gel, cyclohexane:EtOAc 8:2 as eluent.

Brown oil, 75% yield

ESI MS (m/z): 332 [M+H]⁺

¹H NMR (400 MHz, Chloroform-*d*) δ 7.23 (t, J = 8.0 Hz, 1H), 6.55 – 6.48 (m, 2H), 6.43 (t, J = 2.5 Hz, 1H), 4.15 – 4.09 (m, 2H), 4.03 (t, J = 8.5 Hz, 2H), 3.80 (s, 3H), 3.65 (dd, J = 8.5, 5.0 Hz, 2H), 3.52 (d, J = 7.5 Hz, 2H), 2.86 (dtt, J = 13.0, 5.0, 2.5 Hz, 1H), 1.43 (s, 9H)

***Tert*-butyl 3-(((2-acetamidoethyl)(3-methoxyphenyl)amino)methyl)azetidine-1-carboxylate (13)**



13

Compound **13** was prepared following the described general procedure **E** starting from **12**.

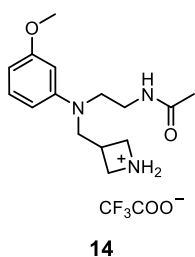
Flash chromatography: silica gel, cyclohexane:EtOAc 1:9 as eluent.

Oil, 70% yield

ESI MS (m/z): 378 [M+H]⁺

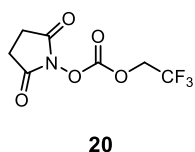
¹H NMR (400 MHz, Chloroform-*d*) δ 7.15 (t, J = 8.5 Hz, 1H), 6.41 – 6.37 (m, 1H), 6.35 – 6.31 (m, 2H), 5.59 (t, J = 4.5 Hz, 1H), 3.97 (t, J = 8.5 Hz, 2H), 3.79 (s, 3H), 3.61 (dd, J = 8.5, 5.5 Hz, 2H), 3.51 – 3.42 (m, 4H), 3.38 (q, J = 6.0 Hz, 2H), 2.89 (dq, J = 10.0, 7.5, 3.5 Hz, 1H), 1.94 (s, 3H), 1.43 (s, 9H)

3-(((2-acetamidoethyl)(3-methoxyphenyl)amino)methyl)azetidinium 2,2,2-trifluoroacetate (14)



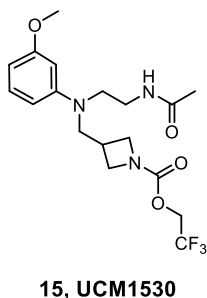
TFA (0.38 ml) was added to a solution of compound **13** (1 equiv., 0.71 mmol) in DCM (1.05 mL) at room temperature. The reaction was stirred at room temperature until the starting material is completely disappeared (about 2h). The solvent was evaporated in vacuo to give the corresponding crude oily azetidinium **14** which was used without any further purification in the next step.

2,5-dioxopyrrolidin-1-yl (2,2,2-trifluoroethyl) carbonate (20)



Bis(2,5-dioxopyrrolidin-1-yl) carbonate (1 equiv., 49.2 mg, 0.19 mmol) is added to a solution of 2,2,2-trifluoroethanol (1 equiv., 0.145 mL, 0.19 mmol) and TEA (3 equiv., 0.780 mL, 0.56 mmol) in dry DCM (1.4 ml) under nitrogen. The reaction is stirred at room temperature for 16h. After 16h, the product **20** in the reaction solution is used as such in the next step.

2,2,2-trifluoroethyl 3-(((2-acetamidoethyl)(3-methoxyphenyl)amino)methyl)azetidinium-1-carboxylate (15, UCM1530)



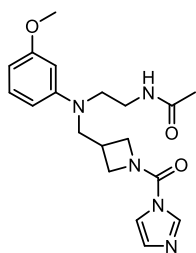
The azetidinium salt **14** (1 equiv., 0.13 mmol) is dissolved in dry DCM (0.44 mL), and TEA (2 equiv., 0.36 mL, 0.26 mmol) to afford a solution that is added dropwise to the reaction mixture of **20** (1.5 equiv., 0.19 mmol) and the mixture is allowed to stir at room temperature for additional 16h. The reaction mixture is diluted in EtOAc, washed with H₂O (x2), then brine. The organic phase is dried over Na₂SO₄, and concentrated in vacuo. The crude product was purified by silica gel column chromatography (cyclohexane:EtOAc 1:9) to give the desired compounds **15** as an oil, 86% yield.

ESI MS (*m/z*): 404 [M+H]⁺

¹H NMR (400 MHz, Chloroform-*d*) δ 7.15 (t, *J* = 8.0 Hz, 1H), 6.39 (ddd, *J* = 8.5, 2.5, 1.0 Hz, 1H), 6.36 – 6.31 (m, 2H), 5.67 (t, *J* = 6.0 Hz, 1H), 4.43 (q, *J* = 8.5 Hz, 2H), 4.09 (t, *J* = 7.0 Hz, 2H), 3.79 (s, 3H), 3.77 – 3.69 (m, 2H), 3.51 (d, *J* = 7.5 Hz, 2H), 3.45 (dd, *J* = 7.5, 6.0 Hz, 2H), 3.40 – 3.33 (m, 2H), 3.00 (dddd, *J* = 15.5, 10.5, 5.0, 2.0 Hz, 1H), 1.93 (s, 3H)

¹³C NMR (101 MHz, Chloroform-*d*) δ 170.6, 161.0, 154.1, 149.3, 130.3, 123.2 (q, *J* = 277.4 Hz), 106.9, 102.7, 100.9, 60.9 (q, *J* = 36.5 Hz), 55.3, 55.0, 53.6, 52.9, 51.0, 37.2, 27.8, 23.2

***N*-2-(((1-(1*H*-imidazole-1-carbonyl)azetid-3-yl)methyl)(3-methoxyphenyl)amino)ethylacetamide (16)**



16

Compound **16** was prepared following the described general procedure **I** starting from **14** with the addition of TEA.

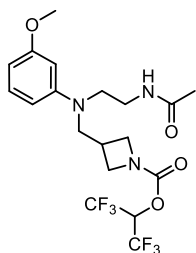
Flash chromatography: silica gel, EtOAc:MeOH 9:1 as eluent.

Oil, 57% yield

ESI MS (*m/z*): 372 [M+H]⁺

¹H NMR (400 MHz, Chloroform-*d*) δ 7.98 (s, 1H), 7.28 (t, *J* = 1.5 Hz, 1H), 7.16 (t, *J* = 8.0 Hz, 1H), 7.08 – 7.06 (m, 1H), 6.39 (dd, *J* = 8.5, 2.5 Hz, 1H), 6.36 (dd, *J* = 8.0, 2.0 Hz, 1H), 6.33 (t, *J* = 2.5 Hz, 1H), 5.69 (t, *J* = 5.0 Hz, 1H), 4.35 (t, *J* = 8.5 Hz, 2H), 4.07 – 3.98 (m, 2H), 3.79 (s, 3H), 3.58 (d, *J* = 7.3 Hz, 2H), 3.46 (t, *J* = 6.5 Hz, 2H), 3.37 (q, *J* = 6.0 Hz, 2H), 3.15 (dt, *J* = 10.0, 7.5, 4.0 Hz, 1H), 1.94 (s, 3H)

1,1,1,3,3,3-hexafluoropropan-2-yl 3-(((2-acetamidoethyl)(3-methoxyphenyl)amino)methyl)azetidine-1-carboxylate (17, UCM1501)



17, UCM1501

Compound **17** was prepared following the described general procedure **K** starting from **16** using 2.5 equivalent of HFIP.

Flash chromatography: silica gel, cyclohexane:EtOAc 2:8 as eluent.

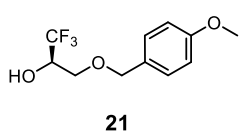
Oil, 96% yield

ESI MS (*m/z*): 472 [M+H]⁺

¹H NMR (400 MHz, Chloroform-*d*) δ 7.16 (t, *J* = 8.0 Hz, 1H), 6.42 – 6.36 (m, 1H), 6.34 (dt, *J* = 4.5, 2.5 Hz, 2H), 5.64 (hept, *J* = 6.0 Hz, 1H), 5.58 (br s, 1H), 4.21 – 4.08 (m, 2H), 3.86 – 3.74 (m, 5H), 3.54 (d, *J* = 7.5 Hz, 2H), 3.48 – 3.43 (m, 2H), 3.41 – 3.34 (m, 2H), 3.07 (dtd, *J* = 15.5, 7.5, 4.0 Hz, 1H), 1.94 (s, 3H)

¹³C NMR (101 MHz, Chloroform-*d*) δ 170.6, 161.1, 151.8, 149.3, 125.81 – 115.33 (m), 107.2, 102.95, 101.2, 67.7 (p, *J* = 34.6 Hz), 55.4, 54.9, 53.8, 53.2, 51.1, 37.3, 27.9, 23.3

(*R*)-1,1,1-trifluoro-3-((4-methoxybenzyl)oxy)propan-2-ol (21)



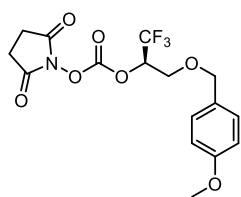
21

NaH 60% (3 equiv., 107 mg, 2.68 mmol) is added portionwise to a stirring solution of 4-methoxyphenol (1.5 equiv., 0.17 mL, 1.34 mmol) in anhydrous THF (2.5 mL) at 0°C under nitrogen atmosphere. After stirring for 1h at 0°C, (*S*)-2-methyloxirane (1 equiv., 0.077 mL, 0.89 mmol) is added to the suspension, and the reaction

mixture is allowed to be stirred at room temperature for an additional 16h. The reaction mixture is quenched with H₂O and extracted with EtOAc (x3). The combined organic phases are dried over Na₂SO₄, and concentrated in vacuo. The crude product was purified by silica gel column chromatography (cyclohexane:EtOAc 1:1) to give the desired compounds **21** as a yellow oil, 49% yield.

The experimental data are in agreement with the ones reported in literature.¹⁷

(R)-2,5-dioxopyrrolidin-1-yl (1,1,1-trifluoro-3-((4-methoxybenzyl)oxy)propan-2-yl) carbonate (22)

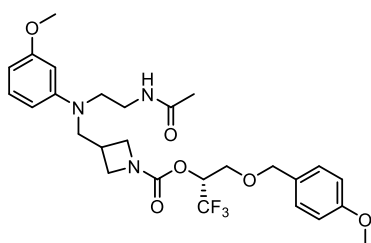


22

Bis(2,5-dioxopyrrolidin-1-yl) carbonate (1 equiv., 82 mg, 0.32 mmol) is added to a solution of (R)-1,1,1-trifluoro-3-((4-methoxybenzyl)oxy)propan-2-ol **21** (1 equiv., 80 mg, 0.32 mmol) and TEA (3 equiv., 0.130 ml, 0.96 mmol) in dry DCM (2.3 mL) under nitrogen. The reaction is stirred at room temperature for 24h.

After 24h, the product **22** is not isolated and the solution is used as such in the next step.

(R)-1,1,1-trifluoro-3-((4-methoxybenzyl)oxy)propan-2-yl 3-(((2-acetamidoethyl)(3-methoxyphenyl)amino)methyl)azetidine-1-carboxylate (18)



18

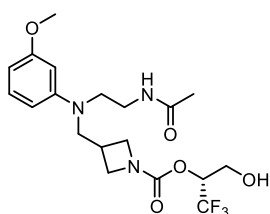
The azetidine salt **14** (1 equiv., 0.215 mmol) is dissolved in dry DCM (2.2 mL), then TEA (4 equiv., 0.120 mL, 0.87 mmol) is added. The solution is added dropwise to the reaction mixture of **22** (1.5 equiv., 0.32 mmol) and the mixture is allowed to stir at room temperature for 16h. The reaction mixture is diluted in DCM, washed with H₂O, then brine. The organic phase is dried over Na₂SO₄, and concentrated in

vacuo. The crude product was purified by silica gel column chromatography (EtOAc as eluent) to give the desired compounds **18** as an oil, 59% yield.

ESI MS (*m/z*): 554 [M+H]⁺

¹H NMR (400 MHz, Chloroform-*d*) δ 7.25 – 7.22 (m, 2H), 7.15 (t, *J* = 8.0 Hz, 1H), 6.88 (d, *J* = 8.5 Hz, 2H), 6.41 – 6.37 (m, 1H), 6.37 – 6.31 (m, 2H), 5.66 (s, 1H), 5.40 (ddq, *J* = 10.0, 7.0, 3.0 Hz, 1H), 4.58 – 4.41 (m, 2H), 4.08 (t, *J* = 8.5 Hz, 2H), 3.80 (s, 3H), 3.79 (s, 3H), 3.77 – 3.70 (m, 3H), 3.67 (d, *J* = 7.5 Hz, 1H), 3.54 – 3.47 (m, 2H), 3.47 – 3.41 (m, 2H), 3.37 (q, *J* = 6.0 Hz, 2H), 3.04 – 2.92 (m, 1H), 1.95 (s, 3H)

(R)-1,1,1-trifluoro-3-hydroxypropan-2-yl 3-(((2-acetamidoethyl)(3-methoxyphenyl)amino)methyl)azetidine-1-carboxylate (19, UCM1529)



19, UCM1529

TFA (0.74 ml, 9.7 mmol) was added to a solution of compound **18** (70 mg, 0.125 mmol) in dry DCM (2.2 ml). The solution was stirred at room temperature for 30 min. Then, the mixture was neutralized with the addition of an aqueous saturated solution of NaHCO₃. The aqueous phase was extracted with DCM (x3). The combined organic phases were dried over Na₂SO₄, and concentrated under reduced pressure. The crude was purified by silica gel column chromatography (EtOAc as eluent) to give the desired compounds **19** as an oil, 75% yield.

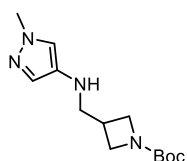
ESI MS (*m/z*): 434 [M+H]⁺

Rotamers are observed when NMR analysis is performed at 25°C. Therefore, NMR analysis has been carried out at 40°C.

¹H NMR (400 MHz, DMSO-*d*₆, 313K) δ 7.85 (t, *J* = 6.0 Hz, 1H), 7.05 (t, *J* = 8.0 Hz, 1H), 6.37 (dd, *J* = 8.0, 2.5 Hz, 1H), 6.33 (t, *J* = 2.5 Hz, 1H), 6.23 (dd, *J* = 8.0, 2.5 Hz, 1H), 5.20 (t, *J* = 6.0 Hz, 1H), 5.14 (qt, *J* = 7.5, 3.5 Hz, 1H), 4.10 (br s, 1H), 4.02 (t, *J* = 8.5 Hz, 1H), 3.80 – 3.67 (m, 3H), 3.72 (s, 3H), 3.63 (dq, *J* = 12.5, 6.5 Hz, 1H), 3.53 (d, *J* = 7.0 Hz, 2H), 3.36 – 3.28 (m, 2H), 3.19 – 3.08 (m, 2H), 3.01 – 2.86 (m, 1H), 1.80 (s, 3H)

¹³C NMR (101 MHz, DMSO-*d*₆, 313K) δ 169.4, 160.5, 153.6, 148.8, 129.7, 125.48 – 112.54 (m), 105.5, 102.0, 98.8, 70.7 (q, *J* = 29.6 Hz), 57.9, 54.7, 53.6, 53.27 – 52.05 (m), 50.0, 35.9, 27.5, 22.4, 20.9

***Tert*-butyl 3-(((1-methyl-1*H*-pyrazol-4-yl)amino)methyl)azetidine-1-carboxylate (24)**



24

Compound **24** was prepared following the described general procedure **C** starting from **23**.

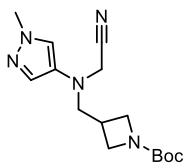
Flash chromatography: silica gel, EtOAc:MeOH 9:1 as eluent.

Red oil, 96% yield

ESI MS (*m/z*): 265 [M+H]⁺

¹H NMR (400 MHz, Chloroform-*d*) δ 7.06 (d, *J* = 1.0 Hz, 1H), 6.88 (d, *J* = 1.0 Hz, 1H), 3.99 (t, *J* = 8.5 Hz, 2H), 3.76 (s, 3H), 3.61 (dd, *J* = 8.5, 5.0 Hz, 2H), 3.12 (d, *J* = 7.5 Hz, 2H), 2.76 – 2.64 (m, 1H), 2.64 – 2.49 (m, 1H), 1.40 (s, 9H)

***Tert*-butyl 3-(((cyanomethyl)(1-methyl-1*H*-pyrazol-4-yl)amino)methyl)azetidine-1-carboxylate (25)**



25

Compound **25** was prepared following the described general procedure **D** starting from **24**.

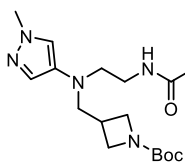
Flash chromatography: silica gel, EtOAc as eluent.

Red oil, 82% yield

ESI MS (*m/z*): 306 [M+H]⁺

¹H NMR (400 MHz, Chloroform-*d*) δ 7.25 (d, *J* = 1.0 Hz, 1H), 7.18 (d, *J* = 1.0 Hz, 1H), 3.96 (dd, *J* = 9.0, 8.0 Hz, 2H), 3.83 (s, 3H), 3.82 (s, 3H), 3.58 (dd, *J* = 9.0, 5.0 Hz, 2H), 3.17 (d, *J* = 7.5 Hz, 2H), 1.41 (s, 9H)

***Tert*-butyl 3-(((2-acetamidoethyl)(1-methyl-1*H*-pyrazol-4-yl)amino)methyl)azetidine-1-carboxylate (26)**



26

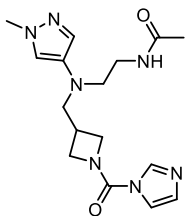
Compound **26** was prepared following the described general procedure **E** starting from **25**.

Flash chromatography: silica gel, EtOAc:MeOH 9:1 as eluent.

Oil, 58% yield

¹H NMR (400 MHz, Chloroform-*d*) δ 7.14 (d, *J* = 1.0 Hz, 1H), 7.00 (d, *J* = 1.0 Hz, 1H), 5.72 (brs, 1H), 3.94 (t, *J* = 8.5 Hz, 2H), 3.82 (s, 3H), 3.56 (dd, *J* = 8.5, 5.5 Hz, 2H), 3.32 (q, *J* = 6.0 Hz, 2H), 3.15 (d, *J* = 7.5 Hz, 2H), 3.06 (t, *J* = 6.5 Hz, 2H), 2.72 (dtt, *J* = 13.0, 5.5, 2.5 Hz, 1H), 1.96 (s, 3H), 1.43 (s, 9H)

***N*-(2-(((1-(1*H*-imidazole-1-carbonyl)azetid-3-yl)methyl)(1-methyl-1*H*-pyrazol-4-yl)amino)ethyl)acetamide (27)**



27

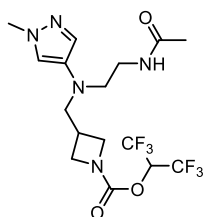
Compound **27** was prepared following the described general procedure **J** starting from **26** with the addition of TEA.

Flash chromatography: silica gel, EtOAc:MeOH 9:1 as eluent. The obtained product was not perfectly clean, thus the yield was not calculated.

ESI MS (*m/z*): 346 [M+H]⁺

¹H NMR (400 MHz, Chloroform-*d*) δ 7.96 (s, 1H), 7.26 (t, *J* = 1.5 Hz, 1H), 7.13 (d, *J* = 1.0 Hz, 1H), 7.04 (t, *J* = 1.0 Hz, 1H), 7.02 (d, *J* = 1.0 Hz, 1H), 6.04 (br s, 1H), 4.36 – 4.26 (m, 2H), 3.99 – 3.90 (m, 2H), 3.79 (s, 3H), 3.29 (q, *J* = 6.5 Hz, 2H), 3.22 (d, *J* = 7.5 Hz, 2H), 3.06 (t, *J* = 6.5 Hz, 2H), 3.03 – 2.91 (m, 1H), 1.93 (s, 3H)

1,1,1,3,3,3-hexafluoropropan-2-yl 3-(((2-acetamidoethyl)(1-methyl-1*H*-pyrazol-4-yl)amino)methyl)azetidine-1-carboxylate (28**, UCM1531)**



28, UCM1531

Compound **28** was prepared following the described general procedure **L** starting from **27**.

Flash chromatography: silica gel, DCM:MeOH 95:5 as eluent.

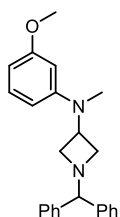
Oil, 55% yield (in two step)

ESI MS (*m/z*): 446 [M+H]⁺

¹H NMR (400 MHz, Chloroform-*d*) δ 7.16 (d, *J* = 1.0 Hz, 1H), 7.03 (d, *J* = 1.0 Hz, 1H), 5.64 (hept, *J* = 6.2 Hz, 1H), 5.64 (br s, 1H), 4.13 (dt, *J* = 17.5, 8.5 Hz, 2H), 3.83 (s, 3H), 3.75 (ddd, *J* = 15.5, 9.0, 5.5 Hz, 2H), 3.32 (q, *J* = 6.0 Hz, 2H), 3.20 (d, *J* = 7.5 Hz, 2H), 3.07 (t, *J* = 6.5 Hz, 2H), 2.90 (dt, *J* = 13.0, 8.0, 2.5 Hz, 1H), 1.96 (s, 3H)

¹³C NMR (101 MHz, Chloroform-*d*) δ 170.4, 151.8, 135.00, 130.5, 119.7, 119.36 (q, *J* = 280.7 Hz), 67.7 (hept, *J* = 34.5 Hz), 58.9, 54.3, 53.9, 53.2, 39.4, 37.2, 27.9, 23.3

1-benzhydryl-*N*-(3-methoxyphenyl)-*N*-methylazetidin-3-amine (30**)**



30

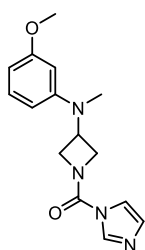
Compound **30** was prepared following the described general procedure **B** starting from commercially available 3-methoxy-*N*-methylaniline **29**.

Flash chromatography: silica gel, cyclohexane:EtOAc 85:15 as eluent.

Yellow oil, 53% yield.

¹H NMR (400 MHz, Chloroform-*d*) δ 7.45 – 7.41 (m, 4H), 7.32 – 7.26 (m, 4H), 7.21 (tt, *J* = 7.5, 2.5 Hz, 2H), 7.11 (t, *J* = 8.2 Hz, 1H), 6.37 – 6.30 (m, 2H), 6.23 (t, *J* = 2.3 Hz, 1H), 4.38 (s, 1H), 4.05 (p, *J* = 6.8 Hz, 1H), 3.76 (s, 3H), 3.65 (td, *J* = 6.4, 1.8 Hz, 2H), 3.00 (td, *J* = 6.9, 1.8 Hz, 2H), 2.80 (s, 3H)

(1*H*-imidazol-1-yl)3-((3-methoxyphenyl)(methyl)amino)azetidin-1-yl)methanone (31**)**



31

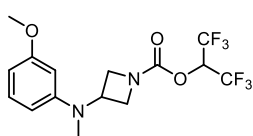
A solution of compound **30** (1 equiv., 240 mg, 0.67 mmol) in MeOH (8 mL) was hydrogenated over Pd/C 10% (61.0 mg) at 5 atm for 16h at r.t. The catalyst was filtered on Celite and the filtrate was concentrated in vacuo to give the corresponding crude oily azetidine which was used without any further purification. CDI (1.2 equiv., 130 mg, 0.81 mmol) was added to a solution of the crude azetidine in dry DCM (1.4 mL). The reaction was stirred at room temperature for 4h. After completion, the solution was diluted with DCM and washed with H₂O (x3). The organic phase was dried over Na₂SO₄ and evaporated under

reduced pressure to yield a crude product which was purified by flash chromatography (EtOAc as eluent) to afford compound **31**, as an oil (56% yield)

ESI MS (m/z): 287 [M+H]⁺

¹H NMR (400 MHz, Chloroform-*d*) δ 8.01 (d, $J = 1.0$ Hz, 1H), 7.30 (d, $J = 1.5$ Hz, 1H), 7.19 (t, $J = 8.0$ Hz, 1H), 7.09 (dd, $J = 1.5, 1.0$ Hz, 1H), 6.47 (ddd, $J = 8.0, 2.5, 1.0$ Hz, 1H), 6.35 (ddd, $J = 8.0, 2.5, 1.0$ Hz, 1H), 6.28 (t, $J = 2.5$ Hz, 1H), 4.53 (t, $J = 8.5$ Hz, 2H), 4.42 (tt, $J = 7.5, 5.0$ Hz, 1H), 4.29 (dd, $J = 9.5, 5.0$ Hz, 2H), 3.79 (s, 3H), 2.91 (s, 3H)

1,1,1,3,3,3-hexafluoropropan-2-yl 3-((3-methoxyphenyl)(methyl)amino)azetidine-1-carboxylate (**32**, UCM1533)



32, UCM1533

Compound **32** was prepared following the described general procedure **K** starting from **31** using 2.5 equivalent of 1,1,1,3,3,3-hexafluoropropan-2-ol.

Flash chromatography: silica gel, cyclohexane:EtOAc 9:1 as eluent.

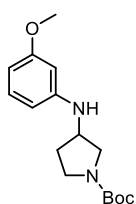
Oil, 68% yield

ESI MS (m/z): 387 [M+H]⁺

¹H NMR (400 MHz, Chloroform-*d*) δ 7.18 (t, $J = 8.0$ Hz, 1H), 6.45 (ddd, $J = 8.0, 2.5, 1.0$ Hz, 1H), 6.35 (ddd, $J = 8.0, 2.5, 1.0$ Hz, 1H), 6.27 (t, $J = 2.5$ Hz, 1H), 5.66 (hept, $J = 6.0$ Hz, 1H), 4.43 – 4.34 (m, 2H), 4.34 – 4.27 (m, 1H), 4.11 (dd, $J = 9.0, 4.5$ Hz, 2H), 3.79 (s, 3H), 2.89 (s, 3H)

¹³C NMR (101 MHz, Chloroform-*d*) δ 160.8, 151.8, 150.9, 130.2, 121.04 (q, $J = 280.4$ Hz), 109.1, 105.0, 103.1, 67.8 (hept, $J = 34.6$ Hz), 55.3, 55.1, 54.3, 50.1, 36.6

Tert-butyl 3-((3-methoxyphenyl)amino)pyrrolidine-1-carboxylate (**33a**)



33a

Under nitrogen atmosphere, 3-pyrrolidone (1.5 equiv., 451 mg, 2.44 mmol) is added to a solution of *m*-anisidine **1a** (1 equiv., 0.18 ml, 1.62 mmol) in MeOH (17.7 mL) and AcOH (1.78 ml). The mixture is stirred at room temperature for 1h, after which NaBH₃CN (2.0 equiv., 203 mg, 3.24 mmol) is added and the reaction is allowed to stir at room temperature for additional 16h. The solvent is evaporated and the residue is dissolved in

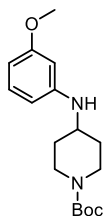
DCM and washed with an aqueous solution of NaHCO₃ 2N (30 ml). The aqueous phase is extracted with DCM (x3). The combined organic phases are dried over Na₂SO₄, and concentrated in vacuo. The residue is purified by silica gel column chromatography (DCM:EtOAc 9:1) to give the desired compounds **33a** as a white solid, 90% yield.

ESI MS (m/z): 293 [M+H]⁺

¹H NMR (400 MHz, Chloroform-*d*) δ 7.09 (t, $J = 8.0$ Hz, 1H), 6.32 – 6.28 (m, 1H), 6.22 (ddd, $J = 8.0, 2.5, 1.0$ Hz, 1H), 6.16 (t, $J = 2.5$ Hz, 1H), 4.02 (s, 1H), 3.77 (d, $J = 4.5$ Hz, 3H), 3.75 – 3.62 (m,

2H), 3.53 – 3.40 (m, 2H), 3.23 (dd, $J = 28.0, 11.5$ Hz, 1H), 2.17 (dtd, $J = 13.0, 7.5, 5.5$ Hz, 1H), 1.89 (s, 1H), 1.46 (s, 9H)

***Tert*-butyl 4-((3-methoxyphenyl)amino)piperidine-1-carboxylate (33b)**



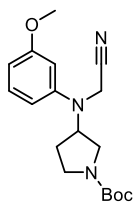
33b

A solution of *tert*-butyl 4-oxopiperidine-1-carboxylate (1.0 equiv., 1105 mg, 5.55 mmol) and *m*-anisidine **1a** (1.05 equiv., 0.65 ml, 5.82 mmol) in dry toluene (7.55 mL) is allowed to stir at room temperature for 1h. After heating to 30-35°C, NaBH(AcOH)₃ (1.5 equiv., 1764 mg, 8.32 mmol) is added portion wise to the solution. The reaction is stirred at 30-35°C for 2h and 30 min. The reaction is diluted with EtOAc and after the addition of H₂O, heated up to 45°C. Then, the organic phase is washed with warm H₂O (x2 at 40°C), dried over Na₂SO₄, and concentrated in vacuo. The residue is purified by silica gel column chromatography (cyclohexane:EtOAc 8:2) to give the desired compounds **33b** as a brown solid, 20% yield.

ESI MS (m/z): 307 [M+H]⁺

¹H NMR (400 MHz, Chloroform-*d*) δ 7.09 (t, $J = 8.0$ Hz, 1H), 6.35 – 6.25 (m, 2H), 6.22 (s, 1H), 4.09 – 3.97 (m, 2H), 3.77 (s, 3H), 3.40 (ddd, $J = 14.0, 10.0, 4.0$ Hz, 1H), 2.90 (t, $J = 11.5$ Hz, 2H), 2.07 – 1.98 (m, 2H), 1.46 (s, 9H), 1.42 – 1.29 (m, 2H)

***Tert*-butyl 3-((cyanomethyl)(3-methoxyphenyl)amino)pyrrolidine-1-carboxylate (34a)**



34a

Compound **34a** was prepared following the described general procedure **D** starting from **33a**.

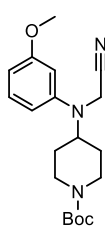
Flash chromatography: silica gel, cyclohexane:EtOAc 8:2 as eluent.

Yellow oil, 86% yield

ESI MS (m/z): 332 [M+H]⁺

¹H NMR (400 MHz, DMSO-*d*₆) δ 7.19 (t, $J = 8.0$ Hz, 1H), 6.62 (dd, $J = 8.0, 2.5$ Hz, 1H), 6.56 (s, 1H), 6.49 (d, $J = 8.5$ Hz, 1H), 4.44 (d, $J = 8.5$ Hz, 2H), 4.41 – 4.31 (m, 1H), 3.74 (s, 3H), 3.53 (dd, $J = 10.5, 7.5$ Hz, 1H), 3.48 – 3.39 (m, 1H), 3.30 – 3.19 (m, 1H), 3.12 (t, $J = 9.0$ Hz, 1H), 2.11 – 2.00 (m, 2H), 1.39 (d, $J = 5.5$ Hz, 9H)

***Tert*-butyl 4-((cyanomethyl)(3-methoxyphenyl)amino)piperidine-1-carboxylate (34b)**



33b

Compound **34b** was prepared following the described general procedure **D** starting from **33b**.

Flash chromatography: silica gel, cyclohexane:EtOAc 8:2 as eluent.

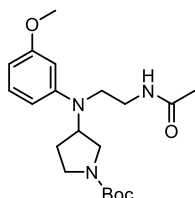
Brown solid, 85% yield

ESI MS (m/z): 346 [M+H]⁺

^1H NMR (400 MHz, Chloroform-*d*) δ 7.23 (t, J = 8.0 Hz, 1H), 6.56 (dd, J = 8.0, 2.5 Hz, 1H), 6.54 – 6.47 (m, 2H), 4.28 – 4.14 (m, 2H), 4.05 (s, 2H), 3.81 (s, 3H), 3.68 (tt, J = 11.5, 3.5 Hz, 1H), 2.80 (t, J = 12.5 Hz, 2H), 1.93 – 1.82 (m, 2H), 1.60 (qd, J = 12.0, 4.5 Hz, 2H), 1.47 (s, 9H).

***Tert*-butyl 3-((2-acetamidoethyl)(3-methoxyphenyl)amino)pyrrolidine-1-carboxylate**

(35a)



35a

Compound **35a** was prepared following the described general procedure **E** starting from **34a**.

Flash chromatography: silica gel, cyclohexane:EtOAc 2:8 as eluent.

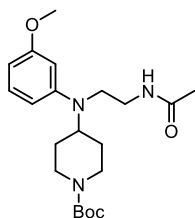
Oil, 61% yield

ESI MS (m/z): 378 [$\text{M}+\text{H}$] $^+$

^1H NMR (400 MHz, DMSO-*d*₆) δ 8.00 (t, J = 5.5 Hz, 1H), 7.07 (t, J = 8.0 Hz, 1H), 6.50 (dd, J = 8.0, 2.0 Hz, 1H), 6.47 (s, 1H), 6.28 (dd, J = 8.0, 2.0 Hz, 1H), 4.38 (tt, J = 16.0, 7.0 Hz, 1H), 3.72 (s, 3H), 3.53 (dd, J = 10.5, 7.5 Hz, 1H), 3.45 – 3.37 (m, 1H), 3.30 – 3.14 (m, 3H), 3.14 – 3.05 (m, 2H), 3.00 (dd, J = 10.5, 8.0 Hz, 1H), 2.07 – 1.89 (m, 2H), 1.81 (s, 3H), 1.40 (d, J = 4.5 Hz, 9H)

***Tert*-butyl 4-((2-acetamidoethyl)(3-methoxyphenyl)amino)piperidine-1-carboxylate**

(35b)



35b

Compound **35b** was prepared following the described general procedure **E** starting from **34b**.

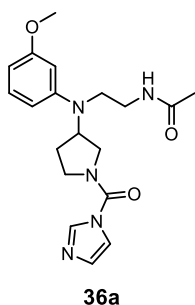
Flash chromatography: silica gel, cyclohexane:EtOAc 2:8 as eluent.

White solid, 57% yield

ESI MS (m/z): 392 [$\text{M}+\text{H}$] $^+$

^1H NMR (400 MHz, Chloroform-*d*) δ 7.16 (t, J = 8.0 Hz, 1H), 6.50 (dd, J = 8.0, 2.5 Hz, 1H), 6.45 (s, 1H), 6.36 (dd, J = 8.0, 2.5 Hz, 1H), 5.80 – 5.62 (m, 1H), 4.33 – 4.12 (m, 2H), 3.81 (s, 3H), 3.68 – 3.56 (m, 1H), 3.42 – 3.32 (m, 2H), 3.32 – 3.21 (m, 2H), 2.82 – 2.67 (m, 2H), 1.97 (s, 3H), 1.80 – 1.71 (m, 2H), 1.57 (qd, J = 12.5, 4.5 Hz, 2H), 1.46 (s, 9H)

***N*-(2-((1-(1*H*-imidazole-1-carbonyl)pyrrolidin-3-yl)(3-methoxyphenyl)amino)ethyl)acetamide (36a)**



Compound **36a** was prepared following the described general procedure **J** starting from **35a**.

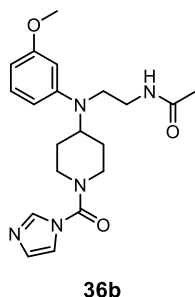
Flash chromatography: silica gel, EtOAc:MeOH 9:1 as eluent.

Yellow oil, 66% yield

ESI MS (*m/z*): 372 [M+H]⁺

¹H NMR (400 MHz, Chloroform-*d*) δ 8.57 (s, 1H), 7.45 (s, 1H), 7.23 – 7.12 (m, 2H), 6.65 – 6.46 (m, 3H), 6.17 (br s, 1H), 4.27 (p, *J* = 7.5 Hz, 1H), 3.93 – 3.80 (m, 2H), 3.80 (s, 3H), 3.76 – 3.59 (m, 2H), 3.42 – 3.31 (m, 3H), 3.31 – 3.18 (m, 1H), 2.27 – 2.11 (m, 2H), 1.97 (s, 3H)

***N*-(2-((1-(1*H*-imidazole-1-carbonyl)piperidin-4-yl)(3-methoxyphenyl)amino)ethyl)acetamide (36b)**



Compound **36b** was prepared following the described general procedure **J** starting from **35b**.

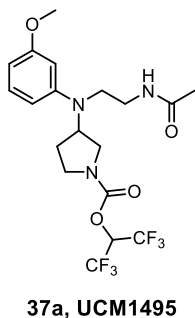
Flash chromatography: silica gel, EtOAc:MeOH 9:1 as eluent.

Oil, 81% yield

ESI MS (*m/z*): 386 [M+H]⁺

¹H NMR (400 MHz, Chloroform-*d*) δ 7.88 (s, 1H), 7.21 (t, *J* = 1.5 Hz, 1H), 7.17 (t, *J* = 8.0 Hz, 1H), 7.09 (s, 1H), 6.51 (dd, *J* = 8.0, 2.5 Hz, 1H), 6.46 (t, *J* = 2.5 Hz, 1H), 6.40 (dd, *J* = 8.0, 2.0 Hz, 1H), 5.81 (br s, 1H), 4.22 (d, *J* = 13.5 Hz, 2H), 3.80 (s, 3H), 3.73 (tt, *J* = 11.5, 3.5 Hz, 1H), 3.36 – 3.26 (m, 4H), 3.13 – 3.03 (m, 2H), 1.97 (s, 3H), 1.94 – 1.87 (m, 2H), 1.73 (qd, *J* = 12.5, 4.0 Hz, 2H)

1,1,1,3,3,3-hexafluoropropan-2-yl 3-((2-acetamidoethyl)(3-methoxyphenyl)amino)pyrrolidine-1-carboxylate (37a, UCM1495)



Compound **37a** was prepared following the above described general procedure **K** starting from **36a** using 2.5 equivalent of HFIP.

Flash chromatography: silica gel, cyclohexane:EtOAc 2:8 as eluent.

Oil, 91% yield

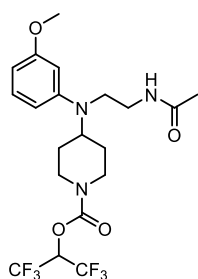
ESI MS (*m/z*): 472 [M+H]⁺

Rotamers are observed when NMR analysis are performed at 25°C. Therefore, NMR analysis have been carried out at 40°C.

¹H NMR (400 MHz, DMSO-*d*₆, 313K) δ 7.93 (s, 1H), 7.09 (t, *J* = 8.0 Hz, 1H), 6.59 – 6.45 (m, 3H), 6.31 (dd, *J* = 8.0, 2.0 Hz, 1H), 4.49 (dp, *J* = 23.5, 8.0 Hz, 1H), 3.73 (s, 3H), 3.68 (dd, *J* = 10.5, 7.5 Hz, 1H), 3.57 (ddd, *J* = 10.5, 8.0, 3.0 Hz, 1H), 3.41 (dtd, *J* = 13.5, 10.0, 7.0 Hz, 1H), 3.24 – 3.06 (m, 5H), 2.16 – 2.00 (m, 2H), 1.80 (d, *J* = 2.0 Hz, 3H)

¹³C NMR (101 MHz, DMSO-*d*₆, 313K) δ 169.2, 160.6, 150.5, 149.2, 129.6, 120.8 (q, *J* = 283.2 Hz), 105.6, 101.7, 99.1, 67.3 (hept, *J* = 33.5 Hz), 54.7, 53.7, 44.1, 43.7, 43.6, 37.7, 28.9 (d, *J* = 15.8 Hz), 22.4

1,1,1,3,3,3-hexafluoropropan-2-yl 4-((2-acetamidoethyl)(3-methoxyphenyl)amino)piperidine-1-carboxylate (37b, UCM1496)



Compound **37b** was prepared following the described general procedure **K** starting from **36b** using 1.2 equivalent of 1,1,1,3,3,3-hexafluoropropan-2-ol.

Flash chromatography: silica gel, cyclohexane:EtOAc 3:7 as eluent.

Yellow oil, 50% yield

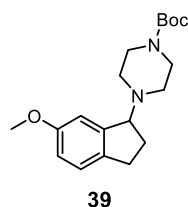
ESI MS (*m/z*): 486 [M+H]⁺

37b, UCM1496

¹H NMR (400 MHz, Chloroform-*d*) δ 7.18 (t, *J* = 8.0 Hz, 1H), 6.52 (dd, *J* = 8.0, 2.0 Hz, 1H), 6.47 (t, *J* = 2.0 Hz, 1H), 6.40 (dd, *J* = 8.0, 2.0 Hz, 1H), 5.75 (hept, *J* = 6.0 Hz, 1H), 5.65 (br s, 1H), 4.34 – 4.20 (m, 2H), 3.81 (s, 3H), 3.66 (tt, *J* = 11.5, 3.5 Hz, 1H), 3.33 (q, *J* = 7.5 Hz, 2H), 3.30 – 3.24 (m, 2H), 3.03 – 2.87 (m, 2H), 1.97 (s, 3H), 1.91 – 1.80 (m, 2H), 1.72 – 1.53 (m, 2H)

¹³C NMR (101 MHz, Chloroform-*d*) δ 170.5, 161.0, 151.5, 149.4, 130.2, 120.8 (q, *J* = 282.2 Hz), 108.7, 103.6, 102.8, 68.3 (hept, *J* = 34.5 Hz), 57.2, 55.4, 44.9, 44.6, 44.3, 38.5, 29.7, 29.5, 23.3

***Tert*-butyl 4-(6-methoxy-2,3-dihydro-1*H*-inden-1-yl)piperazine-1-carboxylate (39)¹⁸**



Under nitrogen atmosphere, sodium borohydride (1.0 equiv., 45 mg, 1.20 mmol) in two portions was added to a suspension of 6-methoxyindan-1-one **38** (1 equiv., 194 mg, 1.20 mmol) in MeOH (2.41 mL). The reaction was stirred at room temperature 1 hour, evaporated, and partitioned between Et₂O and H₂O. The organic phase was washed with H₂O, then with an aqueous solution of HCl 1N, dried over Na₂SO₄, and

evaporated. The resulting oil was dissolved in dry toluene (2.3 mL), adding thionyl chloride (1.5 equiv., 0.13 mL, 1.8 mmol) at room temperature, and stirring at 55-60° for 2h. The solution was cooled, washed with H₂O, dried over Na₂SO₄, and evaporated. The resulting oil was dissolved in dry

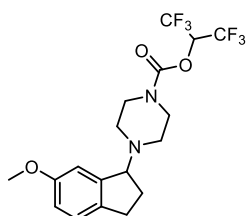
CH₃CN (4.8 mL) and *tert*-butyl piperazine-1-carboxylate (1.2 equiv., 268 mg, 1.44 mmol), K₂CO₃ (2.2 equiv., 364 mg, 2.64 mmol), and a catalytic amount of tetrabutylammonium iodide were added to the solution. The mixture was heated at 75°C for 16 hours, cooled and evaporated. The crude was taken up in EtOAc, washed with H₂O and brine, dried over Na₂SO₄, and evaporated. The residue was chromatographed on silica gel using cyclohexane:EtOAc 7:3 as eluent to afford the desired compound **39** as a yellow oil, 50% yield in three step.

¹H NMR (400 MHz, Chloroform-*d*) δ 7.08 (d, *J* = 8.0 Hz, 1H), 6.88 (d, *J* = 2.5 Hz, 1H), 6.75 (dd, *J* = 8.0, 2.5 Hz, 1H), 4.30 (t, *J* = 7.0 Hz, 1H), 3.77 (s, 3H), 3.49 – 3.35 (m, 4H), 2.82 (dt, *J* = 14.0, 7.0 Hz, 1H), 2.72 (dt, *J* = 15.5, 7.5 Hz, 1H), 2.52 – 2.38 (m, 4H), 2.04 (q, *J* = 7.0 Hz, 2H), 1.44 (s, 9H)

1,1,1,3,3,3-hexafluoropropan-2-yl 4-(6-methoxy-2,3-dihydro-1*H*-inden-1-yl)piperazine-1-carboxylate (40) and (4-(6-methoxy-2,3-dihydro-1*H*-inden-1-yl)piperazin-1-yl)(1*H*-1,2,4-triazol-1-yl)methanone (41)

TFA (0.38 mL) was added to a solution of the *N*-Boc azetidine **39** (1 equiv., 159.5 mg, 0.48 mmol) in dry DCM (0.7 mL) at room temperature. The reaction was stirred at room temperature until the starting material is completely disappeared (about 2h). Then, the reaction was diluted with DCM and washed with an aqueous saturated solution of NaHCO₃. The aqueous phase was extracted with DCM (x3). The combined organic phases were concentrated in vacuo to give the corresponding crude oily azetidine. After dissolution of the crude in anhydrous THF (5.0 mL), the obtained solution was added dropwise to a solution of di(1*H*-1,2,4-triazol-1-yl)methanone (2.5 equiv., 196 mg, 1.2 mmol) and HFIP (15 equiv., 0.75 mL, 7.2 mmol) in anhydrous THF (2.5 mL), previously stirred at room temperature for 15 min. The reaction mixture was stirred an additional 2h at r.t. and then concentrated under reduced pressure. The crude was purified by silica gel flash chromatography using cyclohexane:EtOAc 8:2 as eluent to give the compound **40** and cyclohexane:EtOAc 1:1 as eluent to afford the side product **41**.

40, UCM1500



40, UCM1500

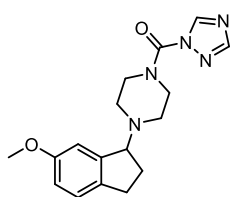
Yellow oil, 22% yield.

ESI MS (*m/z*): 427 [M+H]⁺

¹H NMR (400 MHz, Chloroform-*d*) δ 7.11 (d, *J* = 8.0 Hz, 1H), 6.87 (d, *J* = 2.5 Hz, 1H), 6.79 (dd, *J* = 8.0, 2.5 Hz, 1H), 5.74 (hept, *J* = 6.0 Hz, 1H), 4.34 (t, *J* = 7.0 Hz, 1H), 3.81 (s, 3H), 3.63 – 3.46 (m, 4H), 2.85 (ddd, *J* = 16.0, 8.0, 5.5 Hz, 1H), 2.75 (dt, *J* = 15.5, 7.5 Hz, 1H), 2.59 – 2.45 (m, 4H), 2.13 – 1.98 (m, 2H)

¹³C NMR (101 MHz, Chloroform-*d*) δ 158.9, 151.6, 143.9, 136.1, 125.4, 125.19 – 116.48 (m), 114.1, 110.3, 70.3, 68.2 (p, *J* = 34.4 Hz), 55.6, 48.5, 48.1, 45.3, 44.9, 30.1, 24.9

41



41

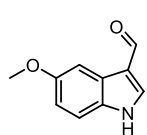
Oil, 17% yield.

ESI MS (m/z): 328 [M+H]⁺

¹H NMR (400 MHz, Chloroform-*d*) δ 8.77 (s, 1H), 7.98 (s, 1H), 7.11 (d, $J = 8.0$ Hz, 1H), 6.89 (d, $J = 2.0$ Hz, 1H), 6.79 (dd, $J = 8.0, 2.5$ Hz, 1H), 4.36 (t, $J = 7.0$ Hz, 1H), 3.96 – 3.82 (m, 4H), 3.81 (s, 3H), 2.86 (dt, $J = 14.0, 7.0$ Hz, 1H), 2.76

(dt, $J = 15.5, 7.5$ Hz, 1H), 2.69 – 2.55 (m, 4H), 2.08 (q, $J = 7.0, 6.5$ Hz, 2H)

5-Methoxy-1H-indole-3-carbaldehyde (43)



43

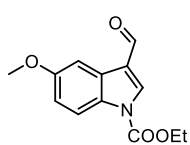
Under nitrogen, in a three-necked flask, the phosphoryl chloride (1.95 equiv., 1.24 ml, 8.83 mmol) is added dropwise to dry DMF (4 ml) at 0°C. After 20 min, the 5-methoxy-1H-indole (1 equiv., 1000 mg, 6.79 mmol), previously dissolved in dry DMF (19 ml), is added dropwise to the solution at 0°C. The reaction is stirred for 2h at room temperature.

After completing, the reaction is poured in a beaker with ice and basified with an aqueous solution of NaOH 2N (40 ml). The aqueous phase is extracted with DCM (3 x 50 ml). The combined organic phases are dried over Na₂SO₄, filtered and evaporated. The residue is dissolved in EtOAc and washed with brine (4 x 50 ml). Finally, the residue is again dried over Na₂SO₄, filtered and evaporated. The crude is used in the next step without further purification.

Yellow solid, 916 mg, 77% yield.

Physicochemical data are in agreement with those previously reported.²²

Ethyl 3-formyl-5-methoxy-1H-indole-1-carboxylate (44)



44

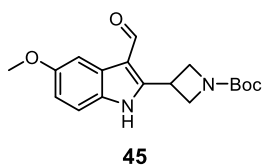
Under nitrogen, the 5-methoxy-1H-indole-3-carbaldehyde **43** (1 equiv., 916 mg, 5.23 mmol) is dissolved in anhydrous THF (13.5 ml) in two-necked flask. NaH 60% (1.5 equiv., 313 mg, 7.84 mmol) is added at 0°C. After stirring for 30 min at 0°C, ethyl carbonochloridate (1.2 equiv., 681 mg, 6.28 mmol) is added at 0°C. Then, the

reaction mixture is allowed to stir at room temperature for 1h. After, H₂O (2 ml) is poured to the mixture and the aqueous phase is extracted with EtOAc (3 x 10 ml). The combined organic phases are washed with brine, dried over Na₂SO₄, filtered and evaporated under reduced pressure. The crude is used in the next step without further purification.

White solid, 1308 mg, 90% yield

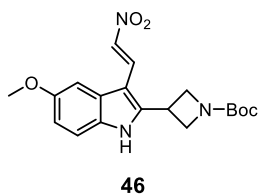
¹H NMR (400 MHz, Chloroform-*d*) δ 10.08 (s, 1H), 8.23 (s, 1H), 8.04 (d, $J = 9.0$ Hz, 1H), 7.77 (d, $J = 3.0$ Hz, 1H), 7.03 (dd, $J = 9.0, 2.6$ Hz, 1H), 4.55 (q, $J = 7.0$ Hz, 2H), 3.90 (s, 3H), 1.51 (t, $J = 7.0$ Hz, 3H)

***Tert*-butyl 3-(3-formyl-5-methoxy-1*H*-indol-2-yl)azetidine-1-carboxylate (45)**



In a Schlenk, previously dried and under nitrogen atmosphere, Pd(PPh₃)₄ (0.1 equiv., 171 mg, 0.15 mmol) and ligand dppp (0.14 equiv., 84 mg, 0.2 mmol) are added to dry toluene (4.5 mL) and the mixture is stirred for 10 min. Ethyl 3-formyl-5-methoxy-1*H*-indole-1-carboxylate **60** (2 equiv., 738 mg, 3 mmol) is added to the mixture with Cs₂CO₃ (2 equiv., 3 mmol, 972 mg) and a solution of *tert*-butyl 3-iodoazetidine-1-carboxylate (1 equiv., 423 mg, 1.5 mmol) in dry toluene (1.5 mL). The reaction is degassed, flushing nitrogen for 15 min. and then is stirred at 110°C for 36h. After cooling to room temperature, the mixture is diluted with EtOAc and washed with H₂O. The organic phase are dried over Na₂SO₄, filtered and evaporated under reduced pressure. The crude is purified by silica gel flash chromatography using DCM:EtOAc 9:1 to give the compound **45** as an transparent solid, 40% yield. ¹H NMR (CDCl₃, 400 MHz): δ 10.2 (bs, 1H), 10.01 (s, 1H), 7.63 (s, 1H), 7.29 (d, *J* = 8.0 Hz, 1H), 6.85-6.91. (m, 1H), 4.38-4.43 (m, 2H), 4.04-4.07 (m, 3H), 3.82 (s, 3H), 1.43 (s, 9H)

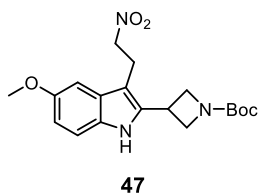
***Tert*-butyl (*E*)-3-(5-methoxy-3-(2-nitrovinyl)-1*H*-indol-2-yl)azetidine-1-carboxylate (46)**



Tert-butyl 3-(3-formyl-5-methoxy-1*H*-indol-2-yl)azetidine-1-carboxylate **45** (1 equiv., 165 mg, 0.5 mmol), nitromethane (6 mL), and ammonium acetate (2.2 equiv., 85 mg, 1.1 mmol) are stirred in a vial at 110°C for 24h. After cooling to room temperature, the nitromethane is evaporated under reduced pressure and the crude is purified by silica gel flash chromatography using DCM:EtOAc 8:2 to give the compound **46** as a yellow solid, 80% yield.

¹H NMR (CDCl₃, 400 MHz): δ 10.16 (bs, 1H), 8.26 (d, *J* = 16.0 Hz, 1H), 7.74 (d, *J* = 8.0 Hz, 1H), 7.40 (d, *J* = 8.0 Hz, 1H), 7.12 (d, *J* = 4.0 Hz, 1H), 6.98 (dd, *J* = 8.0, 4.0 Hz, 1H), 4.48 (m, 2H), 4.21-4.25 (m, 2H), 4.09-4.16 (m, 2H), 3.92 (s, 3H), 1.52 (s, 9H)

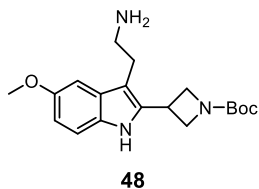
***Tert*-butyl 3-(5-methoxy-3-(2-nitroethyl)-1*H*-indol-2-yl)azetidine-1-carboxylate (47)**



NaBH₄ (7 equiv., 117 mg, 3.09 mmol) is added to a solution of *tert*-butyl (*E*)-3-(5-methoxy-3-(2-nitrovinyl)-1*H*-indol-2-yl)azetidine-1-carboxylate **46** (1 equiv., 165 mg, 0.44 mmol) in MeOH (8.25 mL) at 0°C. The reaction mixture is stirred for 30 min at room temperature, after which is diluted with DCM. The organic phase is washed with a saturated aqueous solution of NH₄Cl (2 x 10 mL), dried Na₂SO₄, filtered and evaporated under reduced pressure. The crude is purified by silica gel flash chromatography using DCM:EtOAc 8:2 to give the compound **47** as a yellow solid, quantitative yield.

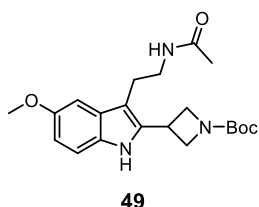
¹H NMR (CDCl₃, 400 MHz): δ 8.66 (bs, 1H), 7.26-7.20 (m, 1H), 6.85-6.90 (m, 2H), 4.58-4.61 (m, 2H), 4.35-4.40 (m, 2H), 3.96-3.98 (m, 3H), 3.88 (s, 3H), 3.35-3.40 (m, 2H), 1.50 (s, 9H)

***Tert*-butyl 3-(3-(2-aminoethyl)-5-methoxy-1*H*-indol-2-yl)azetidine-1-carboxylate (48)**



NaBH₄ (12 equiv., 200 mg, 5.28 mmol) and NiCl₂ (1 equiv., 57 mg, 0.44 mmol) are added to a solution of *tert*-butyl 3-(5-methoxy-3-(2-nitroethyl)-1*H*-indol-2-yl)azetidine-1-carboxylate **47** in MeOH (4.4 mL) at 0°C, then the reaction is stirred for 30 min. The mixture is diluted with DCM and washed with a saturated aqueous solution of NH₄Cl (2 x 10 mL). The organic phase is dried Na₂SO₄, filtered and evaporated under reduced pressure, affording a white solid **48** that is used in the next step without further purification.

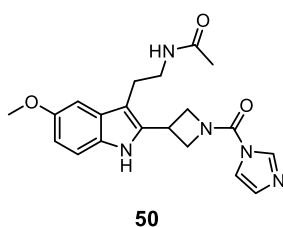
***Tert*-butyl 3-(3-(2-acetamidoethyl)-5-methoxy-1*H*-indol-2-yl)azetidine-1-carboxylate (49)**



Tert-butyl 3-(3-(2-aminoethyl)-5-methoxy-1*H*-indol-2-yl)azetidine-1-carboxylate **48** (1 equiv., 152 mg, 0.44 mmol) is dissolved in dry THF (1.65 mL), then TEA (1.1 equiv., 0.067 mL, 0.48 mmol) and acetic anhydride (1.1 equiv., 0.045 mL, 0.48 mmol) are added. The reaction is stirred at room temperature for 16h. The solvent is evaporated under reduced pressure, and the residue is purified by silica gel flash chromatography using DCM:MeOH 95:5 to give the compound **49** as a colorless solid, 90% yield.

¹H NMR (CDCl₃, 400 MHz): δ 8.81 (br s, 1H), 7.28 (s, 1H), 6.97 (d, *J* = 4.0 Hz, 1H), 6.84-6.87 (m, 1H), 5.62 (br s, 1H), 4.33-4.38 (m, 2H), 3.90-3.95 (m, 3H), 3.86 (s, 3H), 3.41-3.46 (m, 1H), 2.86-2.90 (m, 2H), 1.90 (s, 3H), 1.50 (s, 9H)

***N*-(2-(2-(1-(1*H*-imidazole-1-carbonyl)azetid-3-yl)-5-methoxy-1*H*-indol-3-yl)ethyl)acetamide (50)**



Compound **50** was prepared following the described general procedure **J** starting from **49**.

Flash chromatography: silica gel, DCM:MeOH 9:1 as eluent.

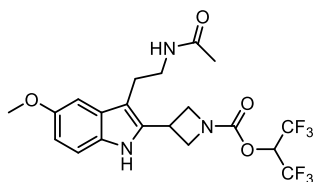
White solid, 44% yield

ESI MS (*m/z*): 382 [M+H]⁺

¹H NMR (400 MHz, DMSO-*d*₆) δ 11.00 (s, 1H), 8.17 (t, *J* = 1.0 Hz, 1H), 7.57 (t, *J* = 1.5 Hz, 1H), 7.21 (d, *J* = 8.5 Hz, 1H), 7.07 (dd, *J* = 1.5, 1.0 Hz, 1H), 6.99 (d, *J* = 2.5 Hz, 2H), 6.71 (dd, *J* = 8.5,

2.4 Hz, 1H), 4.78 – 4.54 (m, 2H), 4.52 – 4.35 (m, 2H), 4.21 (tt, $J = 9.0, 6.5$ Hz, 1H), 3.76 (s, 3H), 3.20 – 3.13 (m, 2H), 2.75 (t, $J = 7.0$ Hz, 2H), 1.78 (d, $J = 1.0$ Hz, 3H).

1,1,1,3,3,3-hexafluoropropan-2-yl 3-(3-(2-acetamidoethyl)-5-methoxy-1H-indol-2-yl)azetidine-1-carboxylate (51, UCM1503)



51, UCM1503

Compound **51** was prepared following the described general procedure **L** starting from **50**.

Flash chromatography: silica gel, DCM:MeOH 95:5 as eluent.

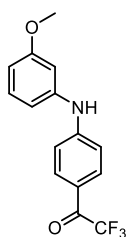
Brown solid, 79% yield

ESI MS (m/z): 482 $[M+H]^+$

^1H NMR (400 MHz, Chloroform-*d*) δ 8.16 (s, 1H), 7.27 (t, $J = 8.5$ Hz, 1H), 6.98 (d, $J = 2.5$ Hz, 1H), 6.88 (dd, $J = 8.5, 2.5$ Hz, 1H), 5.69 (hept, $J = 6.0$ Hz, 1H), 5.56 (br s, 1H), 4.64 – 4.47 (m, 2H), 4.26 – 4.14 (m, 3H), 3.86 (s, 3H), 3.43 (d, $J = 6.5$ Hz, 2H), 2.89 (t, $J = 7.0$ Hz, 2H), 1.93 (s, 3H)

^{13}C NMR (101 MHz, Chloroform-*d*) δ 170.4, 154.5, 151.9, 134.4, 131.2, 128.6, 120.7 (q, $J = 283.6, 282.3$ Hz), 112.6, 111.9, 110.7, 100.7, 67.9 (p, $J = 34.6$ Hz), 56.5, 56.1, 55.6, 40.6, 26.2, 24.3, 23.4

2,2,2-trifluoro-1-(4-((3-methoxyphenyl)amino)phenyl)ethan-1-one (53)



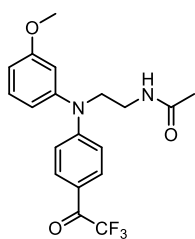
53

In a Schlenk flask, **1a** (1.2 equiv., 0.116 mL, 0.95 mmol) and the commercially available 1-(4-bromophenyl)-2,2,2-trifluoroethan-1-one **52** (1 equiv., 200 mg, 0.79 mmol) were dissolved in dry 1,4-dioxane (10 mL). Then, the XPhos catalyst (0.1 equiv., 58 mg, 0.079 mmol) and Cs_2CO_3 (3 equiv., 772 mg, 2.37 mmol) were added to the solution. The mixture was stirred at 100 °C for 3 h. After cooling to room temperature, the reaction mixture was diluted with EtOAc and filtered through a silica pad, washing with EtOAc. The organic phases were dried over Na_2SO_4 and evaporated under reduced pressure to yield a crude product which was purified by flash chromatography (silica gel, cyclohexane:EtOAc 8:2 as eluent) to give **53** as a yellow solid (90% yield).

ESI MS (m/z): 296 $[M+H]^+$

^1H NMR (400 MHz, Chloroform-*d*) δ 8.00 – 7.93 (m, 2H), 7.29 (t, $J = 8.0$ Hz, 1H), 7.04 – 6.98 (m, 2H), 6.81 (ddd, $J = 8.0, 2.0, 1.0$ Hz, 1H), 6.77 (t, $J = 2.0$ Hz, 1H), 6.71 (ddd, $J = 8.0, 2.0, 1.0$ Hz, 1H), 6.28 (br s, 1H), 3.82 (s, 3H)

***N*-(2-((3-methoxyphenyl)(4-(2,2,2-trifluoroacetyl)phenyl)amino)ethyl)acetamide (54, UCM1491)**



54, UCM1491

Compound **54** was prepared following the described general procedure **A** starting from **53** and *N*-(2,2-dimethoxyethyl)acetamide **2a**.

Flash chromatography: silica gel, cyclohexane:EtOAc 2:8 as eluent. Purification: silica gel, dichloromethane:MeOH 98:2 as eluent. Yellowish amorphous solid, 60% yield.

ESI MS (*m/z*): 381 [M+H]⁺

¹H NMR (400 MHz, Chloroform-*d*) δ 7.86 (d, *J* = 8.5 Hz, 2H), 7.35 (t, *J* = 8.0 Hz, 1H), 6.86 (dd, *J* = 8.5, 2.5 Hz, 1H), 6.84 – 6.77 (m, 3H), 6.76 (t, *J* = 2.5 Hz, 1H), 5.93 (br s, 1H), 3.92 (t, *J* = 7.0 Hz, 2H), 3.80 (s, 3H), 3.50 (q, *J* = 6.5 Hz, 2H), 1.93 (s, 3H).

¹³C NMR (101 MHz, Chloroform-*d*) δ 178.2 (q, *J* = 33.9 Hz), 170.9, 161.4, 154.0, 145.8, 132.5 (q, *J* = 2.2 Hz), 131.2, 119.5, 119.3, 117.40 (q, *J* = 291.7 Hz), 113.5, 113.4, 112.7, 55.6, 51.1, 37.6, 23.2

5.5 References

- ¹ Tordjman S, Chokron S, Delorme R, Charrier A, Bellissant E, Jaafari N, Fougrou C. Melatonin: Pharmacology, Functions and Therapeutic Benefits. *Curr Neuropharmacol*. **2017**, 15(3), 434-443
- ² Scotter EL, Abood ME, Glass M. The endocannabinoid system as a target for the treatment of neurodegenerative disease. *Br J Pharmacol*. **2010**, 160(3), 480-98
- ³ Ikram M, Park HY, Ali T, Kim MO. Melatonin as a Potential Regulator of Oxidative Stress, and Neuroinflammation: Mechanisms and Implications for the Management of Brain Injury-Induced Neurodegeneration. *J Inflamm Res*. **2021**, 14, 6251-6264
- ⁴ Yang W, Zhang Y, Lu D, Huang T, Yan K, Wang W, Gao J. Ramelteon protects against human pulmonary microvascular endothelial cell injury induced by lipopolysaccharide (LPS) via activating nuclear factor erythroid 2-related factor 2 (Nrf2)/heme oxygenase-1 (HO-1) pathway. *Bioengineered*. **2022**, 13(1), 1518-1529
- ⁵ Spadoni G, Bedini A, Furiassi L, Mari M, Mor M, Scalvini L, Lodola A, Ghidini A, Lucini V, Dugnani S, Scaglione F, Piomelli D, Jung KM, Supuran CT, Lucarini L, Durante M, Sgambellone S, Masini E, Rivara S. Identification of Bivalent Ligands with Melatonin Receptor Agonist and Fatty Acid Amide Hydrolase (FAAH) Inhibitory Activity That Exhibit Ocular Hypotensive Effect in the Rabbit. *J Med Chem*. **2018**, 61(17), 7902-7916
- ⁶ Cammarota M, Ferlenghi F, Vacondio F, Vincenzi F, Varani K, Bedini A, Rivara S, Mor M, Boscia F. Combined targeting of fatty acid amide hydrolase and melatonin receptors promotes neuroprotection and stimulates inflammation resolution in rats. *Br J Pharmacol*. **2023**, 180(10), 1316-1338
- ⁷ Bertrand T, Augé F, Houtmann J, Rak A, Vallée F, Mikol V, Berne PF, Michot N, Cheuret D, Hoornaert C, Mathieu M. Structural basis for human monoglyceride lipase inhibition. *J Mol Biol*. **2010**, 396(3), 663-73
- ⁸ a) Stauch B, Johansson LC, McCorvy JD, Patel N, Han GW, Huang XP, Gati C, Batyuk A, Slocum ST, Ishchenko A, Brehm W, White TA, Michaelian N, Madsen C, Zhu L, Grant TD, Grandner JM, Shiriaeva A, Olsen RHJ, Tribo AR, Yous S, Stevens RC, Weierstall U, Katritch V, Roth BL, Liu W, Cherezov V. Structural basis of ligand recognition at the human MT₁ melatonin receptor. *Nature*. **2019**, 569(7755), 284-288; b) Johansson LC, Stauch B, McCorvy JD, Han GW, Patel N, Huang XP, Batyuk A, Gati C, Slocum ST, Li C, Grandner JM, Hao S, Olsen RHJ, Tribo AR, Zaare S, Zhu L, Zatsopin NA, Weierstall U, Yous S, Stevens RC, Liu W, Roth BL, Katritch V, Cherezov V. XFEL structures of the human MT₂ melatonin receptor reveal the basis of subtype selectivity. *Nature*. **2019**, 569(7755), 289-292
- ⁹ Aaltonen N, Savinainen JR, Ribas CR, Rönkkö J, Kuusisto A, Korhonen J, Navia-Paldanius D, Häyriäinen J, Takabe P, Käsnänen H, Panssar T, Laitinen T, Lehtonen M, Pasonen-Seppänen S, Poso A, Nevalainen T,

Laitinen JT. Piperazine and piperidine triazole ureas as ultrapotent and highly selective inhibitors of monoacylglycerol lipase. *Chem Biol.* **2013**, 20(3), 379-90

¹⁰ Mattson RJ, Catt JD, Keavy D, Sloan CP, Epperson J, Gao Q, Hodges DB, Iben L, Mahle CD, Ryan E, Yocca FD. Indanyl piperazines as melatonergic MT₂ selective agents. *Bioorg Med Chem Lett.* **2003**, 13(6), 1199-202

¹¹ Jiang M, Huizenga MCW, Wirt JL, Paloczi J, Amedi A, van den Berg RJBHN, Benz J, Collin L, Deng H, Di X, Driever WF, Florea BI, Grether U, Janssen APA, Hankemeier T, Heitman LH, Lam TW, Mohr F, Pavlovic A, Ruf I, van den Hurk H, Stevens AF, van der Vliet D, van der Wel T, Wittwer MB, van Boeckel CAA, Pacher P, Hohmann AG, van der Stelt M. A monoacylglycerol lipase inhibitor showing therapeutic efficacy in mice without central side effects or dependence. *Nat Commun.* **2023**, 14(1), 8039

¹² Righi M, Bedini A, Piersanti G, Romagnoli F, Spadoni G. Direct, One-Pot Reductive Alkylation of Anilines with Functionalized Acetals Mediated by Triethylsilane and TFA. Straightforward Route for Unsymmetrically Substituted Ethylenediamine. *J Org Chem.* **2011**, 76(2), 704-707

¹³ Spadoni G, Bedini A, Lucarini S, Mari M, Caignard DH, Boutin JA, Delagrange P, Lucini V, Scaglione F, Lodola A, Zanardi F, Pala D, Mor M, Rivara S. Highly Potent and Selective MT₂ Melatonin Receptor Full Agonists from Conformational Analysis of 1-Benzyl-2-acylaminomethyl-tetrahydroquinolines. *J Med Chem.* **2015**, 58(18), 7512-25

¹⁴ Wang BJ, Duncton MAJ. A Single-Step Synthesis of Azetidine-3-amines. *J Org Chem.* **2020**, 85(20), 13317-13323

¹⁵ Aaltonen N, Savinainen JR, Ribas CR, Rönkkö J, Kuusisto A, Korhonen J, Navia-Paldanius D, Häyrynen J, Takabe P, Käsnänen H, Pantsar T, Laitinen T, Lehtonen M, Pasonen-Seppänen S, Poso A, Nevalainen T, Laitinen JT. Piperazine and piperidine triazole ureas as ultrapotent and highly selective inhibitors of monoacylglycerol lipase. *Chem Biol.* **2013**, 20(3), 379-90

¹⁶ Butler CR, Beck EM, Harris A, Huang Z, McAllister LA, Am Ende CW, Fennell K, Foley TL, Fonseca K, Hawrylik SJ, Johnson DS, Knafels JD, Mentel S, Noell GS, Pandit J, Phillips TB, Piro JR, Rogers BN, Samad TA, Wang J, Wan S, Brodney MA. Azetidine and Piperidine Carbamates as Efficient, Covalent Inhibitors of Monoacylglycerol Lipase. *J Med Chem.* **2017**, 60(23), 9860-9873

¹⁷ McAllister LA, Butler CR, Mentel S, O'Neil SV, Fonseca KR, Piro JR, Cianfrogna JA, Foley TL, Gilbert AM, Harris AR, Helal CJ, Johnson DS, Montgomery JI, Nason DM, Noell S, Pandit J, Rogers BN, Samad TA, Shaffer CL, da Silva RG, Uccello DP, Webb D, Brodney MA. Discovery of Trifluoromethyl Glycol Carbamates as Potent and Selective Covalent Monoacylglycerol Lipase (MAGL) Inhibitors for Treatment of Neuroinflammation. *J Med Chem.* **2018**, 61, 3008-3026

¹⁸ Lowe J, Drozda S, Qian W, Peakman MC, Liu J, Gibbs J, Harms J, Schmidt C, Fisher K, Strick C, Schmidt A, Vanase M, Lebel L. A novel, non-substrate-based series of glycine type 1 transporter inhibitors derived from high-throughput screening. *Bioorg Med Chem Lett.* **2007**, 17(6), 1675-8

-
- ¹⁹ Claffey MM, Helal CJ, Verhoest PR, Kang Z, Fors KS, Jung S, Zhong J, Bundesmann MW, Hou X, Lui S, Kleiman RJ, Vanase-Frawley M, Schmidt AW, Menniti F, Schmidt CJ, Hoffman WE, Hajos M, McDowell L, O'Connor RE, Macdougall-Murphy M, Fonseca KR, Becker SL, Nelson FR, Liras S. Application of structure-based drug design and parallel chemistry to identify selective, brain penetrant, *in vivo* active phosphodiesterase 9A inhibitors. *J Med Chem.* **2012**, 55(21), 9055-68
- ²⁰ Rivara S, Pala D, Lodola A, Mor M, Lucini V, Dugnani S, Scaglione F, Bedini A, Lucarini S, Tarzia G, Spadoni G. MT₁-selective melatonin receptor ligands: synthesis, pharmacological evaluation, and molecular dynamics investigation of *N*-{[(3-*O*-substituted)anilino]alkyl} amides. *ChemMedChem.* **2012**, 7(11), 1954-64
- ²¹ Kos I, Jadrijević-Mladar M, Butula I, Biruš M, Maravić-Vlahoviček G, Dabelić S. Synthesis, antibacterial and cytotoxic activity evaluation of hydroxyurea derivatives. *Acta Pharm.* **2013**, 63(2), 175-91
- ²² Sauleau P, Martin MT, Dau ME, Youssef DT, Bourguet-Kondracki ML. Hyrtiazepine, an azepino-indole-type alkaloid from the Red Sea marine sponge *Hyrtios erectus*. *J Nat Prod.* **2006**, 69(12), 1676-9

Chapter 6. Appendix

6.1 Experimental chemistry methods

Melting points were determined on a Buchi B-540 capillary melting point apparatus and were uncorrected. ^1H NMR and ^{13}C NMR spectra were recorded on a Bruker AVANCE 400, using CDCl_3 as solvent unless stated otherwise. Chemical shifts (δ scale) are reported in parts per million (ppm) relative to the central peak of the solvent; coupling constants (J) are given in hertz (Hz). NMR spectra were processed and analyzed using MestReNova software from Mestrelab Research. ESI MS spectra were taken on a Waters Micromass ZQ instrument; molecular ions $[\text{M}+\text{H}]^+$ are given. High-resolution mass spectroscopy was performed on a Micromass Q-ToF Micro mass spectrometer (Micromass, Manchester, UK) using an ESI source. The purity of tested compounds was determined by high performance liquid chromatography (HPLC) and was greater than 95%. These analyses were performed on a Waters HPLC/DAD/MS system (separation module Alliance HT2795, Photo Diode Array Detector 2996, mass detector Micromass ZQ; software: MassLynx 4.1). Column chromatography purifications were carried out under “flash” conditions using Merck 230–400 mesh silica gel. Analytical thin-layer chromatography (TLC) was performed on Merck silica gel 60 F254 plates. Optical rotation analysis was performed using a Perkin-Elmer 241 polarimeter using a sodium lamp (λ 589 nm, D-line), α values were reported in 10^{-1} deg $\text{cm}^2 \text{g}^{-1}$; concentration (c) is in g per 100 mL. Enantiomeric purity was determined by HPLC and performed on AD-H - CHIRALPAK[®] column ($\varnothing = 0.46$ cm, $l = 25$ cm, $5 \mu\text{m}$) on the following apparatus: Shimadzu LC-10AT (liquid chromatograph), Shimadzu SPD-10A (UV detector), Shimadzu C-R6A Chromatopac (integrator); n-hexane/*i*-PrOH 95:5 as eluent, λ 262 nm, flow rate of 1.0 mL/min.

UV-Vis absorption spectra were recorded at 298.1 K on a Varian Cary-100 spectrophotometer equipped with a temperature control unit. Fluorescence emission spectra were recorded at 298.1 K on a Varian CaryEclipse spectrofluorimeter and the spectra are uncorrected. Emission quantum yields were calculated using 2,2'-biphenol in acetonitrile as standard ($\Phi = 0.29$). The HypSpec computer program was used to process the spectrophotometric data.

6.2 *In vitro* pharmacology experiments

Competition binding experiments

Competition binding experiments were performed incubating 2-[¹²⁵I]iodomelatonin (30 pM for MT₁ and 80 pM for MT₂) and different concentrations of the examined compounds in binding buffer (50 mM Tris-HCl, pH 7.4, 5 mM MgCl₂) with hMT₁CHO or hMT₂CHO cell membranes for 90-120 min at 37°C. At the end of the incubation time, bound and free radioactivity were separated in a Brandel cell harvester (Brandel Instruments) by filtering the assay mixture through Whatman GF/B glass fiber filters. Specific binding of MT₁ and MT₂ receptors was always greater than 95%. After incubation, the % of radioligand binding inhibition was determined via a scintillation counting method using a 2 810 TR liquid scintillation counter (Perkin Elmer). The radioligand binding experiments were performed in triplicate. IC₅₀ values were determined by nonlinear regression analysis of the competition curves using Hill equation curve fitting. The pK_i values were calculated from the IC₅₀ values in accordance with the Cheng-Prusoff equation.

cAMP assays

hMT₁CHO or hMT₂CHO cells were washed with phosphate-buffered saline, detached with trypsin and centrifuged for 10 min at 200×g. Cells were seeded in a 96-well white half-area microplate in stimulation buffer composed of Hank Balanced Salt Solution, 5 mM HEPES, 0.5 mM Ro 20–1724, 0.1% BSA. To assess potency, agonists were used in the presence of 1 μM forskolin to stimulate cAMP production. The antagonist's effect was evaluated based on its ability to counteract the melatonin-induced reduction of forskolin-stimulated cAMP production. Melatonin concentrations used in this experiment were 0.3 nM for the MT₁ receptor and 1 nM for the MT₂ receptor. The cAMP levels were quantified by using the AlphaScreen cAMP Detection Kit (Perkin Elmer), following the manufacturer's instructions. The Alpha signal was read with a Perkin Elmer EnSight Multimode Plate Reader.

Assay to measure MAGL inhibitory activity

Inhibitory activity of the newly synthesized compounds was evaluated by incubating human MAGL with 7-hydroxycoumarinyl-arachidonate (a fluorogenic substrate for MAGL), whose cleavage generates a fluorescent metabolite. Fluorescence intensity in the presence of different concentrations of new and reference compounds was monitored with a Perkin Elmer EnSight Multimode Plate.¹

6.3 Molecular modelling

Protein preparation

The crystal structures of MT₁ and MT₂ receptors in complex with 2-PhMLT (PDB id 6ME3 and 6MES) were prepared for molecular modelling studies. Co-expressed proteins and molecules included in crystallization buffers were removed, as well as the unstructured residues in the *N*-terminal sequence of the MT₂ receptor (linked to the apocytochrome b562RIL), leaving Pro36 as the first residue. The missing intracellular loop 3 (ICL3, i.e., Gln219-Pro227 and Arg232-Leu240 in MT₁ and MT₂ receptors, respectively) and residue side chains were added with Modeller 9.21

Ligand docking

The grid for docking calculations was built on the prepared structure of the MT₂ receptor in complex with 2-PhMLT, imposing bounding and enclosing boxes of 10 and 20 Å, respectively, centered on the co-crystallized ligand which was removed before calculations. Docking calculations were performed with Glide 7.9 in standard precision mode. Parameters controlling pose retention after the rough scoring stage for refinement and post-dock minimization stages were increased tenfold from default values. Final ligand poses were ranked according to GScore.

6.4 Molecular dynamics (MD) simulations

Simulations were conducted with Desmond 5.4 with the OPLS3e force field, following a protocol already applied to melatonergic ligands.²

6.5 References

¹ Wang Y, Chanda P, Jones PG, Kennedy JD. A fluorescence-based assay for monoacylglycerol lipase compatible with inhibitor screening. *Assay Drug Dev Technol.* **2008**, 6(3), 387-93

² Elisi GM, Bedini A, Scalvini L, Carmi C, Bartolucci S, Lucini V, Scaglione F, Mor M, Rivara S, Spadoni G. Chiral Recognition of Flexible Melatonin Receptor Ligands Induced by Conformational Equilibria. *Molecules.* **2020**, 25(18), 4057

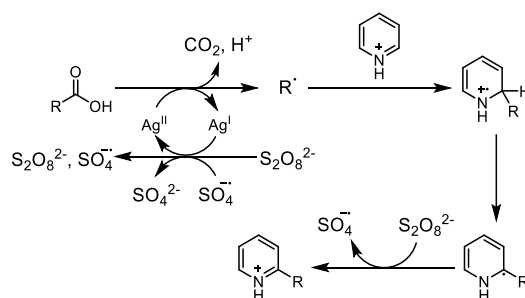
Second Part

Chapter 7. Hydrofunctionalization of olefins driven by a photoinduced halogen atom transfer in flow conditions

This chapter is based on: **Fanini F**, Luridiana A, Mazzarella D, Alfano AI, Van de Heide P, Rincón JA, García-Losada P, Mateos C, Frederick MO, Nuño M, Noël T. Flow photochemical Giese reaction via silane-mediated activation of alkyl bromides. *Tetrahedron Letters* **2023**, 117, 154380

7.1 Introduction

In the past decade, we witnessed the radical chemistry reassessment, which was prompted by the development of new methods for generating crucial radical intermediates. In the past, this powerful chemistry has been limited because of the requirement of harsh reaction conditions, use of toxic reagents (in particular tin-based reagents), high temperature, and difficulties in reaction control.¹ However, the potential of radical chemistry was already disclosed, for example, in the Minisci and Giese reaction. Both of these reactions allow the formation of carbon-carbon bonds, which is fundamental in organic chemistry. In particular, the classic Minisci reaction generates an alkyl radical by decarboxylation of an alkylcarboxylic acid, using silver as a catalyst and persulfate as an oxidant in acidic conditions (**Scheme 18**).² Since the original protocol showed some limitations (regioselectivity, reactivity problems with primary alkylcarboxylic acids, and the use of not ideal reagents and conditions), several improvements have been applied to this protocol, providing new procedures characterized by milder conditions and increased regioselectivity.³



Scheme 18 Minisci classic reaction: proposed mechanism.

Giese reaction is a practical method for the hydrofunctionalization of olefins. The original Giese addition used organotin hydrides to generate the alkyl radicals from alkyl halides, which could undergo the addition of the electron poor-olefin (**Figure 36**).⁴

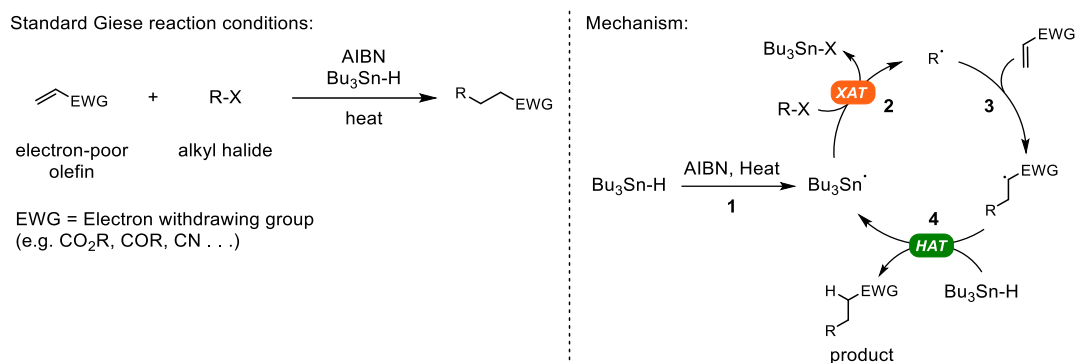


Figure 36 Standard Giese reaction condition and mechanism. **1)** Initiation by AIBN and heat; **2)** halogen atom transfer (XAT); **3)** radical addition; **4)** Hydrogen atom transfer (HAT).

The proposed mechanism of Giese addition initiated by AIBN in the presence of organotin hydride is illustrate in **Figure 36**. Firstly, the organotin radical is formed upon heating of AIBN. Secondly, the organotin radical promotes a XAT process, in which a thermodynamically more stable tin halogen bond and a carbon radical are formed (step 2). Thirdly, the alkyl radical undergoes a radical addition, forming a C-C bond between the electron-poor olefin and the alkyl radical (step 3). Lastly, a hydrogen atom is abstracted from an organotin hydride molecule, through a HAT process, forming the final product (step 4) and generating a new organotin radical. In this way, a radical chain process can be maintained.

The generation of the alkyl radicals can occur in four different ways: direct homolysis, single electron transfer (SET), halogen atom transfer (XAT), and hydrogen atom transfer (HAT). In direct homolysis, the absorption of a specific wavelength of light in the lower region of the visible light spectrum can induce the homolytic cleavage of the C-X bond in an alkyl halide, providing the alkyl radical (**Figure 37A**).⁵ In the SET event, the alkyl halide reduction occurs, generating the desired alkyl radical and negatively charged halide ion (**Figure 37B**).⁶ Alternatively, during a XAT event, a halogen abstractor interacts with a halogen atom of a C-X bond, causing the homolytic cleavage of the bond and forming the carbon radical (**Figure 37C**).⁷ Finally, the HAT process occurs when the radical is formed by the abstraction of a hydrogen atom by a photocatalyst or a radical abstractor (**Figure 37D**).⁴

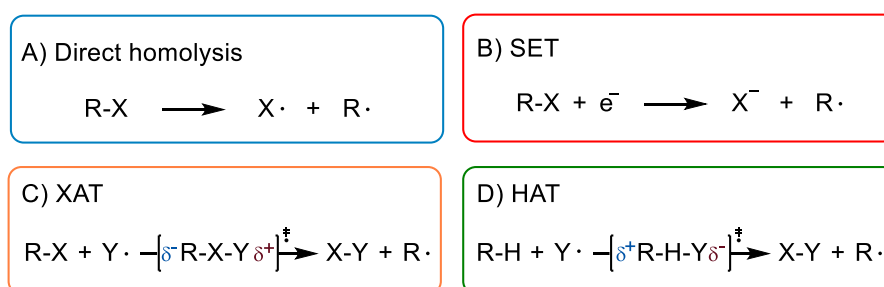


Figure 37 A) Direct homolysis; B) single electron transfer (SET); C) halogen atom transfer (XAT); D) hydrogen atom transfer (HAT)

Enthalpic and polar effects influence XAT events. Regarding the enthalpic effects, it is fundamental that the X-Y bond is stronger than the R-X bond, ensuring that the reaction occurs exothermically. For this reason, the halogen abstraction increases as the R-X bond BDE becomes weaker (in fact, R-I > R-Br > R-Cl).⁷ According to the polar effects, in the transition state of the XAT, if the alkyl group (R) has a partial negative charge and the attacking group (Y) has a partial positive charge, the reaction is highly favorable (**Figure 37C**).⁷ On the contrary, in the HAT process, the alkyl group (R) needs a partial positive charge, while the radical needs a partial negative charge for an efficient HAT reaction (**Figure 37D**).⁸

Nowadays, radicals can be generated using milder and straightforward procedures involving light as a traceless reagent. Radical chemistry is complementary to polar chemistry, allowing access to new chemical space and facilitating the achievement of complex target structures, keeping a good group tolerance.¹

7.1.1 Photochemistry

When a chemical process involves light absorption, we can talk about photochemistry. The development of photochemistry in the past decades can be addressed by other technological innovations, particularly photocatalysis, light sources (LEDs), and reactor technology.⁹ In contrast to the past, where high temperatures were required to generate radicals, the use of photons allows the use of milder conditions and is selective on the species to excite. In fact, the use of LEDs allows the selection of the right wavelength, making the selective excitation of one of the components possible.⁹ In the reaction mixture, a photon-absorbing species, such as a photocatalyst, is responsible for transferring the excited state via different pathways (SET as in photoredox catalysis, HAT or energy transfer).

The Grotthus-Draper law states that only the absorbed light can effectively produce photochemical changes in the molecule, while the Stark-Einstein law states that a singular photon can only activate and form the product for the single molecule that absorbs the photon.¹⁰ The latter notion can be expressed by the quantum yield (Φ), which equation is reported above.¹¹

$$\Phi(\lambda) = \frac{\text{mol of product formed}}{\text{mol of photons absorbed}}$$

The quantum yield is equal to 1 when one mol of product is formed as the absorption of one photon. The Φ can be less than 1 when part of the absorption energy is lost, for example, in a fluorescence event. More interesting is when one mol of absorbed photons results in an amount of product in moles that is higher than one, which means that the reaction propagates itself by means of a radical chain.¹¹

Another critical issue in photochemistry is to ensure the proper irradiation. According to the Bouguer-Lambert-Beer law, the absorbance of the sample depends on the molar absorption coefficient (ϵ), the concentration (c), and the path length of the beam into the sample (l). The absorbance can also be expressed as either the logarithm of the initial intensity of the light (I_0) by the intensity of the light after absorbance has taken place (I) or the logarithm of 1 divided by the transmittance (T). The transmittance is the ratio of the light that has passed through an object (I) to the incident light (I_0).⁹ The equation below describes the Bouguer-Lambert-Beer Law.

$$A = \epsilon \cdot c \cdot l = \log_{10} \frac{I_0}{I} = \log_{10} \frac{1}{T}$$

7.1.2 Flow chemistry: advantages and application in photochemistry

The number of publications regarding photochemical reactions has increased in the past decade. The exploitation of radical chemistry triggered by light enables access to new chemical space or facilitates the formation of complex natural structures. Furthermore, radical chemistry has proven useful for late-stage functionalization, which is crucial in the production of pharmaceuticals and agrochemicals.¹

Most of the procedures developed over the past years in batch conditions showed problem in the scalability of the process, which are due to the attenuation of photon transport when a larger reactor is used (Bouguer-Lambert-Beer law). Since photochemical reactions involve the use of photon-absorbing species, such as photocatalyst⁵, redox-active esters⁴, XAT or HAT reagents⁷ for generating the crucial radical intermediates, the appropriate irradiation of the sample is fundamental. As specified before, the Bouguer-Lambert-Beer law states that the absorbance is influenced by the path length (l), which means that the radiation distribution will not be uniform in all reactors. If, in the sample, there are stronger absorption species (such as photocatalysts or organic dyes), the light intensity will decrease faster along the path length (**Figure 38**). In other words, the lower the light path is, the better the sample is irradiated.¹²

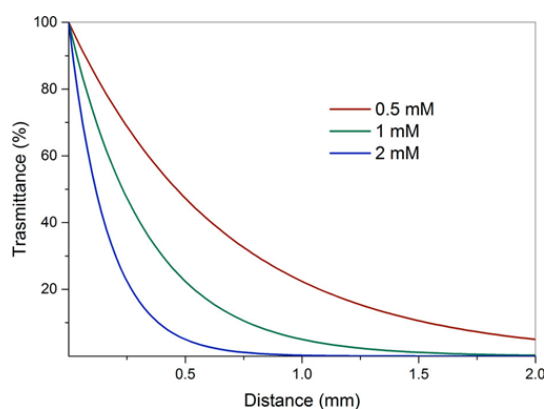


Figure 38 Transmission of light as a function of distance in a photocatalytic reaction using $\text{Ru}(\text{bpy})_3\text{Cl}_2$ ($c = 0.5, 1,$ and 2 mM , $\epsilon = 13\,000 \text{ cm}^{-1} \text{ M}^{-1}$) utilizing the Bouguer–Lambert–Beer correlation.¹²

Furthermore, the over-irradiation of the sample can lead to the formation of byproducts, decomposition, and complications in the purification process.¹² For these reasons, continuous-flow chemistry has gained much interest, especially in photochemistry. The use of narrow tubes ensures the uniform and appropriate irradiation of the reaction, which results in reduced reaction time and lower amount of photocatalyst required. Furthermore, the uniform irradiation and the reduced reaction enhance the productivity of the reaction and simultaneously potentially minimize the formation of byproducts.¹² The scale-up in flow conditions is more straightforward than batch, and new continuous flow reactors have been developed and employed in industrial environments. As observed, the results obtained on a small scale using flow conditions are highly reliable and reproducible on a larger scale.⁹ Other advantages of microreactors are the improved mass- and heat-transfer characteristics, which have been addressed to be responsible for product selectivity. Inline analytical technologies can be used to develop fully automated and/or self-optimizing processes. The mass- and heat-transfer control and the inline analysis enhance the safety of all processes, for example, checking the generation or the consumption of toxic reagents in real-time.¹²

Finally, multiphase reactions, which involve the combination of two or more immiscible phases (e.g., liquid-liquid or gas-liquid reactions), are boosted in flow conditions. The mass transfer and the interfacial area are maximized due to the small specific dimensions of the microreactors.¹³

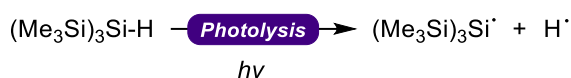
7.1.3 Silyl radicals as halogen abstractors

The Giese reaction is an outstanding reaction for forming C-C bonds, employing cheap and available starting materials, such as alkyl halide and electron-poor olefins, with a good group tolerance.¹⁴ However, as stated before, the main limitation of the first reported procedure is the use of organotin hydrides, which are unsustainable. In fact, both starting organotin hydride and the corresponding organotin product are highly toxic. Moreover, this procedure required relatively elevated temperatures, which are not ideal. Nowadays, discoveries in the photochemistry field have opened new horizons in generating radicals and new reaction protocols.⁴ Several improvements have been made in the past years, including the development of new halogen abstractors. Germanium, boron, phosphorus, and silicon radicals^{4,7}, but also α -aminoalkyl radicals¹⁵ and cyclohexadiene derivatives¹⁶ arose as more sustainable halogen abstractor than tin. Among these XAT reagents, the silicon radicals are considered a valid alternative to organotin hydride. The group of Chatgililoglu demonstrated that tris(trimethylsilyl)silane ((TMS)₃SiH) undergoes hydrogen abstraction in the presence of an alkyl radical (HAT), while the corresponding silyl radical can perform XAT, forming a more stable bond between the silicon atom and the halogen atom (*Scheme 19*).¹⁷



Scheme 19 Reaction equation of HAT process followed by an XAT event.

The generation of the silyl radical from (TMS)₃SiH can be made using an initiator, such as AIBN, or by a photolysis process. The use of AIBN as an initiator requires elevated temperature, which can result not only in the activation of (TMS)₃SiH but also in side reactions and possible decomposition of starting materials/products. In contrast, photolysis can be performed at mild conditions and be selective for the absorbing species. In fact, the absorption of a photon can cause a homolytic cleavage of a Si-H bond, resulting in the generation of silyl radicals (*Scheme 20*).⁴



Scheme 20 Photolysis of (TMS)₃SiH and consequent generation of silyl radical.

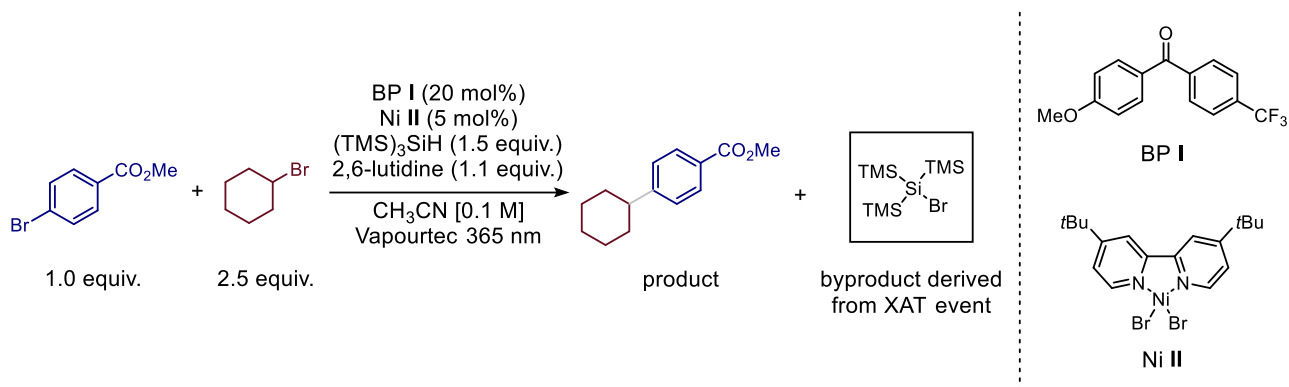
The energy required for cleaving a specific bond by photolytic means is equal to its BDE, which, in the case of (TMS)₃SiH, is 79 kcal/mol.¹⁷ The correct wavelength (λ) of electromagnetic radiation required for the bond to photocleave can be calculated according to Planck's equation described below. In this equation, E is the energy (J), h is Planck's constant, ν is the frequency (Hz) and c is the constant of the speed of light (m/s).

$$E = h \cdot \nu = h \cdot \frac{c}{\lambda}$$

$$E = \frac{7.90 \cdot 10^4 \text{ cal}}{\text{mol}} = \frac{3.31 \cdot 10^5 \text{ J}}{\text{mol}} = 5.50 \cdot 10^{-19} \text{ J} \qquad \lambda = \frac{h \cdot c}{5.50 \cdot 10^{-19}} = 361 \text{ nm}$$

Several works reported the use of (TMS)₃SiH as a suitable XAT reagent with the advantage of being commercially available. The (TMS)₃SiH has been used in combination with metallaphotoredox catalysis to couple alkyl bromides efficiently with aryl or heteroaryl bromides^{18,19} and in the functionalization of poor-olefins^{19,20}.

During my Ph.D., I spent a period abroad in the Noël research group at the University of Amsterdam. While working on a protocol that exploited photocatalytic HAT and silicon-centered radical-promoted XAT to afford a cross-electrophile coupling¹⁹ (**Scheme 21**), my colleagues detected the formation of silyl bromide in the absence of the photocatalyst. However, the latter was necessary for obtaining the desired product in good yield.



Scheme 21 Reaction conditions of cross-electrophile coupling, involving (TMS)₃SiH as XAT reagent.¹⁹

Therefore, we reasoned that a direct photolysis of one of the reaction components can lead to a silicon-centered radical, which cleaves the alkyl bromide bond.¹⁷ Prompted by this observation, we wonder to use this photolysis event as the initiation step for a self-sustaining radical-chain process, such as Giese-type additions. Thus, a remarkable method for the selective hydro-functionalization of poor-olefins with alkyl bromide, using only non-toxic and commercially available (TMS)₃SiH and UV-light in flow conditions, has been reported. Flow conditions allow the activation of the (TMS)₃SiH, faster reaction time, and the possibility of a telescope approach to install allyl fragments.²¹ In the same period of our work on this methodology, the group of Gaunt developed a similar strategy for forming the C(sp³)-C(sp³) bonds, using alkyl iodine instead of alkyl bromide.²²

7.2 Results and discussion

To evaluate our hypothesis, we first turned our attention on the reaction between 2-benzylidenemalonitrile **1** and cyclohexyl bromide **2**, as model substrates, in the presence of $(\text{TMS})_3\text{SiH}$ under UV-light (365 nm) in a Vapourtec UV-150 flow reactor (PFA, ID: 1.3, V: 10 mL).

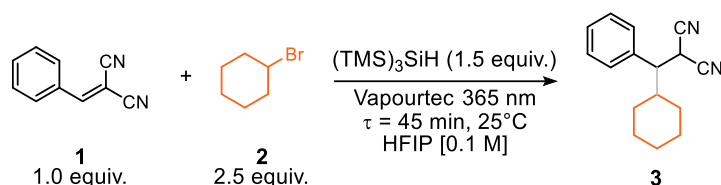


Table 13 Reaction condition: 2-benzylidenemalonitrile **1** (0.30 mmol), cyclohexyl bromide **2** (0.75 mmol), $(\text{TMS})_3\text{SiH}$ (0.45 mmol), HFIP (3 mL), Vapourtec Reactor 16W ($\lambda = 365$ nm and reactor volume = 10 ml), 25°C, 45 min. ^aYields of **3** are calculated by ^1H NMR using 1,1,2,2-tetrachloroethylene as external standard. ^b Yield of the isolated compound.

Entry	Deviation from the reaction condition	^a Conversion % 1	^a Yield % 3
1	CH ₃ CN	15%	7%
2	-	32%	21%
3	40°C	78%	70%
4	120 min	100%	62%
5	120 min, 40°C	100%	73%
6	Dark, 50°C	16%	trace
7	no $(\text{TMS})_3\text{SiH}$	0%	0%
8	405 nm, 40°C	32%	27%
9	60 min, 40°C, 1.1 equiv. $(\text{TMS})_3\text{SiH}$	86%	73%
10	60 min, 40°C, 1.1 equiv. $(\text{TMS})_3\text{SiH}$, 1.5 alkyl bromide	47%	47%
11	120 min, 40°C, 1.1 equiv. $(\text{TMS})_3\text{SiH}$	100%	^b 72%

When the reaction was performed in acetonitrile, we observed the presence of the desired compound **3**, even though in low yield (entry 1, **Table 13**). Switching the acetonitrile with hexafluoroisopropanol (HFIP) resulted in increased yield of **3** (entry 2, **Table 13**). Further optimization experiments have been conducted and a comprehensive survey of reaction conditions is reported in the optimization chapter in the *Experimental section* (6.4.3 Optimization Table). In particular, extending the residence time to 120 minutes and increasing the temperature to 40°C provided a satisfactory 73% yield and full conversion of **1** (entry 3-5, **Table 13**). Separated control

experiments demonstrated that light and $(\text{TMS})_3\text{SiH}$ are fundamental for the observed reactivity (entry 6-7, **Table 13**), while changing the wavelength slow down the reaction (entry 8, **Table 13**). Interestingly, the equivalent of $(\text{TMS})_3\text{SiH}$ can be reduced without affecting the final yield, but the reduction of the amount of alkyl bromide resulted in lower yields (entry 9-10, **Table 13**). Finally, the best results were observed combining 2.5 equiv. of alkylbromide **2** and 1.1 equiv. of $(\text{TMS})_3\text{SiH}$, and performing the reaction at 40°C for 120 minutes (entry 11, **Table 13**).

With the optimized conditions in our hand, we explored the scope of the reaction by using primary, secondary and tertiary alkyl bromide (**Figure 39**). First, we combined 2-benzylidenemalonitrile **1** with a diverse set of secondary heterocyclic alkyl bromides, finding that the system performs well regardless of the ring size, such as for *N*-Cbz-azetidine and *N*-Cbz-piperidine bromide derivatives (**4** and **5**, 51% and 61% respectively) and the heteroatom, for example 3-bromooxetane (**6**, 48% using lutidine as base in acetonitrile). Furthermore, this method allows the introduction of linear chain: 2-bromooctane was readily activated, providing the desired compound **7** in 68% (d.r. 1:1). Unfortunately, when performing the reaction in HFIP, primary alkyl bromides afforded the desired compounds in low yield. However, simply replacing the solvent with acetonitrile overcame this limitation. In fact, the reaction in acetonitrile of aliphatic bromides provided compounds **8** and **9** in moderate yield (62% and 50%, respectively), regardless of the chain length. Furthermore, compound **10** was obtained in 63% yield, highlighting that the process is not sensitive to benzylic positions. As in the case of 2-bromooxetane, the addition of lutidine was necessary when an oxygen-containing primary alkyl bromide is used as coupling partner (**11**, 46% yield). Interestingly, the bromopropyl boronic pinacol ester afforded compound **12**, in good yield, giving opportunities for further functionalization. Similarly to primary alkyl bromide, the tertiary alkyl bromide worked better when acetonitrile is used as reaction solvent instead of HFIP. Under this conditions, acyclic tertiary bromides, such as *tert*-butyl, 2-methylbutyl and 1-benzyl-3-methylbutyl bromide derivatives, afforded the corresponding products in good yield (**13-15**, 40-68%). Additionally, also 1-bromo-1-methylcyclohexane and 1-bromoadamantane provided the desired products **16** and **17** (45% and 54% yield, respectively). Lastly, we performed the scale up of the reaction between 2-bromo-2 methylpropane and **1**, using the same reactor, switching only the coil to a bigger one (from 10 ml to 20 ml). With this simple modification and extending the collection time under flow conditions, we were able to run a 10-fold scale up (5 mmol scale) and to obtain the desired compound **13** in slightly higher yield compared to the model reaction (0.5 mmol scale), further highlighting the central role of flow technology in scale up of photochemical processes⁹.

Next, we moved our attention to electron-poor olefins. Gratifyingly, the method is amenable to olefins bearing esters (**18**, 54% yield), sulphones (**19**, 55% yield), amide (**20**, 53% yield) and

phosphorous based reagents (**21** and **22**, 68% and 60% yield respectively). Notably, triphenylvinylphosphonium bromide, which was used in a conjunctive photocatalytic olefination methodology²³, was successfully reacted with cyclohexyl bromide **2**, to afford compound **23** in good yield (84%).

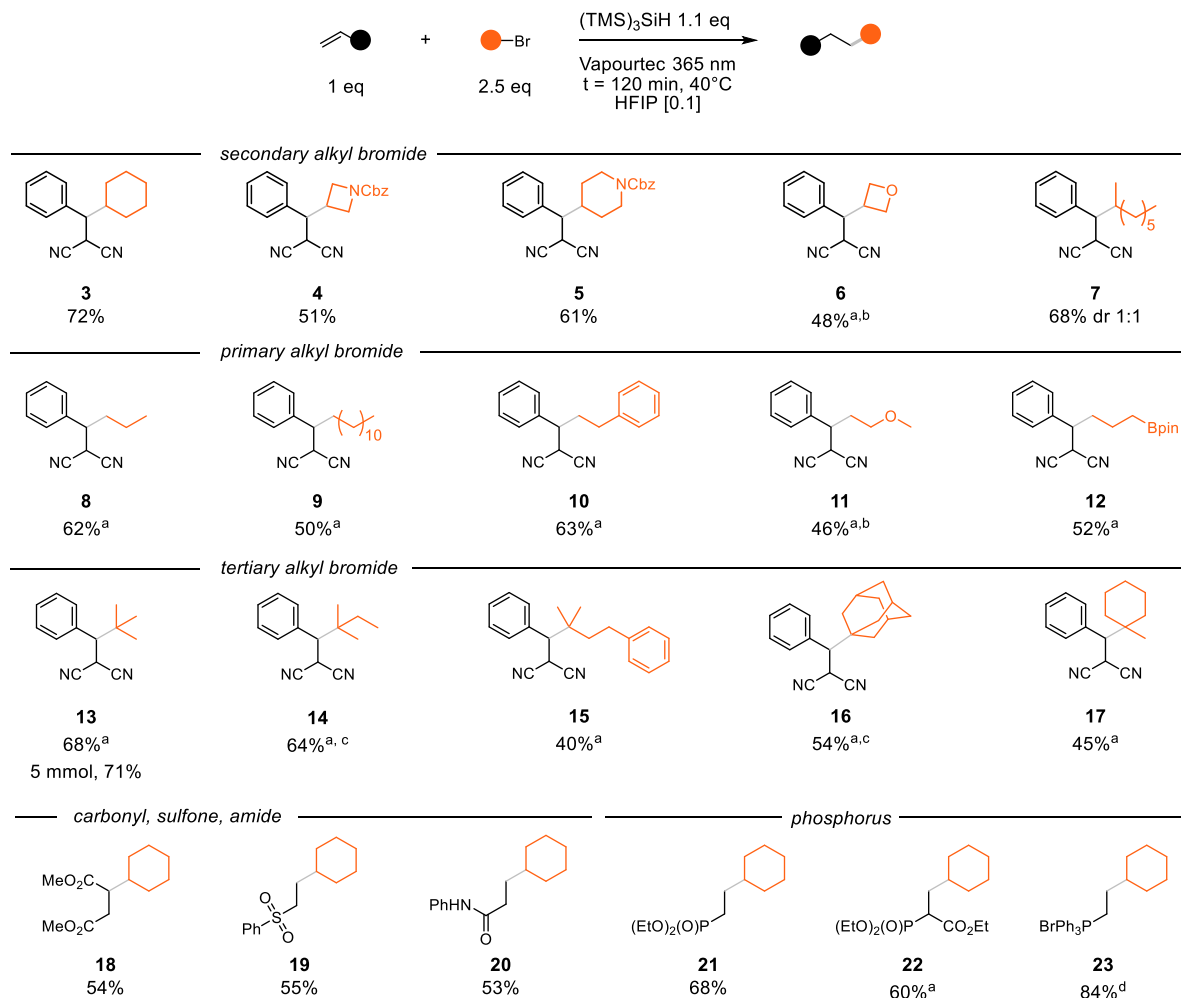


Figure 39 Alkyl bromide and olefin scope. Reaction condition: olefin (0.50 mmol), alkyl bromide (1.25 mmol), tris(trimethylsilyl)silane (0.55 mmol), solvent (5 mL), Vapourtec Reactor 16W ($\lambda = 365$ nm, reactor volume = 10 mL), 40 °C, 120 min. Yield referred to isolated product. ^aCH₃CN in place of HFIP; ^b2,6-lutidine (2 equiv.); ^c180 min; ^dIn batch, purified by crystallization.

A previous work of the Noël research group²⁴ make us envision a telescope protocol, which involves compound **22**, that after the photochemical Giese-type addition, can undergo a classical Horner–Wadsworth–Emmons (HWE) olefination enabling the regioselective allylation of C(sp³)–Br bonds. Therefore, we developed a telescoped flow/fed-batch approach, where after exerting the photochemical reactor, the reaction mixture is dropped in a flask charged with a solution of the suitable aldehyde and lithium *tert*-butoxide in THF (**Figure 40**).

Using this approach, we combined three different aldehydes with **22**, obtaining trisubstituted olefins **24–26** with moderate to good overall yields (38–57 %). Notably, the reaction exhibited perfect selectivity for *E* configuration and the purification of the intermediate was not required.

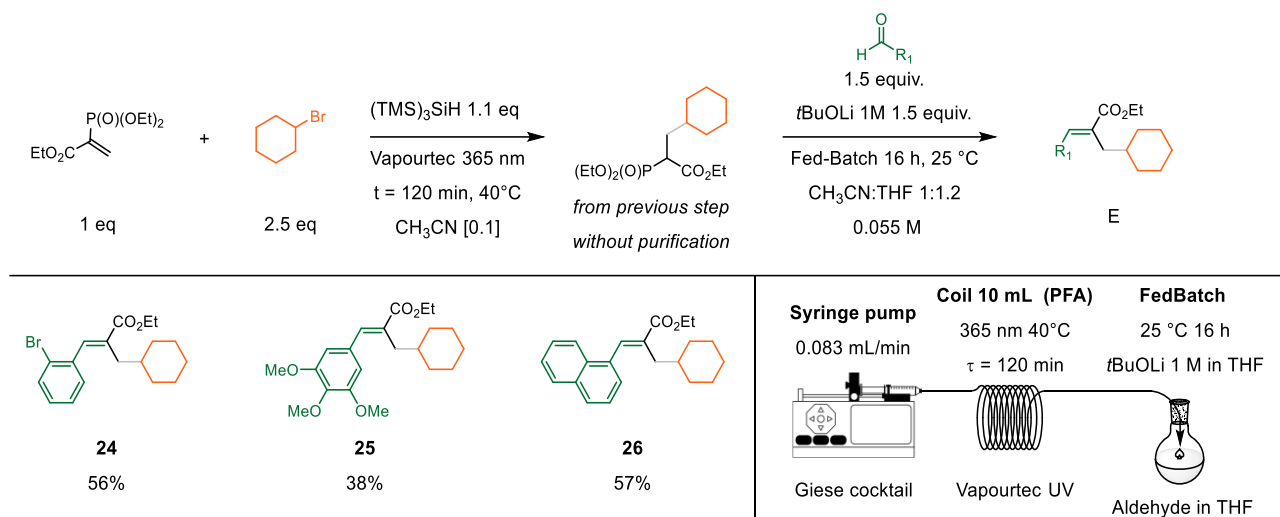


Figure 40 Scope of the Giese addition-HWE olefination. Reaction conditions for the first step as for compound **22**. Reaction conditions for the second step: aldehyde (1.5 mmol), tBuOLi (1.5 mmol) in THF, 25°C, 16 h. Yield referred to isolated product over two steps.

Some experiments have been conducted to elucidate the reaction mechanism (**Figure 41**). First, the reaction does not occur without the presence of $(\text{TMS})_3\text{SiH}$, confirming the central role of the silicon reagent. Furthermore, without the silane, no reaction neither degradation of starting materials are observed.

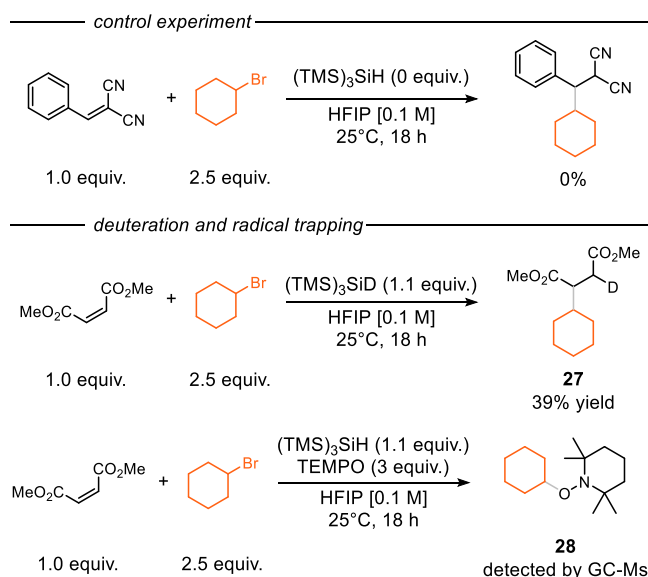


Figure 41 Control experiment without $(\text{TMS})_3\text{SiH}$, labelling experiment with deuterium and radical trapping.

When deuterated silicon-based reagent was used in the model reaction, the product **27** incorporated the deuterium in the α -position of the cyano group, suggesting that after the radical addition over **1**, the ensuing electrophilic radical abstracts the deuterium/hydrogen from the silane, starting the radical chain propagation. Lastly, the model reaction was performed in the presence of (2,2,6,6-tetramethylpiperidin-1-yl)oxyl (TEMPO). In this case, no product was detected, but the formation of the radical adduct between cyclohexyl radical and TEMPO (compound **28**) was observed

by crude analysis by GC-MS. Considering all the results obtained, a photochemical and radical pathway occur.¹¹

7.3 Conclusion

In conclusion, we have disclosed a simple protocol for the hydroalkylation of electron-poor olefins using alkyl bromide, in the presence of commercially available $(\text{TMS})_3\text{SiH}$ and UV-light irradiation in flow conditions. Remarkably, this methodology does not require the use of a photocatalyst. Furthermore, the scale up of the reaction was easily performed, without the need for further optimization of the reaction conditions. To extend this protocol, a telescoped approach has been developed for achieving a modular and regioselective allylation of $\text{C}(\text{sp}^3)\text{-Br}$ bonds.

7.4 Experimental section

7.4.1 Materials and methods

All reagents and solvents were purchased from commercial suppliers and used without further purification. The 1,1,1,3,3,3-hexamethyl-2-(trimethylsilyl)trisilane-2-*d* was prepared according to reported procedures.²⁵ The 1-bromo-1-methylcyclohexane, (3-bromo-3-methylbutyl)benzene and 2-bromo-2-methylbutane was synthesized according to literature procedures.²⁶

¹H (300 and 400 MHz), ¹³C (75 and 101 MHz) and ¹⁹F (282 and 376 MHz) spectra were recorded at ambient temperature using Bruker AV 300-I, AV 400. ¹H NMR spectra are reported in parts per million (ppm) downfield relative to CDCl₃ (7.26 ppm) and all ¹³C NMR spectra are reported in ppm relative to CDCl₃ (77.16 ppm) unless stated otherwise. The multiplicities of signals are designated by the following abbreviations: s (singlet), d (doublet), t (triplet), q (quartet), m (multiplet), dd (doublet of doublets), dt (doublet of triplets), td (triplet of doublets), ddd (doublet of doublet of doublets). Coupling constants (*J*) are reported in hertz (Hz). NMR data was processed using the MestReNova 14 software package. High resolution mass spectra (HRMS) were collected on an AccuTOF LC, JMS-T100LP Mass spectrometer (JEOL, Japan) or on an AccuTOF GC v 4g, JMS-T100GCV Mass spectrometer (JEOL, Japan). Disposable syringes were purchased from Laboratory Glass Specialist. Syringe pumps were purchased from Chemix Inc. model Fusion 200 Touch. Product isolation was performed manually, using silica (P60, SILICYCLE). TLC analysis was performed using Silica on aluminum foils TLC plates (F254, SILICYCLE) with visualization under ultraviolet light (254 nm and 365 nm) or appropriate TLC staining (Potassium Permanganate). Organic solutions were concentrated under reduced pressure on a Büchi rotary evaporator (in vacuo at 40 °C, ~5 mbar).

UV-Vis spectra were recorded with a double beam spectrophotometer Shimadzu UV2700 equipped with a deuterium lamp (190-350 nm), a halogen lamp (330-900 nm) and a photomultiplier (Hamamatsu R928). Measurements were performed in a quartz cuvette (optical path: 1 cm). All spectra were recorded in CH₃CN (solvent cutoff: 190 nm) in quartz cuvettes (optical path: 1 cm) with a bandwidth of 5 nm and a data pitch of 1 nm.

Luminescence spectra were recorded with a Horiba Fluorolog-3 equipped with a 450W Xenon lamp and a photomultiplier (Hamamatsu R636). Measurements were performed in a quartz cuvette (optical path: 1 cm) sealed with a rubber septum. The solution was bubbled with N₂ for 10 minutes before irradiation at 362 nm (*A* = 0.1). The slits of the excitation monochromator were kept at 10 nm, while those of the emission monochromator at 5 nm. Integration time was 0.1 s, each spectrum is an average of 2 acquisitions with a data pitch of 1 nm. A long-pass filter was used to minimize the

intensity of the Raman band. The nature of the latter was verified by observing its shift by changing the excitation wavelength (data not shown).

Nanosecond transient absorptions were recorded with an in-house assembled setup. An excitation wavelength of 319 nm was used. The excitation wavelength of 319 nm was generated using a tunable Nd:YAG-laser system (NT342B, Ekspla) comprising the pump laser (NL300) with harmonics generators (SHG, THG) producing 355 nm to pump an optical parametric oscillator (OPO) with SHG connected in a single device. The laser system was operated at a repetition rate of 5 Hz with a pulse length of 5 ns. The probe light running at 10 Hz was generated by a high-stability short arc xenon flash lamp (FX-1160, Excelitas Technologies) using a modified PS302 controller (EG&G). Using a 50/50 beam splitter, the probe light was split equally into a signal beam and a reference beam and focused on the entrance slit of a spectrograph (SpectraPro-150, Princeton Instruments) with a grating of 150 ln/mm blaze at 500nm. The probe beam ($A = 1 \text{ mm}^2$) was passed through the sample cell and orthogonally overlapped with the excitation beam on a $1 \text{ mm} \times 1 \text{ cm}$ area. The excitation energy was recorded by measuring the excitation power at the back of an empty sample holder. In order to correct for fluctuations in the flash lamp spectral intensity, the reference was used to normalize the signal. Both beams were recorded simultaneously using a gated intensified CCD camera (PI-MAX3, Princeton Instruments) which has an adjustable gate of minimal 2.9 ns (20 ns were used). Two delay generators (DG535 and DG645, Stanford Research Systems, Inc.) were used to time the excitation pulse, and to change the delay of the flash lamp and gate of the camera during the experiment. The setup was controlled by an in-house written Labview program.

7.4.2 Reactors

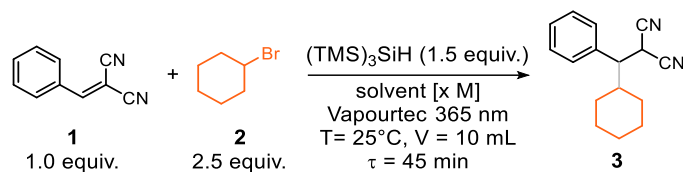
For the reactions performed in batch, we have used a homemade, 3D-printed reactor (UFO reactor). The reactor was designed to fit reaction vials and to be equipped with a Kessil lamp. The reactor was designed in Adobe Inventor 2021 with 4 different parts. The reactor is designed to host up to 8 reactions vials and holds the Kessil lamp in the center. The box is designed with holes to allow the air flow to escape the reactor and keep the temperature stable.²¹

For reactions performed in flow, a Vapourtec device with a UV-150 photochemical reactor was used, equipped with 16 W 365 nm LED and a one layer coil ($V = 10 \text{ ml}$, internal diameter 1.3 mm, external diameter 1.6 mm). The temperature of the photochemical chamber was kept constant at 40 °C. For the scale-up the set up was the same except for the coil, that has been replaced by a two layers coil ($V = 20 \text{ mL}$, internal diameter 2.0 mm, external diameter 3.0 mm).

More information about the reactors used in this project are available in the supporting information of the published paper (*Tetrahedron Letters* **2023**, 117, 154380)

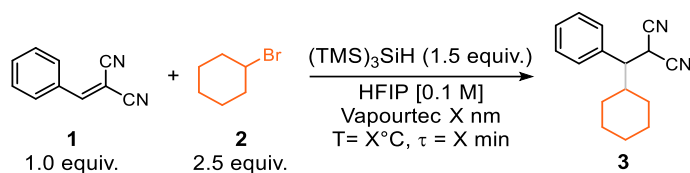
7.4.3 Optimization Table

Table Optimization of the solvent and reaction concentration.



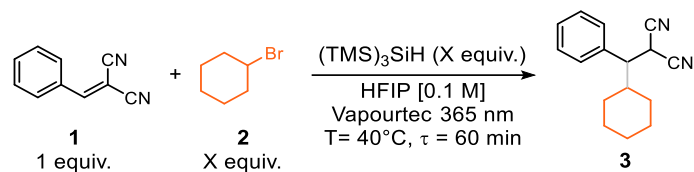
Entry	Solvent	Concentration	Yield
1	CH ₃ CN	0.1 M	7%
2	CH ₃ CN	0.5 M	4%
3	TFT	0.1 M	7%
4	TFT	0.5 M	7%
5	HFIP	0.1 M	21%
6	Acetone	0.5 M	7%
7	DCM	0.5 M	7%
8	iPrOH	0.1 M	11%
9	THF	0.1 M	8%

Table Light source, retention time and temperature optimization



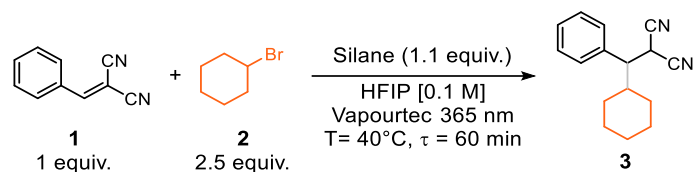
Entry	Light Wavelength	Temperature	τ	Conversion	Yield
1	365 nm	25°C	45 min	35%	21%
2	365 nm	25°C	120 min	100%	62%
3	365 nm	40°C	45 min	78%	70%
4	365 nm	40°C	60 min	91%	73%
5	365 nm	40°C	120 min	100%	73%
6	405 nm	25°C	45 min	13%	7%
7	405 nm	40°C	45 min	32%	27%
8	Dark	50°C	45 min	16%	6%

Table Optimization of the stoichiometry



Entry	Equiv. of 2	Equiv. of $(\text{TMS})_3\text{SiH}$	Conversion	Yield
1	2.5	1.5	91%	73%
2	2.5	1.1	86%	73%
3	2.5	1.0	84%	69%
4	1.5	1.1	47%	47%
5	2.5	0	0%	0%

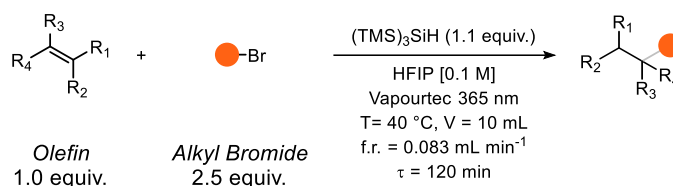
Table Silane derivatives screening



Entry	Silane	Conversion	Yield
1	dimethyl(phenyl)silane	-	-
2	triphenylsilane	7%	-
3	triisopropylsilane	-	-
4	triethoxysilane	-	-

7.4.4 Experimental procedures

General procedure A



To a flame-dried nitrogen-purged screw-capped vial, fitted with a rubber septum, charged with the electron poor olefin (1 equiv., 0.500 mmol) in HFIP (5 mL, 0.1 M), the alkyl bromide derivative (2.5 equiv., 1.250 mmol) and $(\text{TMS})_3\text{SiH}$ (1.1 equiv., 170 μL , 0.550 mmol) were added. After, the solution was sparged with nitrogen for 30 seconds and the reaction vessel was sealed with parafilm. This solution was taken with a 6 mL syringe (12.4 mm inner diameter), positioned on a syringe pump and connected to a Vapourtec UV-150 reactor, equipped with a 10 mL PFA coil prefilled with CH_3CN (internal diameter 1.3 mm, external diameter 1.6 mm), and with a check valve and a back-pressure regulator (2.8 psi). The solution was pumped, unless differently specified, with a total flow rate of 0.083 mL min^{-1} and collected at the end of the reactor. The solvent of the resulting reaction mixture was removed under reduced pressure. The residue was purified by flash column chromatography on silica gel affording the corresponding products in the stated yield.

General procedure B

To a flame-dried nitrogen-purged screw-capped vial, fitted with a rubber septum, charged with the electron poor olefin (1 equiv., 0.500 mmol) in dry CH_3CN (5 mL, 0.1 M), the alkyl bromide derivative (2.5 equiv., 1.250 mmol) and $(\text{TMS})_3\text{SiH}$ (1.1 equiv., 170 μL , 0.550 mmol) were added. After, the solution was sparged with nitrogen for 30 seconds and the reaction vessel was sealed with parafilm. This solution was taken with a 6 mL syringe (12.4 mm inner diameter), positioned on a syringe pump and connected to a Vapourtec UV-150 reactor, equipped with a 10 mL PFA coil prefilled with CH_3CN (internal diameter 1.3 mm, external diameter 1.6 mm), and with a check valve and a back-pressure regulator (2.8 psi). The solution was pumped, unless differently specified, with a total flow rate of 0.083 mL min^{-1} and collected at the end of the reactor. The solvent of the resulting reaction mixture was removed under reduced pressure. The residue was purified by flash column chromatography on silica gel affording the corresponding products in the stated yield.

General procedure C

To a flame-dried nitrogen-purged screw-capped vial, fitted with a rubber septum, charged with the electron poor olefin (1 equiv., 0.500 mmol) in dry CH_3CN (5 mL, 0.1 M), the alkyl bromide

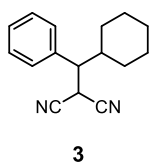
derivative (2.5 equiv., 1.250 mmol), (TMS)₃SiH (1.1 equiv., 170 μ L, 0.550 mmol) and 2,6-lutidine (2.0 equiv., 116 μ L, 1.000 mmol) were added. After, the solution was sparged with nitrogen for 30 seconds and the reaction vessel was sealed with parafilm. This solution was taken with a 6 mL syringe (12.4 mm inner diameter), positioned on a syringe pump and connected to a Vapourtec UV-150 reactor, equipped with a 10 mL PFA coil prefilled with CH₃CN (internal diameter 1.3 mm, external diameter 1.6 mm), and with a check valve and a back-pressure regulator (2.8 psi). The solution was pumped, unless differently specified, with a total flow rate of 0.083 mL min⁻¹ and collected at the end of the reactor. The solvent of the resulting reaction mixture was removed under reduced pressure. The residue was purified by flash column chromatography on silica gel affording the corresponding products in the stated yield.

General procedure for the scale-up

To an oven dried flask, fitted with a rubber septum, charged with benzylidenemalononitrile (1.0 equiv., 770.8 mg, 5.000 mmol) in CH₃CN (50 mL, 0.1 M), tert-butyl bromide (2.5 equiv., 1.4 ml, 12.500 mmol) and (TMS)₃SiH (1.1 equiv., 1.70 ml, 5.500 mmol) were added. After, the solution was sparged with nitrogen for less than 1 minute and the vessel was sealed with parafilm. This solution was taken with a 50 mL syringe (28.9 mm inner diameter), positioned on a syringe pump and connected to Vapourtec UV-150 equipped with a 20 mL PFA coil prefilled with CH₃CN (internal diameter 2.0 mm, external diameter 3.0 mm), and with a check valve and a back-pressure regulator (2.8 psi). The solution was pumped with a total flow rate of 0.166 mL min⁻¹ and collected at the end of the reactor. The solvent of the resulting reaction mixture was removed under reduced pressure. The residue was purified by flash column chromatography on silica gel (100% pentane to pentane:Et₂O 8:2) to give product **13** as a colourless oil (755 mg, 71% yield).

7.4.5 Experimental data

2-(cyclohexyl(phenyl)methyl)malononitrile (**3**)



Compound **3** was prepared following the general procedure **A** starting from cyclohexyl bromide **2** (2.5 equiv., 154 μ L, 1.250 mmol) and benzylidenemalononitrile **1** (1 equiv., 77.1 mg, 0.500 mmol).

Flash chromatography: silica gel, 100% pentane to pentane:Et₂O 8:2 as eluent.

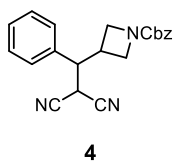
Colorless oil, 86 mg, 72% yield.

¹H NMR (400 MHz, Chloroform-*d*) δ 7.45 – 7.34 (m, 3H), 7.34 – 7.28 (m, 2H), 4.19 (d, *J* = 5.5 Hz, 1H), 2.89 (dd, *J* = 9.8, 5.5 Hz, 1H), 2.02 (dtd, *J* = 14.5, 11.2, 3.4 Hz, 1H), 1.93 (dt, *J* = 12.3, 3.3 Hz, 1H), 1.87-1.80 (m, 1H), 1.73 – 1.61 (m, 2H), 1.53 – 1.42 (m, 1H), 1.37 (tt, *J* = 12.8, 3.6 Hz, 1H), 1.29 – 0.99 (m, 3H), 0.90 – 0.75 (m, 1H)

^{13}C NMR (101 MHz, Chloroform-*d*) δ 136.8, 129.2, 128.8, 128.4, 112.4, 112.1, 52.4, 39.3, 31.3, 30.7, 27.2, 25.9, 25.9, 25.8

Physicochemical data are in agreement with those previously reported.²⁷

Benzyl 3-(2,2-dicyano-1-phenylethyl)azetidone-1-carboxylate (4)



Compound **4** was prepared following the general procedure **A** starting from benzyl 3-bromoazetidone-1-carboxylate (2.5 equiv., 203 mg, 0.750 mmol) and benzylidene malononitrile **1** (1 equiv., 77.1 mg, 0.500 mmol).

Flash chromatography: silica gel, pentane:acetone 95:5 to pentane:acetone 8:2 as eluent.

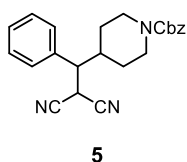
Colorless oil, 54 mg, 52% yield.

^1H NMR (400 MHz, Chloroform-*d*) δ 7.46 – 7.27 (m, 10H), 5.07 (s, 2H), 4.36 (t, J = 8.5 Hz, 1H), 4.02 (dd, J = 9.1, 5.6 Hz, 1H), 3.96 (t, J = 8.8 Hz, 1H), 3.90 (d, J = 5.7 Hz, 1H), 3.54 – 3.45 (m, 2H), 3.39 – 3.27 (m, 1H)

^{13}C NMR (101 MHz, Chloroform-*d*) δ 156.2, 136.4, 134.4, 129.7, 129.6, 128.6, 128.3, 128.1, 127.9, 111.4, 111.3, 66.9, 53.3, 50.0, 31.4, 28.2

HRMS (GC-EI) m/z calcd for $\text{C}_{21}\text{H}_{19}\text{N}_3\text{O}_2$: 345.1477; found: 345.1488.

Benzyl 4-(2,2-dicyano-1-phenylethyl)piperidine-1-carboxylate (5)



Compound **5** was prepared following the general procedure **A** starting from benzyl 4-bromo-1-piperidinecarboxylate (2.5 equiv., 271 μL , 1.250 mmol) and benzylidene malononitrile **1** (1 equiv., 77.1 mg, 0.500 mmol).

Flash chromatography: silica gel, pentane:Et₂O 9:1 to pentane:Et₂O 7:3 as eluent.

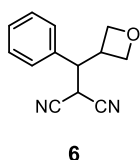
Colorless oil, 114 mg, 61% yield.

^1H NMR (400 MHz, Chloroform-*d*) δ 7.47 – 7.27 (m, 10H), 5.11 (s, 2H), 4.32 (brs, 1H), 4.21-4.05 (m, 2H), 2.90 (dd, J = 9.9, 5.3 Hz, 2H), 2.71 (brs, 1H), 2.27 – 2.12 (m, 1H), 1.88 (d, J = 12.6 Hz, 1H), 1.46 – 1.37 (m, 1H), 1.37-1.19 (m, 1H), 1.12 – 1.01 (m, 1H)

^{13}C NMR (101 MHz, Chloroform-*d*) δ 155.1, 136.7, 135.9, 129.5, 129.2, 128.6, 128.2, 128.2, 127.9, 111.9, 111.8, 67.3, 51.7, 43.8, 43.6, 38.0, 27.1

HRMS (GC-EI) m/z calcd for $\text{C}_{23}\text{H}_{23}\text{N}_3\text{O}_2$: 373.1790; found: 373.1795.

2-(oxetan-3-yl(phenyl)methyl)malononitrile (6)



Compound **6** was prepared following the general procedure **C** starting from 3-bromooxetane (2.5 equiv., 150 μL , 1.250 mmol) and benzylidene malononitrile **1** (1 equiv., 77.1 mg, 0.500 mmol).

Flash chromatography: silica gel, pentane:acetone 95:5 to pentane:acetone 8:2 as eluent.

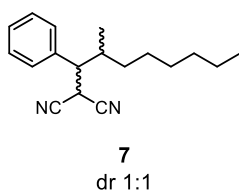
Colorless oil, 51 mg, 48% yield.

^1H NMR (400 MHz, Chloroform-*d*) δ 7.49 – 7.35 (m, 3H), 7.30 – 7.25 (m, 2H), 5.01 (t, $J = 6.7$ Hz, 1H), 4.74 (t, $J = 6.1$ Hz, 1H), 4.62 (t, $J = 7.0$ Hz, 1H), 4.21 (t, $J = 6.3$ Hz, 1H), 3.88 – 3.72 (m, 3H)

^{13}C NMR (101 MHz, Chloroform-*d*) δ 134.6, 129.8, 129.6, 127.9, 111.3, 75.8, 74.9, 50.0, 37.2, 28.4

HRMS (GC-FI) m/z calcd for $\text{C}_{13}\text{H}_{12}\text{N}_2\text{O}$: 212.0950; found: 212.0960.

2-(2-methyl-1-phenyloctyl)malononitrile (7a and 7b)



Compound **7** was prepared following the general procedure **A** starting from 2-bromooctane (2.5 equiv., 219 μL , 1.250 mmol) and benzylidenemalononitrile **1** (1 equiv., 77.1 mg, 0.500 mmol).

Flash chromatography: silica gel, pentane:Et₂O 95:5 to pentane: Et₂O 92:8 as eluent to afford a mixture of diastereomers **7a** and **7b** in a 1:1 ratio.

Colorless oil, 91 mg, 68% yield.

7a

^1H NMR (400 MHz, Chloroform-*d*) δ 7.45 – 7.34 (m, 3H), 7.34 – 7.25 (m, 2H), 4.18 (d, $J = 6.7$ Hz, 1H), 3.01 (dd, $J = 8.6, 6.8$ Hz, 1H), 2.29 – 2.18 (m, 1H), 1.54 – 1.45 (m, 1H), 1.45 – 1.27 (m, 8H), 1.25 – 1.11 (m, 1H), 0.94 – 0.86 (m, 3H), 0.81 (d, $J = 6.7$ Hz, 3H)

^{13}C NMR (101 MHz, Chloroform-*d*) δ 136.4, 129.2, 128.9, 128.6, 112.4, 112.1, 51.7, 34.9, 34.5, 31.9, 29.5, 27.6, 26.5, 22.7, 16.5, 14.2

HRMS (FD) m/z calcd for $\text{C}_{18}\text{H}_{24}\text{N}_2$: 268.1939; found: 268.1932.

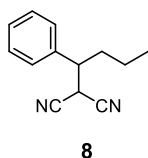
7b

^1H NMR (400 MHz, Chloroform-*d*) δ 7.46-7.35 (m, 3H), 7.34 - 7.28 (m, 2H), 4.17 (d, $J = 5.4$ Hz, 1H), 2.90 (dd, $J = 10.1, 5.4$ Hz, 1H), 2.30 - 2.15 (m, 1H), 1.28 – 1.14 (m, 8H), 1.12 (m, 4H), 0.97 (m, 1H), 0.83 (t, $J = 7.1$ Hz, 3H)

^{13}C NMR (101 MHz, Chloroform-*d*) δ 136.9, 129.3, 128.9, 128.5, 112.3, 111.9, 52.5, 34.8, 33.6, 31.8, 29.3, 27.9, 26.4, 22.6, 17.6, 14.2

HRMS (GC-FI) m/z calcd for $\text{C}_{18}\text{H}_{24}\text{N}_2$: 268.1939; found: 268.1947.

2-(1-phenylbutyl)malononitrile (8)



Compound **8** was prepared following the general procedure **B** starting from 1-bromopropane (2.5 equiv., 154 mg, 1.250 mmol) and benzylidenemalononitrile **1** (1 equiv., 77.1 mg, 0.500 mmol).

Flash chromatography: silica gel, 100% pentane to pentane: Et₂O 9:1 as eluent.

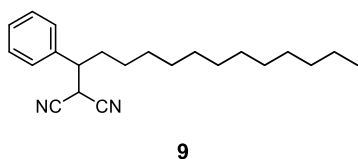
Pale yellow oil, 61.5 mg, 62% yield.

^1H NMR (400 MHz, Chloroform-*d*) δ 7.46 – 7.27 (m, 5H), 3.87 (d, J = 6.3 Hz, 1H), 3.29 – 3.14 (m, 1H), 2.06 – 1.92 (m, 2H), 1.36 – 1.18 (m, 2H), 0.93 (t, J = 7.4 Hz, 3H)

^{13}C NMR (101 MHz, Chloroform-*d*) δ 136.9, 129.4, 129.0, 127.9, 112.1, 112.0, 46.5, 34.3, 30.4, 20.4, 13.7

Physicochemical data are in agreement with those previously reported.²⁸

2-(1-phenyltridecyl)malononitrile (9)



Compound **9** was prepared following the general procedure **B** starting from 1-bromodocecane (2.5 equiv., 312 mg, 1.250 mmol) and benzylidenemalononitrile **1** (1 equiv., 77.1 mg, 0.500 mmol).

Flash chromatography: silica gel, 100% toluene to toluene:pentane 9:1 as eluent.

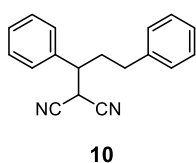
Pale yellow oil, 83 mg, 50% yield.

^1H NMR (400 MHz, Chloroform-*d*) δ 7.44 – 7.33 (m, 3H), 7.34 – 7.28 (m, 2H), 3.87 (d, J = 6.2 Hz, 1H), 3.24 – 3.13 (m, 1H), 2.06 – 1.92 (m, 2H), 1.35 – 1.18 (m, 20H), 0.88 (t, J = 6.7 Hz, 3H)

^{13}C NMR (101 MHz, Chloroform-*d*) δ 136.9, 129.4, 129.0, 127.9, 112.1, 46.7, 32.2, 32.0, 30.4, 29.8, 29.7, 29.7, 29.6, 29.5, 29.4, 29.3, 27.1, 22.8, 14.3

HRMS (FI) m/z calcd for: $\text{C}_{22}\text{H}_{32}\text{N}_2$ 324.2565, found 324.2565.

2-(1,3-diphenylpropyl)malononitrile (10)



Compound **10** was prepared following the general procedure **B** starting from (2-bromoethyl)benzene (2.5 equiv., 231 mg, 1.250 mmol) and benzylidenemalononitrile **1** (1 equiv., 77.1 mg, 0.500 mmol).

Flash chromatography: silica gel, 100% pentane to pentane:Et₂O 9:1 as eluent.

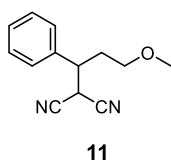
Pale yellow oil, 81 mg, 63% yield.

^1H NMR (300 MHz, Chloroform-*d*) δ 7.68 – 7.27 (m, 10H), 4.03 (d, J = 6.2 Hz, 1H), 3.43 – 3.30 (m, 1H), 2.91 – 2.75 (m, 1H), 2.71 – 2.60 (m, 1H), 2.59 – 2.47 (m, 2H)

^{13}C NMR (75 MHz, Chloroform-*d*) δ 140.0, 136.3, 129.6, 129.2, 128.8, 128.5, 128.1, 126.6, 111.9, 111.8, 45.7, 33.6, 32.8, 30.5

HRMS (FI) m/z calcd for: $\text{C}_{18}\text{H}_{16}\text{N}_2$ 260.1313, found 260.1313.

2-(3-methoxy-1-phenylpropyl)malononitrile (11)



Compound **11** was prepared following the general procedure **C** starting from 1-bromo-2-methoxyethane (2.5 equiv., 174 mg, 1.250 mmol) and benzylidenemalononitrile **1** (1 equiv., 77.1 mg, 0.500 mmol).

Flash chromatography: silica gel, 100% pentane to pentane:Et₂O 8:2 as eluent.

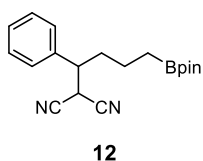
Pale yellow oil, 50 mg, 60% yield.

¹H NMR (400 MHz, Chloroform-*d*) δ 7.46 – 7.36 (m, 3H), 7.36 – 7.29 (m, 2H), 4.25 (d, *J* = 6.0 Hz, 1H), 3.50 – 3.41 (m, 2H), 3.33 – 3.23 (m, 4H), 2.39 – 2.26 (m, 1H), 2.19 – 2.06 (m, 1H)

¹³C NMR (101 MHz, Chloroform-*d*) δ 136.9, 129.4, 129.0, 128.0, 112.3, 112.1, 69.6, 58.9, 44.1, 32.3, 29.8

HRMS (FI) *m/z* calcd for: C₁₃H₁₄N₂O 214.1106, found 214.1106.

2-(3-bromopropyl)-4,4,5,5-tetramethyl-1,3,2-dioxaborolane (12)



Compound **12** was prepared following the general procedure **B** starting from 2-(3-bromopropyl)-4,4,5,5-tetramethyl-1,3,2-dioxaborolane (2.5 equiv., 311 mg, 1.25 mmol) and benzylidenemalononitrile **1** (1 equiv., 77.1 mg, 0.500 mmol).

Flash chromatography: silica gel, 100% pentane to pentane:Et₂O 9:1 as eluent.

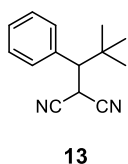
Pale yellow oil, 85 mg, 52% yield.

¹H NMR (300 MHz, Chloroform-*d*) δ 7.46 – 7.34 (m, 3H), 7.34 – 7.26 (m, 2H), 3.89 (d, *J* = 6.1 Hz, 1H), 3.33 – 3.14 (m, 1H), 2.08 – 1.95 (m, 2H), 1.47 – 1.18 (m, 13H), 0.89 – 0.71 (m, 2H)

¹³C NMR (75 MHz, Chloroform-*d*) δ 136.9, 129.3, 128.9, 128.1, 112.1, 112.0, 83.3, 46.5, 34.4, 30.3, 25.0, 24.9, 21.5

HRMS (FI) *m/z* calcd for: C₁₉H₂₅BN₂O₂: 304.2009, found: 324.2013.

2-(2,2-dimethyl-1-phenylpropyl)malononitrile (13)



Compound **13** was prepared following the general procedure **B** starting from *tert*-butyl bromide (2.5 equiv., 140 μL, 1.250 mmol) and benzylidenemalononitrile **1** (1 equiv., 77.1 mg, 0.500 mmol).

Flash chromatography: silica gel, pentane:Et₂O 99:1 to pentane:Et₂O 8:2 as eluent.

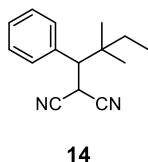
Colorless oil, 72 mg, 68% yield.

¹H NMR (400 MHz, Chloroform-*d*) δ 7.41 – 7.37 (m, 5H), 4.22 (d, *J* = 5.7 Hz, 1H), 3.01 (d, *J* = 5.7 Hz, 1H), 1.11 (s, 9H)

¹³C NMR (101 MHz, Chloroform-*d*) δ 136.4, 129.4, 128.8, 128.7, 113.3, 113.2, 56.9, 35.1, 28.6, 25.2

Physicochemical data are in agreement with those previously reported.²⁹

2-(2,2-dimethyl-1-phenylbutyl)malononitrile (14)



Compound **14** was prepared following the general procedure **C** starting from 2-bromo-2-methylbutane (2.5 equiv., 189 mg, 1.250 mmol) and benzylidenemalononitrile **1** (1 equiv., 77.1 mg, 0.500 mmol).

Flash chromatography: silica gel, pentane:Et₂O 98:2 to pentane:Et₂O 8:2 as eluent.

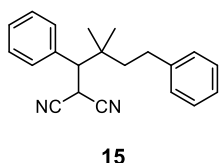
Pale yellow oil, 72 mg, 64% yield.

¹H NMR (400 MHz, Chloroform-*d*) δ 7.44 – 7.33 (m, 5H), 4.21 (d, *J* = 5.4 Hz, 1H), 3.08 (d, *J* = 5.4 Hz, 1H), 1.47 – 1.31 (m, 2H), 1.13 (s, 3H), 1.00 (s, 3H), 0.90 (t, *J* = 7.4 Hz, 3H)

¹³C NMR (101 MHz, Chloroform-*d*) δ 136.1, 129.7, 128.9, 128.8, 113.4, 113.2, 55.3, 37.6, 33.6, 25.0, 24.9, 24.7, 8.3

Physicochemical data are in agreement with those previously reported.³⁰

2-(2,2-dimethyl-1,4-diphenylbutyl)malononitrile (15)



Compound **15** was prepared following the general procedure **C** starting from 2-bromo-2-methylbutane (2.5 equiv., 189 mg, 1.25 mmol) and benzyldenemalononitrile **1** (1 equiv., 77.1 mg, 0.500 mmol).

Flash chromatography: silica gel, pentane:Et₂O 95:5 to pentane:Et₂O 8:2 as eluent.

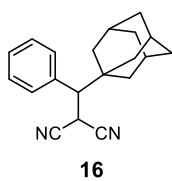
Colorless oil, 60 mg, 40% yield.

¹H NMR (400 MHz, Chloroform-*d*) δ 7.46 – 7.35 (m, 5H), 7.30 – 7.21 (m, 2H), 7.21 – 7.13 (m, 1H), 7.12 – 7.05 (m, 2H), 4.20 (d, *J* = 5.5 Hz, 1H), 3.14 (d, *J* = 5.5 Hz, 1H), 2.69 – 2.51 (m, 2H), 1.69 – 1.56 (m, 2H), 1.24 (s, 3H), 1.12 (s, 3H)

¹³C NMR (101 MHz, Chloroform-*d*) δ 141.8, 135.9, 129.7, 128.8, 128.7, 128.7, 128.4, 126.2, 113.3, 113.2, 55.5, 43.4, 37.7, 30.4, 25.5, 25.4, 25.1

HRMS (GC-EI) *m/z* calcd for C₂₁H₂₂N₂: 302.1783; found: 302.1783.

2-(((3*r*,5*r*,7*r*)-adamantan-1-yl)(phenyl)methyl)malononitrile (16)



Compound **16** was prepared following the general procedure **B** starting from 1-bromoadamantane (2.5 equiv., 269 mg, 1.250 mmol) and benzyldenemalononitrile **1** (1 equiv., 77.1 mg, 0.500 mmol).

Flash chromatography: silica gel, pentane:Et₂O 99:1 to pentane:Et₂O 9:1 as eluent.

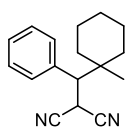
White solid, 78 mg, 54% yield.

¹H NMR (400 MHz, Chloroform-*d*) δ 7.45 – 7.33 (m, 5H), 4.24 (d, *J* = 5.3 Hz, 1H), 2.81 (d, *J* = 5.3 Hz, 1H), 2.07 – 1.99 (m, 3H), 1.75 – 1.56 (m, 12H)

¹³C NMR (101 MHz, Chloroform-*d*) δ 135.4, 129.8, 128.7, 128.6, 113.6, 113.4, 58.1, 40.5, 36.7, 36.5, 28.5, 23.9

Physicochemical data are in agreement with those previously reported.³¹

2-((1-methylcyclohexyl)(phenyl)methyl)malononitrile (17)



Compound **17** was prepared following the general procedure **B** starting from 1-bromo-1-methylcyclohexane (2.5 equiv., 221 mg, 1.250 mmol) and benzylidenemalononitrile **1** (1 equiv., 77.1 mg, 0.500 mmol).

17 Flash chromatography: silica gel, pentane:Et₂O 99:1 to pentane:Et₂O 9:1 as eluent.

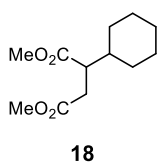
Colorless oil, 57 mg, 45% yield.

¹H NMR (400 MHz, Chloroform-*d*) δ 7.45 – 7.35 (m, 5H), 4.25 (d, *J* = 5.4 Hz, 1H), 3.06 (d, *J* = 5.3 Hz, 1H), 1.65 – 1.20 (m, 10H), 1.16 (s, 3H)

¹³C NMR (75 MHz, Chloroform-*d*) δ 135.8, 129.9, 128.8, 128.7, 113.6, 113.3, 56.9, 37.5, 36.9, 36.7, 25.8, 24.4, 21.9, 21.6, 20.5

Physicochemical data are in agreement with those previously reported.³²

Dimethyl 2-cyclohexylsuccinate (18)



Compound **18** was prepared following the general procedure **A** starting from cyclohexyl bromide **2** (2.5 equiv., 154 μL, 1.250 mmol) and dimethyl maleate (1 equiv., 62.6 μL, 0.500 mmol).

Flash chromatography: silica gel, pentane:Et₂O 99:1 to pentane:Et₂O 9:1 as eluent.

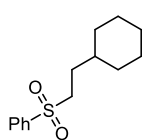
Colorless oil, 62 mg, 54% yield.

¹H NMR (400 MHz, Chloroform-*d*) δ 3.68 (s, 3H), 3.65 (s, 3H), 2.77 – 2.66 (m, 2H), 2.50 – 2.39 (m, 1H), 1.77 – 1.68 (m, 2H), 1.68 – 1.52 (m, 4H), 1.28 – 0.93 (m, 5H)

¹³C NMR (101 MHz, Chloroform-*d*) δ 175.1, 173.0, 51.8, 51.7, 47.1, 40.0, 33.3, 30.7, 30.2, 26.4, 26.2

Physicochemical data are in agreement with those previously reported.³³

((2-cyclohexylethyl)sulfonyl)benzene (19)



Compound **19** was prepared following the general procedure **A** starting from cyclohexyl bromide **2** (2.5 equiv., 154 μL, 1.250 mmol) and (vinylsulfonyl)benzene (1 equiv., 91.1 mg, 0.500 mmol).

19 Flash chromatography: silica gel, pentane:Et₂O 99:1 to pentane:Et₂O 8:2 as eluent.

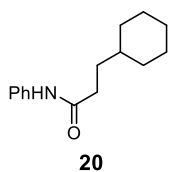
Colorless oil, 71 mg, 55% yield.

¹H NMR (400 MHz, Chloroform-*d*) δ 7.93 – 7.86 (m, 2H), 7.69 – 7.61 (m, 1H), 7.56 (dd, *J* = 8.4, 7.0 Hz, 2H), 3.12 – 3.05 (m, 2H), 1.71 – 1.57 (m, 7H), 1.32 – 1.03 (m, 4H), 0.92 – 0.78 (m, 2H)

¹³C NMR (101 MHz, Chloroform-*d*) δ 139.4, 133.7, 129.4, 128.1, 54.5, 36.7, 32.9, 29.7, 26.4, 26.1

Physicochemical data are in agreement with those previously reported.³⁴

3-cyclohexyl-N-phenylpropanamide (20)



Compound **20** was prepared following the general procedure **A** starting from cyclohexyl bromide **2** (2.5 equiv., 154 μ L, 1.250 mmol) and *N*-phenylacrylamide (1 equiv., 73.6 μ L, 0.500 mmol).

Flash chromatography: silica gel, pentane:Et₂O 50:2.5 to pentane:Et₂O 50:20 as eluent.

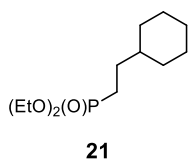
White solid, 61 mg, 53% yield.

¹H NMR (400 MHz, Chloroform-*d*) δ 7.51 (d, *J* = 8.0 Hz, 2H), 7.31 (t, *J* = 7.8 Hz, 2H), 7.17 – 7.05 (m, 2H), 2.41 – 2.32 (m, 2H), 1.79 – 1.66 (m, 4H), 1.63 (q, *J* = 7.3 Hz, 3H), 1.36 – 1.07 (m, 4H), 1.00 – 0.86 (m, 2H).

¹³C NMR (101 MHz, Chloroform-*d*) δ 171.9, 138.2, 129.1, 124.3, 119.9, 37.4, 35.4, 33.2, 33.1, 26.6, 26.4.

Physicochemical data are in agreement with those previously reported.³⁵

Diethyl (2-cyclohexylethyl)phosphonate (21)



Compound **21** was prepared following the general procedure **A** starting from cyclohexyl bromide **2** (2.5 equiv., 154 μ L, 1.250 mmol) and diethyl vinylphosphonate (1 equiv., 77.1 μ L, 0.500 mmol).

Flash chromatography: silica gel, DCM:EtOAc 95:5 to DCM:EtOAc 7:3 as eluent.

Colorless oil, 84 mg, 68% yield.

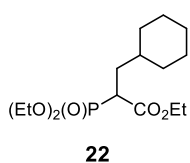
¹H NMR (400 MHz, Chloroform-*d*) δ 4.17 – 3.99 (m, 4H), 1.78 – 1.59 (m, 7H), 1.47 (m, 2H), 1.31 (t, *J* = 7.0 Hz, 6H), 1.28 – 1.09 (m, 4H), 0.94 – 0.80 (m, 2H)

¹³C NMR (101 MHz, Chloroform-*d*) δ 61.5 (d, *J* = 6.5 Hz), 38.5 (d, *J* = 16.8 Hz), 32.9, 29.7 (d, *J* = 5.1 Hz), 26.7, 26.3, 23.3 (d, *J* = 140.5 Hz), 16.6 (d, *J* = 6.0 Hz)

³¹P NMR (162 MHz, Chloroform-*d*) δ 33.37 (tp, *J* = 17.4, 8.7 Hz).

Physicochemical data are in agreement with those previously reported.³⁶

Ethyl 3-cyclohexyl-2-(diethoxyphosphoryl)propanoate (22)



Compound **22** was prepared following the general procedure **B** starting from cyclohexyl bromide **2** (2.5 equiv., 154 μ L, 1.250 mmol) and ethyl 2-(diethoxyphosphoryl)acrylate (1 equiv., 118 mg, 0.500 mmol).

Flash chromatography: silica gel, pentane:EtOAc 6:4 as eluent.

Colorless oil, 96 mg, 60% yield.

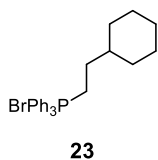
¹H NMR (400 MHz, Chloroform-*d*) δ 4.24 – 4.06 (m, 6H), 3.05 (ddd, *J* = 23.1, 11.5, 3.4 Hz, 1H), 1.94 (m, 1H), 1.76 – 1.57 (m, 6H), 1.33 – 1.10 (m, 13H), 0.98 – 0.77 (m, 2H)

^{13}C NMR (101 MHz, Chloroform-*d*) δ 169.6 (d, $J = 5.0$ Hz), 62.91 – 62.61 (m), 61.4, 43.4 (d, $J = 130.6$ Hz), 36.5 (d, $J = 14.1$ Hz), 34.2 (d, $J = 5.0$ Hz), 32.8 (d, $J = 155.8$ Hz), 26.5, 26.2 (d, $J = 13.5$ Hz), 16.5 (dd, $J = 6.0, 2.6$ Hz), 14.3

^{31}P NMR (162 MHz, Chloroform-*d*) δ 23.57.

Physicochemical data are in agreement with those previously reported.²⁴

Bromo(2-cyclohexylethyl)triphenyl- λ^5 -phosphane (23)



Cyclohexyl bromide **2** (2.5 equiv., 154 μL , 1.250 mmol) and $(\text{TMS})_3\text{SiH}$ (1.1 equiv., 170 μL , 0.550 mmol) were added to a flame-dried nitrogen-purged screw-capped vial, fitted with a rubber septum, charged with the triphenyl(vinyl)phosphonium bromide (1 equiv., 185 mg, 0.500 mmol) in CH_3CN (5 mL, 0.1 M). After, the solution was sparged with nitrogen for 30 seconds and the reaction vessel was sealed with parafilm. The vial was then placed in a 3D-printed photoreactor using a Kessil Lamp (390 nm, 100% intensity) as light source and irradiated overnight. The solvent of the resulting reaction mixture was removed under reduced pressure. The residue was purified by crystallization (pentane:MeOH 20:1) giving the desired product **23** as a yellowish solid (190 mg, 84% yield).

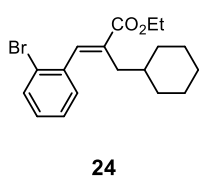
^1H NMR (400 MHz, Chloroform-*d*) δ 7.77 (m, 9H), 7.67 (m, 6H), 3.59 (td, $J = 12.7, 7.1$ Hz, 2H), 1.75 (dd, $J = 12.8, 3.4$ Hz, 2H), 1.65 – 1.40 (m, 6H), 1.25 – 1.11 (m, 2H), 1.04 (m, 1H), 0.87 – 0.74 (m, 2H)

^{13}C NMR (101 MHz, Chloroform-*d*) δ 135.1 (d, $J = 3.0$ Hz), 133.7 (d, $J = 10.1$ Hz), 130.6 (d, $J = 12.5$ Hz), 118.2 (d, $J = 86.0$ Hz), 37.9 (d, $J = 14.5$ Hz), 32.8, 29.6 (d, $J = 4.6$ Hz), 26.2, 25.8, 20.8 (d, $J = 50.3$ Hz)

^{31}P NMR (162 MHz, CDCl_3) δ 24.96

HRMS (LC-UV-ESI) m/z calcd for $\text{C}_{26}\text{H}_{30}\text{BrP}$: 373.2085; found 373.2093.

Ethyl (*E*)-3-(2-bromophenyl)-2-(cyclohexylmethyl)acrylate (24)



Compound **24** was prepared following the general procedure **D** starting from cyclohexyl bromide **2** (2.5 equiv., 154 μL , 1.250 mmol), ethyl 2-(diethoxyphosphoryl)acrylate (1 equiv., 118 mg, 0.500 mmol) and 2-bromobenzaldehyde (3.0 equiv., 197 μL , 1.500 mmol).

Flash chromatography: silica gel, pentane:EtOAc 98:2 as eluent.

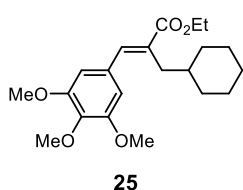
Colorless oil, 98 mg, 56% yield. Only one of the possible diastereomer, with *E* configuration, was detected via ^1H NMR of the reaction crude, and confirmed by the NOESY spectrum.

^1H NMR (300 MHz, Chloroform-*d*) δ 7.65 – 7.58 (m, 2H), 7.34 – 7.24 (m, 3H), 4.29 (q, $J = 7.1$ Hz, 2H), 2.30 (d, $J = 7.0$ Hz, 2H), 1.65 – 1.55 (m, 5H), 1.35 (t, $J = 7.1$ Hz, 3H), 1.19 – 0.97 (m, 3H), 0.80 – 0.62 (m, 2H)

^{13}C NMR (101 MHz, CDCl_3) δ 168.3, 138.9, 136.9, 134.4, 132.8, 130.4, 129.4, 127.2, 124.1, 60.9, 37.6, 34.7, 33.2, 26.5, 26.4, 14.4

HRMS (GC-EI) m/z calcd for 350.0881; found 350.0874.

Ethyl (*E*)-2-(cyclohexylmethyl)-3-(3,4,5-trimethoxyphenyl)acrylate (**25**)



Compound **25** was prepared following the general procedure **D** starting from cyclohexyl bromide **2** (2.5 equiv., 154 μL , 1.250 mmol), ethyl 2-(diethoxyphosphoryl)acrylate (1 equiv., 118 mg, 0.500 mmol) and 3,4,5-trimethoxybenzaldehyde (3.0 equiv., 294 mg, 1.500 mmol).

Flash chromatography: silica gel, pentane:EtOAc 98:2 as eluent.

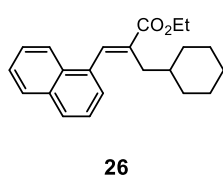
Colorless oil, 68 mg, 38% yield. Only one of the possible diastereomer, with *E* configuration, was detected via ^1H NMR of the reaction crude, and confirmed by the NOESY spectrum.

^1H NMR (400 MHz, Chloroform-*d*) δ 7.58 (s, 1H), 6.64 (s, 2H), 4.27 (q, $J = 7.1$ Hz, 2H), 3.88 (s, 3H), 3.87 (s, 6H), 2.53 (d, $J = 7.1$ Hz, 2H), 1.64 (m, 8H), 1.35 (t, $J = 7.1$ Hz, 3H), 1.16 (m, 3H)

^{13}C NMR (101 MHz, Chloroform-*d*) δ 169.2, 153.2, 139.1, 138.3, 132.5, 131.6, 106.9, 61.1, 60.9, 56.3, 38.4, 34.8, 33.6, 26.6, 26.5, 14.5

HRMS (GC-EI) m/z calcd for 362.2093; found 362.2085.

Ethyl (*E*)-2-(cyclohexylmethyl)-3-(naphthalen-1-yl)acrylate (**26**)



Compound **26** was prepared following the general procedure **D** starting from cyclohexyl bromide **2** (2.5 equiv., 154 μL , 1.250 mmol), ethyl 2-(diethoxyphosphoryl)acrylate (1 equiv., 118 mg, 0.5 mmol) and 1-naphthaldehyde (3.0 equiv., 81.5 μL , 1.50 mmol).

Flash chromatography: silica gel, pentane:EtOAc 98:2 as eluent.

Colorless oil, 92 mg, 57% yield. Only one of the possible diastereomer, with *E* configuration, was detected via ^1H NMR of the reaction crude, and confirmed by the NOESY spectrum.

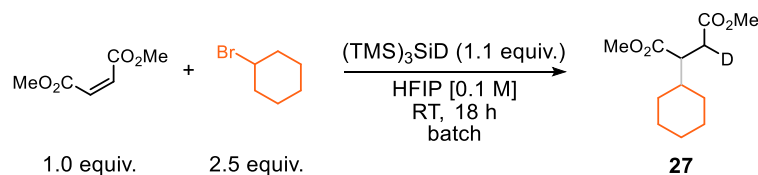
^1H NMR (400 MHz, Chloroform-*d*) δ 8.12 (s, 1H), 7.92 – 7.85 (m, 2H), 7.82 (d, $J = 8.2$ Hz, 1H), 7.54 – 7.45 (m, 3H), 7.36 (d, $J = 7.0$ Hz, 1H), 4.34 (q, $J = 7.1$ Hz, 2H), 2.33 (d, $J = 7.0$ Hz, 2H), 1.61 – 1.50 (m, 5H), 1.40 (t, $J = 7.1$ Hz, 3H), 1.08 (m, 2H), 0.89 (m, 2H), 0.72 – 0.58 (m, 2H)

^{13}C NMR (101 MHz, Chloroform-*d*) δ 168.6, 138.1, 135.2, 133.8, 133.5, 131.6, 128.6, 128.3, 126.3, 126.2, 126.2, 125.3, 125.1, 60.9, 37.5, 35.1, 33.2, 32.0, 26.4, 26.3, 22.8, 14.5, 14.3

HRMS (GC-EI) m/z calcd for 322.1933; found 322.1936.

7.4.6 Mechanistic studies

Incorporation of deuterium from silane

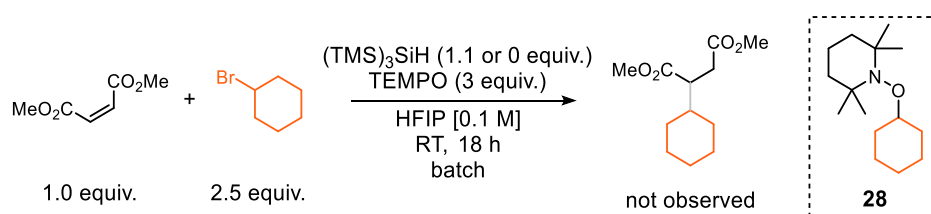


To a flame-dried nitrogen-purged screw-capped vial, fitted with a rubber septum, charged with the dimethyl maleate (1 equiv., 25 μL , 0.200 mmol) in HFIP (2 mL, 0.1 M), cyclohexyl bromide (2.5 equiv., 61.4 μL , 0.500 mmol) and $(\text{TMS})_3\text{SiD}$ (1.1 equiv., 54.9 mg, 0.220 mmol) were added. After, the solution was sparged with nitrogen for 30 seconds and the reaction vessel was sealed with parafilm. Then, the vial was placed in a 3D-printed photoreactor using a Kessil Lamp (390 nm, 100% intensity) as light source and irradiated overnight. The solvent of the resulting reaction mixture was removed under reduced pressure. The crude mixture was purified by flash column chromatography (pentane:Et₂O 9:1) to afford product **27** as a colorless oil (18 mg, 39% yield).

¹H NMR (400 MHz, Chloroform-d) δ 3.69 (s, 3H), 3.66 (s, 3H), 2.74 – 2.66 (m, 2H), 1.78 – 1.69 (m, 2H), 1.69 – 1.58 (m, 4H), 1.28 – 1.07 (m, 3H), 1.07 – 0.95 (m, 2H)

HRMS (GC-FI) m/z calcd for 229.1424; found 229.1419.

Trapping with TEMPO



To a flame-dried nitrogen-purged screw-capped vial, fitted with a rubber septum, charged with the dimethyl maleate (1 equiv., 25 μL , 0.200 mmol) and TEMPO (3.0 equiv., 93.8 mg, 0.600 mmol) in HFIP (2 mL, 0.1 M), cyclohexyl bromide (2.5 equiv., 61.4 μL , 0.500 mmol) and $(\text{TMS})_3\text{SiH}$ (1.1 or 0 equiv., 68 or 0 μL , 0.220 or 0 mmol) were added. After, the solution was sparged with nitrogen for 30 seconds and the reaction vessel was sealed with parafilm. The vial was then placed in a 3D-printed photoreactor using a Kessil Lamp (390 nm, 100% intensity) as light source and irradiated overnight. The solvent of the resulting reaction mixture was removed under reduced pressure. An external standard was added (trichloroethylene, 18 μL , 1 equiv.) and the sample was analyzed by ¹H NMR spectroscopy and GC-MS.

From the NMR spectra, both reactions with and without $(\text{TMS})_3\text{SiH}$ did not afford the product, suggesting that the radical process was inhibited by the presence of TEMPO. GC-MS analysis of the

reaction in the presence of $(\text{TMS})_3\text{SiH}$ shows new peaks different from the starting materials. As it is possible to see from the spectra in **Figure 42**, there is the formation of the adduct **28** between the in situ formed cyclohexyl radical and the TEMPO. The spectroscopic data is consistent with that reported previously.³⁷ Furthermore, GC-MS analysis of the reaction in the absence of TTMS confirmed the no presence of the product and no reaction neither degradation of the starting materials.

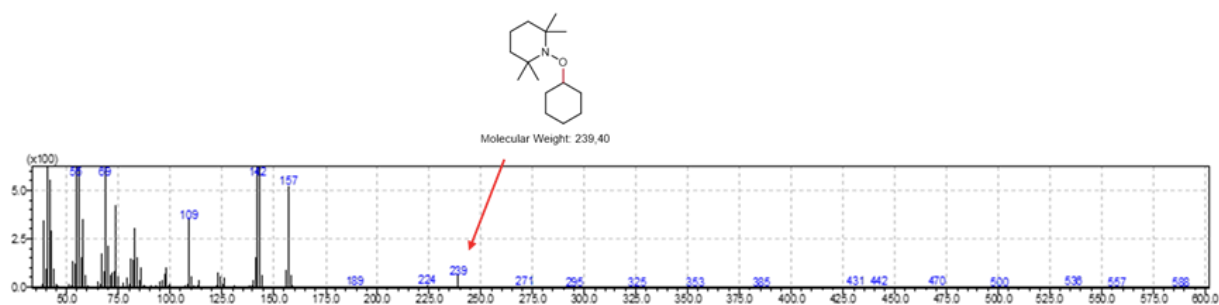


Figure 42 Mass spectra of the adduct between cyclohexyl and TEMPO.²¹

7.5 References

- ¹ Yan M, Lo JC, Edwards JT, Baran PS. Radicals: Reactive Intermediates with Translational Potential. *J Am Chem Soc.* **2016**, 138(39), 12692-12714
- ² Minisci F, Bernardi R, Bertini F, Galli R, Perchinummo M. Nucleophilic character of alkyl radicals—VI: A new convenient selective alkylation of heteroaromatic bases. *Tetrahedron* **1971**, 27(15), 3575-3579
- ³ Proctor RSJ, Phipps RJ. Recent Advances in Minisci-Type Reactions. *Angew Chem Int Ed.* **2019**, 58(39), 13666-13699
- ⁴ Crespi S, Fagnoni M. Generation of Alkyl Radicals: From the Tyranny of Tin to the Photon Democracy. *Chem Rev.* **2020**, 120(17), 9790-9833
- ⁵ Prier CK, Rankic DA, MacMillan DW. Visible light photoredox catalysis with transition metal complexes: applications in organic synthesis. *Chem Rev.* **2013**, 113(7), 5322-63
- ⁶ Zhang N, Samanta SR, Rosen BM, Percec V. Single electron transfer in radical ion and radical-mediated organic, materials and polymer synthesis. *Chem Rev.* **2014**, 114(11), 5848-958
- ⁷ Juliá F, Constantin T, Leonori D. Applications of Halogen-Atom Transfer (XAT) for the Generation of Carbon Radicals in Synthetic Photochemistry and Photocatalysis. *Chem Rev.* **2022**, 122(2), 2292-2352
- ⁸ Roberts BP. Polarity-reversal catalysis of hydrogen-atom abstraction reactions: concepts and applications in organic chemistry. *Chem. Soc. Rev.* **1999**, 28(1), 25-35
- ⁹ Buglioni L, Raymenants F, Slattery A, Zondag SDA, Noël T. Technological Innovations in Photochemistry for Organic Synthesis: Flow Chemistry, High-Throughput Experimentation, Scale-up, and Photoelectrochemistry. *Chem Rev.* **2022**, 122(2), 2752-2906
- ¹⁰ Bonfield HE, Knauber T, Lévesque F, Moschetta EG, Susanne F, Edwards LJ. Photons as a 21st century reagent. *Nat Commun.* **2020**, 11(1), 804
- ¹¹ Buzzetti L, Crisenza GEM, Melchiorre P. Mechanistic Studies in Photocatalysis. *Angew Chem Int Ed.* **2019**, 58(12), 3730-3747
- ¹² Cambié D, Bottecchia C, Straathof NJ, Hessel V, Noël T. Applications of Continuous-Flow Photochemistry in Organic Synthesis, Material Science, and Water Treatment. *Chem Rev.* **2016**, 116(17), 10276-341
- ¹³ Laudadio G, Deng Y, van der Wal K, Ravelli D, Nuño M, Fagnoni M, Guthrie D, Sun Y, Noël T. C(sp³)-H functionalizations of light hydrocarbons using decatungstate photocatalysis in flow. *Science.* **2020**, 369(6499), 92-96
- ¹⁴ Kitcatt DM, Nicolle S, Lee AL. Direct decarboxylative Giese reactions. *Chem Soc Rev.* **2022**, 51(4), 1415-1453

-
- ¹⁵ Constantin T, Zanini M, Regni A, Sheikh NS, Juliá F, Leonori D. Aminoalkyl radicals as halogen-atom transfer agents for activation of alkyl and aryl halides. *Science*. **2020**, 367(6481), 1021-1026
- ¹⁶ Constantin T, Gorski B, Tilby M, Chelli S, Juliá F, Llaveria J, Gillen KJ, Zipse H, Lakhdar S, Leonori D. Halogen-atom and group transfer reactivity enabled by hydrogen tunneling. *Science*. **2022**, 377(6612), 1323-1328
- ¹⁷ Chatgililoglu C, Griller D, Lesage M. Tris(trimethylsilyl)silane. A new reducing agent. *J. Org. Chem.* **1988**, 53(15), 3641–3642
- ¹⁸ Zhang P, Le CC, MacMillan DW. Silyl Radical Activation of Alkyl Halides in Metallaphotoredox Catalysis: A Unique Pathway for Cross-Electrophile Coupling. *J Am Chem Soc.* **2016**, 138(26), 8084-8087
- ¹⁹ Luridiana A, Mazzarella D, Capaldo L, Rincón JA, García-Losada P, Mateos C, Frederick MO, Nuño M, Jan Buma W, Noël T. The Merger of Benzophenone HAT Photocatalysis and Silyl Radical-Induced XAT Enables Both Nickel-Catalyzed Cross-Electrophile Coupling and 1,2-Dicarbonylfunctionalization of Olefins. *ACS Catal.* **2022**, 12(18), 11216-11225
- ²⁰ ElMarrouni A, Ritts CB, Balsells J. Silyl-mediated photoredox-catalyzed Giese reaction: addition of non-activated alkyl bromides. *Chem Sci.* **2018**, 9(32), 6639-6646
- ²¹ Fanini F, Luridiana A, Mazzarella D, Alfano AI, Van de Heide P, Rincón JA, García-Losada P, Mateos C, Frederick MO, Nuño M, Noël T. Flow photochemical Giese reaction via silane-mediated activation of alkyl bromides. *Tetrahedron Letters* **2023**, 117, 154380
- ²² Mistry S, Kumar R, Lister A, Gaunt MJ. C(sp³)-C(sp³) coupling of non-activated alkyl-iodides with electron-deficient alkenes via visible-light/silane-mediated alkyl-radical formation. *Chem Sci.* **2022**, 13(44), 13241-13247
- ²³ Filippini D, Silvi M. Visible light-driven conjunctive olefination. *Nat Chem.* **2022**, 14(1), 66-70
- ²⁴ Capaldo L, Bonciolini S, Pulcinella A, Nuño M, Noël T. Modular allylation of C(sp³)-H bonds by combining decatungstate photocatalysis and HWE olefination in flow. *Chem Sci.* **2022**, 13(24), 7325-7331
- ²⁵ Pickford HD, Nugent J, Owen B, Mousseau JJ, Smith RC, Anderson EA. Twofold Radical-Based Synthesis of *N,C*-Difunctionalized Bicyclo[1.1.1]pentanes. *J Am Chem Soc.* 2021, 143(26), 9729-9736
- ²⁶ Harris JR, Haynes MT 2nd, Thomas AM, Woerpel KA. Phosphine-catalyzed reductions of alkyl silyl peroxides by titanium hydride reducing agents: development of the method and mechanistic investigations. *J Org Chem.* **2010**, 75(15), 5083-91
- ²⁷ Deng HP, Zhou Q, Wu J. Microtubing-Reactor-Assisted Aliphatic C-H Functionalization with HCl as a Hydrogen-Atom-Transfer Catalyst Precursor in Conjunction with an Organic Photoredox Catalyst. *Angew Chem Int Ed.* **2018**, 57(39), 12661-12665

-
- ²⁸ Jin Y, Zhang Q, Wang L, Wang X, Meng C, Duan C. Convenient C(sp³)-H bond functionalisation of light alkanes and other compounds by iron photocatalysis. *Green Chem.* **2021**, 23(18), 6984-6989
- ²⁹ Li J, Lear MJ, Hayashi Y. Direct Cyclopropanation of α -Cyano β -Aryl Alkanes by Light-Mediated Single Electron Transfer Between Donor-Acceptor Pairs. *Chem Eur J.* **2021**, 27(19), 5901-5905
- ³⁰ Xu QH, Wei LP, Xiao B. Alkyl-GeMe₃: Neutral Metalloid Radical Precursors upon Visible-Light Photocatalysis. *Angew Chem Int Ed.* **2022**, 61(14), e202115592
- ³¹ Zhang K, Chang L, An Q, Wang X, Zuo Z. Dehydroxymethylation of Alcohols Enabled by Cerium Photocatalysis. *J Am Chem Soc.* **2019**, 141(26), 10556-10564
- ³² Feng G, Wang X, Jin J. Decarboxylative C-C and C-N Bond Formation by Ligand-Accelerated Iron Photocatalysis. *Eur. J. Org. Chem.* **2019**, 2019(39), 6728-6732
- ³³ de Pedro Beato E, Spinnato D, Zhou W, Melchiorre P. A General Organocatalytic System for Electron Donor-Acceptor Complex Photoactivation and Its Use in Radical Processes. *J Am Chem Soc.* **2021**, 143(31), 12304-12314
- ³⁴ Xue F, Wang F, Liu J, Di J, Liao Q, Lu H, Zhu M, He L, He H, Zhang D, Song H, Liu XY, Qin Y. A Desulfurative Strategy for the Generation of Alkyl Radicals Enabled by Visible-Light Photoredox Catalysis. *Angew Chem Int Ed.* **2018**, 57(22), 6667-6671
- ³⁵ Zhou Z, Kweon J, Jung H, Kim D, Seo S, Chang S. Photoinduced Transition-Metal-Free Chan-Evans-Lam-Type Coupling: Dual Photoexcitation Mode with Halide Anion Effect. *J Am Chem Soc.* **2022**, 144(20), 9161-9171
- ³⁶ Geant P, Mohamed BS, Pèrigaud C, Peyrottes S, Uttaro J, Mathè C. Probing the reactivity of H-phosphonate derivatives for the hydrophosphonylation of various alkenes and alkynes under free-radical conditions. *New J. Chem.* **2016**, 40(6), 5318-5324
- ³⁷ Sha W, Yu JT, Jiang Y, Yang H, Cheng J. The benzoyl peroxide-promoted functionalization of simple alkanes with 2-aryl phenyl isonitrile. *Chem Commun.* **2014**, 50(65), 9179-81

List of abbreviations

1,2-DAG: 1,2-diacylglycerol	EC: endocannabinoid system
3D-QSAR: three-dimensional quantitative structure-activity relationships	ECs: endocannabinoids
(CD ₃) ₂ CO: deuterated acetone	e.e.: enantiomeric excess
(TMS) ₃ SiH: Tris(trimethylsilyl)silane	equiv.: equivalent
[¹²⁵ I] MLT: 2-[¹²⁵ I]iodomelatonin	EtOAc: ethyl acetate
[³ H] MLT: [³ H]melatonin	EtOH; ethanol
2-AG: 2-arachidonoyl glycerol	F= phenylalanine
4P-PDOT: 4-Phenyl-2-propionamidotetralin	FAAH: fatty-acid amide hydrolase
aa: amino acids	FFA: free fatty acid
AcOH: acetic acid	GABA: γ -aminobutyric acid
AEA: Anandamide or <i>N</i> -arachidonylethanolamine	GPCR: G protein-coupled receptor
AIBN: Azobisisobutyronitrile	HAT: hydrogen atom transfer
BDE: bond-dissociation energy	HFIP: 1,1,1,3,3,3-Hexafluoroisopropanol
Boc: tert-Butyloxycarbonyl protecting group	HPLC: high performance liquid chromatography
BODIPY: 4,4-difluoro-4-bora-3a,4a-diaza-s-indacene	HWE: Horner–Wadsworth–Emmons reaction
Cbz: carboxybenzyl protecting group	IV: intravenous bolus
CD ₃ OD: deuterated methanol	M.p.: melting point
CDCl ₃ : deuterated chloroform	MAGL: monoacylglycerol lipase
CDI: 1,1'-carbonyldiimidazole	MAGs: monoacylglycerols
CH ₃ CN: acetonitrile	MD: μ s-long molecular dynamics
CNS: central nervous system	MLT: melatonin
COX: cyclooxygenase	MW: molecular weight
d.r.: diastereomeric ratio	N: asparagine
DCM: dichloromethane	NMR: nuclear magnetic resonance
DIPEA: <i>N,N</i> -diisopropylethylamine	NREM: non-rapid eye movement
DMAC: <i>N,N</i> -Dimethylacetamide	PFA: perfluoroalkoxy alkanes
DMF: <i>N,N</i> dimethylformamide	PK: pharmacokinetic
DMSO: dimethyl sulfoxide	PO: oral gavage
ECL: extracellular loop	Q= glutamine
	REM: rapid eye movement
	r.t.: room temperature

SAR: structure-active relationship

SET: single electron transfer

TEA: triethylamine

TEMPO: (2,2,6,6-tetramethylpiperidin-1-yl)oxyl

TES: triethylsilane

TFA: trifluoroacetic acid

THF: tetrahydrofuran

TM: transmembrane helix

TMSCN: trimethylsilyl cyanide

TMSOTf: trimethylsilyl trifluoromethanesulfonate

XAT: halogen atom transfer

XFEL: X-ray free-electron laser